Context Dependent Processing in the Mouse Olfactory Bulb

Rebecca Jordan

University College London

PhD

Declaration

I, Rebecca Jordan, confirm that the work presented in this thesis is my own. Where information has been derived from other sources, I confirm that this has been indicated in the thesis.

The full word count for this document, including all figure legends and references, is 61,784.

Parts of this dissertation have and will be published as the following journal articles and conference poster abstracts:

1. ‘Massive normalization of olfactory bulb output in mice with a 'monoclonal nose''. *Roland, B., *Jordan, R., *Sosulski, D.L., Diodato, A., Fukunaga, I., Wickersham, I., Franks, K.M., Schaefer, A.T., and Fleischmann, A. ELife. 2016.
   **equal first authors*

2. ‘Active sampling state dynamically enhances olfactory bulb odor representation’. Jordan, R., Fukunaga, I., Kollo, M., and Schaefer, A.T. (2017a). BioRxiv 222588, Submitted.

3. ‘Sniff-invariant intensity perception using olfactory bulb coding of inhalation dynamics.’ Jordan, R., Kollo, M., and Schaefer, A.T. (2017b). BioRxiv 226969. Submitted.

4. ‘Learning-related changes in odour representations in mitral and tufted cells of the mouse olfactory bulb’. Jordan, R., Fukunaga, I., Kollo, M., and Schaefer, A.T. Poster presented at Neuroscience 2015, San Diego, California.

5. ‘Learning-related changes in mitral and tufted cell responses reflect changes in sniffing behaviour’. Jordan, R., Fukunaga, I., Kollo, M., and Schaefer, A.T. Poster presented at Neuroscience 2016, Chicago, Illinois.

6. ‘Sniff-invariant odour intensity perception via reafference of inhalation in the olfactory bulb’. Jordan, R., Schaefer, A.T. Poster presented at Neuroscience 2017, Washington DC.

Signed,

Rebecca Jordan

Acknowledgments

Many people have been indispensable in their help with this work. First and foremost, those include Andreas Schaefer and colleagues/ex-colleagues from Schaefer lab, including Mihaly Kollo and Izumi Fukunaga, Tobias Ackels, Andrew Erskine, William Wray, Isabell Whitely, Debanjan Dasgupta, Carles Bosch and Romeo Racz. Further, the whole division of Neurophysiology at the National Institute for Medical Research (NIMR), including Ede Rancz, Denis Burdakov and Troy Margrie labs, consistently provided a fun and supportive academic atmosphere which greatly facilitated my work. I thank the biological services of both the NIMR and Francis Crick Institute for their tireless work in providing animal care. I thank Ronan cottage neuroelectronics of Mill Hill – in particular Nicholas Burczyck and Martyn Stopps – as well as the mechanical workshop team, for always helping me so efficiently and effectively with custom made equipment. I would also like to thank Keith Fairhall for knowing everything and everyone within both the NIMR and Francis Crick Institute, and consistently providing support when all manner of problems arose. I thank my thesis committee, Denis Burdakov, Troy Margrie and Iris Salecker for numerous sharp questions, observations, and ideas for my project. I thank Mostafa Abdelhamid and Edward Bracey for initially helping me with setting up the head-fixed training and behaviour, as well as Christoph Schmidt-Hieber who, via email, provided essential advice on whole cell recordings in awake mice. I would like to thank Alexander Fleischmann and his lab for the opportunity to collaborate on a very interesting project and ultimately publish a paper, the data from which is not presented in this thesis. For my personal funding (as well as wonderful hikes and academic enrichment in Austria) I am enormously grateful to Boerhinger Ingelheim Fonds for their generous provision of a PhD fellowship. Finally, on a more personal note, I would like to thank Helena Aegerter for not hindering me too much during the three years that I lived with her, and similarly Mahesh Karnani for only getting in my way some of the time.

Two datasets were contributed for the sake of analysis by other members of the lab. Firstly, Mihaly Kollo provided me with a dataset of 325 after-hyperpolarisation waveforms to facilitate cell identification of my own recordings via cluster analysis (Fig. 2.4). Second, Izumi Fukunaga provided sniffing data from anaesthetised mice to allow my comparison across behavioural states in Chapter 4 (Fig. 4.1).

Summary

Context Dependent Processing in the Mouse Olfactory Bulb

Rebecca Jordan

Optimal behavioural strategies necessitate the ability to flexibly respond to sensory stimuli according to behavioural context. Contextual information can be defined as internally-generated information that gives behavioural meaning to primary sensory stimuli, for example: hunger state, reward associations and other learned information. The olfactory bulb (OB) is the very first site of odour information processing, yet a large variety of contextual information has been described in its activity. To investigate the mechanistic basis of this, I used whole cell patch recordings from identified mitral and tufted cells in the olfactory bulb of the behaving mouse *in vivo* to measure how odour responses are shaped across rapid olfactory go/no-go learning episodes. While basic physiological properties do not differ between passively exposed and learning mice, I find that a variety of response changes occur specifically in the learning mouse within the very first sniff cycle. Mice acquire active sniffing behaviours during the odour stimulus across learning, a strategy associated with high motivation and fast reaction times. Responses can be tightly modulated on a trial by trial basis by the active sampling state of the mouse, though some inhibitory response changes occur independent of sniffing behaviour. Response changes due to active sampling appear to enhance both the discriminability and detectability of OB odour representation across the olfactory bulb, and exceed that predicted from feed-forward input alone, suggesting the involvement of top-down mechanisms. Response changes are highly correlated in tufted cells, but not mitral cells, indicating that mitral cell response changes may selectively increase discriminability of odourants. Altogether, active sampling overtly shapes odour responses on rapid timescales, likely enhancing odour representation to facilitate rapid olfactory behaviour. Finally, I explore how perception and coding for odour intensity remain robust despite variance in sniffing, and suggest that the olfactory bulb encodes sniffing parameters to allow sniff-independent perception of stimulus features. This dissertation thus begins to demonstrate the functional impact of active sampling on early sensory processing, and provides new perspectives on olfactory bulb function.

List of abbreviations

IN	Interneuron
PC	Principal cell
OB	Olfactory bulb
MTC	Mitral and tufted cell
MC	Mitral cell
TC	Tufted cell
PSTH	Peristimulus time histogram
V_m	Membrane potential
FR	Firing rate
MID	Mean inhalation duration
FID	First inhalation duration
PiC	Piriform cortex
EPL	External plexiform layer
MCL	Mitral cell layer
GL	Glomerular layer
GC	Granule cell
JG cell	Juxtaglomerular cell
ET cell	External tufted cell
SA cell	Short axon cell
PG cell	Periglomerular cell
AP	Action potential
AHP	After hyperpolarisation
WC	Whole cell (recording)
GPCR	G-protein coupled receptor
OR	Olfactory receptor
ORN	Olfactory receptor neuron
Ri	Input resistance
V_{rest}	Resting membrane potential
pTC	Putative tufted cell
pMC	Putative mitral cell
HDB	Horizontal limb of the diagonal band of Broca
SD	Standard deviation
SE	Standard error
IQR	Interquartile range
STA	Spike-triggered average
sccm	Standard cubic centimetre per minute

List of figures and tables

Introduction figures

Figure 1.1 - Mechanisms for contextual modulation of early sensory circuits.

Figure 1.2. – Feedforward pathway in the olfactory system.

Figure 1.3. - Simplified diagram of OB circuitry.

Figure 1.4. – Centrifugal projections to the olfactory bulb.

Methods figures

Figure 2.1 – Olfactometer diagram.

Figure 2.2 – Odour stimuli.

Figure 2.3 – Spike-subtraction

Figure 2.4 - Principal cell vs interneuron identification analysis and recording parameters.

Figure 2.5 - Go/no-go acqusition and performance.

Figure 2.6 - Widespread responses to odour mixtures.

Results figures

Figure 3.1 - Comparison of passive properties and spontaneous activity between behavioural states.

Figure 3.2 - Comparison of MTC odour response properties between passive and behaving mice.

Figure 3.3 - Diverse response changes occur across learning and not during passive exposure.

Figure 3.4 - Response changes do not depend on reward contingency of odour.

Figure 3.5 – Utility of odour response changes for olfactory behaviour.

Figure 4.1 – Modulation of sniffing by behavioural state.

Figure 4.2 - Learning-related changes in sniffing behaviour.

Figure 4.3 - Sniff changes represent the emergence of an active sampling strategy.

Figure 4.4 - Changes in MID are strong predictor of excitatory response change across learning.

Figure 4.5 - Rapid modulation of active sampling behaviour through task engagement switches.

Figure 4.6 - Dynamic switches in response according to active sampling state.

Figure 4.7 - Rapid sniffing reduces response onset latency and sniff modulation amplitude.

Figure 5.1 - Sniff-related response changes in passive mice evoked by surprising tactile stimulation.

Figure 5.2 - Sniff changes in double-tracheotomised anaesthetised mice result in response changes.

Figure 5.3 - Response changes due to fast sniffing in behaving mice exceed those predicted by bottom-up mechanisms.

Figure 5.4 - Activity changes during baseline during spontaneous rapid sniff bouts.

Figure 5.5 - Comparison of putative mitral and tufted cell response changes.

Figure 6.1 - Effect of puff on sniffing and covariance between sniffing parameters.

Figure 6.2 - Sniff change and concentration change have similar effects on FR responses of MTCs.

Figure 6.3 - Changes in subthreshold response are more inhibitory for concentration increase than for fast sniffing.

Figure 6.4 - Excitatory onset latencies shift in response to inhalation change and concentration change in similar ways.

Figure 6.5 - Fast sniffing does not replicate effect of concentration change when aligning to sniff phase.

Figure 6.6 - Mice rapidly learn to discriminate concentrations on fast timescales.

Figure 6.7 - Mice are capable of good concentration discrimination in the face of fluctuating inhalations.

Figure 6.8 - Inhalation duration transforms mean baseline MTC activity in a large proportion of cells.

Figure 6.9 - Population activity allows detection of an inhalation change on behavioural timescales.

Figure 6.10 - Cell type specificity of effect of inhalation.

General Discussion figures

Table 7.1 - Context dependent modulation of MTC activity and sniffing in the literature.

Figure 7.1 - Potential mechanisms for top-down control of olfactory bulb responses during active sampling.

Contents

Declaration 3

Summary 5

List of abbreviations 6

List of figures and tables 7

Contents 9

1. *General Introduction* 13

1.1. Introduction to contextual information in sensory circuits 14

1.2. The Olfactory Bulb 18

1.3. The Olfactory Bulb Circuit 19

1.3.1. The basic feed-forward pathway 19

1.3.2. Interneurons in the OB 22

1.3.3. Centrifugal Projections 25

1.3.4. Plasticity 28

1.4. Coding of information within the Olfactory bulb 29

1.4.1. Odour identity 30

1.4.2. Odour intensity 31

1.4.3. The sniff cycle 32

1.4.4. Contextual information 34

1.5. Mechanisms of context dependent processing in the OB 36

1.5.1. Top down mechanism: centrifugal afferents 36

1.5.2. Bottom-up mechanism: contextual modulation of sniffing behaviour 38

Conclusion 39

1.6. Aims 39

1.7. Approach 41

2. *General Methods* 45

2.1. Surgery 46

2.2. Head-fixed behaviour 47

2.2.1. Habituation to head-fixation 47

2.2.2. One-odour operant conditioning 47

2.2.3. Two-odour discrimination learning 48

2.2.4. Second pair discrimination learning 48

2.3. Passive exposure 49

2.4. Odourant Delivery 49
2.5. Electrophysiology 53
2.5.1. Craniotomy 53
2.5.2. Whole cell Recordings 53
2.5.3. Recovery of cell morphology 54
2.5.4. Sniff measurement 54
2.6. Data Analysis 55
2.6.1. Principal cell identification 55
2.6.2. Spike subtraction 55
2.6.3. Statistics 56
2.6.4. Decision and reaction time calculation 57
2.6.5.. Odour responses 57
2.7. Optimisation of experimental techniques 58
2.7.1. Stable whole cell recordings in awake mice 58
2.7.2. Rapid acquisition of olfactory go/no-go behaviour 61
2.7.3. Widespread odour responses to multi-component mixtures 64
3. *Physiological differences of MTCs according to behavioural state and learning* 67
3.1. Introduction 68
3.2. Chapter methods 70
3.2.1. Basic cellular properties 70
3.2.2. Response onsets and durations 70
3.2.3. Sniff modulation amplitudes 71
3.2.4. Odour responses and changes 72
3.2.5. Response change onset detection 72
3.2.6. Detectability/Discriminability euclidean distance analysis 73
3.3. Results 73
3.3.1. Baseline properties 73
3.3.2. Odour responses 76
3.3.3. V_m responses undergo changes during learning 80
3.3.4. Response changes are useful for decision 84
3.4. Discussion 86
4. *Learned active sampling strategies and their impact on odour responses* 91
4.1. Introduction 92
4.2. Chapter methods 95
4.2.1. Measuring changes in sniffing 95

4.2.2. Response onset analysis 96
4.2.3. Task engagement/disengagement....96
4.3. Results 97
4.3.1. There are behavioural state-dependent differences in sniffing behaviour....97
4.3.2. There are task specific changes in mean inhalation duration 99
4.3.3. Changes in Sniffing indicate the emergence of active sampling strategies....101
4.3.4. Changes in sniff strategy correspond well with mean response changes 104
4.3.5. Dynamically altering active sampling state causes dynamic switches in response....107
4.3.6. Effect of sniffing on temporal features of the response....112
4.4. Discussion.... 115
5. *Mechanistic relationship between sniffing and response change* 121
5.1. Introduction 122
5.2. Chapter methods 124
5.2.1. Effect of fast sniffing on baseline V_m....124
5.2.2. Surprising tactile stimulus experiments....124
5.2.3. Double tracheotomy 125
5.2.4. Putative mitral cell versus tufted cell identification from theta tuning 125
5.3. Results 126
5.3.1. Fast sniffing evokes odour response changes in passively exposed awake mice126
5.3.2. Fast sniffing evokes odour response changes in anaesthetised mice 129
5.3.3. Response changes during behaviour exceed that predicted by sniff locking properties....132
5.3.4. Spontaneous sniff bouts in absence of odour cause activity changes 135
5.3.5. Tufted cells show more highly correlated changes during behaviour than mitral cells 139
5.4. Discussion.... 142
6. *Impact of sniff variance on intensity perception and neural correlates of odour concentration* 147
6.1 Introduction 148
6.2 Chapter methods 149
6.2.1. Behavioural task and training 149
6.2.2. Odours used 150
6.2.3. Cell numbers 151
6.2.4. Spike rate responses and onsets....151

6.2.5. Correlations between response changes due to sniffing and concentration change 152
6.2.6. Euclidean distance analysis of concentration discriminabilty 152
6.2.7. Baseline activity correlations with inhalation duration 153
6.2.8. Euclidean distance analysis of detectability of sniff change 153
6.2.9. Modulation of sniff-activity relationships across phase preference 154
6.3 Results 154
6.3.1 Changes in sniffing can mimic effect of increased concentration on firing rate response 154
6.3.2. Faster inhalation mimics effect of concentration increase on latency response in the timescale of a single sniff 160
6.3.3. Phase advance within sniff cycle remains stable despite changes in sniff rise time 163
6.3.4. Mice can successfully discriminate concentrations on rapid timescales 166
6.3.5. Variance in sniffing has no overt impact on performance in a fine concentration discrimination task 169
6.3.6. Mitral and tufted cells encode changes in the inhalation on rapid behavioural timescales 172
6.3.7. Putative Mitral and Tufted respond to changing inhalation parameters in divergent ways 177
6.4. Discussion 180
7. *Overall conclusions and general discussion* 185
Overall conclusions 186
General discussion 188
7.1 New perspectives on olfactory bulb function 189
7.1.1 The bulb as an olfactory thalamus 189
7.1.2 'Contextual information' in the bulb - a misnomer? 191
7.1.3 The olfactory bulb as an encoder of sniff dynamics 194
7.2. Active sampling modulation of olfactory responses – potential mechanisms 195
7.2.1 Local circuit mechanism 196
7.2.2 Top down control 198
7.2.3 Population level effects 200
7.3 The impact on future research 202
7.3.1 Research in the olfactory system 202
7.3.2 Broader impact on sensory neuroscience 204
References 206

CHAPTER 1

GENERAL INTRODUCTION

1.1. Introduction to contextual information in sensory circuits

The nervous system evolved to generate behaviours optimal for survival. This function is further complicated since the optimal behaviour in response to a stimulus in one situation may be completely different in another. A rat can gain nutrition by eating discarded cheese out of a trash can, but when set out on a kitchen floor trap this could mean certain death, while the mating call of a male bird is salient to a receptive female with no mate, but is of no interest to a paired female with chicks to feed. An animal's internal and external environment is in constant flux – when the animal moves or migrates, with physiological stressors, when weather or season changes, when other animals move into or out of the area. This means that optimal behavioural strategies, as well as the fraction of sensory information important to the control of action are both subject to dynamic change. Thus, for an organism to generate optimal behaviour, it must be able to flexibly encode and respond to sensory stimuli according to the contextual information present. This latter information can be defined as internally-stored information that gives behavioural meaning to primary sensory stimuli. This can include the homeostatic state of the animal's internal environment, the behavioural state of the animal, the type of task the animal is engaged in, and predictive information about the situation that the animal has learned through experience, such as reward expectations. For a long time since the basic hierarchical model of sensory processing was brought forward by Hubel and Wiesel (Hubel and Wiesel, 1959, 1962), it has been thought that these more cognitive, contextual forms of information are integrated with incoming sensory stimuli only in downstream multimodal circuits, such as the lateral entorhinal cortex and hippocampus. In recent years, however, there has been a gentle shift away from this passive, feedforward model of sensory processing toward a more complex system which incorporates a large amount of feedback from higher centres to earlier ones, since this is a pervasive feature of sensory circuits (Engel et al., 2001). It is also becoming increasingly apparent that contextual information is indeed present in the ongoing activity of relatively early

sensory circuits of all modalities: for example, locomotion, expectation and reward timing modulate visual cortex activity (Chubykin et al., 2013; Fiser et al., 2016; Niell and Stryker, 2010; Shuler and Bear, 2006), and barrel cortex activity is profoundly influenced by active tactile exploration and social context (Crochet and Petersen, 2006; Lenschow and Brecht, 2015). In the olfactory system, contextual information apparently even reaches the earliest sensory processing circuit - the olfactory bulb (see later). This latter circuit, and the role of context in its processing, will be the focus of this dissertation.

Contextual information could conceivably have great utility for early sensory processing. The sensory environment is extremely rich in information, and only a small fraction of this information is behaviourally relevant - a fraction which is likely to change according to the particular situation encountered. Because there is limited coding capacity within the nervous system in terms of both neuronal number and energetic resources, encoded information needs to be filtered of the irrelevant information as early as possible to ensure efficient use of these resources. Some believe this to be the reason that early sensory pathways include information bottlenecks in neuronal number. These arise from substantial convergence from the sensory periphery to the secondary projection neurons and thalamic circuits and constitute a substantial drop in information coding resources before the information is divergently sent to a much larger number of neurons in the cortex. For example, there are 63 million rods and cones collecting light information in each macaque retina (Packer et al., 1989), while just under 2 million retinal ganglion cells pass this information on to the lateral geniculate nucleus of the thalamus (Potts et al., 1972). Here, only 1 million neurons divergently send on the visual information to primary visual cortex, V1, where there are around 160 million neurons (O'Kusky and Colonnier, 1982).

These bottleneck circuits are an ideal location to discard redundant or irrelevant information prior to generating a cortical representation. Some redundant information can be removed by intrinsic processing of the incoming information, for example by differentiating the incoming

signals and encoding spatiotemporal changes in sensory stimuli, rather than the static features. This is known to occur in retinal circuits, where contrast and movement is encoded in the RGCs instead of absolute luminance levels encoded by the photoreceptors (Dowling, 1996). While this kind of processing can remove a big chunk of redundant information, the sensory circuit is still liable to encode a lot of information that is not necessarily of any use to the animal. To further increase coding efficiency in the nervous system, it would conceivably be useful to bias coding resources towards information that is more likely to be of importance. In this respect, contextual information could be utilised in information bottleneck circuits to mediate dynamic changes in the information filter that selectively facilitates the passage of important information. Further, contextual information could also be utilised in sensory circuits in general to shape exactly how stimuli are processed according to the current behavioural demands of an animal. For example, if the animal is engaged in detection of low threshold stimuli, reduced inhibition may be beneficial, while if the animal making fine discrimination between very similar stimuli, increased inhibition may be the optimal choice to facilitate pattern separation.

Broadly, two mechanisms underlying contextual modulation of early sensory circuits are possible in the adult brain: top-down and bottom up mechanisms (Fig. 1.1). A common feature of sensory systems is the presence of sensory-driven feed-forward pathways as well as top-down pathways originating in higher centres. The former carry information about the external environment, while the latter are often hypothesised to be cognitively activated by higher-order contextual information (Engel et al., 2001), such as reward expectations. As such, contextual information could reach early sensory circuits through these ubiquitous top-down circuits. A second pervasive feature of sensation is that sensory information is not only passively collected, but actively sampled from the environment with behaviour; e.g. eye movements, whisking, pinnae orientation and sniffing. Such behaviour could be modulated to either increase sensory information flow for a particular modality or direct acquisition towards particular features of the

sensory environment according to attentional or exploratory processes. Any context-dependent modulation of this behaviour will alter the overall pattern of incoming information from bottom-up sensory-driven circuits.

While there is accumulating evidence of contextual information being represented in sensory circuit activity, far less is known about the underlying mechanisms. The aim of the current dissertation is to elucidate some of the mechanistic basis of contextual modulation of very early sensory circuit activity in the olfactory bulb, the first stage of olfactory information processing.

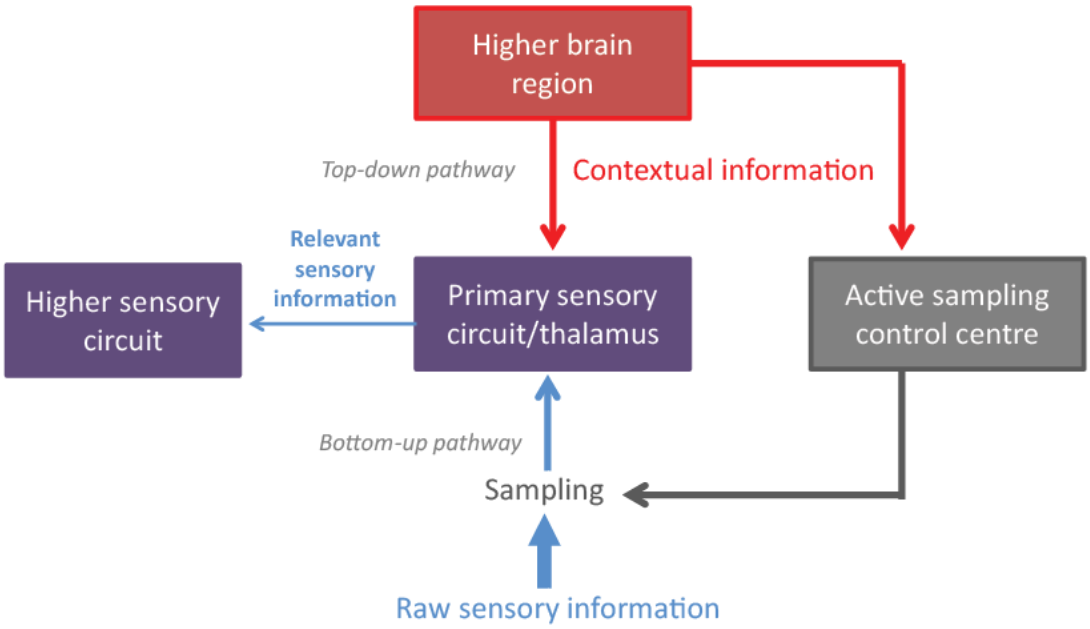

Figure 1.1. Mechanisms for contextual modulation of early sensory circuits

Higher brain regions encoding contextual information could a) deliver this via top-down connections to the sensory circuit itself, altering processing to selectively facilitate the passage of important information, and b) use this information to alter active sampling behaviour which in turn is directed to facilitate the delivery of important sensory information from the pool of raw information available. Since these are non-mutually exclusive, coordination of the two mechanisms may occur.

1.2. The Olfactory Bulb

The olfactory bulb (OB) is the first site of odour information processing. In contrast to other sensory modalities, olfactory information is not subject to thalamic processing prior to reaching the primary olfactory cortices. Instead, olfactory information is delivered directly from the sensory periphery (the olfactory epithelium) to the OB, which is ontogenetically part of the paleocortex. However, it has been noted that the circuitry of the olfactory bulb is similar in architecture to that of the sensory thalamus, such as the lateral geniculate nucleus of the visual system, and some have hypothesized that the two structures may have convergently evolved to provide the same function of controlling sensory information flow to the cortex (Kay and Sherman, 2007).

The OB is an ideal circuit for studying context-dependent changes in processing. Like the sensory thalamus, it represents the only major bottleneck in the number of neurons along the olfactory pathway: olfactory receptor neurons (ORNs) converge onto excitatory principal cells (mitral and tufted cells; MTCs) of the OB on the order of 1000s to 1 (Mombaerts et al., 1996), while MTCs send widely divergent and non-topographic projections to the cortex (Ojima et al., 1984; Sosulski et al., 2011). Additionally, in contrast to other sensory systems, the OB represents the only layer of processing between sensory periphery and cortex, and with its large number of INs relative to PCs compared to the cortex, it is hypothesised the OB may be required to perform a large number of differing processing functions (see section 1.3.2). Moreover, there is already abundant evidence for contextual information reaching the OB both anatomically and physiologically (see section 1.3.3). Taken together, there is ample reason to believe that adaptive changes in OB processing could be of high importance in efficiently and selectively shaping odour representation according to behavioural context.

The OB is also an ideal model circuit from an experimental standpoint: it lies dorsally at the anterior-most point of the brain, largely isolated from other brain structures, with no through-

running axonal fibres. This allows the OB to be discretely manipulated without disrupting other brain structures, and allows good access for imaging and intracellular electrophysiology – techniques critical for investigating circuit mechanisms. Secondly, the circuit structure of the OB is highly tangible yet non-trivial, providing a good level of complexity for studying circuit functionality. Finally, the olfactory system is of high ethological importance to nocturnal and crepuscular animals such as the mouse, a model organism in which many specific genetic manipulations of neuronal circuitry are possible. This also means that olfactory behaviour in rodents is also very rapidly learned in laboratories compared to other sensory modalities (Nigrosh et al., 1975).

1.3. The Olfactory Bulb Circuit

The OB circuit has been relatively well deciphered so far, with a distinct layered arrangement of interneurons that separates information flow into discrete stages of processing. Despite many references to the OB as a 'relay' of olfactory information, the OB is far from such a simple device: interneurons (INs) outnumber projection neurons by 100s to 1, indicating massive processing of olfactory information within the circuit (Shepherd, 2004).

1.3.1. The basic feed-forward pathway

1.3.1.1 Olfactory epithelium

In the olfactory epithelium (OE) ORNs first transduce olfactory information. Each ORN expresses just one of 1000 different olfactory receptor (OR) genes in the rodent (Zhang and Firestein, 2002), which is selected for stochastically (reviewed in Magklara and Lomvardas, 2013). ORNs expressing different ORs are intermingled throughout the nasal epithelium, but each type is restricted to 1 of 4 zones, the functionality of which is unknown. Each OR binds a range of odour volatiles with varying affinity. The large majority of ORs are G-protein coupled receptors (GPCRs; Buck and Axel, 1991), and the binding of the odour volatile sets off a transduction cascade

(Kleene, 2008), simplified as follows: conformational changes in the GPCR release the G-protein (G_{olf}), which then binds and activates adenylate cyclase, converting ATP to cyclic AMP, which then binds cyclic nucleotide-gated ion channels (CNG), allowing influx of Na^+ and Ca^{2+} (Nakamura and Gold, 1987). Increased internal calcium ion concentration in turn activates Ca^{2+}-gated chloride channels, causing an efflux of chloride which is thought to greatly amplify the depolarisation (Lowe and Gold, 1993). Termination of the response comes about through multiple mechanisms, largely triggered by the increased internal Ca^{2+} (Kleene, 2008). Note, however, that variations on this cascade exists within and between ORNs (Spehr and Munger, 2009). The ORN depolarisation elicits a train of action potentials (APs) which are transmitted to the OB, where they synapse onto MTCs and periglomerular neurons in contained input structures called glomeruli. ORNs expressing one kind of OR most often converge exclusively onto just one glomerulus in each hemibulb (Mombaerts et al., 1996).

1.3.1.2 MITRAL AND TUFTED CELLS

MTCs are the glutamatergic output neurons of the OB. They sample from just one glomerulus with their apical dendrite and send on olfactory information to a number of cortical regions via the lateral olfactory tract, including the piriform cortex, anterior olfactory nucleus, olfactory tubercle, amygdala and entorhinal cortex (Ghosh et al., 2011; Haberly and Price, 1978; Miyamichi et al., 2011; Sosulski et al., 2011; Fig. 1.2). While mitral and tufted cells are similar in these basic respects, it is becoming clear that these two cell types constitute two different channels of olfactory bulb output. Firstly, they differ in morphology: their cell bodies lie in different layers of the olfactory bulb, with mitral cell bodies lying tightly packed within the mitral cell layer, and tufted cells sitting much further away in the external plexiform layer (EPL) and glomerular layer (GL) – this is often how the different cell types are distinguished experimentally (e.g. Fukunaga et al., 2012; Yamada et al., 2017). TCs have often further been broken down into three sub-types depending on where they sit within the GL or EPL: superficial (GL), middle (upper

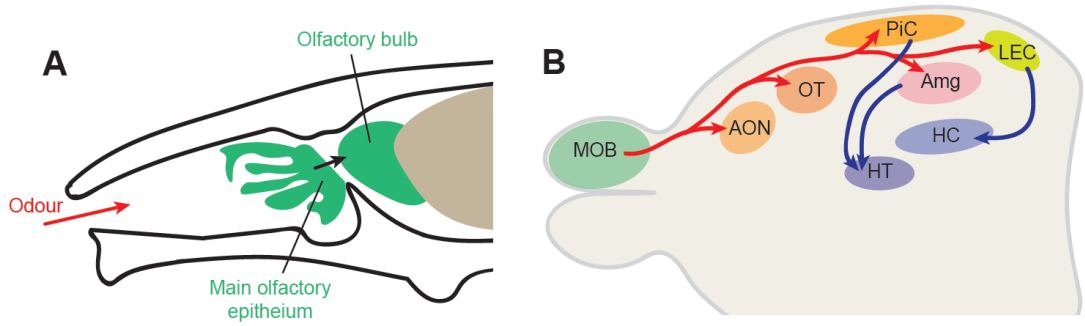

Figure 1.2. Feedforward pathway of the olfactory system.

(**A**) When the animal takes an inhalation, odour enters the nasal cavity and is first transduced at the main olfactory epithelium, which in turn sends projections to the olfactory bulb. (**B**) Transverse plane diagram of the mouse brain to show the main projection targets of the main olfactory bulb (MOB). Primary projections are shown in red. AON = anterior olfactory nucleus, OT = olfactory tubercle, PiC = Piriform cortex, Amg = amygdala, LEC = lateral entorhinal cortex. Some second-order projections are also depicted in blue: HC = hippocampus, HT = hypothalamus.

ELP) and deep (lower EPL) TCs. Additionally, mitral cells have a larger extent of lateral (basal) dendrites (Mori et al., 1983; Orona et al., 1984), and congruently, in slice recordings, mitral cells appear to receive more lateral inhibition (Christie et al., 2001). Other aspects of response properties also, differ, with TC response profiles tending to show stronger odour-evoked excitation (Fukunaga et al., 2012; Griff et al., 2008a; Nagayama et al., 2004) congruent with their lower thresholds for activation following olfactory nerve stimulation (Schneider and Scott, 1983), while mitral cells show longer timescale excitatory responses in anaesthetised animals (Fukunaga et al., 2012; Griff et al., 2008a; Igarashi et al., 2012). Neuromodulators also have different effects on the two cell types: stimulation of the raphe nuclei for example causes potentiation of tufted cell responses to odours, rendering them more excitatory, while having more heterogeneous effects on mitral cell responses, serving to decorrelate them (Kapoor et al., 2016). This kind of divergent effect on MCs and TCs has similarly been reported during task learning (Yamada et al., 2017). Altogether, this has led to a sense that TCs are driven by feedforward inputs primarily, and thus provide a rapid 'snapshot' of the olfactory scene, while

mitral cells incorporate more processing into their responses which occur at later timescales, and may provide more detailed olfactory information.

MTCs divergently project their axons to multiple cells in the olfactory cortices, with each pyramidal receiving input from multiple MTCs (Ojima et al., 1984; Sosulski et al., 2011). The two cell types differ in their precise projection targets: tufted cells project to focal, anterior regions of the cortex, and MCs project diversely to all areas (Igarashi et al., 2012; Nagayama et al., 2010). It is apparent that different olfactory cortices receive a different arrangement of input from the olfactory bulb. For example, the anterior olfactory nucleus and amygdala receive highly topographic input from the olfactory bulb, while the piriform cortex and olfactory tubercle receive input in a much more stochastic way, with no preservation of topography (Giessel and Datta, 2014; Sosulski et al., 2011).

1.3.2. INTERNEURONS IN THE OB

The OB is not a simple relay for olfactory information, however: there exists a range of inhibitory interneurons (INs) which serve to process the information. These are conveniently segregated into discrete layers of processing (Fig. 1.3), however, surprisingly little is known about the functionality of the different interneuron circuits for information processing *in vivo*, though *in vitro* work has driven much hypothesizing.

In the glomerular layer, a highly heterogeneous population of juxtaglomerular INs (JGs) surround each glomerulus and mediate processing within and between glomeruli. These can be segregated into three main types: excitatory external tufted cells (ET), excitatory short axon cells (SA) and inhibitory periglomerular cells (PG), the latter of which are highly diverse in terms of their expression profiles, electrophysiology and morphology (Hayar et al., 2004). The diversity of these neuronal types would suggest a range of different processing functions, however due to the current lack of simple classification methods for each cell type, their different functionality *in vivo* have not been well established. Most evidence thus either comes from slice

for the specific cell types, or is based on the bulk heterogenous population *in vivo*. Altogether JGs are proposed to process the olfactory information in a number of different ways: for example, recently the inhibitory glomerular neurons have been shown to mediate odour-driven inhibition of MTCs, and setting the theta phase-preference of MCs via feed-forward inhibition (Fukunaga et al., 2014). They are also thought to mediate feedback inhibition onto the incoming olfactory sensory neuron terminals (Ennis et al., 2001; Wachowiak et al., 2005), perhaps serving as the gate-keepers of olfactory input. They also provide lateral inhibition between adjacent glomeruli (Aungst et al., 2003; Economo et al., 2016), potentially serving to refine the tuning of mitral and tufted cells (Tan et al., 2010), and normalise overall activity across large changes in input strength alongside concentration increases (Roland et al., 2016). Excitatory ET cell activity is highly rhythmic and appears to entrain the activity of other JG neurons to theta rhythms which may be entrained by the sniff cycle (Hayar et al., 2004).

The sparser external plexiform layer INs include parvalbumin expressing INs. Recent studies suggest that these play an important role in computations such gain control of OB output (Kato et al., 2013; Miyamichi et al., 2013).

In the granule cell layer (GCL), axonless inhibitory granule cells (GCs) provide the final stage of processing before the information is sent on to cortical areas. GCs are by far the most numerous IN in the olfactory bulb, and greatly outnumber MTCs (Shepherd, 2004), which presumably is suggestive of their great importance in OB processing. They form inhibitory dendrodendritic bi-directional synapses onto MTCs lateral dendrites and mediate recurrent inhibition within the same synapse when activated by back-propagating action potentials (Margrie et al., 2001) however their precise roles within the OB remain elusive. The granule cell dendritic spines at which these dendrodendritic synapses occur (known as gemmules) contain voltage activated currents, and can be relatively electrically isolated from the rest of the neuron. Thus they can act as individual computational units in absence of GC spiking activity (Bywalez et al., 2015).

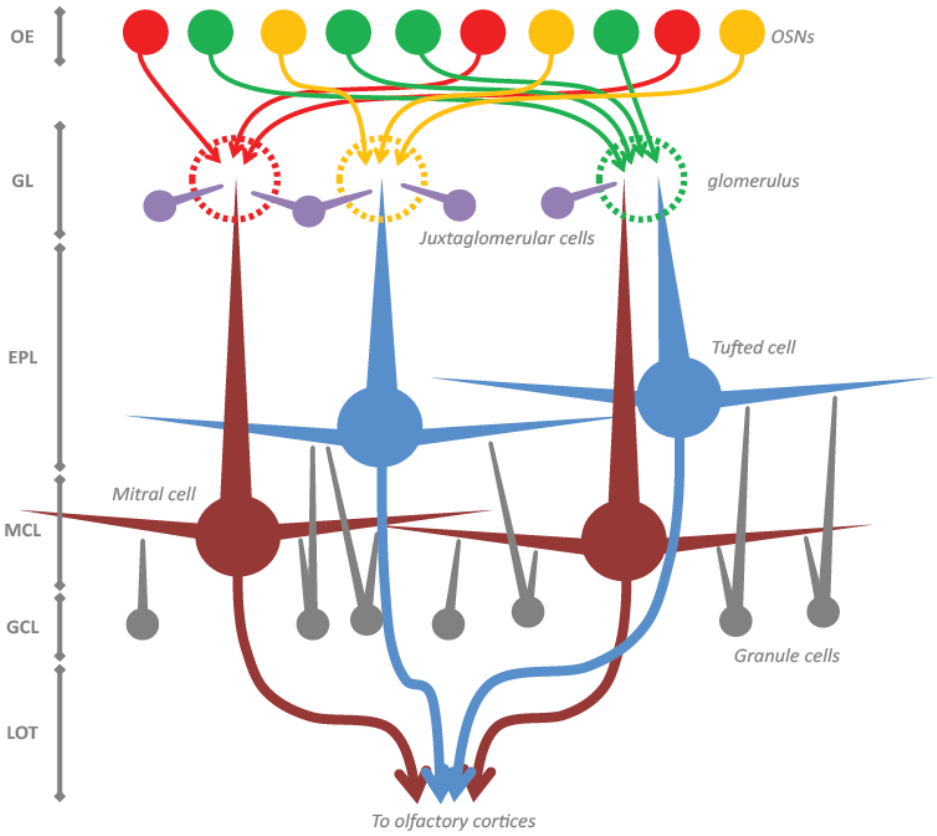

Figure 1.3. Simplified diagram of OB circuitry.

Unprocessed odour information is sent from the olfactory receptor neurons (ORNs) of the olfactory epithelium (OE), where it synapses onto mitral cells (MCs) and tufted cells (TCs) in input structures called glomeruli. A heterogeneous population of glomerular layer INs (JGs) mediates processing at this stage. Inhibitory granule cells (GCs) provide a second stage of processing, before the information is sent on to the olfactory cortex. Note: EPL INs not shown.

LOT: lateral olfactory tract; GCL: granule cell layer; MCL: mitral cell layer; EPL: external plexiform layer; GL: glomerular layer; ONL: olfactory neuron layer; OE: olfactory epithelium

They are thought to play a key role in the generation of gamma oscillations (30-100Hz) and synchronous spiking of MTCs (Fukunaga et al., 2014; Schoppa, 2006). These are proposed to be important for odour discrimination (Lepousez and Lledo, 2013): enhancing gamma oscillations genetically increases the ability of mice for fine odour-discrimination (Nusser et al., 2001), while fine odour discrimination is also accelerated when GC-MC inhibition is increased via specific targeted modification of the MC-GC synapse (Abraham et al., 2010), or targeted disinhibition of

GCs (Nunes and Kuner, 2015). Since granule cells sit very deep within the OB, and are very small, direct recordings *in vivo* are rare and thus their odour response features are fairly elusive. Recent loose-patch recordings from GCs in anaesthetised and awake mice however, show that they are highly active and odour-responsive in the awake state (Cazakoff et al., 2014).

A much smaller population of stellate-shaped Blanes cells also exists within the GCL, and these provide feedforward inhibition onto GCs (Pressler and Strowbridge, 2006), though their function is unknown.

Recently there has been much interest in finding out how bulb interneurons may diversify information within a single glomerular column (i.e. all of the mitral and tufted cells which sample from a single shared glomerulus, known as 'sister' mitral and tufted cells). Do such sister mitral and tufted cells carry redundant information, or does inhibition shape each cell's response profile differently? This is difficult to answer given the issues surrounding identifying true sister MTCs, however the first unit recording evidence suggests that spike rate responses to odours are highly correlated between sister cells, but temporal responses show divergence (Dhawale et al., 2010). However, unit recordings will greatly underestimate inhibitory input, as well as bias toward highly active cell types. Newer imaging evidence has provided conflicting results – one study suggests that response polarity to an odourant is shared by sister mitral and tufted cells (Economo et al., 2016), but another suggests clear response heterogeneity within a module (Kikuta et al., 2013). Since single glomerular labelling suggests spatial overap between MTCs from different glomeruli (Kikuta et al., 2013), the matter is as yet unresolved.

1.3.3. CENTRIFUGAL PROJECTIONS

Given that the olfactory bulb is the very first site of olfactory information processing, it is perhaps surprising that it receives a huge amount of top-down input coming from a variety of regions (Shipley and Adamek, 1984). The sheer abundance of centrifugal afferents and the first indications that they have profound effects in the circuit suggest they are of critical importance

in shaping olfactory bulb processing. The OB interneuron layers are prominent targets for top-down centrifugal projections from higher centres, so it is conceivable that higher centres encoding contextual information actively shape OB processing. While knowledge of centrifugal afferents dates back decades, surprisingly little is known about what kind of information these top-down afferents carry, and what functionality they have for olfactory bulb processing (Matsutani and Yamamoto, 2008). There are two main kinds of centrifugal projection to the olfactory bulb based on their origin: input from the neuromodulatory centres of the brainstem, and cortical input from areas which the olfactory bulb itself projects to (Fig. 1.4). The two are hypothesized to have very different roles in olfactory bulb processing.

1.3.3.1. NEUROMODULATORY INPUT

The first kind of projection comes from neuromodulatory centres of the brain stem. These include cholinergic and GABAergic fibres from the horizontal limb of the diagonal band of Broca, as well as massive projections from the noradrenergic fibres of the locus coeruleus, and serotonergic and GABAergic fibres from the dorsal raphe nuclei (Shipley and Adamek, 1984; Steinfeld et al., 2014). These are proposed to have a wide range of functions related to altering the network state according to behavioural context, however the contributions of individual projections are hard to quantify since neuromodulatory centres also send projections to the olfactory cortices which in turn send projections to cortex.

An estimated 40% of cells in the locus coeruleus project to the olfactory bulb, with multiple and widespread release variscosities on terminals here (McLean et al., 1989). The large majority of these terminals sit in the external plexiform layer and granule cell layer. Noradrenergic action in OB slices appears to have excitatory effects on MCs, enhancing MTC response to weak input (Jahr and Nicoll, 1982), and appears to inhibit transmission at the MC-GC synapse (Trombley and Shepherd, 1992). *In vivo*, despite the fact that noradrenergic terminals have not been abundantly found in the glomerular layer, activation of noradrenergic afferents appears to

suppress pre-synaptic OSN input to the olfactory bulb (Eckmeier and Shea, 2014). Behaviourally, noradrenergic action in the olfactory bulb has been linked to olfactory recognition (Guerin et al., 2008; Pissonnier et al., 1985).

The horizontal limb of the diagonal band of Broca (HDB) sends abundant cholinergic afferents to the olfactory bulb. Activation of this pathway *in vivo* can have profound consequences on circuit state, for example optogenetic activation of the cholinergic neurons of the HDB adds an excitatory bias to both spontaneous and evoked MTC activity in the anaesthetised mouse (Rothermel et al., 2014), potentially by amplifying glomerular input to weak sensory input (Bendahmane et al., 2016).

Finally, the dorsal raphe nuclei (DRN) sends both serotonergic and GABAergic projections to the olfactory bulb. The action of serotonergic projections from the raphe nuclei appear to have contradictory effects in the literature: one study shows that serotonin acts to increase juxtaglomerular inhibitory feedback onto OSN terminals, reducing olfactory input indiscriminately (Petzold et al., 2009), while another shows that MTC odour responses are potentiated or decorrelated for MCs and TCs respectively (Kapoor et al., 2016).

1.3.3.2. CORTICAL INPUT

The second type of centrifugal input to the olfactory bulb comes from the cortex. A number of cortical areas project to the bulb: the piriform cortex, the anterior olfactory nucleus and the lateral entorhinal cortex (LEC). These largely project to the granule cell layer (Niedworok et al., 2012; Shipley and Adamek, 1984). Little is known about the precise role these cortical projections serve in the olfactory bulb. Slice studies have shown that olfactory cortex pyramidal cells excite a diverse range of OB INs, and can gate odour responses in MTCs *in vivo* (Boyd et al., 2012; Markopoulos et al., 2012). Similar studies also suggest possible roles for the cortex in both gating the activity of GCs (Balu et al., 2007) and mediating plasticity within the GC circuit (Gao and Strowbridge, 2009). The function of this cortical feedback is as yet unclear, but models of

olfactory coding have recently incorporated it as a predictive coding feature: the cortical projections deliver a prediction of the olfactory scene to the olfactory bulb, and here the prediction is subtracted via GCs from the actual olfactory activity to generate an olfactory error signal (Grabska-Barwińska et al., 2017; Kepple et al., 2016). There is not a large amount of evidence to support these kinds of predictive coding models, and it is still unresolved whether these cortical projections even constitute true 'feedback', i.e. whether the cortical neuron projects back to the same neurons that activate it to form a closed loop. However, first imaging studies suggest odour information provided by cortical projections does not locally relate to MTC odour responses, suggesting that cortical projections may in fact function to decorrelate mitral cell activity (Otazu et al., 2015) instead of providing feedback in the literal sense.

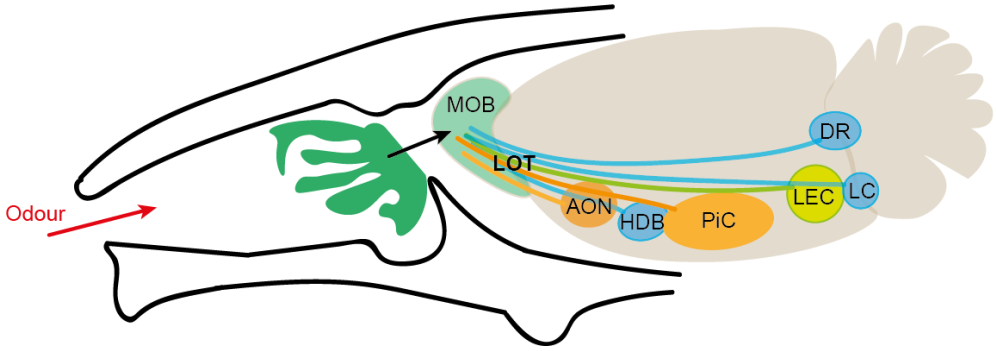

Figure 1.4. Centrifugal input to the olfactory bulb.

Sagital plane diagram of the mouse brain to show main projections coming to the olfactory bulb via the lateral olfactory tract (LOT). These include cortical areas: AON, PiC and LEC, as well as neuromodulatory nuclei (shown in blue), the dorsal raphe (DR), locus coeruleus (LC) and the horizontal limb of the diagonal band of Broca (HDB).

1.3.4. PLASTICITY

There are multiple sources of plasticity within the olfactory bulb circuit (Wilson et al., 2004). First are the more conventional types of plasticity, evidence for which comes from paired slice recordings. MTCs and granule cells within the olfactory bulb both express NMDA receptors.

Input synapses from OSNs to MTCs have been shown to undergo long term potentiation in slice (Ennis et al., 1998), while excitatory synapses onto granule cells (at least some of which come from cortical input) are also strongly potentiating on proximal dendrites, while depressing in more distal dendrites (Gao and Strowbridge, 2009). While this suggests a great toolset for plasticity in olfactory processing, the precise function of this plasticity remains unclear, partly because the function of the interneuron circuits is still a matter of speculation.

Aside from conventional forms of plasticity, the olfactory bulb is unique from other sensory circuits in that in maintains neurogenesis into adulthood, just like the hippocampus (Mouret et al., 2009). This would suggest a selective pressure for a high degree of ongoing flexibility in the olfactory bulb. Neuroblasts are generated in the subventricular zone and migrate into the olfactory bulb circuit via the rostral migratory stream, and here they integrate into the circuit as either granule cells or periglomerular cells (Mizrahi, 2007). The latter have been targeted in two photon patch recordings, which showed that their olfactory responses are refined as they mature and integrate into the circuit (Livneh et al., 2014). Furthermore, even after integration into the circuit, both the spines and dendrites undergo continual remodelling (Mizrahi, 2007). While again, the precise function of this plasticity is not clear, discrimination learning is accompanied by an elevated survival rate of adult-born interneurons, and blocking neurogenesis results in impaired olfactory learning (Moreno et al., 2009).

1.4. Coding of information within the Olfactory bulb

Currently, a large portion of work on the olfactory bulb focuses on which features of olfactory bulb output are reliable indicators of odour features. This is a difficult problem, since many features of olfactory neural activity are good candidates for coding: the spatial map of activity, the intensity of responding, the synchronicity of cell activity, the timing of activity in absolute terms or relative to the sniff cycle, and these features can covary. Moreover, there are a number of different kinds of information to extract from an odour stimulus: the identity, intensity, the

quality or the location, and these can covary (e.g. identity is known to alter intensity perception even when odour concentrations are matched (Wojcik and Sirotin, 2014); while intensity of an odour stimulus scales with the distance to the source (Louis et al., 2008). Thus it is difficult to know if one or a number of activity features are necessary or sufficient for perception of an individual odour feature. What we do know is that many of these features are indeed accessible to perception: using optogenetic activation of a single glomerulus, it was found that mice can perceive identity, intensity and timing of glomerulus activation (Smear et al., 2013). While even more sophisticated experiments using this technique are ongoing in the same lab to elucidate how features of the input may warp perception in trained animals, there is also a wealth of physiological evidence for different coding schema, and here I will focus on such evidence for odour identity, odour intensity and sniff cycle coding.

1.4.1. ODOUR IDENTITY

Rodents are very efficient at discriminating odour identities (Nigrosh et al., 1975). The olfactory bulb receives raw olfactory information from OSNs, with each glomerulus receiving information from OSNs expressing only one type of receptor. As each olfactory receptor (OR) has a certain range of affinities for volatile odourants, and each kind of receptor converges onto two particular glomeruli within the bulb in a fixed pattern (Mombaerts et al., 1996; Vassar et al., 1994), odour stimuli produce a spatial pattern of glomerular activation that has been thought to code for odour identity (Malnic et al., 1999; Rubin and Katz, 1999, 2001; Uchida et al., 2000). The similarity of these evoked patterns of activity by two different odours indeed predicts the difficulty with which an animal learns to distinguish them, and as the sniff progresses, pattern separation occurs within the OB potentially to enable better distinction (Gschwend et al., 2015). Several ‘sister’ MTCs sample from each glomerulus (Shepherd, 2004). MTCs show sustained firing rate changes, both increases and decreases, in response to odour stimuli (Adrian, 1950; Kollo et al., 2014). However, newer hypotheses, taking into account the extremely rapid

olfactory decision times of mice (as low as tens of milliseconds; Abraham et al., 2004, 2010; Resulaj and Rinberg, 2015; Uchida and Mainen, 2003), have shifted focus away from mean firing rates, and instead focus on faster temporal features of neuronal activity (Homma et al., 2009), such as the earliest MTC firing transients within a sniff, referred to as 'Primacy coding' (Cury and Uchida, 2010; Kepple et al., 2016; Wilson et al., 2017), phase coding relative to the sniff cycle (Shusterman et al., 2011), and synchronous firing of neuronal ensembles (Saha et al., 2015). The idea that only the first portion of odour response matters for odour identity coding corresponds with the fact that activation of pyramidals of the piriform cortex relies on coincident input from just a few (less than 5) MTCs (Franks and Isaacson, 2006), and the observation that excitatory odour responses in piriform cortex pyramidal cells occurs within a very short time-window, before intracortical inhibition removes the later activity (Bolding and Franks, 2017).

1.4.2. ODOUR INTENSITY

Though mice are capable of extrapolating odour identity over large (10 fold) concentration ranges (Uchida and Mainen, 2008), they are also capable of distinguishing odour concentrations (Abraham et al., 2004; Shusterman et al., 2011; Wojcik and Sirotin, 2014). The concentration of an odour appears to relate perceptually to the intensity of the odourant, and different odourants have different concentration-intensity functions (Wojcik and Sirotin, 2014). The concentration of the odourant is represented in olfactory activity in various ways (Mainland et al., 2014). At the level of the glomerulus, increasing concentrations increases the level of activity of responsive glomeruli, and incorporates additional glomeruli into the activation pattern, causing a broadening of the activation pattern (Bendahmane et al., 2016; Rubin and Katz, 1999; Spors and Grinvald, 2002) . At the same time, increasing concentrations activate ORNs at increasingly short latencies (Ghatpande and Reisert, 2011; Rospars et al., 2000), giving rise to potential temporal coding of intensity. In the olfactory bulb, firing rate responses to concentration change are a little more complex, with both increases in excitation and inhibition in response to

increasing concentration (Bathellier et al., 2008; Cury and Uchida, 2010; Fukunaga et al., 2012; Meredith, 1986). While more MTCs can become responsive at higher odourant concentrations, the activity of certain interneurons is known to normalise MTC responsiveness according to input strength to a certain degree, presumably such that the dynamic range of neuronal firing activity can represent concentration over such a vast logarithmic scale (Kato et al., 2013; Miyamichi et al., 2013; Roland et al., 2016).

The more ubiquitous feature for intensity coding appears to be temporal features of responding: latency of mitral and tufted cell excitation is progressively reduced as intensity increased (Cang and Isaacson, 2003; Fukunaga et al., 2012; Shusterman et al., 2011). In anaesthetised mice, it was found that mitral cells respond with shorter latency after each sniff as intensity increased, causing a phase advance of firing relative to the sniff cycle, while tufted cells show more stable temporal features (Fukunaga et al., 2012). Together, this gives rise to increase numbers of MTCs responding at the same time as odour intensity is increased, a feature which is enhanced between the olfactory bulb and the piriform cortex (Bolding and Franks, 2017).

1.4.3. THE SNIFF CYCLE

Terrestrial vertebrates continually sample air from the environment through breathing and sniffing behaviour. Thus air, odourised or otherwise, is delivered to the nasal epithelium in discrete packets. As well as transducing odour information, it is now known that ORNs are mechanoceptive (Grosmaitre et al., 2007), and in fact transduce information about pressure change. Thus even in absence of odourant, ORN firing is patterned by the sniff cycle (Ghatpande and Reisert, 2011). ORNs transduce odour information within a restricted temporal window with each inhalation: after the transduction cascade eliciting depolarisation following odourant binding, there are several mechanisms by which the depolarisation is shut off. This means ORN firing can follow odour stimulation at respiration frequencies *in vitro* (Ghatpande and Reisert,

2011), although at higher sniff frequencies this patterning seems to disappear (Verhagen et al., 2007).

Activity in the OB is similarly strongly patterned by the sniff cycle. Each inhalation provides a packet of sensory input from OSNs into the olfactory bulb. During both odour stimulus and during baseline, MTC activity is entrained to the sniff cycle (Adrian, 1950; Cang and Isaacson, 2003; Fukunaga et al., 2012; Macrides and Chorover, 1972; Margrie and Schaefer, 2003). During baseline, it has been found in anaesthetised mice that mitral cells and tufted cells lock to different phases of the cycle - inhalation and exhalation respectively (Fukunaga et al., 2012; Griff et al., 2008b), likely reflecting differing sniff-driven feedforward circuits: mitral cells are thought to be driven by feedforward inhibition, and tufted cells by feedforward excitation (Fukunaga et al., 2012). This patterning completely disappears if the naris is occluded, meaning this baseline sniff coupling is inherited from mechanosensory input from OSNs rather than efference copy of sniffing motor activity (Margrie and Schaefer, 2003). During odour presentation, features of sniff locking can change when compared to baseline, for example the phase of activity can shift relative to the sniff cycle (Fukunaga et al., 2012). Far less is known about the underlying circuit causing changes in theta locking during odour presentation, and how the phasic mechanoceptive and chemoceptive activation of olfactory sensory neurons interacts. Recently it has been shown that the sniff cycle strongly gates sensory input, such that optogenetic activation of OSN input can only evoke increased firing rates in MTCs at particular phases of the sniff cycle (Short et al., 2016). This is both congruent with older studies which show that in absence of sniffing in humans, odours do not evoke a perception at all, even when directly applied to the nasal epithelium (Mainland and Sobel, 2006; Proetz, 1938), and the idea that mechanoception in OSNs gates sensory input (Grosmaitre et al., 2007). While most work on sniff locking has been done in anaesthetised animals, less has been done in awake animals. The data available suggests that while sniff patterning is reduced in prominence (Bhalla and Bower, 1997;

Cazakoff et al., 2014), it still has a profound influence on activity (Fukunaga et al., 2012; Kay and Laurent, 1999).

1.4.4. CONTEXTUAL INFORMATION

There is mounting evidence for the presence of contextual information in the OB. The large majority of this comes from extracellular (EC) recording techniques (unit recordings or LFP/EEG recordings) in awake animals either passively or actively engaging in odour sampling, but more recent evidence comes from imaging studies.

Behavioural state has a profound influence over activity in the OB. Odour firing rate (FR) responses of MTCs in awake animals show a great reduction in overt excitatory components (Rinberg, 2006) and a much greater variance compared to anaesthetised animals (Bhalla and Bower, 1997; Blauvelt et al., 2013; Kollo et al., 2014), perhaps eluding to the increased engagement of inhibitory networks in the awake state - a conclusion that would be supported physiologically (Blauvelt et al., 2013; Cazakoff et al., 2014; Kato et al., 2012).

Further evidence comes from experiments employing behaving animals in an attempt to reveal the correlates of specific kinds of contextual information in MTC activity. Unit recordings have appeared to demonstrate MTC responses to non-olfactory task events and behavioural events, i.e. the light stimulus predicting an upcoming odour, and mouse nose-poke behaviour (Kay and Laurent, 1999; Rinberg, 2006). Similar recordings in trained rats showed that presumptive MTC firing rate (FR) responses to odours were modulated by the hunger state of the animal, with responses to food odours being selectively enhanced relative to non-food odours (Pager, 1974). MTC FR responses also appear to be modulated by non-food odours associated with rewards: responses to the rewarded odours tend to increase during learning of a go/no-go task, while responses to the unrewarded odours tend to decrease (Doucette and Restrepo, 2008; Doucette et al., 2011), while a similar effect is seen on the percentage of synchronous action potentials in the MTC population during the odour period (Doucette et al., 2011). In addition to reward

information, information about punishment is also documented in the OB: imaging glomerular inputs to the OB shows a long-lasting amplification during learning of inputs specifically for odours associated with foot-shock (Kass et al., 2013), possibly mediated by altered GABAergic feedback from JGCs onto ORNs.

Facilitation of the transmission of important information according to context is additionally suggested by studies showing evidence for activity in the OB in the absence of odours. EEG recordings from the rabbit OB surface shows that the spatial pattern of gamma oscillations in the control state reflects that evoked by an expected salient odourant, e.g. one that predicts a footshock (Freeman and Schneider, 1982), or a reward (Di Prisco and Freeman, 1985).This gave rise to the idea of an olfactory 'search image' in the OB. However, while evidence may suggest that gamma oscillations represent the interplay between MTCs and inhibitory INs (Lepousez and Lledo, 2013; Schoppa, 2006; Fukunaga et al., 2014), the underlying cause of these EEG-recorded oscillations was not investigated. Mapping of immediate early genes similarly suggests that the pattern of activity in the OB not only represents physically present odours, but may also represent odours that the animal expects to be present (Mandairon et al., 2014).

Context-dependent information could also have utility in optimising IN networks for processing according to the behavioural demands placed upon an animal. Unit recordings provide some evidence that the activity of the inhibitory network may change according to the task engagement: the proportion of inhibitory responses to odours increases when the animal is actively discriminating between odours, as opposed to when passively exposed to them (Fuentes et al., 2008). Recent imaging data from MTCs during both simple and difficult discrimination learning suggests that odour responses change across learning in different ways according to task type, with detectability being amplified when the odours are very different, and discriminability being increased when the odours are highly similar (Chu et al., 2016; Yamada et al., 2017). LFP recordings additionally show that oscillatory activity in the OB evolves during

learning of olfactory tasks (Kay and Beshel, 2010; Martin et al., 2006; Ravel et al., 2003), in a way that depends on the specific task that is being learned - for example go/no-go (GNG) versus two alternative force choice (2AFC) (Beshel et al., 2007).

Thus, there is abundant evidence for many different kinds of contextual modulation of OB activity.

1.5. MECHANISMS OF CONTEXT DEPENDENT PROCESSING IN THE OB

While EC recordings provide evidence that there are correlates of contextual information in MTC activity, they are not suited to definitively pinpoint the mechanisms giving rise to such observations: EC recording makes cell type identification challenging, is likely to impose a significant bias in sampling from very active cells only (Kollo et al., 2014; Margrie et al., 2003; Shoham et al., 2006), and sub-threshold responses (such as synaptic inputs and membrane excitability) are not seen. LFP and EEG recordings are even more ambiguous, with no evidence supplied as to the likely complex underlying causes of the signal (i.e. which cells are responsible, and how cell activity might translate into LFP activity).

As briefly introduced earlier (Fig. 1.1), there are two broad, non-mutually-exclusive mechanisms that could underlie contextual representations in early sensory circuits: 1) transmission of contextual information to the circuit through top-down projections from higher centres; 2) context-dependent control of the active sampling process, altering the bottom-up transmission of sensory input.

1.5.1. TOP DOWN MECHANISM: CENTRIFUGAL AFFERENTS

In sensory cortices of other modalities, the activation of top-down afferents has already been noted during particular contexts. For example in the barrel cortex, cholinergic afferents are known to become active and alter network state in profound ways during spontaneous whisking behaviour (Eggermann et al., 2014). In the olfactory bulb, however, only a very limited number

of papers have attempted to link the presence of contextual information to the activity of centrifugal afferents, and in the few cases that exist this was done via pharmacological blockade. Spatial patterns of gamma oscillation reflecting expected reinforced odourants did not arise when noradrenaline action was pharmacologically blocked in the OB (Gray et al., 1986), while the divergence in synchronous spike train activity in response to rewarded and unrewarded odours also appeared to be dependent on the action of noradrenaline in the OB (Doucette et al., 2011).

While direct evidence is entirely lacking, there is much evidence that top down projections could in principal supply cognitively-driven contextual information to the OB circuit. This is primarily due to their sheer abundance, and the observation that most areas projecting to the OB are known to encode contextual information. In the locus coeruleus, noradrenergic cells fire at various times during olfactory tasks, e.g. in response to rewards (Bouret and Sara, 2004). These cells fire homogenously and a large proportion of them project to the OB (Shipley and Adamek, 1984). Activity in cholinergic cells of the HDB is thought to relate to behavioural variables such as attention (D'Souza and Vijayaraghavan, 2014), while serotonergic neurons of the raphe nuclei have been implicated in gating information flow and sensorimotor coordination (Jacobs and Fornal, 1993; Petzold et al., 2009). Meanwhile there is evidence in the behaving rat that piriform cortex pyramidal cell odour responses are modulated by the reward value associated with an odour (Schoenbaum and Eichenbaum, 1995; Zinyuk et al., 2001) and whether the odour presentation was predictable or not (Schoenbaum and Eichenbaum, 1995). However it is unclear whether this information is internally generated within the cortex or inherited from the OB itself, since all of these areas receive OB input directly.

Given the evidence, top-down modulation of the OB network during ongoing behaviour is highly plausible candidate for contextual modulation of OB activity.

1.5.2. BOTTOM-UP MECHANISM: CONTEXTUAL MODULATION OF SNIFFING BEHAVIOUR

As most studies into contextual modulation of OB were carried out in freely moving mice, they lack fine temporal monitoring or control over behavioural state and odour stimuli, making it difficult to distinguish the underlying causes of the physiological observations. Critically, most of these studies did not record sniffing behaviour, making it impossible to interpret the results in the framework of active sampling. In only very few cases can this possibility be somewhat excluded, for example in a recent study where the mouse was under anaesthesia for the imaging process, with aversive conditioning taking place between the two imaging epochs (Kass et al., 2013).

Contextual modulation of sensory input patterns is highly likely since sniffing behaviour is orchestrated in a highly complex and context-dependent way. Rodents increase inhalation frequency when presented with novel odourants (Verhagen et al., 2007; Welker, 1964; Wesson et al., 2008a), in anticipation of reward (Clarke, 1971; Ikemoto and Panksepp, 1994; Kepecs et al., 2007; Wesson et al., 2008a), during behavioural events such as locomotion (Bramble and Carrier, 1983), in response to surprising non-olfactory stimuli (Wesson et al., 2008a), and finally during stimulus sampling in olfactory tasks (Cury and Uchida, 2010; Kepecs et al., 2007; Macrides et al., 1982; Rajan et al., 2006; Uchida and Mainen, 2003; Youngentob et al., 1987). This latter rapid sniff behaviour can emerge over the course of learning a simple olfactory discrimination task, and is highly variable between experimental animals (Wesson et al., 2009). As such, it is likely that such sniffing strategy is not crucial for odour identification (Cenier et al., 2013), but may aid it in a some respect (e.g. increased reliability, or faster acquisition of the information).

As discussed above, the sniff cycle profoundly patterns activity in the OB. Less is known about how changes in sniff pattern affect OB activity, since most work is done in anaesthetised animals. Using double-tracheotomy to control air flow through the nares in anaesthetised rodents, it has been demonstrated that the later phase of glomerular activity is dampened during fast sniffing,

perhaps owing to adaptation mechanisms intrinsic to OSNs (Verhagen et al., 2007). One notable study found that the much more irregular temporal dynamics of MTC activity seen in passive awake compared to anaesthetised animals could in fact be predicted well by external sniff measurements (Blauvelt et al., 2013), and another study showed that sniffing frequency may even have a profound impact on the state of the OB network, for example by altering the activity of inhibitory interneurons in the bulb (Kato et al., 2012).

Given that sniffing has a profound role in patterning OB activity, it seems plausible that contextual changes in sniffing may have a role to play in contextual modulation of activity, yet such modulations have never been interpreted in the framework of sniffing.

CONCLUSION

Overall, while there is abundant descriptive evidence for context dependent changes in OB cell responses, it is unclear whether OB processing itself has been altered, and if so, exactly how it has been altered. It is unclear whether the pattern of OSN input is changing, or whether centrifugal afferences are altering the circuit properties. Both bottom-up and top-down mechanisms seem highly plausible according to the available evidence. Thus the mechanisms of context dependent processing in the OB at this point are left largely to speculation.

1.6. AIMS

The key purpose of this project was to analyse the mechanisms and consequences of context dependent processing in the OB. Specifically, the following aims and questions were addressed:

A. Define the nature of context-dependent modulation in the responses of identified neurons

- How does cellular physiology differ between behavioural states?
- How do OB representations of odour change during simple odour discrimination learning?

- How could these changes facilitate behaviour?

2. Determine the mechanisms responsible for mediating contextual changes in processing

- What is the relative contribution of sniffing (odour sampling) behaviour compared to other sources of modulation (e.g. top-down input) in causing response changes?
- What is the relative contribution of feed-forward and feedback mechanisms for response changes modulated by active sampling state?

3. Investigate how contextual changes in response can inform us about the nature of odour coding in the olfactory bulb.

- Since perception of certain odour features should remain stable across contexts, what features of odour response are subject to change, and which are stable across states?

1.7. APPROACH

Whole cell recordings were employed in the OB of head-fixed mice in various behavioural scenarios. These were made according to blind patching procedures described previously (Fukunaga et al., 2012; Kollo et al., 2014; Margrie and Schaefer, 2003). These intracellular recordings allow observation of sub-threshold and supra-threshold changes in a cell's response. This is important for elucidating circuit mechanisms, as it allows direct observation of the membrane potential of a neuron, including synaptic inputs and changes in membrane state that may prime the neuron according to the context. In addition, the blind-patching procedure used to establish recordings prevents bias in cell selection that can arise from unit recordings which are often guided by baseline cell activity, giving rise to oversampling from highly active cells which are not in fact very common (Margrie et al., 2002; Kollo et al., 2014; Shoham et al., 2006). Finally, whole cell recording allows identification of the cell type being recorded from, either electrophysiologically or via dialysis with anatomical markers. With regard to the olfactory bulb, previous whole cell recordings *in vivo* in conjunction with recovery of cell morphology has revealed that the spike after-hyperpolarisation waveform provides a reliable way to discern between interneuron and principal cell (Kollo et al., 2014), while patterning of subthreshold membrane potential by the sniff cycle can provide information about tufted cell and mitral cell phenotype in anaesthetised mice (Fukunaga et al. 2012). Whether the latter can also be used in the awake state is currently untested.

Mice recorded from here were either passively exposed to odours, performing or learning olfactory tasks, or in rare cases anaesthetised during the whole cell recording. The head-fixed nature of behavioural tasks allows greater control over stimuli, something which is extremely important for olfaction given the dynamic nature of odour plumes in air. It also provides greater control over behavioural state, with very rapid learning of tasks previously described in head-fixed mice (Guo et al., 2014), and allows precise measurement of sniffing patterns via pressure

or flow sensors placed externally at the nostril contralateral to the side of recording – something which is crucial for explaining variability in cellular activity (Kato et al., 2012), and allows interpretation of contextual changes in terms of changes in active sampling.

Throughout the course of this dissertation, WC recordings took place in six different cohorts of mice:

a) Learning mice: mice learning to perform a simple olfactory discrimination task: the olfactory go-no-go task, in which one odour predicts a reward, and the animal must respond to it to receive the reward, while the other odour is unrewarding, and the animal must inhibit responding.

b) Passive mice: these mice were exposed to the same odour stimuli over the same timescale of recording, but no task was performed. This allows assessment of the specificity of response changes observed to the learning condition.

c) Task engagement versus disengagement: these behaving mice are engaged in successful performance of the go/no-go task, having learned the task prior to recording. After a given number of trials, the task is disengaged (the reward spout removed), such that the animal can no longer perform the task and is effectively now passively exposed. The task can then be re-engaged to recommence behaviour. This allows assessment of dynamic changes in behavioural state on response changes.

d) Passive mice exposed randomly on a small number of trials to an unexpected tactile stimulus to induce fast sniffing during the odour stimulus. This allows assessment of sniff frequency on odour response in absence of learning.

e) Double-tracheotomised anaesthetised mice: in these anaesthetised mice, breathing is de-coupled from sniffing through the nostrils, airflow can be controlled experimentally

through the nostrils, and thus sniff frequency can be varied to determine its impact on odour responses in absence of top-down input.

f) Passive mice exposed to both high and low concentration stimuli, alongside unexpected tactile stimuli to evoke fast sniffing. This allowed analysis of the stability of odour intensity perception and responses in the face of changing sniff cycles.

Whole cell recordings, while providing the best measure of single cellular activity, come with issues of throughput and stability. The following chapter will address how these were optimised alongside behavioural procedures to allow recording from single cells over the full time-course of learning.

CHAPTER 2.

GENERAL METHODS

For all chapters, behavioural and recording procedures were undertaken as outlined here in general methods. The 'chapter methods' sections within each results chapter outline specific analytical methods used to calculate the results in the chapter, or specific experimental methods which are used only in that chapter.

All animal procedures were performed in accordance with the guidelines of the UK Home Office under the Animals (Scientific Procedures) Act 1986, and approved by the local ethics panel of the National Institute for Medical Research and the Francis Crick Institute. All mice were male and from wild type lines (C57BL/6 Jax from Jackson Laboratories), aged 5 to 10 weeks old. All reagents (including odourants) were obtained from Sigma-Aldrich unless otherwise stated.

2.1. SURGERY

Strict sterile practice was maintained for all surgical procedures. Mice were anaesthetised either with ketamine and xylazine intraperitoneally (100 and 20 mg/kg body weight respectively), or with isoflurane mixed in medical oxygen (5% for induction, 1.5-3% for maintenance) and given meloxicam (2.5 mg/kg) or carprofen (5mg/kg) subcutaneously. Local analgesia around the site of incision was also used (0.5% mepivicaine or levobupivicaine). An incision was made dorsally above the skull, and the bone cleaned and dried. The surface layer of the skull plates was removed using a dental drill (EXL-40, Osada - Los Angeles, USA). In preparation for whole cell recordings, the flexible joints between the intraparietal and parietal skull plates were fortified: a blunt metal rod was lowered 1 mm anterior to lambda, until additional force applied to the parietal plates does not visibly cause deflection between plates. Thin layers of tissue adhesive (Histoacryl - Michigan USA) were then applied to the sutures until no flexibility between skull plates remained. This step ensures that animal locomotive movement did not translate to movement of the brain relative to the skull. Tissue adhesive was then applied to the base of a custom-made stainless steel or PEEK head-plate, and this was adhered to the surface of the parietal and intraparietal plates. The join to the skull at the base of the head-plate was then

reinforced with dental cement (Simplex Rapid, Kemdent - Swindon, UK). For whole cell recordings, a recording chamber was additionally implanted over the OB: the surface of the overlying skull was similarly roughened, and a 5 mm diameter plastic ring (custom sculpted from a Pasteur pipette) was adhered with tissue adhesive. The recording chamber was built up and attached to the head-plate using dental cement, then filled with silicone (Qwik-Cast Sealant, World Precision Instruments – Florida, USA) and sealed with a thin layer of dental cement, before the incision was closed with tissue adhesive. Animals were monitored during recovery from anaesthesia and allowed at least 48 hours to recover in their home cage, with wet-food supplied.

2.2. HEAD-FIXED BEHAVIOUR

For animals going on to discrimination learning, prior head-plated animals began water deprivation on day two post-surgery. On day three, mice were handled and supplied 0.5ml of diluted sweetened condensed milk (approximately 2% v/v, Farmlea – SHS, Gloucester, UK) by hand from a Pasteur pipette. On all days thereafter, it was ensured that mice consumed at least 1ml of water, and maintained weight above 80% of their original weight, adjusted according the weight of littermate control mice with free water access.

2.2.1. HABITUATION TO HEAD-FIXATION

On day four, mice were briefly anaesthetised with isoflurane and head-fixed above a custom-made treadmill. In this training session, mice simply learned to lick at a spout for 15 µl diluted sweetened condensed milk rewards, while habituating to the head-fixed state. Licks were detected via the crossing of an infrared beam close to the reward spout.

2.2.2. ONE-ODOUR OPERANT CONDITIONING

On day five, the animal learned to lick in response to an odour CS+ via delay classical conditioning. A CS+ of almond oil (AL) was introduced. The odour was signalled by an LED that

turns on 2.5 s prior to odour onset, and remained on until odour offset. In the 1 s period post-odour, the animal had the opportunity to lick the spout (at least once) in order to trigger a reward. At the beginning of the session, delayed 15 µl rewards were automatically presented 500 ms after the odour if the animal failed to lick. If the animal licked prior to this, a larger reward of 30 µl was instantaneously received. Once this had occurred at least 10 times, rewards were made contingent only upon licking, with no automatic rewards received further. Criterion was achieved when the animal responded correctly for at least 80% of trials for two consecutive blocks of 10 trials.

2.2.3. TWO-ODOUR DISCRIMINATION LEARNING

On day six, the CS- of peppermint oil was introduced. There was a 50:50 pseudorandom sequence of CS+ and CS-. If animals licked in the response period following a CS+, a 15 µl reward was received. If they licked in the response period following the CS-, a punishment of a 4 s extension to the ITI was triggered. Criterion was achieved when the animal responded correctly for at least 80% of trials for two consecutive blocks.

2.2.4. SECOND PAIR DISCRIMINATION LEARNING

On day seven, learning to discriminate a second novel pair of odours would occur. WC recordings would be obtained before the start of each learning epoch in animals implanted with recording chambers. After ensuring the animal had retained performance on pair 1 discrimination, the animal was introduced to a second, novel pair of odour stimuli, and had to learn to discriminate between the two as for the first odour pair. The first block usually had more than five CS+ presentations to initially encourage licking to the CS+, before the CS- was introduced. Once criterion was met for the learning of the second pair discrimination (and /or the WC recording came to an end), a third novel odour pair would be presented, and the process repeated.

2.3. PASSIVE EXPOSURE

For mice undergoing passive exposure to odour stimuli, 2 days post-surgery the mouse would have one session of 'head-fix habituation'. This would consist of a 20 minute session simply head-fixed with no rewards or stimuli, until the mouse learned how to sit comfortably and run on the treadmill. This session was required to reduce disruptive behaviour on the subsequent day of recording.

2.4. ODOURANT DELIVERY

Odourants were delivered using a custom built olfactometer consisting of 8 different odour channels connecting two manifolds, a clean air channel, and a final dilution channel carrying clean air (Fig. 2.1). Air was carbon-filtered and pressure-controlled at 1mbar with a pressure regulator (IR 1000, SMC Pneumatics - California, USA). In the control state, the odour channels are closed via two way valves (4W1-LW, Asco Valves – New York, USA), and air through the manifolds is diverted to waste via the final four way valve (0W3-AR, Asco Valves – New York, USA), while the clean air channel is directed to the mouse via the final valve (Fig. 2.1A). When an odour is given, 3 s prior to odour onset, the odour pulse is prepared: the selected odour channel opens and air through the manifold is directed through the odour bottle with a computer-controlled flow waveform (Q, Fig. 2.1B). 3 s later resulting odourised air is diverted to the mouse via the 4 way valve, while clean air is diverted to waste. The final dilution channel mixes clean air into the final air stream reaching the animal at all times. Flow was controlled at various points using flow regulators (Key Instruments – Pennsylvania, USA) so that the channel supplying the mouse provided a constant flow of 2000 sccm/N_2 at all times, meaning that no tactile stimulus accompanied odour pulses. Each odour or odour mixture was calibrated to form an approximate 2 s square pulse of 1% saturated vapour pressure (e.g. Fig. 2.2B) using a mini photo ionisation detector (miniPID, Aurora Scientific) and custom written calibration programs

in LabView which optimise the flow waveform through the manifolds during odour preparation and odour pulse.

Odour stimuli for the first pair consisted of almond oil and peppermint oil. Second and third pair odour stimuli were randomly selected from a set of 4 odour mixtures made up from three to six monomolecular components, selected for their ability to activate dorsal OB glomeruli (Takahashi et al., 2004; Fig. 2.2A). The components of each mixture were grouped according to similarity of vapour pressure, and added in ratios weighted according to their vapour pressure such that the contribution of each component to the overall vapour pressure would be roughly equal.

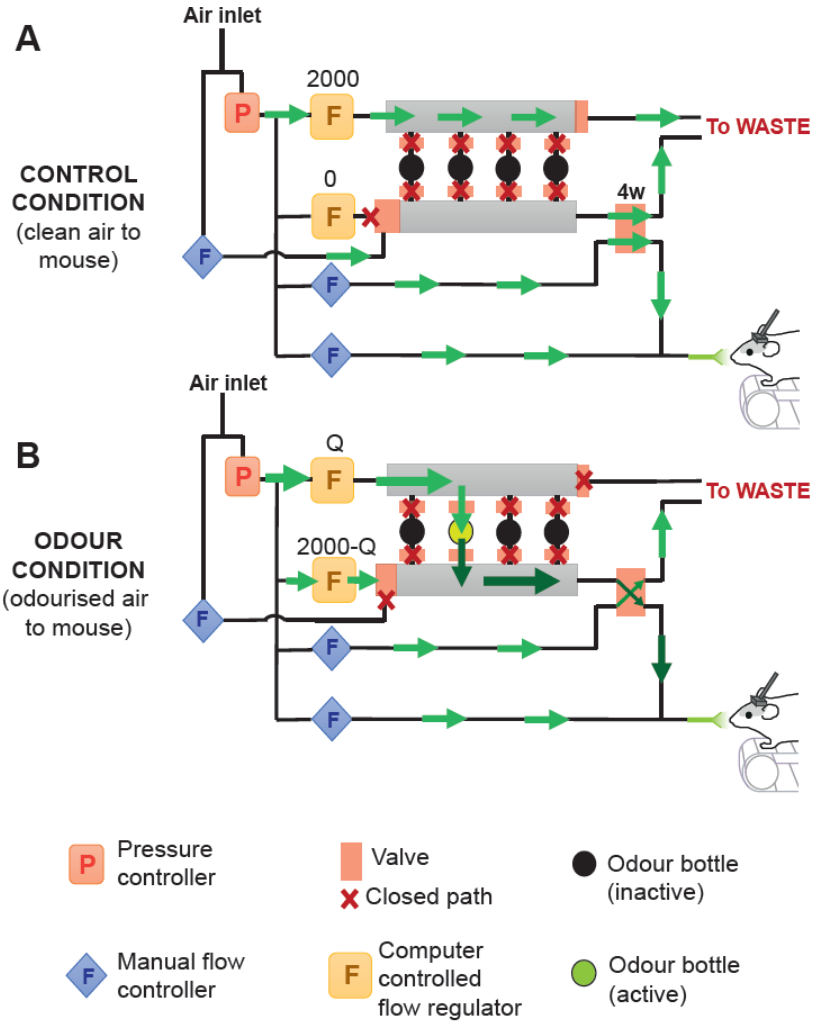

Figure 2.1. Olfactometer.

(**A**) The olfactometer in the control state, when mouse is receiving clean air between odours. Arrows indicate direction of air flow, red crosses indicate channels closed off via valves, and numbers near flow meters indicate flow in sccm/N_2. An in-house air supply provided the source of air at the inlet to the system, which was then carbon filtered. Key for symbols is at bottom of figure. '4w' indicates 4 way (final) valve. Flow Q is a computer controlled waveform and calibrated for delivery of a 2s 1% square pulse. (**B**) Olfactometer in the odour pulse state, when mouse is receiving odourised air. Dark green arrows indicate odourised air, light green arrows indicate clean air.

A

	Odor	Vapor pressure (mmHg)	% vol
Mixture 1	methyl salicylate	0.034	15
	eugenol	0.022	23
	cinnamaldehyde	0.029	18
	creosol	0.024	22
	1-nonanol	0.023	22
Mixture 2	1-heptanol	0.22	25
	0-ethylphenol	0.15	35
	acetophenone	0.37	14
	ethyl heptanoate	0.2	26
Mixture 3	guaiacol	0.11	24
	valeric acid	0.2	14
	(+)-carvone	0.16	17
	2-phenyl ethanol	0.09	32
	4-allyanisole	0.21	13
Mixture 4	α-terpinene	1.66	20
	butyric acid	1.65	19
	limonene	1.55	21
	benzaldehyd	1.5	21
	eucalyptol	1.65	19

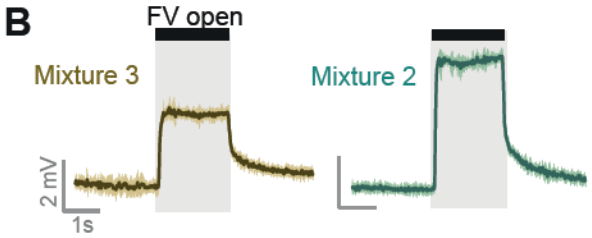

Figure 2.2. Odour mixture components

(**A**) Each table shows the components added to each of the four mixtures. The components were added in proportion to their relative vapor pressure, such that higher vapor pressure components were added in lesser volume. This was done in attempt to keep the relative contribution of each component fairly similar in the olfactory headspace, though the possibility of interactions between chemicals within the mixture cannot be excluded. (**B**) Average odour square pulse waveforms recorded by the miniPID over 9 pulses for mixture 3 and mixture 4. Shaded areas indicate standard deviation.

2.5. ELECTROPHYSIOLOGY

2.5.1. CRANIOTOMY

Animals were anaesthetised with isoflurane (1.5-3% in medical oxygen) and given carprofen (subcutaneous, 5 mg/kg). The recording chamber was re-opened and filled with external recording solution (in mM: 135 NaCl, 5.4 KCl, 5 Hepes, 1 $MgCl_2$, 1.8 $CaCl_2$), and a 1-2 mm craniotomy was made over the OB. A careful durectomy was then performed, before application of approximately 30-40 °C low-melting point agar (4-5% w/v in external recording solution), solidifying at 0.5-2 mm thickness over the OB. External recording solution then filled the chamber. The animal was then head-fixed at the treadmill and allowed to recover from anaesthesia for at least 20 minutes before engagement in the olfactory task. Criterion (80% correct) or above performance in discrimination of the first odour pair was confirmed before recordings took place.

2.5.2. WHOLE CELL RECORDINGS

Recordings in awake mice were performed as previously described (Fukunaga et al., 2014; Kollo et al., 2014; Margrie et al., 2003). In brief, 5-6 MΩ micropipettes were pulled using a P-1000 micropipette puller (Sutter Instrument Company – Novato, USA) from borosilicate glass (2mm diameter, 0.5 mm wall thickness Hilgenberg – Malsfeld, Germany). These were back-filled with intracellular solution (in mM: 130 K-$MeSO_4$, 10 Hepes, 7 KCl, 2 ATP-Na, 2 ATP-Mg, 0.5 GTP, 0.05 EGTA, and pH adjusted to 7.4 with KOH, osmolarity: 280 mOsm). Signals were amplified and filtered at 30 kHz by an Axoclamp 2B (Molecular Devices – West Berkshire, UK) and digitized at 20 kHz with a micro 1401 (Cambridge Electronic Design –Cambridge, UK). In voltage clamp, a 10 Hz, 10ms long step of 30-40 mV was applied, and the resistance across the micropipette tip monitored via the current trace on an oscilloscope (HM1007, Hameg – Mainhausen, Germany). High pressure (>1000 mbar) was applied to the micropipette as it was descended through the agar layer and 180 µm into the OB, where the pressure reduced to 9-12 mbar. The micropipette

was then advanced in 2 µm steps until a large sudden reduction in pipette resistance, and an oscillatory waveform was observed (indicating proximity to a cell), and the pressure was abruptly removed. Once a gigaohm seal was formed, WC configuration was obtained by gentle suction pulses. Cell type identification was largely based on electrophysiological properties (see later).

2.5.3. RECOVERY OF CELL MORPHOLOGY

Morphologies of a subset of recorded cells were acquired as previously described (Kollo et al. 2014; Fukunaga et al., 2012). Recordings were made with intracellular solution including 10 mM biocytin. Mice were perfused following recordings with cold phosphate-buffered saline, followed by 4% (wt/vol) paraformaldehyde solution in phosphate-buffered saline. Fixed olfactory bulbs were embedded in porcine gelatin (10% wt/vol), before being fixed overnight in 4% paraformaldehyde. The OBs were then cut into 150 µm slices with a vibratome (Microm, Idaho, USA) and stained with avidin-biotinylated peroxidase (ABC kit, Vector Labs, California, USA) and the DAB reaction. Biocytin stained cells were traced using a Neurolucida system (Micro Bright Field, Vermont, USA). Principal cells were identified via soma size, cell body location with respect to the mitral cell layer, an apical dendrite reaching the glomerular layer and lateral dendrites branching in the external plexiform layer, while mitral and tufted cells were largely distinguished by proximity of the soma with respect to the MCL.

2.5.4. SNIFF MEASUREMENT

Sniffing behaviour was recorded either with a pressure sensor or flow sensor (Sensortechnics, Berlin, Germany), externally located in close proximity to the left naris (contralateral to recording side). The precise orientation relative to the nostril was manually optimised prior to each recording in order to acquire the full sniff waveform in spite of any movement of the naris. The signal was amplified by a custom-made amplifier and digitised at 1000 Hz with a micro 1401.

2.6. DATA ANALYSIS

All data was pre-processed using custom-written scripts in Spike2 (version 7.10, Cambridge Electronic Design – Cambridge, UK) and analysed using custom-written functions in MatLab 2014b (MathWorks - Massachusetts, USA).

Note that for every odour response trace in this dissertation, responses were aligned to the onset of the first inhalation after odour stimulus onset.

2.6.1. PRINCIPAL CELL IDENTIFICATION

Mitral and tufted cells were distinguished from interneurons as previously (Kollo et al. 2014). The current data set was pooled with the much larger data set of neurons recorded in the OB of awake mice acquired previously, and independent component analysis was performed on the AHP waveform (2 to 25 ms from spike onset) to reveal three independent components, upon which hierarchical cluster analysis was used to band the cells into two groups, 'principal' and 'other'. Based on cell morphologies from the previous data set, and an additional 12 acquired in the current data set, 100% of the 20 morphologies obtained from the 'principal' group were confirmed as MTCs, while 86% of the 13 morphologies from the 'other' group were confirmed interneurons.

2.6.2. SPIKE SUBTRACTION

To analyse subthreshold responses in absence of spiking activity, spikes and their AHPs were subtracted from the trace. This was done by first using the 'wavemark' tool in Spike2 to detect spikes by thresholding and matching them to a generated spike waveform template. The length of this spike waveform template was manually adjusted for each cell according to its AHP length, but was usually around -4 ms to 30 ms post spike peak. A trace was then generated with all detected spike waveforms, and this was subtracted from the original voltage trace (Fig 3.3).

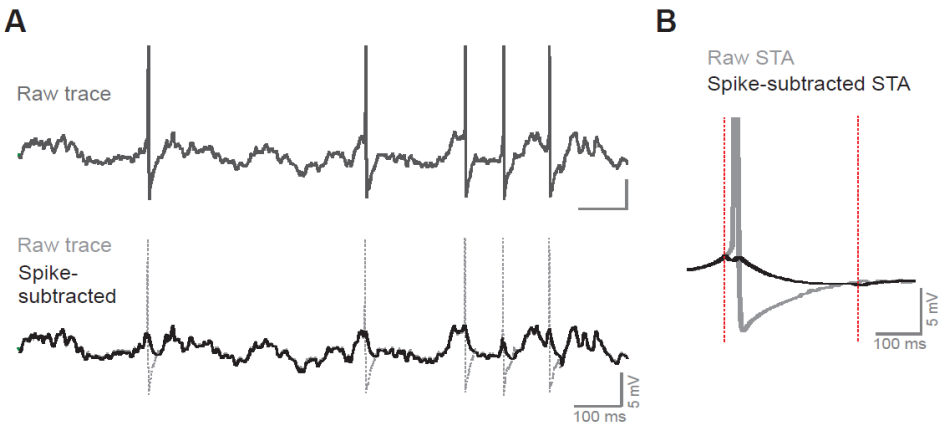

Figure 2.3. Spike subtraction.

(**A**) Top: example raw membrane potential trace prior to spike subtraction. Below: black trace shows membrane potential after spike subtraction. Grey dotted trace shows raw trace for comparison. Spikes are clipped for display (**B**) Spike-peak-triggered average of membrane potential traces both prior to spike subtraction (grey) and after spike subtraction (black).

2.6.3. STATISTICS

In all cases, 5-95% confidence intervals were used to determine significance unless otherwise stated. In all figures, a single asterisk denotes $p<0.05$, double asterisk denoted $p<0.01$ and a triple asterisk denotes $p<0.001$. Means and error bars showing a single standard deviation either side are used in all cases for normally distributed data of equal variance. Two-sided Student's t-tests were used for comparison of means and Bartlett tests used to compare variances, unless otherwise stated. Boxplots are used to represent any other data (data comparisons of unequal variance, or non-normally distributed data), where median is plotted as a line within a box formed from 25th (q1) and 75th (q3) percentile. Points are drawn as outliers if they are larger than q3 + 1.5 x (q3 - q1) or smaller than q1 – 1.5(q3 - q1). For such data, Ranksum tests were used to compare the medians, and Browne-Forsythe tests used to compare variance, unless otherwise stated. To determine points of significant difference between cumulative histograms, a bootstrapping method was used. Firstly, data underlying the two histograms would be shuffled between datasets, and cumulative histograms would be calculated from these shuffled sets. The

difference at each point between the two histograms would then be calculated. This was repeated 10,000 times, and the differences between the real cumulative histograms would then be compared to the shuffled distribution at each point. An arrow was drawn on the points at which the actual difference exceeded the 99th percentile of the shuffled distribution.

2.6.4. DECISION AND REACTION TIME CALCULATION

Decision and reaction time calculations were based on 10 or more trials of 80% correct responses or higher. **From lick behaviour:** For each CS+ and CS-, lick probability was calculated in a moving time window of 100 ms, aligned to the first inhalation after final valve opening. The difference between the probability of licking for CS+ and CS- for each time window was calculated, and the leading edge of the first window at which this calculated difference significantly deviated from the values calculated from the 2 s window prior to odour onset was considered the reaction time. **From sniff behaviour**: inhalation and exhalation duration values were calculated for CS+ and CS- as a function of sniff number from odour onset. These values were compared between those calculated for CS+ and CS- using a t-test, and the decision time was calculated based on the first inhalation or exhalation within the series to show a significant difference. For 12/21 mice there was a significant difference between CS+ and CS- sniffing.

2.6.5. ODOUR RESPONSES

For firing rate (FR) responses, for each trial spikes were calculated in 250ms time-bins aligned to the first inhalation post odour onset. The values were quadrupled to estimate FR. These time bins were then normalised to the average value for time bins within the 4 seconds prior to odour onset to get FR response values. These values were then averaged across all trials for the full 2 s of the stimulus to get a mean and standard deviation of FR response. To determine significance of response a paired t-test was used to compare the mean FR value within the 2 s prior to stimulus onset, and the mean value within the odour stimulus for each trial. Responses with a p value <0.05 were considered significant.

Responses were analysed very similarly for V_m. These were calculated from spike-subtracted traces as outlined in general methods, and time bins were 10 ms instead of 250 ms.

2.7. Optimisation of experimental techniques

Whole cell recordings *in vivo* provide an excellent method to mechanistically investigate circuit function: they provide an unbiased sample of the neuronal population, since cell-selection is blind, and they provide a high resolution description of both the subthreshold membrane potential and spiking activity of the cell, allowing both neuronal input and output to be quantified. Their key limitations lie in stability. The recording only lasts as long as the pipette tip is adhered in a high resistance gigaohm seal to the cell membrane, and small mechanical disturbances can disrupt this seal. While this is not such a problem for *in vitro* preparations or even anaesthetised animals, this becomes particularly problematic in the awake animal, where, due to animal movement, recordings are typically of limited duration and quality compared to more stable settings. For example, previous whole cell recordings in the OB of the passive awake animal lasted only 0.5-35 minutes, with a median of 11.34 minutes (Kollo et al., 2014). This can result in experimental design issues. For example, task acquisition must be very rapid if you want to study the effects of learning across the timescale of a single recording. Additionally, unlike unit recordings, you can usually only record from one cell at a time, making throughput limited. Thus, the probability of recording from an odour-responsive cell must be high to increase throughput. Overall, optimisation needed to occur to a) increase recording stability in awake mice, b) reduce the acquisition time for olfactory behaviour, and c) increase the throughput of the technique by increasing the incidence of olfactory response in the OB.

2.7.1. Stable whole cell recordings in awake mice

The following experiments (results chapters 3 to 5) describe results obtained from 60 recordings from principal cells in awake mice. For principal cell identification analysis (Fig. 2.4A-C), my data was pooled with data from Kollo et al. (2014). Principal cells were identified from interneurons

based on independent component analysis and hierarchical cluster analysis of the spike after hyperpolarisation (AHP) waveform (see general methods for details; Kollo et al., 2014), and for a small number of cells, recovered morphologies were used to confirm this. This allowed identification of mitral and tufted cells with a 0% false positive rate (20/20 recovered morphologies were MTC; 9 from my own data, 11 from Kollo et al. 2014), however, due to a high threshold for inclusion in the MTC group, some recovered MTCs were identified as INs in the cluster analysis, such that identification of INs occurred with a 18% false positive rate (2/11). Since only MTC data has been analysed in the following sections, this is not an issue.

Over the course of months, head-plate surgery and craniotomy procedures were optimised for minimal brain movement. Critical steps included fusing of the intraparietal skull plate to the parietal skull plates with extensive tissue glue, and addition of 1-2 mm 4% agar to the surface of the craniotomy prior to every electrode descent. Additionally, each mouse was subjected to head-fixation habituation sessions on the day prior to recording such that animal movement was minimised on the day of recording. After such measures were routinely implemented, recordings typically lasted 14±4 mins (Fig. 2.4Di), with an access resistance of 36±19 MΩ (Fig. 2.4Dii). Corrected for drift using spike thresholds, baseline membrane potential changed on average by only 0.9±1 mV over the course of the recording (Fig. 2.4Diii). The junction potential was measured at 8 mV, and all absolute potentials have been corrected using this value in all subsequent sections.

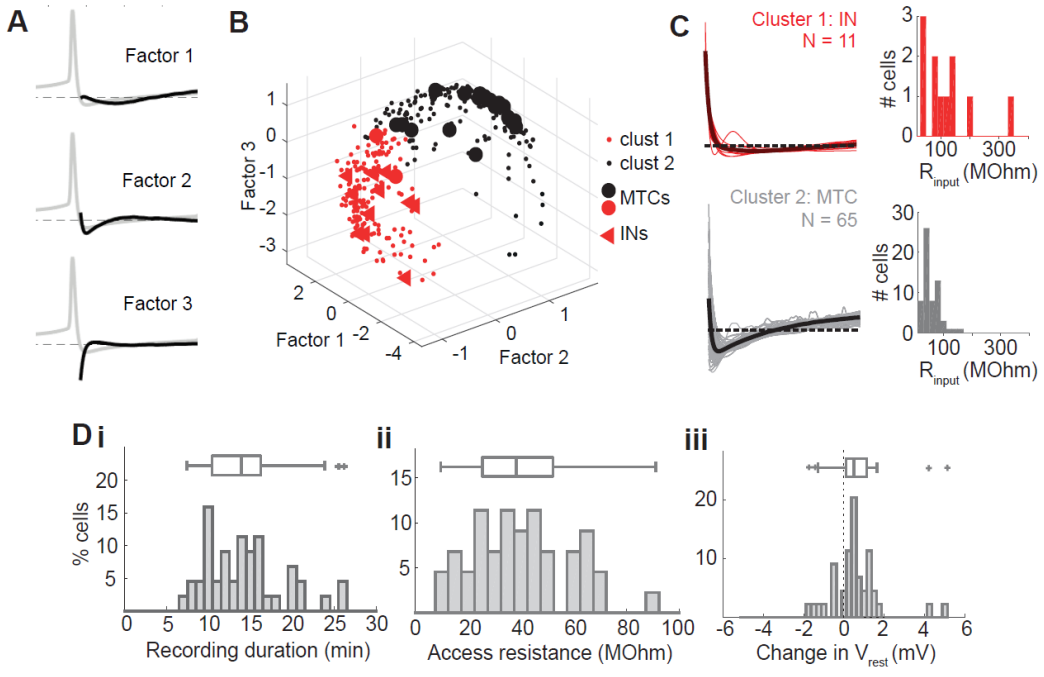

Figure 2.4. Principal cell vs interneuron identification analysis and recording parameters

(**A**) Three factors identified using independent component analysis on AHP waveforms (2-250ms from onset of action potential) of entire dataset (76 neurons from my dataset, 325 neurons from Kollo et al., 2014 dataset). A weighted combination of these factors can be used to reconstruct any AHP in the dataset. (**B**) Scatter of the weights of each factor for each cell in the dataset. Heirarchical cluster analysis was used to divide the dataset into two clusters based on these weights. In red is cluster 1, and described IN-like AHPs; in grey is cluster 2, describing MTC-like AHPs. Dots show cells without morphological reconstruction, while larger points show cells with reconstructions: circles show confirmed MTCs, and triangles show confirmed INs. Two confirmed MTCs were missed from the MTC cluster (black), indicating a conservative threshold for inclusion. (**C**) Left: AHPs from my own dataset only that fall into either cluster 1 (red, INs), or cluster 2 (grey, mitral and tufted cells). Thick black plot shows the average of all AHPs in the cluster. Recordings with biocytin–fill and reconstruction from each cluster showed that 100% of cluster 2 neurons were MTC (9/9 of my own reconstructions, and 11/11 from Kollo et al.), while 82% of recovered cluster 1 neurons were INs (2/4 of my own, 7/7 from Kollo et al.). Right: histograms of input resistance for cells from each group. (**D**) Distributions of recording parameters for 44 recorded MTCs: (**i**) recording duration, (**ii**) Access resistance and **iii**) Change in resting membrane potential (V_{rest}), between early in recording (first 3 minutes) and later in recording (last 3 minutes).

2.7.2. RAPID ACQUISITION OF OLFACTORY GO/NO-GO BEHAVIOUR

For examining the effect of olfactory learning on MTC responses, I utilised a simple olfactory go/no-go task: on each trial one of two possible odours is presented following an LED cue. If the CS+ (rewarded) odour is presented, the mouse must make a licking response (GO trial) in order to obtain a reward. If the alternate CS- (unrewarded) odour is presented, he must refrain from licking to avoid a 5 s addition to the inter-trial interval (punishment time-out) (Fig. 2.5B). Due to the limited timescale of whole cell recordings in awake animals, the training protocol for olfactory task learning was optimised such that discriminations could be rapidly learned within the timescale of a typical WC recording (for a detailed description, see general methods). In brief, the protocol consists of four sessions (Fig. 2.5C). In session one (S1), water-restricted mice were head fixed for the first time, and learned to lick a reward spout for rewards of sweetened condensed milk. In session 2 (S2), the CS+ odour was introduced. The mouse learned to lick in the one second response period following odour offset in order to gain a reward. In the third training session (S3), both the CS+ and CS- odours were presented, in a 50:50 pseudorandom sequence. Mice had to learn to lick in the reward period following CS+ odour presentations, and inhibit responding following CS- presentations. If the mouse licked in the response period following a CS-, this was deemed a false alarm (FA), and a punishment of 4s addition to the inter-trial interval (ITI) was triggered. Mice reached criterion performance when 80% or more of responses were correct in two consecutive blocks of ten trials. In session 4, mice were presented two new pairs of odourants in sequence, and were trained to discriminate these as in S3. The timing of each trial is depicted in Fig. 2.5B.

I optimised this training protocol for rapid acquisition of the task. Key aspects for rapid acquisition included a) training of animals only during the night cycle, b) sphinx-like comfortable posture of the animal, c) large rewards (20 microliters) during initial operant conditioning (S1 – later training steps utilised half this value), and finally, delay operant conditioning techniques

(see methods for details). Mice typically reached criterion for the first odour pair (S2) within 10 blocks (Fig. 2.5D, n=15 mice), equating to roughly 30 minutes - a time in excess of the typical whole cell recording duration. However, learning times for the second odour pair (S3) are much reduced, with mice typically reaching criterion by the third block (learning time of 8 minutes). All mice reached criterion within a maximum of four blocks (11 minutes) for both pair two and pair three learning. For mice undergoing whole cell recording procedures during S3 (including a craniotomy just prior), small distractions and task disruptions imposed by the experimenter may incur small increases in learning times. However, for animals undergoing whole cell recording procedures, over 80% of mice reached criterion by block 4. These learning times are within the typical WC recording timescale reported previously, and recordings thus took place over S3 during second pair learning (and in some rare cases, third pair learning).

While the paradigm was designed to separate odour stimulus and response epochs, mice would often make their decision prior to the response window and lick to the CS+ during the odour stimulus itself (Fig. 2.5E). Across mice, the median reaction time based on divergent licking to CS+ and CS- during criterion performance was 500 ms (Fig. 2.5E). It was also noted however that sniff waveforms could also diverge between CS+ and CS- odours during criterion performance, with sniffing to the CS+ becoming faster than for the CS- (Fig. 2.5F). Analysing the point of earliest significant divergence between these waveforms gave us an earlier estimate of reaction time compared to licking behaviour. Most often, significant divergence of sniffing could be seen as early as the first exhalation, as in Fig. 2.5F. The median reaction time calculated by this method was 240 ms, while the minimum reaction was 170 ms (Fig. 2.5G), i.e. a single sniff cycle, congruent with estimates made previously for olfactory decision (Abraham et al., 2004, 2010; Resulaj and Rinberg, 2015; Uchida and Mainen, 2003).

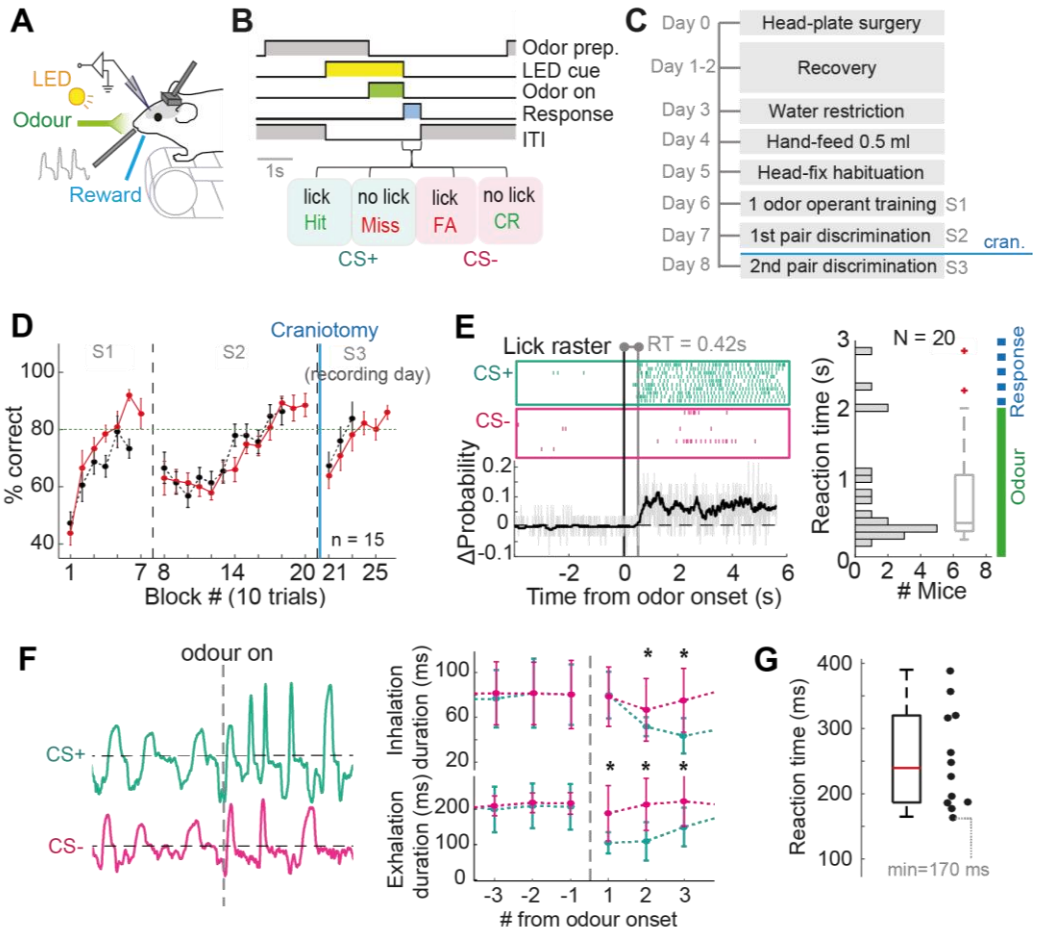

Figure 2.5. Go/no-go acqusition and performance

(**A**) Experimental set up for head-fixed recordings in awake learning mouse. (**B**) Schematic of a single go/no-go trial sequence. ITI=inter-trial interval, FA=false alarm, CR=correct rejection. (**C**) Training scheme optimised for rapid learning of task on day 8. 'CRAN.' Indicates where craniotomy woul occur prior to recording in S3. (**D**) Average learning curves for the three phases of operant learning (S1-S3, see panel C) for 15 mice in each cohort. In red shows data from mice undergoing craniotomy before S3, in black shows data from mice undergoing no such craniotomy. (**E**) Left: example reaction time (RT) calculation for one mouse. Lick rasters for CS+ and CS- during criterion performance are compared. Bottom trace: grey: shows for each 10ms time window the difference in probability of lick occurrence between CS+ and CS-. In black: Average of the grey trace with a sliding time window of 100ms. Reaction time is calculated where this exceeds 2x the SD of baseline. Right: distribution of reaction times calculated for 20 mice. (**F**) Left: example nasal flow (sniffing) traces from one mouse during criterion performance for both the CS+ odour and the CS- odour. Right: quantification of inhalation duration and exhalation durations as a function of sniff number from odour onset over 10 trials of CS+ and 10 trials of CS-. Reaction time was estimated at the point of first divergence between CS+ and CS- sniff patterns. E.g. in this example, sniff patterns significantly diverge as early as the first exhalation duration. (**G**) Distribution of reaction times estimated from the sniff patterns according to panel F for 12 mice in which this was possible.

2.7.3. WIDESPREAD ODOUR RESPONSES TO MULTI-COMPONENT MIXTURES

Since single cell recordings only allow very limited numbers of recordings per mouse (1 per mouse on average), and MTCs show responses to only a small subset (<20%) of monomolecular odours (Davison and Katz, 2007), I designed odour stimuli to provide a high probability of response. These consisted of four mixtures of 4-6 components (Fig. 2.6A, detailed list in Fig. 2.2A) selected for their reported ability to activate dorsal glomeruli (Takahashi et al., 2004). These were presented at 1% vapour pressure for 2 seconds (Fig. 2.6B).

To exemplify the high fidelity with which the mixtures evoked response, I here focus on 46 responses recorded from passively exposed awake mice. 67% were responsive to the odour when averaging FR responses over all trials for the full 2 s stimulus, with 43% showing inhibitory responses, 24% showing excitatory responses (Fig. 2.6C). Spike-clipping the traces and measuring the mean membrane potential responses, which allows a more sensitive estimation of inhibition, revealed an even greater portion of responsiveness, with 75% showing significant changes in potential (Fig. 2.6D). Of this responsive portion, 98% were inhibitory, while 2% were excitatory. Interestingly, the proportion of inhibition calculated here is larger compared to that reported previously for passive mice, where excitation and inhibition was roughly balanced (Kollo et al., 2014). The discrepancy is presumably due to the nature of the odour stimuli: the previous study used single monomolecular odourants. The increased inhibitory portion seen here could be due to the widespread nature of responses across the dorsal surface of the bulb: presumably this would engage a large amount of local lateral inhibitory mechanisms that act to normalise MTC responses according to input strength (Kato et al., 2013; Miyamichi et al., 2013; Roland et al., 2016)

Thus, the randomly selected odour mixtures provide a high probability of MTC response even without a screening step.

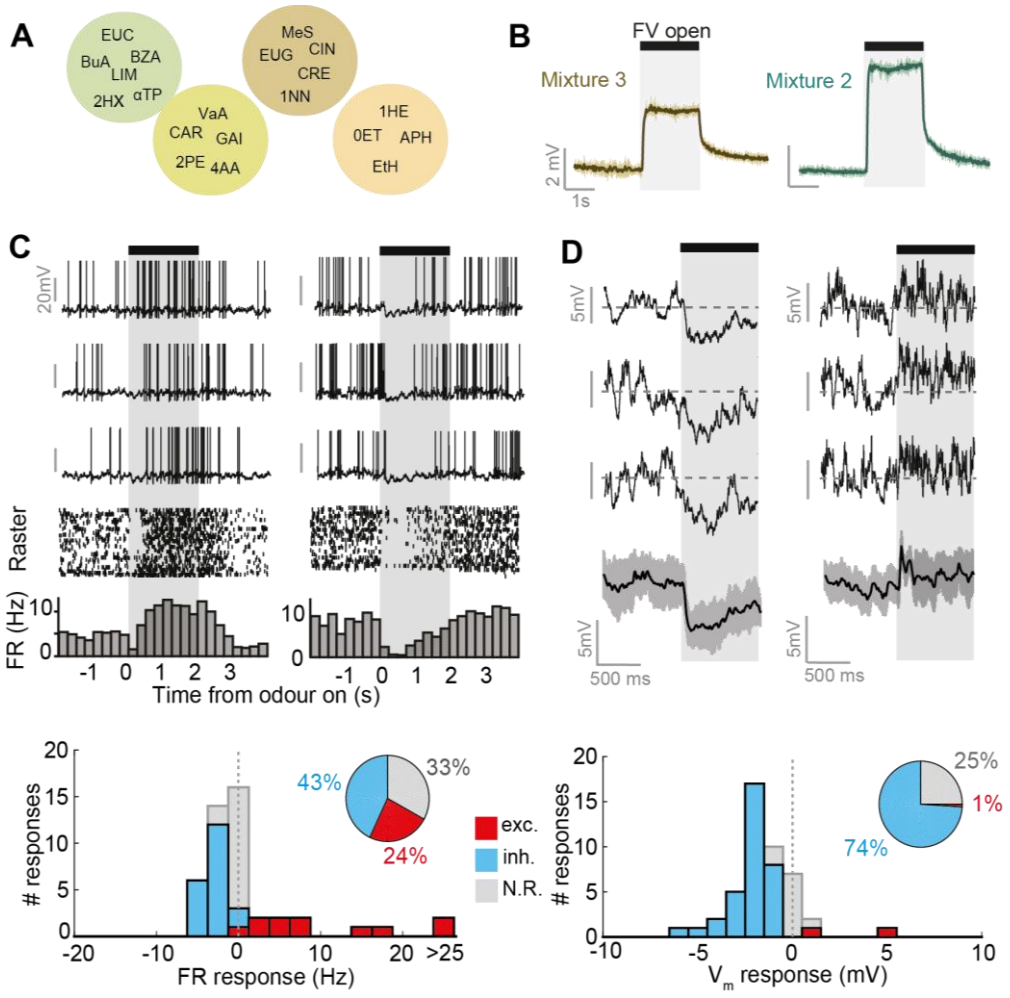

Figure 2.6. Widespread responses to odour mixtures for MTCs in passive mice

A) Schematic of four odour mixtures used (see Fig. 2.2 for full description). **B**) Example mini-photoionisation (miniPID) signal of odour mixture square pulse. Shaded area represents final valve of olfactometer open. **C**) FR responses to odour mixtures recorded via whole cell configuration in MTCs of awake passive mice. Top: two example responses (left = excitatory, right = inhibitory). Individual traces show examples from 1min, 5min and 10min (top to bottom) into recording, exemplifying the stability of the recording. Below are rasters of spikes across all recorded trials for each response, which is quantified below in peristimulus time histogram. Below shows histogram of mean FR responses averaged across all trials in awake passive mice. In blue shows portion of significant inhibitory responses, in red shows portion of significant excitatory responses, and in grey shows non-significant responses (N.R.). **D**) As for C, but for subthreshold responses after spike-subtraction. Note that these examples do not correspond to the examples in panel C.

CHAPTER 3. **RESULTS**

PHYSIOLOGICAL DIFFERENCES OF MTCS ACCORDING TO BEHAVIOURAL STATE AND LEARNING

3.1. INTRODUCTION

The relevance of sensory information is dependent on the behavioural state of the animal. For example, if an animal is anaesthetised or asleep, food odours will have very little behavioural consequence. However, if the animal is awake, the food odours may have consequence, but this in turn depends on the hunger state of the mouse. It would thus make sense that sensory circuit physiology and sensory representations depend on the behavioural state of the animal.

Arousal state is indeed known to have a profound influence on the physiology of principal cells in cortical sensory circuits (McGinley et al., 2015; Vinck et al., 2015), such as the barrel cortex in which overt changes in pyramidal cell physiology occurs during active exploration compared to passivity (Crochet and Petersen, 2006). In the OB, it is known that MTCs can become relatively more hyperpolarised during passive wakefulness compared to anaesthesia (Kollo et al., 2014). There are also large differences in interneuron cell activity according to the state change between anaesthesia and passive wakefulness, with interneuron activity tending to increase during wakefulness (Cazakoff et al., 2014; Kato et al., 2012), alongside overt changes in oscillatory activity (Chery et al., 2014).

Behavioural state changes can also profoundly alter sensory responses. For example during locomotion in V1, visual responses are amplified compared to rest (Niell and Stryker, 2010), while selective attention has profound effects on visual responses at various locations along the visual pathway (Han et al., 2009; Herrero et al., 2008). In the olfactory bulb, the transition from anaesthetised to awake state results in a shift towards more sparse odour representations (Rinberg et al., 2006). Even distinct states in awake rodents can apparently alter sensory responses. In somatosensory thalamus and barrel cortex, responses to tactile stimuli are highly modulated by both active whisking and the behavioural context of touch (Ferezou et al., 2006; Lenschow and Brecht, 2015; Urbain et al., 2015). In the OB, unit recordings from presumptive MTCs have previously shown that inhibitory responses tend to be more probable in rats engaged

in odour discrimination compared to passive exposure and response onsets were of shorter latency and longer duration in behaving mice compared to passive mice (Fuentes et al., 2008), while unit recordings in freely moving rats has provided evidence that hunger state could modulate responses to food odour in a highly reversible manner upon satiation (Pager, 1974).

There is also evidence for learning-related changes within odour responses of the OB. Firstly, the physiological basis for learning in the OB is present: *In vitro* work has shown that cortical inputs have potentiating synapses onto granule cells (Gao and Strowbridge, 2009). Secondly, the OB receives an abundance of connections from neuromodulatory centres and cortical regions (Shipley and Adamek, 1984), which are known to have a wide range of effects on the circuit. Thus, if learning occurs within a circuit outside of the OB, learned information could be delivered to the OB and indirectly alter responses.

There is also some evidence for changes in the suprathreshold odour responses of MTCs during task learning over the course of days. In animals learning a simple go/no-go task, Doucette and colleagues found transient changes in odour representation in terms of average FR responses (Doucette and Restrepo, 2008), and the proportion of synchronised spikes across the MTC population (Doucette et al., 2011). Meanwhile, imaging from MTC responses in mice learning discrimination tasks has shown that responses change in variable ways depending on the difficultly of the task being learned (Chu et al., 2016; Yamada et al., 2017). Imaging of glomerular input to the OB has shown that aversive conditioning can enhance inputs specifically for the conditioned odourant, perhaps via modulation of feedback inhibition onto OSN terminals (Kass et al., 2013). Finally, EEG and LFP recordings have shown changes in oscillatory activity of the OB throughout task learning and classical conditioning procedures (Freeman and Schneider, 1982; Di Prisco and Freeman, 1985; Beshel et al., 2007; Kay and Beshel, 2010).

Thus, there is evidence for both state-dependent shifts and learning related changes in OB activity. Therefore I sought to determine how basic physiology and odour-evoked responses of MTCs could change according to behavioural state, as well as across the rapid learning episode.

3.2. CHAPTER METHODS

3.2.1. BASIC CELLULAR PROPERTIES

Within the first 20 s of the recording, a current-voltage curve was calculated. In current-clamp, a series of current steps were applied to the cell three times, starting from -0.2 nA and increasing in 0.05 steps to 0.15 nA. After spike-subtraction, at each 10 ms time point, the mean potential was plotted against the applied current, and a linear regression fitted. Where this model intersected the Y axis (at 0 current), the resting membrane potential was estimated. The slope of the curve represented the linear sum of input resistance and access resistance (and no effort was made during recordings to compensate for access resistance via the bridge balance). To estimate the relative contribution of the two resistances, the mean voltage response waveform was taken for the most hyperpolarising (-0.2 nA) current pulse. A double exponential curve was fitted to the voltage trace between 0 and 10 ms, with a slow and fast time constant. The relative amplitude of the slow and fast components represented the relative contribution of input resistance and access resistance respectively, and were used as an estimate of each. The time constant for the slow exponential was used as a measure of membrane time constant. Spontaneous firing rate was calculated as the average firing rate in the 4 s prior to odour stimulus across all trials.

3.2.2. RESPONSE ONSETS AND DURATIONS

Response onsets were calculated using the mean subthreshold response waveform as triggered by the first inhalation onset after odour stimulus application. Only response onsets within the time range of the first sniff cycle (170 ms) were considered. Using the mean membrane potential

waveform as averaged over all trials, upper and lower bounds for significant response were calculated as the mean ± 2 standard deviations of the membrane potential in the 2 seconds prior to odour onset. Response onsets were considered as the first point at which the potential crossed the upper or lower bound and remained above or below for the next 100 ms.

Response duration was calculated by subtracting the response onset from the response offset. The response offset was calculated similarly to the response onset: the first point after response onset at which the potential returned to a value between the upper and lower bound for at least 100 ms.

3.2.3. SNIFF MODULATION AMPLITUDES

For baseline V_m during ITI: The theta modulation properties of each cell were calculated as previously (Fukunaga et al. 2012). Due to the high variability of sniff behaviour in awake mice, analysis was restricted to sniff cycles between 0.25 and 0.3s in duration, given that the preceding sniff cycle was also within this range. Mean V_m from the spike-subtracted V_m trace was taken as a function of sniff cycle phase for at least 150 sniffs, and this was plotted as Cartesian coordinates. The angle of the mean vector calculated by averaging these Cartesian coordinates was taken as the phase preference of the cell, while the difference between the mean V_m at the preferred phase, and the minimum value on the mean V_m waveform was taken as the amplitude of modulation. To determine significance, a bootstrapping method was used: 100 ms segments of V_m data were randomly selected for each cell and connected to form a shuffled dataset. The phase analysis was then performed on these shuffled datasets, and a modulation amplitude calculated and this was repeated 100 times. Significant modulation was assigned when the actual modulation amplitude exceeded that of the 95th percentile of shuffled data amplitudes.

During odour response: This was calculated as for baseline, but based on the first four sniffs post odour onset for the 10 trials of lowest sniff rates. As odour responses can have both tonic

and sniff-modulated components, the phase-V_m trace for each sniff had to be normalised according to the linear vector connecting the V_m at the beginning and end of the sniff.

3.2.4. ODOUR RESPONSES AND CHANGES

For all analyses, the first presentation of each odour was excluded due to the elicitation of high frequency sniffing by the novel odourant, which rapidly decayed by the second presentation. All traces were aligned to the odour onset, defined as the first inhalation following final valve opening. For V_m response calculations, spike waveforms, including the AHP, were subtracted from the V_m trace as outlined in general methods. Responses for each trial were calculated as the mean V_m within the first 500 ms post odour onset, normalised to the baseline membrane potential in the 2 s prior to odour onset. FR responses were calculated as the mean number of spikes per 250 ms time bin in the first 500 ms post odour onset, normalised to that calculated for 2 s prior to odour onset. Significant responses were determined for both V_m and FR using a paired t-test to compare baseline and odour-evoked activity for all trials. Significant changes between early and late trials for each odour response were identified by comparing the five 'early trials' in block 1, with the 5 last presentations of the stimulus using a t-test. Since this is a very weak test in this situation, there is likely to be a relatively high false-negative error rate.

3.2.5. RESPONSE CHANGE ONSET DETECTION

For each response, the mean V_m response waveform calculated for early trials was subtracted from that calculated from late trials, to generate a response change waveform at each time-point from odour onset. This was then normalised by the standard deviation of this resulting waveform during the baseline period 2 s prior to odour onset. Response change onset was detected where the response change magnitude first exceeded 2 standard deviations and remained there for at least 50 ms.

3.2.6. DETECTABILITY/DISCRIMINABILITY EUCLIDEAN DISTANCE ANALYSIS

For each cell-odour pair, mean V_m response waveforms were averaged over 3 trials for early, mid-point, and late trials. This was repeated 5 times to get five average membrane potential waveforms each for early, mid-point and late trials, each averaged across a different subset of 3 trials. Next, corresponding baseline waveforms were made in the same way by averaging inhalation-triggered waveforms from the ITI. Population response vectors were then constructed from these mean response waveforms for all cell-odour pairs recorded. At each time point relative to inhalation onset, the Euclidean distance was calculated between response and baseline vectors, and this was repeated five times for each baseline vector to gain a mean detectability over time, and a standard deviation. Minimum detection times were calculated as the first time post-inhalation where the mean detectability exceeded 2.5x the SD of the baseline mean detectability, and remained so for at least 50 ms. Peaks of detectability were defined as the maximum detectability within the first 150 ms after odour onset. Discriminability was analysed similarly, however the response vectors used to calculate the Euclidean distances were calculated between CS+ and CS- mean V_m response waveforms for the five sets of early, mid-point and late trials, i.e. the Euclidean distance was generated between population responses for CS+ and CS- separately.

3.3. RESULTS

3.3.1. BASELINE PROPERTIES

I recorded from 23 MTCs in passive mice exposed to repeated stimulation of odour mixtures (Fig. 3.1A), as well as 21 MTCs in mice during learning of the simple olfactory go/no-go discrimination task with the same mixtures (Fig. 3.1B).

To first determine whether the two behavioural states cause any general change in olfactory bulb physiology, I stimulated cells with a current step series (Fig. 3.1C) and compared basic

properties of cells between the states. The passive properties of cells showed no noticeable difference in either average values or variance. Resting membrane potential (V_{rest}) was indistinguishable (Passive: mean = -53.5±3.4 mV; Behaving: mean = -53.4±3.1 mV; p = 0.94, unpaired t-test; p = 0.68, Bartlett test; Fig. 3.1D), as were membrane time constants (Passive: mean = 17.5±6.8 ms; Behaving: mean = 16.7±7.0 ms; p = 0.81, unpaired t-test; p = 0.86, Bartlett test; Fig.3.1E), and input resistances (Passive: median = 47 MΩ, IQR = 37–79 MΩ; Behaving: median = 57 MΩ, IQR = 34-76 MΩ; p = 0.68, Ranksum; p = 0.54, Brown-Forsythe test; Fig. 3.1F),.

I also compared baseline spontaneous activity between the two states. I found that average spontaneous firing rates were not significantly different (passive: mean = 4.9 ± 2.9 Hz; behaving: mean = 6.5 ± 5.2 Hz; p = 0.31, unpaired t-test; Fig. 3.1G), however variance for spontaneous firing rates was significantly higher in behaving mice relative to passive mice (p = 0.01, Bartlett test). It has been widely observed in anaesthetised mice that baseline membrane potential of MTCs is modulated by the sniff cycle (Cang and Isaacson, 2003; Fukunaga et al., 2014). Consistently, I find that subthreshold activity in 83% of MTCs in awake mice is significantly modulated by the sniff cycle (see methods), with various amplitudes of modulation. Such sniff modulation amplitudes were indistinguishable between the two behavioural states (Behaving: median = 1.1 mV, IQR = 0.7-2.3 mV, Passive: median = 1.2 mV, IQR = 0.8-2.0 mV; p = 0.9, Ranksum; p = 0.8, Brown-Forsythe test; Fig. 3.1H).

Thus, basic passive and spontaneous properties of MTCs in awake passive and behaving states are almost entirely indistinguishable, with the exception of variance in spontaneous firing rates.

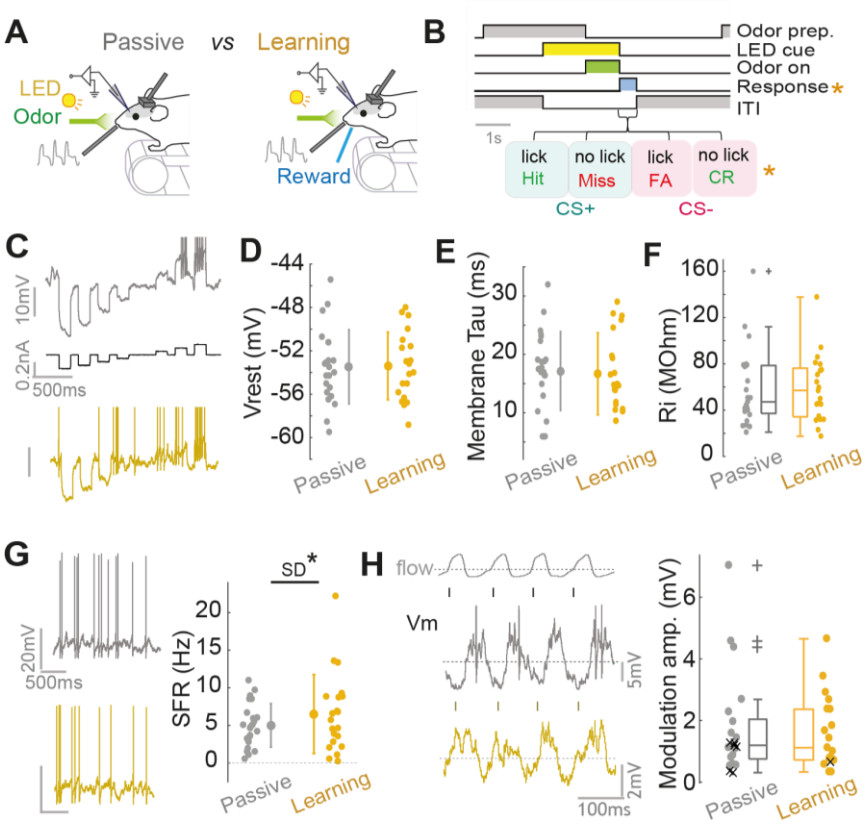

Figure 3.1. Comparison of passive properties and spontaneous activity between behavioural states

(**A**) Diagram of recording paradigms. (**B**) Diagram of trial sequence. Gold asterisks indicate segments/features that are only present for the learning mice. (**C**) Example current steps and concurrent voltage responses measured in current clamp in a MTC from passive (grey) and a MTC from a learning mouse (gold). (**D**) Resting membrane potential (V_{rest}) compared for passive (N=23) and behaving MTCs (N=21). (**E**) Comparison of membrane time constant (Tau). (**F**) Comparison of input resistance (R_i). (**G**) Left: example baseline firing activity from two MTCs. Right: comparison of spontaneous firing rates (SFR) across the two distributions (**H**) Left: example subthreshold activity during the inter-trial interval across 4 sniff cycles for 2 MTCs. Flow trace shows nasal flow, ticks show inhalation onsets. Spikes have been clipped for display. Right: Amplitude of modulation of membrane potential by the sniff cycle compared for passive and learning mice. Crosses show points which did not show significant modulation.

3.3.2. ODOUR RESPONSES

Next, basic odour response properties were compared between MTCs in passive and behaving mice. 46 responses in passive mice were compared with 42 responses in behaving mice. Since mice identify odours within very short timeframes of tens to hundreds of milliseconds (Abraham et al., 2004; Resulaj and Rinberg, 2015; Uchida and Mainen, 2003; and Fig. 2.6E-G), and my mice showed average reaction times of 500 ms as calculated from licking behaviour (Chapter 2, Fig. 2.5E), I chose only to average over the first 500 ms of the stimulus, since this is the behaviourally relevant part of the stimulus.

Averaging responses across all trials for a given cell-odour pair, it was apparent that FR responses did not differ in distribution between passive and behaving mice (Fig. 3.2Ai and Aii). Median FR responses were virtually identical (passive: median = -0.84 Hz, IQR = -2.2 to 1.1 Hz; behaving: median = -0.51 Hz, IQR = -2.8 to 2.1 Hz, p = 0.84, Ranksum), as was response variance across cells (p = 0.42, Brown-Forsythe test). Proportions of responsiveness were relatively similar between the two: in passive mice 43% were significant inhibitory responses, 24% were excitatory and 33% were non-responsive, while in behaving mice, the corresponding percentages were 40% inhibitory, 33% excitatory and 27% non-responsive.

Subthreshold responses offer us a more sensitive measure of many response parameters, including temporal features and inhibition. Taking mean membrane potential responses revealed that these also do not differ much between the two behavioural states in terms of means (passive: mean = -1.5±1.8 mV; behaving: mean = -1.7±2.4 mV; p=0.67, unpaired t-test; Fig. 3.2Bi and Bii). Weak inhibition (between 0 and -2 mV) described the large majority of significant responses in passive mice, while in behaving mice, inhibitory responses tended to be stronger (Fig. 3.2Bii). The proportion of excitation was increased in behaving mice, with an almost 5 fold increase in significant excitatory responses and fewer non responsive cells (passive: 74% inhibitory, 4% excitatory, 25% non-responsive; learning: 67% inhibitory, 19%

excitatory, 14% non-responsive). These effects were reflected in larger response variance across cells in learning mice relative to passive mice, though this did not quite reach significance ($p = 0.05$, unpaired t-test, $n = 42$ vs 46; Fig. 3.2Bii). To test whether this increase proportion of significant responses was due in fact to a reduction in between-trial response variability, the standard deviation of responses across trials was calculated for each cell-odour pair. While standard deviations were slightly lower on average in behaving mice, this did not reach significance (passive: mean = 1.2±0.4 mV; behaving: mean = 1.0±0.4 mV, $p = 0.14$, unpaired t-test).

Analysing the subthreshold responses allows us to more accurately extract temporal features of the responses, such as response durations and onsets. For response onset analysis, only onsets within the first 250 ms were considered. Comparing response onsets between passive and learning mice revealed a highly significant shift towards earlier onsets in learning mice (passive: median = 85 ms, IQR = 70-110 ms, $n = 39$; learning: median = 70ms, IQR = 60-90, $n = 36$; $p = 0.004$, Ranksum; Fig. 3.2C), with 33% of responses occurring before 70 ms in learning mice, and only 10% in passive mice. Response durations were then calculated by subtracting the response offset from the response onset. Responses in both passive and behaving animals showed a bimodal distribution, with around half showing short responses of ~500 ms, and the other half showing responses which lasted around the full duration (2 s) of the stimulus (Fig. 3.2D). Only a few responses showed durations that extended beyond the stimulus offset, and consistent with previous findings in awake passive mice (Kollo et al., 2014), no persistent long-lasting responses over tens of seconds were noted, as are known to occur in anaesthetised mice.

Finally, just as for baseline activity, activity during odour response is often locked to the sniff cycle. I calculated a sniff modulation amplitude from sub-threshold activity during the odour response (see chapter methods for details) to quantify to what degree each cell-odour pair was locked to the sniff cycle during odour stimulation, and compared this for passive and learning

mice (Fig. 3.2E). Overall, passive cell-odour pairs showed a significantly higher degree of patterning by the sniff cycle than learning cell-odour pairs (passive sniff modulation amplitude = 3.1±1.7 mV, n = 42; learning: 2.4±1.4 mV, n = 38, p = 0.03, unpaired t-test; Fig. 3.2F). Thus, odour responses in passive mice appear to be significantly more coupled to the sniff cycle than in learning mice.

Overall, compared to passive mice, responses in learning mice show an increased variance, occur with a significantly shorter latency and are less coupled to the sniff cycle than in passive mice.

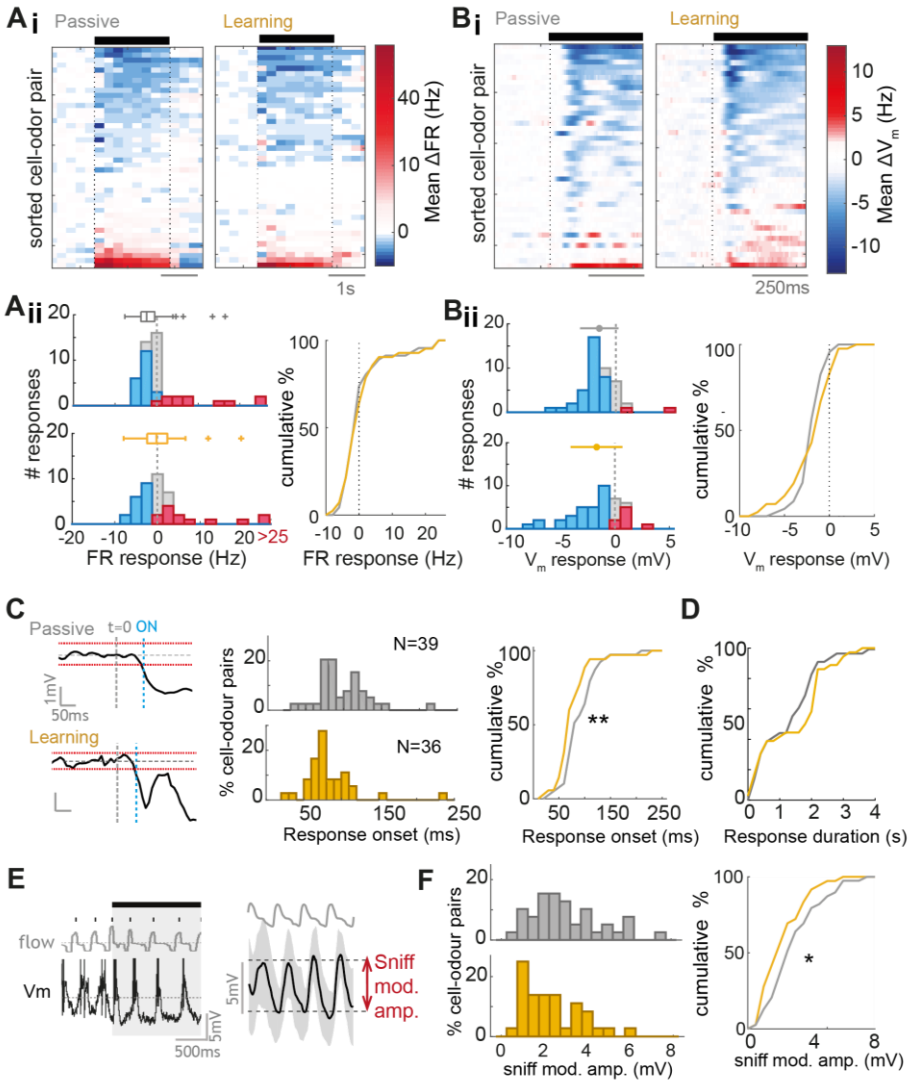

Figure 3.2. Comparison of MTC odour response properties between passive and behaving mice

(**Ai**) Heatmap of FR responses averaged across all trials for each cell-odour pair, sorted by mean 2 s FR response, for both passive (n = 46) and learning (n = 42) datasets. Black bar indicates odour stimulus. (**Aii**) Left: Histograms of average 2 s FR responses for (top) passively exposed and (bottom) learning mice. Right: cumulative histograms comparing average FR response data for passive (grey) and learning (gold) cell-odour pairs. (**Bi**) As for panel Ai, but for V_m responses. (**Bii**) As for panel Aii, but for V_m responses averaged over the first 500 ms of the stimulus. (**C**) Comparison of response onset latency for learning and passive mice. Left shows examples: average membrane potential waveforms averaged over all trials. t = 0 indicates when the odour turned on. Red dotted lines indicate upper bounds and lower bounds (calculated as mean±2SD of the baseline membrane potential). When the V_m waveform rises above or below the line for at least 100 ms, this is when response onset is defined (blue dotted line, ON). Histograms compare the distribution of response onsets for learning and passive mice, and cumulative histograms of the same data are shown to the right. P = 0.004, Ranksum. *Continued on next page…*

(**D**) Cumulative histograms to compare response durations for passive and learning mice. (**E**) Left: example of a highly sniff-locked odour response from a passive mouse across the first 4 sniff cycles. Flow shows nasal flow trace. Right: example average phase aligned membrane potential for first four sniffs of the odour response. 'Sniff mod. Amp.' Indicates the calculation of sniff modulation amplitude (see methods). (**F**) Left: histograms to show distributions of sniff modulation amplitudes of cell odour pairs in passive and behaving mice. Right: Cumulative histograms to compare sniff-modulation amplitudes for passive and learning mice.

3.3.3. V_M RESPONSES UNDERGO CHANGES DURING LEARNING

Recent imaging work has suggested that MTC responses are subject to change in both learning and passive mice over days (Chu et al., 2016; Yamada et al., 2017). In my task-learning mice, after pre-training on different odourants (see previous chapter), mice underwent very rapid learning in a matter of minutes on a novel pair of odour stimuli, reaching criterion within 10-20 minutes. Could the differences in response variance seen between passive and behaving average V_m responses come about across this learning timeframe, or are they there already from the beginning of learning?

To observe whether and how responses change across learning, I first compared the cell's response in five early trials where the mouse is performing at chance levels, to the same response in five late trials where the mouse is performing at criterion or above (Fig. 3.3A).

It was apparent that there were diverse changes in odour response occurring across learning: for example, overt increases in excitatory response (Fig. 3.3B), as well as increases in inhibitory response (Fig. 3.3C), which developed gradually across trials. Overall, in learning mice, 30% (13/42) of cell-odour pairs showed a significant change across learning ($p<0.01$, unpaired t-test between 5 early and 5 late trials), with 19% (8/42) showing a positive change, and 11% (5/42) showing a negative change (Fig. 3.3D and F). These changes led to an increase in the variance of responses between early and late trials across the sample, though this did not quite reach

significance (early SD = 2 mV, late SD = 2.6 mV; p = 0.06, Bartlett test). By contrast, cell-odour pairs recorded in passive mice showed far less frequent significant change (4%, 2/46 cell-odour pairs), and no change in response diversity across the sample (SD early = 1.9 mV, SD late = 2.0 mV, p = 0.58, Bartlett test; Fig. 3.3E and F). Overall, there was significantly higher variance in response changes for cell-odour pairs recorded in learning compared to passive mice (Learning response change SD = 1.5 mV, passive SD = 1.1 mV, p = 0.02, Bartlett test; Fig. 3.3G). Learning-related changes were not due to time-dependent effects of recording, since recording durations in passive and learning were matched (passive recording duration = 13±5 mins, learning = 15±5 mins; p = 0.12, unpaired t-test; p = 0.91, Bartlett test).

A previous study found that response changes across learning were dependent on reward value of the stimulus, with responses to the CS+ tending to increase, and responses to the CS- tending to decrease (Doucette and Restrepo, 2008). The response changes were not dependent on the reward value of the stimuli (Fig. 3.4A), with no systematic difference between changes for CS+ and changes for CS- (p = 0.77, paired t-test; Fig. 3.4B). In fact, response changes showed a significant correlation between CS+ and CS- within cells (R^2 = 0.44, p = 0.001, n = 21; Fig. 3.4C).

Thus, diverse response changes occur across learning that are not reflected in passive odour exposure. Similar analysis of changes in response onset and sniff modulation amplitude is marred due to the low trial number, which makes it much more challenging to gain accurate results. However, the underlying factors for this difference between passive and behaving odour representation is addressed in chapter 4.

Thus, the differences in odour representation between passive and behaving mice arise over the course of learning.

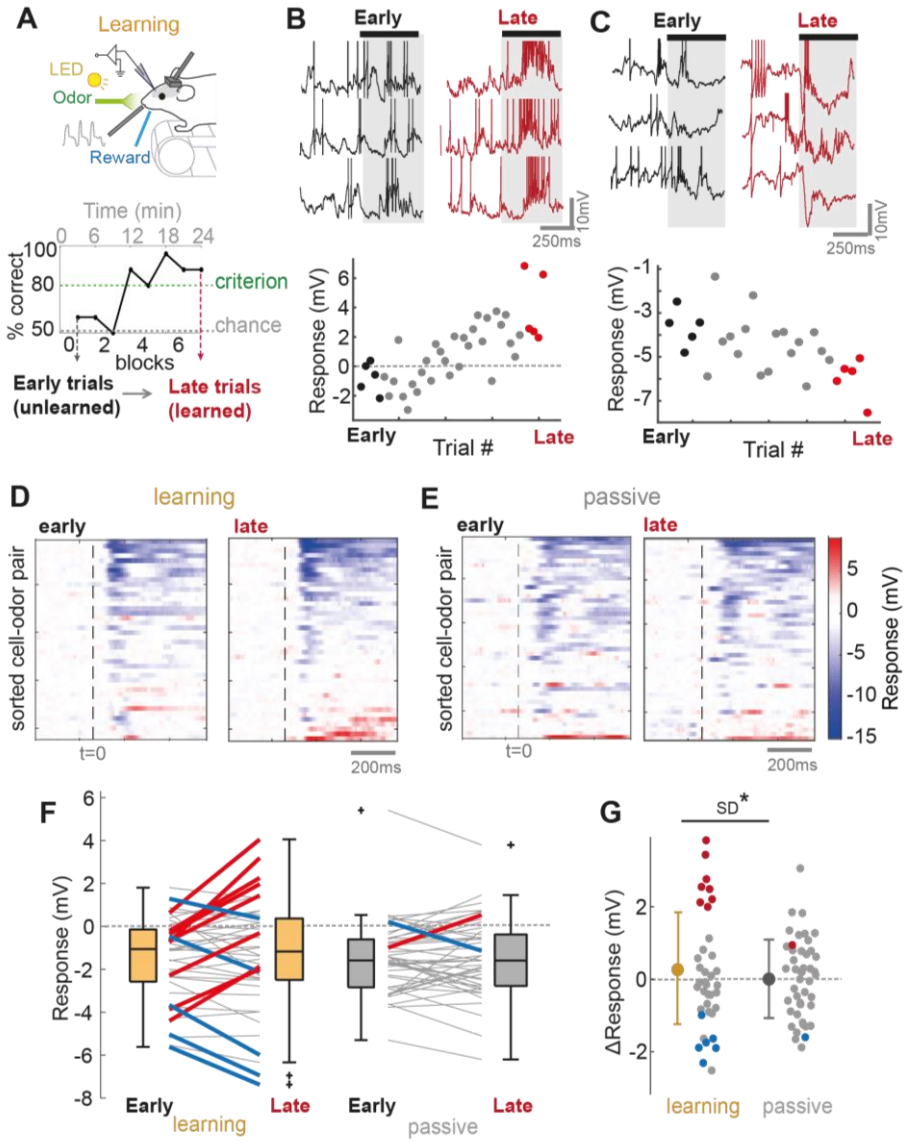

Figure 3.3. Diverse response changes occur across learning and not during passive exposure

(**A**) Diagram of the recording paradigm (above) and example learning curve for one mouse across the recording timeframe (below). Responses are compared between early trials (unlearned) and late trials (learned). (**B**) Above: example odour response traces in early and late for a cell-odour pair undergoing increase in excitation across learning (spikes have been clipped). Shaded area indicates odour stimulus (aligned to first inhalation onset). Below: mean membrane potential response across trials (averaged over first 500 ms of stimulus). Black dots indicate early trials, and red dots indicate late trials used for comparison. (**C**) As for panel B, but for a response undergoing an increase in inhibition. *Continued on next page…*

(**D**) Heat-map of average V_m responses across whole dataset for both early (left) and late (right) trials in learning mice, sorted by their mean late response. Dotted lines indicate start of the odour stimulus (t = 0). (**E**) As for panel D but for cell odour pairs recorded in passively exposed mice. (**F**) Plot of early and late membrane potential responses (first 500 ms) across learning for learning mice (left; n = 42 cell-odour pairs) and passive mice (right; n = 46 cell-odour pairs) separately. Thick red lines indicate significant positive change ($p<0.01$), thick blue lines indicate significant negative change. (**G**) Comparison of response changes (late-early) for learning and passive mice. Red dots show significant positive changes, blue dots show significant negative changes.

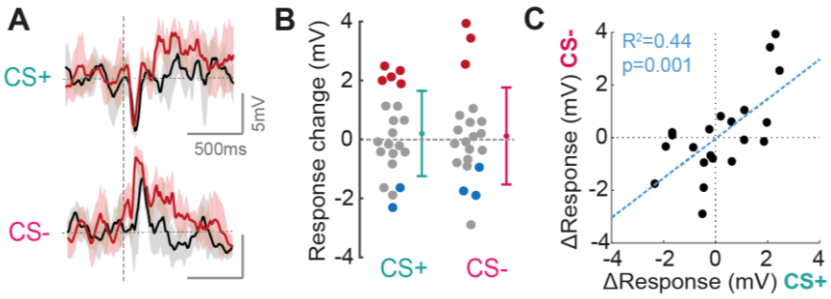

Figure 3.4. Response changes do not depend on reward contingency of odour.

(**A**) Example mean V_m response waveforms between early (black) and late (red) trials, for the CS+ odour and the CS- odour. Both responses show increased excitation. (**B**) Comparison of response changes (late-early) for CS+ and CS- in learning mice. (**C**) Scatter of response change for CS+ versus response change for CS- for each cell in learning mice.

3.3.4. RESPONSE CHANGES ARE USEFUL FOR DECISION

Could such response changes be used in behaviour? Mice are known to make simple olfactory discriminations within the timescale of a single sniff cycle (Abraham et al., 2004; Uchida and Mainen, 2008; Wesson et al., 2008b). Congruently here, we find reaction times as low as 170 ms (see previous chapter). When identifying the onset of response change (see methods), a large fraction of identifiable onsets occurred prior to 170 ms (Fig. 3.5A). Thus, it is possible that such changes are useful for the mouse in guiding behaviour.

I next wanted to address whether and how changes in odour response across learning could mediate enhancement of odour representation at the level of the 'population'. Here (and at all points in my results) I use this word to refer to a 'faux' population constructed from individual responses for different cell odour pairs recorded in different animals, much like those seen in Fig. 3.3D and E. However it must be remembered that these recordings were made in different animals, and thus do not constitute a real population response. To extract a measure of the detectability of the odour response across the constructed population, I calculated the Euclidean distance of the population odour response vector from baseline population response vectors constructed from cell activity in absence of odour (see chapter methods). I found that peak detectability in the first 150 ms of the odour stimulus significantly increased between early and late trials for learning mice (peak early = 31.9±0.8 mV, late = 40.1±1.0 mV; $p = 4x10^{-5}$, unpaired t-test, n=5; Fig. 3.5B), while no such significant changes were observed for passive exposure (peak early = 35.3±0.3 mV, late = 37.1±1.6 mV; p = 0.06 unpaired t-test, n=5; Fig. 3.5B).

To determine the effects of response changes on the discriminability of the two odour stimuli, I next calculated the Euclidean distance between population response vectors for the CS+ and CS- across different trial subsets. Here I observed a significant increase in peak discriminability of the two odours across the recording for learning (peak early = 19.8±1 mV, late = 25.0±2 mV, p =

$5x10^{-4}$; Figure 3.5C) but not passive mice (peak early = 20.4±1.9 mV, late = 19.9±1.3 mV, p = 0.68).

Thus, it appears that the changes observed are potentially useful for both increased detectability of the response across the population, as well as increased discriminability between the two presented odours.

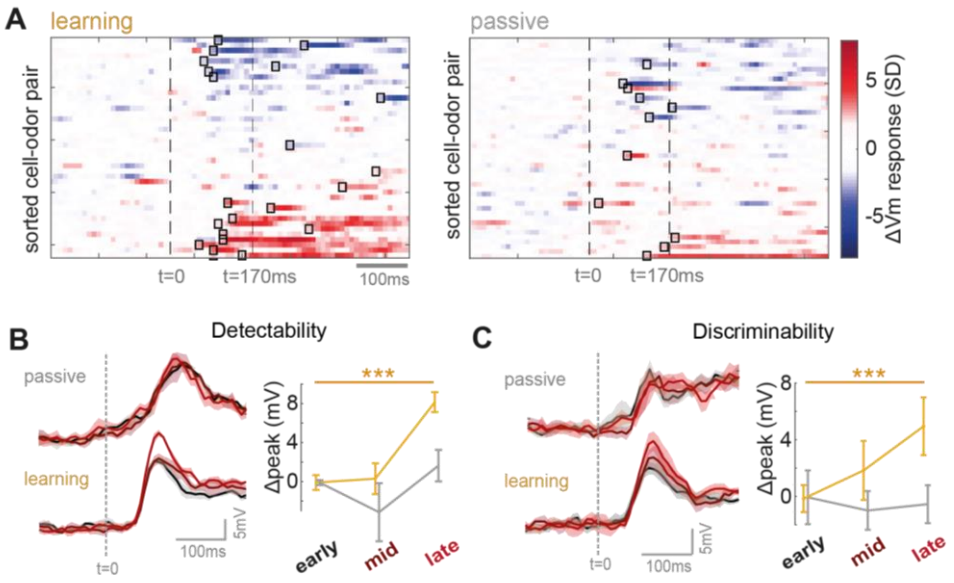

Figure 3.5. Changes in odour response could be useful for olfactory behaviour.

(**A**) Response change heatmaps (late-early average membrane potential waveforms) normalized by baseline SD. Black boxes indicate onset of change (>2.5 SD for at least 5 consecutive points). t = 170 ms is indicated as the shortest detected reaction time (see previous chapter). (**B**) Left plots: Euclidean distance as a function of time since odour onset (t = 0) between population vectors for odour response, and control vectors initiated by an inhalation during the inter-trial interval. This gives an indication of the detectability of the odour response across the sample. Black plot is calculated for early trials, maroon plot is calculated from mid-point trials, and red plot is calculated from late trials. Each is averaged over 5 trial subsets (see methods for details), and shaded area indicates standard deviation. Right: plot to show peak detectability within the first 150 ms of the stimulus across early, mid-point and late trials. Plot shows mean across the 5 trial subsets, and errorbars show standard deviation. Gold plot is for learning mice (n = 42 cell-odour pairs), and grey plot is for passive mice (n = 46 cell-odour pairs). (**C**) As for B, but with the Euclidean distance measured between population vectors for the CS+ and CS- to give an indication of the discriminability of the two responses across the sample.

3.4. DISCUSSION

Here I have shown that while baseline MTC properties are relatively similar between the passively exposed and actively learning states, there are aspects of odour response profiles (such as onset latency, variance, and sniff locking) that do indeed differ.

Behavioural state changes between anaesthetised and awake passive states has often revealed prominent shifts in the properties of the circuit including the OB (Chery et al., 2014; Cazakoff et al., 2014; Kato et al., 2012; Rinberg et al., 2006) , where inhibition seems to be dramatically increased, and MTCs can have more hyperpolarised membrane potentials (Kollo et al., 2014). There is much less evidence about shifts according to behavioural state. In the barrel cortex, changes between passive and active states as signified by spontaneous whisking behaviour cause highly overt changes in single cell baseline activity: pyramidal cells become relatively depolarized and show much reduced variance in baseline membrane potential (Crochet and Petersen, 2006). In comparison, here in the principal cells of the OB I find surprisingly little indication of changes in baseline or spontaneous properties, aside from increased variance in the spontaneous firing rates of behaving mice. This of course does not mean that subtle changes do not occur, since here I am not comparing direct shifts of the properties of a single cell between shifts in the behavioural context of the animal. The only apparent difference is a larger spread of spontaneous firing rates in behaving relative to passive mice (Fig. 3.1G).

Principal cell sensory responses are also known to be greatly modulated by behavioural state in the primary sensory cortices. For example, in visual cortex, visual responses are facilitated during attention (Ito and Gilbert, 1999) or locomotion (Niell and Stryker, 2010), while in the whisker system, passive touch causes reduced responses during spontaneous whisking compared to baseline, yet active touch evokes larger responses (Ferezou et al., 2006). Responses can subtly change between anaesthetised and awake states in the olfactory bulb - for example, awake mice do not show prolonged responses to odour stimuli as seen in anaesthetised mice (Kollo et al.,

2014), while unit recordings show an increased sparseness of odour responses in awake state compared to anaesthetised state (Rinberg et al., 2006). Here we find some differences in response profile between the passive and behaving population, particularly when analysing the sub-threshold membrane potential. There is a greater variance of mean V_m response across cells in behaving animals, resulting from an increased proportion of weak excitatory responses and a tendency for stronger inhibitory responses overall.

This result is hard to relate with previous results comparing FR responses of MTCs in rats either passively exposed to odours, or engaged in two alternative force choice discrimination: in the latter case, proportion of inhibitory responses was larger (Fuentes et al., 2008). Here, such a notable increase in the proportion of inhibition was not apparent, though amplitudes of inhibitory responses were larger. There could be several contributing factors for such a discrepancy. Firstly, unit recordings tend to oversample from cells with high baseline FR, while blind patching samples from a more representative MTC population that have low baseline activity (Kollo et al., 2014). Since cells with high baseline FR preferentially show inhibitory responses (Kollo et al., 2014), the difference in result could lie here. Secondly, the study used a very low sample size in terms of cells and animals, and the results appear to be highly variable between animals (see cited study Figure 2F-G). In additional conflict with their results, I found no indication of increased response duration in behaving animals, whilst the mentioned study does. This may result from the fact they used freely moving animals, in which both the odour pulse and the duration of stimulus sampling by the animal is out of experimenter control. Here we also find that response onset latency is significantly reduced in behaving mice relative to passively exposed mice, on the order of a tens of milliseconds. A similar result has been reported before from unit recordings (Fuentes et al., 2008), however, this occurred on the order of a few hundred milliseconds.

I have shown that odour responses change in diverse ways across learning episodes, but not in passively exposed mice, and that this gives rise to increased response variance across the sample (Fig. 3.3F).

The learning-related odour response seen here could conceivably be useful for behaviour, since they occur prior to our earliest estimates of decision (Fig. 3.5A). The reduced response onsets compared to passive mice could reflect the utility for more rapid acquisition of odour information during olfactory behaviour, as seen in glomerular imaging in mice performing the same task (Wesson et al., 2009). To determine how the changes may improve the stimulus representation I used analysis of population response vectors constructed across my sample of cells to analyse effects of response changes on odour representation (Fig. 3.5B and C). The results of this analysis must be treated with some caution, since the number of cells is limited (which can lead to problems with baseline noise when calculating discriminability and detectability from the vectors) and the responses come from different animals, and were not recorded simultaneously. As such, I may miss subtle changes in odour representation. However, the results I report here are congruent with recent studies imaging MTCs in mice learning discrimination tasks over days (Chu et al., 2016; Yamada et al., 2017). Here, they showed that stimulus representation 'reliability' is selectively increased over the course of learning a simple discrimination between highly dissimilar odourants, while stimulus discriminability was increased only when learning difficult discriminations where the stimuli were alike. In our task, given the high probability of response in any given cell-odour pair, the odour mixtures presumably activate overlapping populations of cells. As such, it would be useful to mediate changes in processing that enhance the discriminability of the stimulus, and this is indeed what we see specifically in our learning mice (Fig. 3.5C). Early stimulus detectability (analogous to 'reliability' in the cited study) was also increased, such that the stimulus was detectible more robustly across learning (Fig. 3.5B). Thus the response changes may allow the animal to make a

more reliable decision, and conceivably could alter perceptual features such as stimulus salience or strength.

Previously studies have also shown that response changes can occur across learning over longer timescales (Chu et al., 2016; Doucette and Restrepo, 2008; Yamada et al., 2017). It is difficult to directly compare the response changes seen here with those reported in the imaging studies, due to the different recording methods used, the fact they are looking at learning over days rather than minutes, and the way in which results are reported for large population data (Chu et al., 2016; Yamada et al., 2017). However, my results are consistent with these studies in that I show both an increase in detectability and discriminability across learning. Previous studies from Doucette and colleagues using unit recordings in freely behaving mice tracked changes in odour response over the course of go/no-go learning (Doucette and Restrepo, 2008; Doucette et al., 2011). Here they found that odour responses changed transiently over the learning period, with a large proportion of cells showing 'divergent' response changes: typically increases in response for the rewarded odour, and decreases for the unrewarded odour. Here, we found no such difference in response changes between CS+ and CS-; on the contrary, response changes were found to correlate very well between CS+ and CS- for a cell (Fig. 3.4). As discussed for other discrepancies, this contrast could come from the unit recording vs whole cell recording difference: in the mentioned study, cells with very high baseline firing rate are exemplary and, if representative of their sample, they may be sampling from an uncommon sub-type of MTC, since in the whole cell recordings here, cells with such high firing rate are not common. Differences in the learning paradigm may also contribute.

Overall, I find that diverse response changes occurred specifically over the course of very rapid learning epochs, potentially enabling enhanced early detection and discrimination of the odour stimuli. The next chapter will begin to address potential mechanisms underlying these phenomena, in particular how changes emerge across the learning episode.

CHAPTER 4. **RESULTS**

LEARNED ACTIVE SAMPLING STRATEGIES AND THEIR IMPACT ON ODOUR RESPONSES

4.1. INTRODUCTION

What are the mechanisms underlying the learning-related changes in odour responses? While previous studies have described learning related changes in average firing rate responses across learning (Chu et al., 2016; Doucette and Restrepo, 2008; Yamada et al., 2017), none have identified the mechanism of the change. There are two broad mechanisms that could explain such an effect. The first and most highly touted explanation comes from the huge abundance of top-down connections projecting to the olfactory bulb from higher cortical circuits and neuromodulatory regions of the brainstem. These regions are known themselves to encode contextual information, including learned information (Bouret and Sara, 2004; Schoenbaum and Eichenbaum, 1995; Zinyuk et al., 2001). Thus, learned information could be delivered to the OB from these higher centres, and alter circuit physiology, giving rise to the changes in response.

The second, and remarkably under-acknowledged explanation comes from sniffing, which comprises active sampling behaviour in the olfactory system. Rodents orchestrate their sniffing behaviour in a complex and highly dynamic way according to context (Wachowiak, 2011). Sniffing behaviour is modulated for all kinds of reasons, including in non-olfactory situations, such as locomotion (Bramble and Carrier, 1983), reward anticipation (Clarke, 1971; Ikemoto and Panksepp, 1994; Kepecs et al., 2007; Wesson et al., 2008a) and auditory stimuli (Wesson et al., 2008a), as well as during sampling of olfactory stimuli, such as novel odours (Roland et al., 2016; Verhagan et al., 2007), or odour stimuli during olfactory discrimination tasks (Kepecs et al., 2007; Macrides et al., 1982; Rajan et al., 2006; Uchida and Mainen, 2003; Youngentob et al., 1987). It is thus necessary to distinguish active sniff changes that are directed towards sampling a relevant olfactory stimulus (which I will term 'active sampling'), and sniff changes that arise as a bi-product of another behavioural variable, which have nothing to do with sampling an olfactory stimulus.

A particularly relevant study showed that rapid sniff strategies emerged as mice learned to perform an olfactory go/no-go discrimination task (Wesson et al., 2009). Since activity in the olfactory system is profoundly shaped by active sniffing behaviour (Adrian, 1950; Cang and Isaacson, 2003; Fukunaga et al., 2012; Macrides and Chorover, 1972; Margrie and Schaefer, 2003), with a packet of sensory input to the OB arising with each inhalation, we might expect changes in sniff pattern to affect MTC activity. The development of sniff strategies across learning could thus potentially explain the changes in response described in the previous chapter. As prior studies have largely been undertaken in freely moving animals, sniff rates are hard to measure, and thus rarely reported. Recording sniffing behaviour in a head-fixed animal is by contrast very simple – making it surprising that even recent high-profile head-fixed studies reporting contextual change in the bulb fail to even mention sniffing (e.g. Chu et al., 2016).

It has been hypothesized that active sampling strategies serve to enhance or optimise early sensory representation. In the whisker system, it is known that spontaneous whisking bouts correlate with large changes in the state of pyramidal cells in barrel cortex and affect the responses to tactile stimuli (Crochet and Petersen, 2006; Ferezou et al., 2006; Lenschow and Brecht, 2015; Urbain et al., 2015). In the visual system, saccades biphasically modulate the firing rates of visual cortex neurons (McFarland et al., 2015). Exactly what functional impact these changes have for sensory coding is still a matter of speculation, and whether task specific changes in active sampling strategies serves to improve sensory representation is not yet demonstrated physiologically.

The current state of evidence about how active sniffing strategies during behaviour may affect OB activity is limited to two studies imaging from OSN glomerular inputs. The first has shown that rapid sniffing during olfactory discrimination behaviour served to reduce the latency of glomerular response onset, yet the amplitude of responses stayed the same (Wesson et al., 2009). The latencies reported, however, were in the region of hundreds of milliseconds. By

contrast, the changes in MTC response I observe occur within the first sniff cycle, and the shortening of onset latency I observe occurs in the order of tens of milliseconds. A second study showed that long bouts of rapid sniffing reduces the amplitude of glomerular responses over long timescales via an adaptation mechanism (Verhagan et al., 2007), however, whether this is true for the initial few hundred milliseconds is unclear. The only study to my knowledge that examines the effect of rapid active sniffing on odour responses of MTCs shows that while sniffing does have an impact on average firing responses, the earliest sub-sniff transients of firing response remain stable, and can be used to reliably code for odour identity across different sniff frequencies (Cury and Uchida, 2010). In contrast, the response changes I observe occur as early as 50 ms after inhalation onset (Chapter 3, Fig. 3.5A) - the very initial portion of activity in response to an odour.

There is a much larger set of evidence from an analysis of firing patterns in anaesthetised mice. Since MTC activity is modulated by the sniff cycle, it seems plausible that changes in the sniff pattern will cause changes in MTC firing patterns. Indeed, changes in inhalation frequency in anaesthetised, double-tracheotomised rats is known to alter the basal firing patterns of MTCs (Carey and Wachowiak, 2011), such that inhalation-locked burst of action potentials during odour stimulation follows the profile of inhalation frequency even at high sniff rates. Increased flow rate of simulated sniffs has also been found to modulate MTC responses to odours (Courtiol et al., 2011). Imaging of glomerular signals in a similar set up showed that peak glomerular responses to odours were found to increase with increasing flow rate of the sniff in anaesthetised mice (Cenier et al., 2013; Oka et al., 2009), though sniff frequency was found to have less of an impact (Oka et al., 2009). The latter study showed in particular that flow rate had varying effects on the glomerular response according to odourant type, such that an entirely different pattern of glomerular activity would occur for an odour mixture presented at high compared to low flow rate sniffing. However, how far these user-controlled sniff patterns match

that seen in actively sampling behaving animals is unclear, and in a particular study, no correlation could be found between peak glomerular responses to odours and flow rates of sniffing when the animal was awake and actively discriminating (Cenier et al., 2013). The importance of the sniff cycle in awake mice has further been called into question over reports that the sniff cycle does not modulate firing patterns in awake mice, or at awake sniff frequencies, nearly so much as it does in anaesthetised mice where sniffing frequency is always lower (Cazakoff et al., 2014; Rinberg et al., 2006; Spors et al., 2006). Thus, currently the impact of active sampling on odour response is a matter of speculation.

During the course of my whole cell recordings, either flow or pressure sensors were placed externally in close proximity to the naris contralateral to the side of recording, allowing sniffing behaviour to be measured. Using this information, it was possible to identify a) whether changes in sniffing emerged, b) whether such changes were reflective of an olfactory active sampling strategy, and c) what explains variation in such strategies between mice. I then wanted to investigate whether changes in active sampling across learning could explain the changes in average response across learning described in chapter 3, as well as differences in other response features (onset latency and sniff modulation) seen between passive and learning mice.

4.2. CHAPTER METHODS

4.2.1. MEASURING CHANGES IN SNIFFING

Since the time-window of analysis of the odour response changes in the previous chapter was only 500 ms (corresponding to relevant reaction times), it was necessary to take a measure of sniffing behaviour within this time window that could be easily quantifiable, provide the most data points, and be most relevant to olfaction. The mean inhalation duration (MID) of all inhalations completed within the time window was selected for this purpose, since it is during the inhalation period that odour molecules are delivered to the olfactory system. To extract

inhalation durations from flow traces, firstly inhalation peaks were detected as any peak above a certain threshold arbitrarily set according to the amplitude of the signal. Inhalation onset was set at the nearest point pre-peak that the flow trace touches zero, while inhalation offset was set at the nearest point post-peak that the flow trace reaches zero. The distance between these points was taken as the inhalation duration. The mean inhalation duration for the first 500 ms of each odour presentation was calculated from the duration of all complete inhalations within that time period.

4.2.2. RESPONSE ONSET ANALYSIS

To determine the effect of sniff changes on response onset, only the first inhalation after odour onset was considered, since only response onsets less than or equal to 250 ms were analysed. For each response, trials were categorised into 'slow' (first inhalation duration in upper 50^{th} percentile of all trials) or 'fast' (first inhalation duration in lower 50^{th} percentile of all trials) sniff trials. The mean normalised V_m response waveform was averaged across these trial sets. Response onsets were calculated as described in the previous section using these waveforms. Only cases where there were five or more trials in each category as well as a detectable response onset within 250 ms of odour onset were analysed. Response onsets from fast vs. slow trials were then compared across all responses for either behaving or passive MTCs to determine the effect of sniffing within each group. Response onsets were then compared between passive and behaving MTCs calculated from sniffs within a restricted subset of inhalation durations (80-100 ms), to determine any effect of behavioural state independent of sniff variance.

4.2.3. TASK ENGAGEMENT/DISENGAGEMENT

For mice undergoing the task engagement/disengagement paradigm, acquisition of the task occurred prior to recording such that criterion performance was already achieved from the start of the recording. After around 20 trials, the water port was manually moved away to disengage the task. Mice would continue to attempt to lick the port (as detected by infrared beam) for a

variable number of trials before 'giving up' (i.e. at least 3 consecutive 'miss' trials), after which the port was returned. Often a free reward was used as a salient stimulus to the mouse that the task was re-engaged. To compare changes in response across task engagement, disengagement and re-engagement, 5 trials were taken from each. For task engagement, these were the 5 trials just preceding removal of the reward port. For task disengagement, these were 5 trials prior to return of the reward port, so long as anticipatory licks for the CS+ were at a very low average rate (<4 licks in 2 s), and at least 2 subsequent misses for the CS+ had occurred. Re-engagement trials were taken as the 5 trials proceeding the mouse 'realising' the port had returned, i.e. the first self-initiated hit onwards.

4.3. RESULTS

4.3.1. THERE ARE BEHAVIOURAL STATE-DEPENDENT DIFFERENCES IN SNIFFING BEHAVIOUR

To first assess general differences in sniffing according to behavioural state, the durations of all sniffs collected across the inter-trial intervals were compared between passive, behaving and anaesthetised mice anaesthetised with ketamine/xylazine (latter data provided by Izumi Fukunaga; Fig. 4.1A-B). Sniffing in anaesthetised mice showed the lowest variation (median SD = 28 ms, IQR = 20-37 ms, n = 12 mice), while passive mice displayed significantly larger variation (median SD = 71 ms, IQR = 59-82 ms, n = 29 mice; anaesthetised vs passive: $p = 6x10^{-7}$; Fig. 4.1C), and learning mice displayed significantly larger variation than passive mice (median SD = 56 ms, IQR = 44-71 ms, passive vs learning: $p = 4x10^{-4}$, unpaired t-test; n = 30 mice). Mean frequencies were also modulated, with passive and learning mice showing significantly shorter sniff durations (higher frequency sniffing) than anaesthetised mice (anaesthetised: median = 370 ms, IQR = 331-406 ms, n = 12; passive: median = 277 ms, IQR = 251-304 ms, n = 30; learning: median = 258 ms, IQR = 233-285 ms, n = 29; anaesthetised vs learning: $p = 3x10^{-10}$, unpaired t-test; anaesthetised vs passive: $p = 9x10^{-7}$, unpaired t-test; Fig. 4.1D). Thus, sniffing behaviour is overtly modulated by behavioural state even in absence of odour.

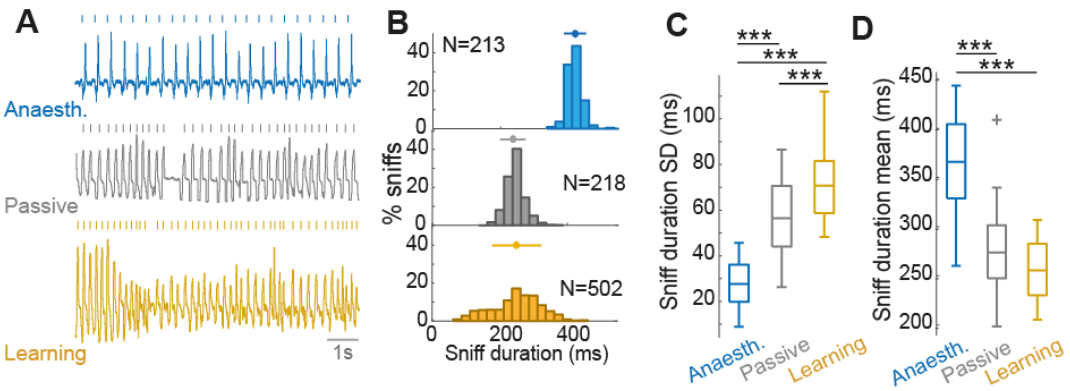

Figure 4.1. Sniffing is modulated by behavioural state.

(**A**) Example sniff traces from example anaesthetised (using piezo strap to measure chest distension - data provided by Izumi Fukunaga), passive (flow measurement) and learning mice (flow measurement) during the inter-trial interval. Vertical dashes represent inhalation onset (top) and inhalation peaks (middle and bottom). (**B**) Histograms from example mice showing distribution of sniff durations during baseline for an anaesthetized (top), passively exposed (middle) and behaving mouse (bottom). (**C**) Boxplots to compare standard deviation in sniff duration distributions between anaesthetized (n = 12), passive (n = 30) and learning mice (n = 29), ($p<0.001$, unpaired T-test). (**D**) Boxplots to compare mean sniff durations across all mice. Mean sniff durations are significantly higher for anaesthetized mice ($p<0.001$, unpaired T-test).

4.3.2. THERE ARE TASK SPECIFIC CHANGES IN MEAN INHALATION DURATION

To analyze sniff changes across learning within the short 500 ms time-window of the odour stimulus (as was used to measure the changes in membrane potential response in chapter 3), I quantified the mean inhalation duration (MID) of all inhalations completed within the first 500 ms of the stimulus (Fig. 4.2A). Four cell-odour pairs from the learning dataset were excluded due to periods of corrupted sniff data, while four were excluded from the passively exposed dataset, resulting in sample size of n = 38 in learning mice and n = 42 in passive mice. When comparing early and late learning trials, it was apparent that mice showed striking changes in sniff behavior during the odour stimulus, for example some mice displayed faster, sharper inhalations (reduced duration) emerging in the late learning phase (Fig. 4.2B), which developed gradually across trials (Fig. 4.2C). Changes in MID mirrored changes in sniffing frequency across trials (Fig. 4.2C). Thus when I refer to 'fast sniffing', I am necessarily referring to both a reduction in MID alongside an increase in sniff frequency.

Across all cell-odour pairs, a large fraction underwent significant changes in MID during learning (26%, 10/38 cell odour pairs; Fig. 4.2D). In stark contrast, passively exposed mice showed far more stable MID, with only 12% of cell-odour pairs showing significant change (Fig. 4.2D), and substantially less variation in the changes in MID occurring across the recording (learning: ΔMID SD = 24 ms, passive: SD = 9 ms, $p = 3x10^{-8}$, Bartlett test). It was apparent that, while in learning mice 18% (7/38) of cell-odour pairs underwent reductions in MID resulting in fast sniffing (late MID<60 ms), this never occurred for passive mice (Fig. 4.2D). Comparing cumulative histograms of the MID change between learning and passive mice revealed that a significantly larger proportion of learning mice underwent reductions in MID exceeding 20 ms (learning: 26%, passive: 2%; p<0.01, bootstrapping; Fig. 4.2E). Changes in MID across the population of learning mice again correlated very well with changes in sniff frequency ($R^2 = 0.59$, $p = 3x10^{-8}$; Fig. 4.2F).

Thus there are indeed learning specific changes in sniffing behaviour during the odour stimulus.

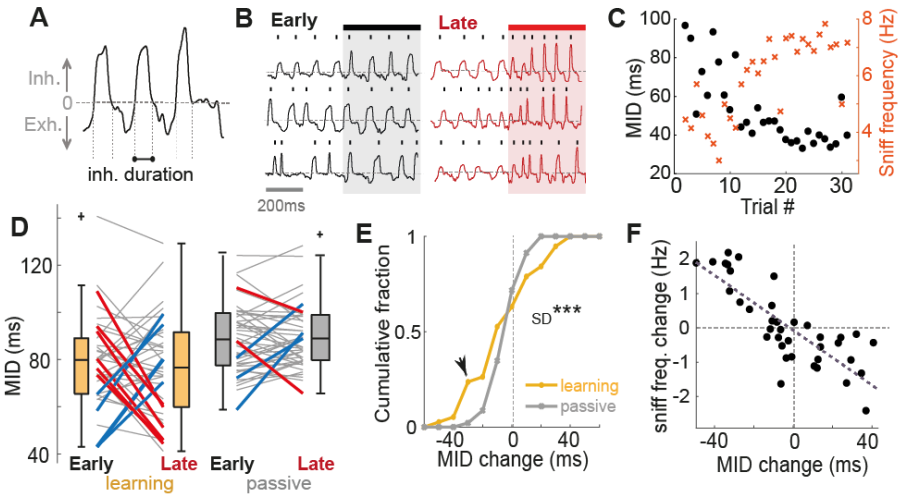

Figure 4.2. Learning-related changes in sniffing behaviour

(**A**) Diagram to show extraction of inhalation duration from example nasal flow trace. (**B**) Example nasal flow traces from one mouse showing emergence of rapid sniffing between early and late trials. (**C**) MID for example cell-odour pair in panel B calculated for each trial (first 500 ms of stimulus) in black dots. Orange crosses show corresponding sniff frequency for each trial. (**D**) Plot showing how MID changes between early and late trials, for learning (n = 38) and passive (n = 42) mice. Thick red lines show significant reductions in MID, thick blue lines show significant increases in MID. (**E**) Cumulative histograms of MID change for learning and passive mice compared. Black arrowhead shows significant difference in the histograms. (**F**) Scatter between change in MID and change in sniff frequency between early and late trials for all learning cell-odour pairs.

4.3.3. CHANGES IN SNIFFING INDICATE THE EMERGENCE OF ACTIVE SAMPLING STRATEGIES

I next wanted to further analyse features of the MID change that would indicate the nature of the sniff change – i.e. is it an effect of reward anticipation, as has previously been described (Wesson et al., 2008a, Kepecs et al., 2007) which would indicate the sniff change is the result of the decision already being made, or could the sniff changes be utilised for decision? Further – why do some mice show the MID change while others do not?

I first considered the time course of the MID change. To do this, I analysed the first four inhalations in the odour stimulus and calculated the change in their duration between early and late trials. I noticed that often the first inhalation after odour onset already showed a pronounced change in duration in cases of large MID change – both for reductions and increases (Fig. 4.3A). When relating the change in the first inhalation duration (FID) to the change in MID across learning, I found a very tight correlation ($R^2 = 0.77$, $p = 7x10^{-13}$; Fig. 4.3B). Since the first inhalation is only a few tens of milliseconds, this suggests that the sniff change is occurring prior to a decision being made.

While this is suggestive that the MID change constitutes an active sampling strategy, it is clearly not absolutely necessary for accurate olfactory behaviour in this paradigm since there is large variance in MID changes across all mice who successfully learn the task (Fig. 4.2D). What could explain this variance in strategy?

While all mice underwent the same water deprivation program, motivation for the task is difficult to control precisely during the recording due to individual variation (e.g. in percentage body fat), as well as variation in the sequence of events (e.g. how long it takes to obtain a stable whole cell recording, and thus how many rewards are acquired prior to this). I noted that mice respond with variable vigour in their licking behaviour during the odour stimulus, making it possible that different mice are motivated to different degrees for the task, and that this could explain the differences in sampling. I noticed that the mice who tended to show fast sniffing

strategies also tended to show high rates of licking during the odour stimulus compared to mice which did not sniff fast (Fig. 4.3C). The number of anticipatory licks in late trials in fact correlated well with the change in MID across learning, with reductions in MID associated with larger frequency of anticipatory licking ($R^2 = 0.54$, $p = 0.0004$; MID change averaged across CS+ and CS- for each cell-odour pair; Fig. 4.3D). Thus it appears that the reduction in MID is selectively seen in mice with high motivation, as indicated by their anticipatory licking ('response vigour', Berditchevskaia et al., 2016). Reduced MID was also significantly associated with shorter reaction time ($R^2 = 0.23$, $p = 0.04$, MID change averaged across CS+ and CS- for each cell-odour pair; Fig. 4.3E).

Could the change in MID be linked to the motor response or reward anticipation in some way? To test this, I compared for each mouse the change in MID for the CS+ and the CS- across learning. This revealed a significant positive correlation between the two variables ($R^2 = 0.54$, $p = 0.0003$; Fig. 4.3F), such that every time MID reduced for the CS+, it did so also for the CS-. Secondly, the correlation between MID change and anticipatory lick rates could be seen for both MID changes for the CS+ and CS- alone (CS+: $R^2 = 0.58$, $p = 1x10^{-4}$; CS-: $R^2 = 0.36$, $p = 0.006$; Fig. 4.3G). Given that mice are not licking for the CS- in late trials, it is hard to argue that the changes in MID across learning reflect licking response or reward anticipation. The effect of reward anticipation on sniffing could be seen, however, when considering the absolute MID rather than the change across trials: MID values were indeed mildly but significantly smaller (faster sniffing) for CS+ than for CS- in both early trials (MID = 9±17 ms smaller for CS+, $p = 0.02$, $n = 18$, paired t-test) and late trials (MID = 10±12 ms smaller for CS+, $p = 0.003$, $n = 18$, paired t-test), indicating that reward prediction indeed drives mice to sniff more rapidly (data not shown). Indeed I rely on this effect to calculate reaction times from the divergence of sniffing behaviour between CS+ and CS- stimuli, resulting in reaction times smaller than those calculated from sniffing behaviour (see Chapter 2).

Altogether, this argues that the MID changes across learning most likely constitute an active sampling strategy for the task in highly motivated mice, and could be functional for decision.

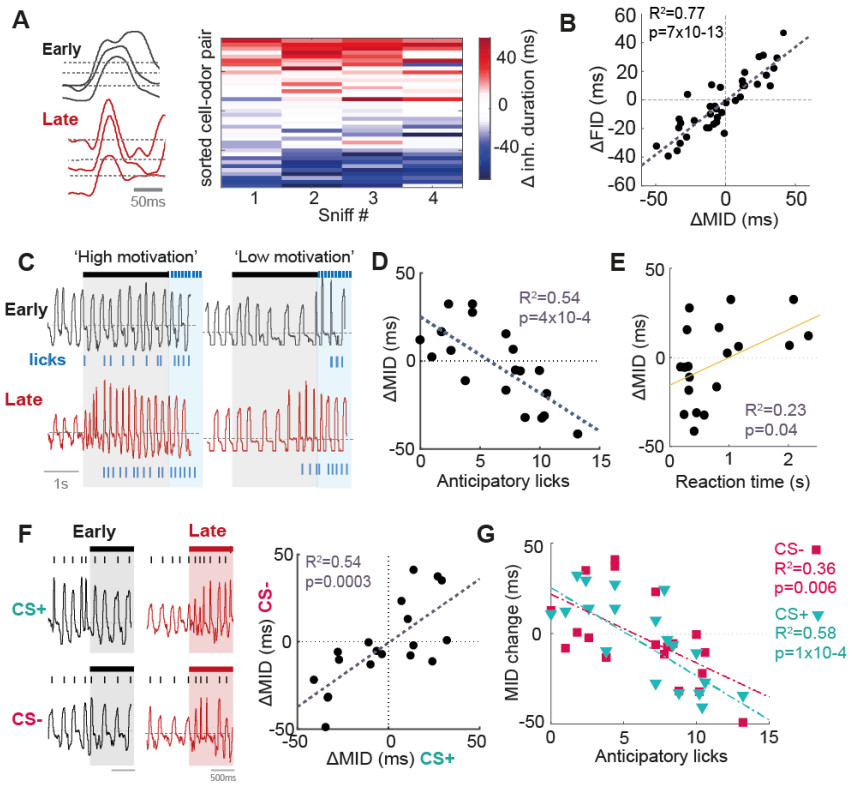

Figure 4.3. Sniff changes represent the emergence of an active sampling strategy

(**A**) Left: example flow traces showing duration of the first inhalation (FID) after odour onset between early and late trials. Right: Heatmap to show change in inhalation duration as a function of sniff number since odour onset. (**B**) Scatter of changes in MID versus changes in FID. (**C**) Example nasal flow traces during CS+ presentations for 'high motivation' (left) and 'low motivation' mice (right). 'Motivation' here refers to the number of licks during the odour stimulus (500-2000 ms, 'anticipatory' licks). Note sniff changes only occur for the 'high motivation' mouse. (**D**) MID change (averaged for each cell across CS+ and CS- stimuli) across learning as a function of the mean number of anticipatory licks in late trials for CS+ trials. (**E**) MID change (averaged for each cell across CS+ and CS- stimuli) across learning as a function of the reaction time calculated from divergent lick patterns. (**F**) Left: example traces showing how sniffing changes for one mouse between early and late trials for corresponding CS+ and CS- odours. Right: scatter of MID changes for the CS+ versus MID changes for the CS- for all 19 cells. (**G**) As for panel D, but now plotted separately for MID changes for CS+ stimuli and MID changes for CS- stimuli.

4.3.4. CHANGES IN SNIFF STRATEGY CORRESPOND WELL WITH MEAN RESPONSE CHANGES

Since the responses of MTCs recorded in awake animals were widely modulated by sniffing (Chapter 3, Fig. 3.2F), and mice displayed changes in sniff strategy across learning (Fig. 4.2 and 4.3), I next wanted to test what impact the changes in active sampling had on the response changes observed across learning.

I first split the dataset according to MID change: large MID change (>20 ms absolute change between early and late trials, n = 18), and small MID change (<20 ms absolute change, n = 20). Comparing heatmaps of response change between early and late trials for each dataset revealed that positive changes were exclusively displayed alongside large MID change (Fig. 4.4A). There was a significant increase in response variance for cell-odour pairs recorded alongside large MID change (early SD = 1.8 mV, late SD = 3.2 mV, p = 0.02 Bartlett test), but not for small MID change (early SD = 2.2 mV, late SD = 2.2 mV; p = 0.98 Bartlett test; Fig. 4.4B). Altogether, responses recorded alongside large MID changes accounted for 7/8 significant positive response changes, and 2/5 inhibitory response changes, and showed significantly larger variance in response changes compared to those recorded alongside small MID changes (large sniff change: SD = 1.9 mV, n = 18; small sniff change: SD = 1.1 mV, n = 20; p = 0.002, Bartlett test), and response changes in passive mice (passive SD = 1.1 mV, p = 0.002, Bartlett test, n = 18 vs 46), while the small change dataset was indistinguishable from passive controls (p = 0.94, Bartlett test, n = 20 vs 46). In particular, there were significantly more positive response changes (>1 mV) in the large sniff change group (39%) compared to small sniff change (5%) and passive mice (11%; p<0.01, bootstrapping, see methods; Fig. 4.4C).

To test the strength of associations between V_m response and active sampling further, I correlated the mean MID and V_m response across trials for each cell-odour pair. For cells undergoing positive response changes across learning, this resulted in striking, significant

correlations, as in Fig. 4.4D (left example), while those undergoing increases in inhibition showed no such tight correlation (Fig. 4.4E, right example). Overall, 88% (7/8) cell-odour pairs showing significant positive changes across learning displayed highly significant correlations ($p<0.01$) between V_m response and inhalation duration across trials. Increased inhibition (negative response change) however could not be explained by active sampling changes, with no significant correlations between changes in V_m response and inhalation duration for these 5 cell-odour pairs. This effect across the population resulted in a significant positive relationship between the response change occurring across learning and the R^2 of the correlation between MID and response across trials ($R^2 = 0.38$, $p = 4x10^{-5}$, $n = 42$; Fig. 4.4F).

In the previous chapter, I found that changes in response across learning, but not passively exposed mice, contributed to increased detectability and discriminability of the odour responses across the population. How did changes in active sampling impact on these changes in representation? To test this I again split the learning population according to large or small MID change as before (Fig. 4.4A-C). When recalculating the Euclidean distances for these individual datasets, I found that the increase in detectability largely occurred alongside large MID change (early peak = 25.1±1.0 mV, late peak = 33.7±1.4 mV, $p = 7x10^{-4}$, unpaired t-test; Fig. 4.4G), and was far smaller and less significant in those undergoing small MID change (early peak = 20.0±1.2 mV, late peak = 23.1±2.6 mV, $p = 0.04$, unpaired t-test; Fig. 4.4G). I found the same result for changes in discriminability, with a significant increase only in cases where ΔMID for both CS+ and CS- stimuli was large (large ΔMID: peak early = 13.2±0.8 mV, late = 19.6±1.8 mV, $p = 0.002$, unpaired t-test; small ΔMID: peak early = 15.4±1.0 mV, late = 16.1±1.5 mV, $p = 0.28$, unpaired t-test; Fig. 4.4H).

Thus, positive response changes and enhanced stimulus representation are associated with animals undergoing changes in active sampling, while negative response changes (increased inhibition), cannot be explained by sniff changes.

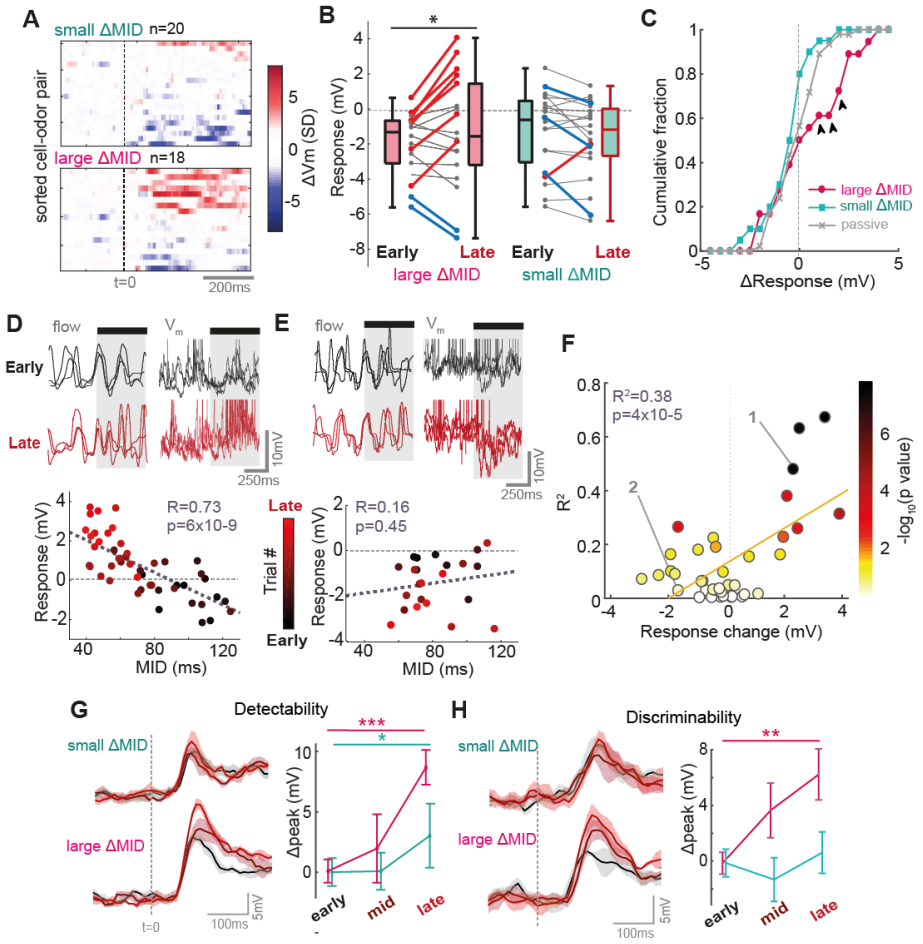

Figure 4.4. Changes in MID are strong predictor of excitatory response change across learning.

All data is from the learning dataset. (**A**) Response change heatmaps (late-early average V_m response) normalized by baseline SD, for small MID change (ΔMID<20ms) and large MID change (ΔMID>20 ms). (**B**) Plot of early and late membrane potential responses (first 500 ms) across learning for large ΔMID (left; n = 18 cell-odour pairs) and small ΔMID (right; n = 20 cell-odour pairs) separately. Thick red lines indicate significant positive change (p<0.01), thick blue lines indicate significant negative change. (**C**) Cumulative histograms for response changes in large ΔMID, small ΔMID and passive mice. Black arrowheads show significant differences between large ΔMID vs both small ΔMID and passive histograms. (**D**) Above: example nasal flow and V_m traces overlayed for 3 early and 3 late trials for a cell-odour pair undergoing significant increase in excitation across learning. Spikes have been clipped for display. Below: Scatter between MID and V_m response across trials for this cell-odour pair. Points have been colored according to trial number. (**E**) As for panel D, but for a cell undergoing a significant increase in inhibition across learning. (**F**) Scatter between the response change across learning (late-early), and the R^2 value for correlations as in panels D-E, coloured according to the p-value of the correlation. Note how all cases of strong positive response change exclusively show strong correlations with sniffing. *Continued on next page….*

(**G**) Euclidean distance as a function of time since odour onset (t = 0) between population vectors for odour response, and control vectors initiated by an inhalation during the inter-trial interval. This gives an indication of the detectability of the odour response across the sample. Black plot is calculated for early trials, maroon plot is calculated from mid-point trials, and red plot is calculated from late trials. Each is averaged over 5 trial subsets (see previous chapter methods for details), and shaded area indicates standard deviation. Response vectors were constructed from learning data that was split into cell-odour pairs recorded alongside large ΔMID (n = 18) and small ΔMID (n = 20). (**H**) As for G, but with the Euclidean distance measured between population vectors for the CS+ and CS- to give an indication of the discriminability of the two responses across the sample. Data was split into cell-odour pairs recorded alongside large MID change (>20 ms change for both CS+ and CS-, n = 8 cells) and small MID change (any other cell, n = 11 cells).

4.3.5. DYNAMICALLY ALTERING ACTIVE SAMPLING STATE CAUSES DYNAMIC SWITCHES IN RESPONSE

If the rapid sniffing is indeed an active strategy for odour acquisition during behaviour, we would expect the strategy to disappear if the task comes to an end (i.e. transition to passive odour exposure), and re-emerge only when the task reinitiates. To test this, I implemented a paradigm in which task engagement could be reversibly changed by physically removing and re-introducing the water reward spout (Fig. 4.5A), resulting in rapid switches between olfactory behaviour and passive exposure. Here I recorded from an entirely new cohort of mice, resulting in 8 cell-odour pairs. Mice would adapt their licking response after the port was removed, with licking to the CS+ eliminated after a variable number of trials, and in particular the anticipatory licking that predicts fast sniffing was abolished (Fig. 4.5B). Task disengagement was designated at the point where there was a very low rate of anticipatory licks (<4), and at least 2 consecutive misses (Fig. 4.5C-D). As predicted, animals robustly adapted their sniffing strategy upon elimination of the licking response after removal of the reward port (Fig. 4.5E), with MID increasing (slower sniffing). Reintroduction of the reward port rapidly restored fast sniff behavior (Fig. 4.5E). This reversible switch in sniffing strategy was observed for 6/8 of the cell-odour pairs recorded (Fig. 4.5F). Thus, sniffing behavior of an animal is dynamically dependent

on engagement in an olfactory task, congruent with the previous analysis in learning mice that indicated MID changes were an active sampling strategy (Fig. 4.3).

If active sampling determines neural responses as predicted from learning mice (Fig. 4.4), we would expect largely positive response changes to occur alongside emergence of the rapid sniffing strategy. For recorded cells during task engagement and disengagement, there were clear cases where responses were profoundly modulated according to task engagement, with excitatory responses only occurring when the task was engaged, and the animal sniffing rapidly (Fig. 4.6Ai and Bi). I found that 60% (5/8) of cell-odour pairs changed in this way robustly and reversibly between task engagement, disengagement and re-engagement (Fig. 4.6Aii and Bii). Consistent with the learning-related changes, positive changes in response always coexisted with the emergence of rapid active sampling (reduction in MID). Changes in response were again tightly linked to the sniff changes on a trial-by-trial basis, showing robust correlations between MID and response (Fig. 4.6C-D; FR: $R = -0.77 \pm 0.08$, $p < 1 \times 10^{-5}$; V_m: $R = -0.53 \pm 0.3$, $p < 0.05$), consistent with the idea that changes in neural responses are directly driven by sniff strategy. The correlations between MID and V_m were highly similar regardless of the current task engagement – i.e. if a mouse sniffed slowly during task engagement, this resulted in the same response as if he were sniffing slowly during task disengagement. This makes it more likely that the response change is solely the result of the change in active sampling state. Strikingly, response changes could occur within only a single trial upon recognition of task re-engagement (Fig. 4.6E) emphasizing the dynamic nature with which changes in active sampling state influence neural responses.

Presumably, for a cell to undergo increases in excitation during active sampling, it must receive weak direct excitation from a glomerulus (the only recorded cases of lateral indirect excitation occur within MTCs belonging to the same glomerulus - Christie and Westbrook, 2006). To get some idea of whether this was the case, I correlated the firing rate responses to odours during

task engagement, with the change in firing rate response between engagement and disengagement. Indeed, there was a strong correlation between the two variables, i.e. the more excitatory the response during engagement, the bigger the drop in excitation during disengagement ($R^2 = 0.77$, $p = 0.0008$, $n = 10$; Fig. 4.6F). The only insignificant response showed no change, while the only inhibitory response in fact showed a reduction in inhibition. We can thus potentially predict how a given cell-odour pair will change its response according to shifts in active sampling state according to its level of excitation during task engagement.

Thus, dynamic switches in active sampling state likely drive overt alterations in response, with rapid active sampling associated with a bias toward excitatory responses.

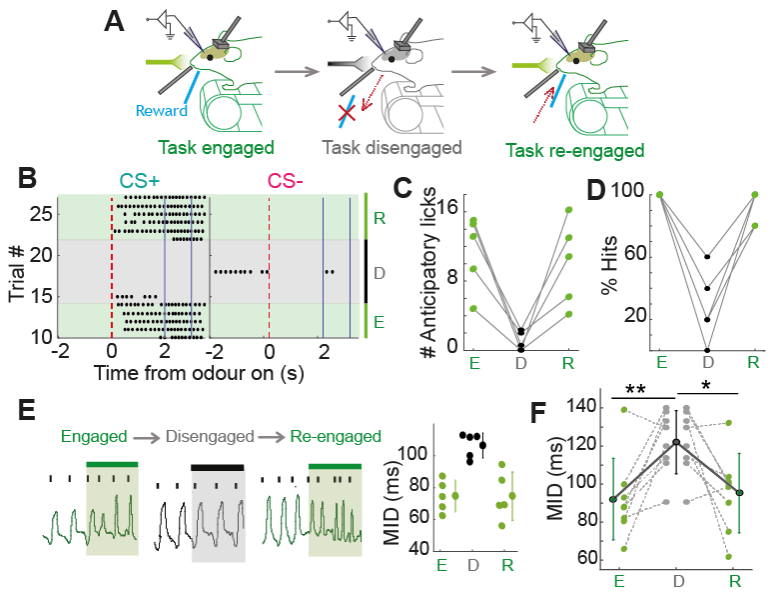

Figure 4.5. Rapid modulation of active sampling behaviour through task engagement switches

(**A**) Task engagement/disengagement paradigm. Mouse begins the recording performing the task at criterion (task engaged, E), then after some trials the reward port is removed from mouse reach, preventing the mouse from performing the conditioned response (task disengaged, D). After the mouse has given up trying to respond for some trials, the port is returned (task re-engaged, R). (**B**) Raster of licks made for one mouse across task engagement switches for the CS+ and the CS-. (**C**) Change in mean number of anticipatory licks to the CS+ across task disengagement switches for all 5 mice recorded from. (**D**) As for C but for the percentage of hits for the CS+. (**E**) Example sniff traces during the odour between task engagement switches, quantified for 5 trials of each state in the plot to the right. (**F**) Change in MID across the task engagement switches for all 8 cell-odour pairs (asterisks indicate p-values from paired t-tests between MID values. Engaged vs disengaged: mean MID change = 30±22 ms, p = 0.008; disengaged vs engaged: mean MID change = -26±25 ms, p = 0.03).

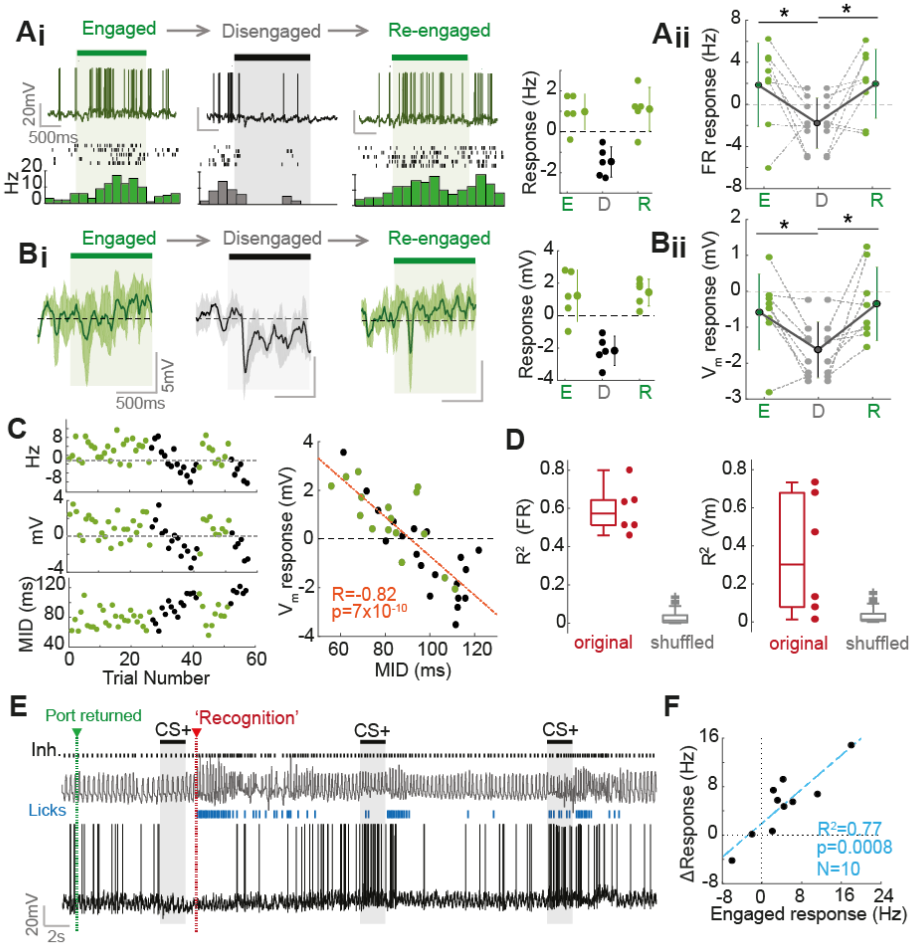

Figure 4.6. Dynamic switches in response according to active sampling state.

(**Ai**) Example FR responses corresponding to sniff traces in Fig. 4.5E across engagement switches: individual traces (top) and spike rasters and PSTHs below. Mean 2 s FR responses across 5 trials of each state are plotted on the right. (**Aii**) 2 s FR response change across all 8 cell-odour pairs. P-values obtained through paired t-tests. (**Bi**)-(**Bii**) as for A, but for membrane potential responses. (**C**) Left: top: FR response, middle: V_m response, bottom: MID for example in panels A and B as a function of trial number. Right: correlation between MID and V_m response on each trial for the same example cell-odour pair. (**D**) Boxplots to show corresponding R values for all 6 responses showing significant changes across engagement shifts, with R values for bootstrapped data below. Left: FR responses, right: V_m responses. (**E**) Example trace showing 3 consecutive CS+ trials across task re-engagement for one response. Port returned indicates when the reward port was returned and the task re-engaged. 'Recognition' indicates the point at which a free reward was used to indicate to the animal that the port had returned, and licking thus resumed. Note the rapid switch in valence of the FR response after recognition of task re-engagement. (**F**) Change in FR responses between engagement and disengagement (engage-disengage) plotted as a function of average 2 s FR response during task engagement.

4.3.6. EFFECT OF SNIFFING ON TEMPORAL FEATURES OF THE RESPONSE

In chapter 3, I showed that response onsets for V_m responses averaged over all trials were significantly earlier in behaving mice relative to passive mice. It is conceivable that differences in the properties of the first sniff within the stimulus could drive this change, since fluid dynamic models of nasal air flow show that faster air speed should influence odour response onsets (Shusterman et al., 2017). To first test this, response onsets were calculated for each mouse from a) trials in which the first sniff was 'slow' (>50th percentile first inhalation durations) and b) trials in which the first sniff was 'fast' (<50th percentile first inhalation durations). When comparing response onsets for each cell in between the fast and slow condition, there was a significant shift towards shorter latency onsets for fast sniffs which was similar in both passive (median latency shift = -10 ms, IQR = -5 to 35 ms n = 36, p = 0.03, paired T-test; Fig. 4.7A) and behaving animals (latency shift = -10 ms, IQR = 0- to 20 ms, n = 33, p = $3x10^{-5}$, paired T-test; Fig. 4.7A). The variance in response onset change across passive and learning mice could to a degree be explained by how fast the response was already during slow sniffs: there was a significant negative relationship between the response onset during slow sniffs, and the change in onset between slow and fast sniffs (R^2 = 0.26, p = $6x10^{-6}$, n = 69; Fig. 4.7B). This indicates that indeed, fast sniffs reduce response onsets. To test whether sniff variance could account for the difference in response onsets between passive and learning mice, I calculated response onsets across trials for inhalation durations within a specific narrow band (80-100 ms). Comparing response onsets for cell-odour pairs with more than 5 such eligible trials now resulted in no significant detectable difference between the two populations (passive: median = 90 ms, IQR = 80-110 ms, n = 27; learning: median = 80 ms, IQR = 70-110 ms, n = 22; p = 0.21, Ranksum; p = 0.14, Brown-Forsythe test; Fig. 4.7C). This strongly indicates that the shift towards shorter latency onsets seen between passive and behaving animals across all trials is driven by faster sniffs, rather than any physiological circuit change associated with behavioural state.

In the previous chapter I also showed that the degree of sniff locking during odour responses was enhanced in passive mice relative to learning mice (Chapter 3, Fig. 3.2F). It is known that fast sniffing attenuates sniff locking (Carey and Wachowiak, 2011), so I wanted to test whether differences in sniffing could explain the difference between passive and learning mice. I thus split trials according to the mean duration of the first four sniffs (over which sniff locking is calculated), either fast sniffs (<50th percentile mean duration) or slow sniffs (>50th percentile mean duration), and calculated the sniff modulation amplitude of each cell-odour pair. Consistent with previous reports that increased sniff frequency reduces sniff modulation, fast sniffing significantly reduced sniff modulation amplitudes in both passive (mean change (fast-slow) = -0.5±1.1 mV, p = 0.003, n = 41; Fig. 4.7D) and learning cell-odour pairs (mean change (fast-slow) = -0.8±0.9 mV, p = $9x10^{-6}$, n = 35; Fig. 4.7D). This reduction depended to a degree on how locked the cell was already during slow sniffing, with the most highly locked cells undergoing the greatest reduction in amplitude between slow and fast sniffs (R^2 = 0.22, p = $2x10^{-5}$, n = 76; Fig. 4.7E). To test difference between passive and behaving cell odour pairs without the confounding factor of sniff variance, I re-analysed the sniff modulation amplitudes for only trials which had a mean sniff duration between 0.25 and 0.33 ms (3-4 Hz sniffing), and compared the resulting amplitudes for cell-odour pairs with more than 10 eligible trials. While the mean sniff modulation strength did not significantly differ between passive and behaving mice as it had before (learning: median = 2.9 mV, IQR = 1.8-3.3 mV, n = 19; passive: median = 3.1, IQR = 2.2-5.1 mV, n = 20; p = 0.2, Ranksum; Fig. 4.7F), there was still a tendency for passive cell-odour pairs to display strong sniff locking of over 4mV sniff modulation amplitude (35% cell-odour pairs) compared to learning mice (10%). This was reflected in significantly higher variance in the sniff modulation amplitudes of passive relative to learning samples (p = 0.02, Bartlett test). Thus, while sniff frequency does affect sniff locking, it likely does not account for the entirety of the differences between the passive and learning mice.

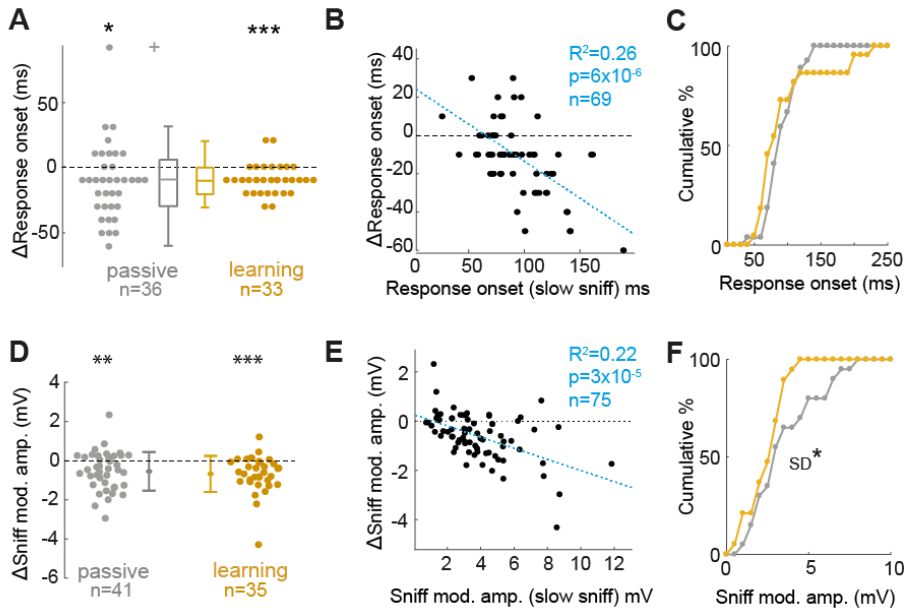

Figure 4.7. Rapid sniffing reduces response onset latency and sniff modulation amplitude.

(**A**) Changes in response onset between fast inhalation trials (<50th percentile first inhalation duration) and slow first inhalation trials (>50th percentile first inhalation durations) for both passive and learning cell-odour pairs. Asterisks refer to significance of paired t-test between response onsets for fast and slow inhalation trials. (**B**) Change in response onset between fast and slow sniff trials as a function of the response onset during slow sniff trials. (**C**) Cumulative histograms for response onsets of learning (n = 22) and passive cell-odour pairs (n = 27) across trials with first inhalation duration between 80 and 100 ms (only n>5 trials included). (**D**) As for A, but for the difference in sniff modulation amplitude of the odour response between fast sniff (mean duration first 4 sniffs < 50th percentile) and slow sniff trials (>50th percentile). Asterisks refer to significance of paired t-test between response onsets for fast and slow sniff trials. (**E**) As for B, but for the change in sniff modulation amplitude. (**F**) Cumulative histograms for sniff modulation amplitude of odour responses in learning (n = 19) and passive cell-odour pairs (n = 20) across trials with mean sniff duration between 250 and 330 ms (only n>10 trials included).

4.4. DISCUSSION

Animals universally acquire sensory information from the environment via active sampling behaviours, such as saccadic eye movement, whisking and sniffing. It is hypothesized that animals dynamically regulate active sampling for optimal sensory acquisition according to behavioural context (Ahissar and Assa, 2016; Yang et al., 2016). Eye movement, for example, is modulated according to the task at hand and varies between individuals (Rayner et al., 2007), while rodents dynamically modulate whisking behaviour to apparently optimise information acquisition, something which also varies between individuals (Zuo et al., 2011). Here I have shown that rapid inhalation (as indicated by reduced MID), emerges over the course of learning as an active sampling strategy for olfactory behaviour, with variance between individuals at least partly explained by motivational state. Additionally, I show that changes in sniff strategy are strong predictors of response change in behaving mice, with shorter latency responding and overtly increased excitation emerging alongside rapid active sniffing during the odour stimulus. This is the first direct physiological evidence, to my knowledge, that active sampling strategies are used to enhance sensory representation during behavioural tasks.

Mice change their sniffing behaviour for many reasons (Wachowiak, 2011): it has been reported that fast sniffing is exhibited in mice in response to non-olfactory specific events, such as auditory stimuli (Wesson et al., 2008a), and reward anticipation (Kepecs et al., 2007; Wesson et al., 2008a), while breathing rate increases during locomotion, presumably to meet increased respiratory demands (Bramble and Carrier, 1983). In such cases, the sniffing is unlikely to represent a strategy for olfactory decision. At the same time it has been noted that rodents do sniff fast during the odour stimuli for olfactory tasks, which more likely represents an active sampling strategy (Kepecs et al., 2007; Macrides et al., 1982; Rajan et al., 2006; Uchida and Mainen, 2003; Youngentob et al., 1987). Here, while reward prediction did affect absolute MID values, the sniff changes over the course of learning were not affected by reward contingency,

and in fact were correlated for the two odours (Fig. 4.3F). Moreover, these changes occurred even in the first inhalation after odour onset (Fig. 4.3A-B). Together this makes it more likely that the sniff changes reflect an active sampling strategy that mice may use to aid olfactory decision.

Consistent with previous studies (Wesson et al., 2009), we found a high variability of sniff strategy between mice. What this variance suggests is that, while this strategy may aid decision, it is not critical for odour identification, since some mice do not show fast sniffing and yet still perform the task perfectly well. As such the strategy is not critical for fundamental processes, such as identity coding. Rather, it may have an effect on perception of stimulus strength, as suggested by some studies in humans, where stronger sniffing decreased concentration thresholds for odour detection (Laing, 1983; Sobel et al., 2000), and by the increase in stimulus detectability across learning seen here (Fig 4.4G). Additionally, fast sniffing appears to aid discriminability of odours (Fig 4.4H), and could increase the speed of stimulus acquisition to accelerate decision, as suggested from imaging (Wesson et al., 2009), our analyses on stimulus detection time within the population, and the reduced response onsets during fast sniffing (Fig 4.7A).

I have found that around half of the between-animal variation in sniffing strategy can be explained by the motivational state of the mouse. If the sniffing strategy can indeed account for the improved early odour representation in MTCs, then the fact that only highly motivated mice show fast sniffing strategy makes sense, since they are driven to acquire the stimulus more quickly. Meanwhile less motivated mice are still capable of identifying the odour, and wait until the end of the stimulus to respond and acquire the reward. It is interesting to note that activation of orexin neurons in the lateral hypothalamus precedes rapid sniffing behaviour (personal communication with Conni Schoene and Denis Burdakov), and that the activity of such orexin neurons are thought to represent a general drive for exploration, e.g. during hunger

(Mahler et al., 2014). Fast sniffing may thus be intertwined with fundamental drives to explore, such as hunger and thirst. This is congruent with the fact that even sniffing in absence of odour is modulated by behavioural state, with learning (and therefore motivated) mice displaying increased variance in sniff frequency (Fig. 4.1).

The external flow and pressure sensors used here to measure sniffing have the great advantage in that they are quick and easy to use, with little chance of failure. However, in the awake mouse they prevent us from investigating some aspects of the sniff strategy, such as amplitudes, since changes in amplitude are ambiguous: they could occur by lateral movement of the naris relative to the sensor rather than actual amplitude changes. As such, there may be some aspects of the sniff change that I cannot quantify.

Emergence of active sampling during the task was in most cases associated strongly with positive response changes, and this largely came from cells which showed only weak responses during slower sniff cycles (Fig. 4.4A-B). Thus, rapid sniffing may boost weak excitation from OSNs. Secondly, response onset latency could be reduced through a rapid first inhalation during odour sampling. This can only be explained if such shortened inhalation durations reflect increased flow rates of air (and thus accelerated odourant delivery) into the nasal passage, rather than a simple shortened inhalation in absence of changed flow rate - an idea which is supported physiologically (Courtiol et al., 2011). Further, response type appears to have an impact on the effect of sniff changes on response: in the task engagement/disengagement paradigm, the greater the excitation during task engagement, the larger the drop in excitation during disengagement (Fig. 4.6F). While we must be aware that the sample size in this paradigm is small, I could hypothesize that rapid sniffing acts to increase the excitatory component of the response by boosting weak direct excitation from OSNs. Cases of indirect excitation have only been noted mitral cells of the same glomerulus via spillover glutamate and gap junctions, so it makes sense that such a phenomenon cannot occur if there is no direct feedforward excitation

(Christie and Westbrook, 2006). This could occur, for example, by an increase in the strength of OSN response with higher flow-rate sniffing, which would be supported by glomerular imaging studies (Cenier et al., 2013; Oka et al., 2009). Or, there could be a state change in the circuit during the olfactory task causing disinhibition of OSN input via reduced periglomerular feedback onto the incoming OSN terminals. The alternative hypothesis is that lateral inhibition in the circuit is in some way down-regulated during active sniffing, and this is to some degree supported by the observation that switches in valence – from inhibitory to excitatory – can occur as active sniffing emerges (e.g. Fig. 4.4D, 4.6Ai & Bi).

Changes in sniffing cannot account for all variation in response changes. Particularly, sniffing does not seem a good explanation for increases in inhibition, which occur in both passive and behaving animals at a low rate, and show only weak relationships with MID on a trial by trial basis (Fig. 4.4B and E). Firstly, there are some features of the sniffing behaviour we cannot acquire from our sniff recordings due to their external nature, for example sniff amplitudes, which could change across learning and account for other aspects of the variation. Secondly, other factors outside of sniffing could contribute to the remaining variance, such as top-down inputs or changes due to whole cell recording technique.

What could be the function in such a phenomenon? Rapid sniffing during olfactory sampling would indicate high levels of attention toward the olfactory stimulus, and previously it has been demonstrated that rapid sniffing improves olfactory performance, even on the timescale of a single sniff cycle (Kepecs et al., 2007). During odour sampling in the task-engaged context, olfactory information is important for behaviour, and thus the transfer of information should be increased (via increased number of spikes coding for the odourant). Conversely, during passive exposure, the odourant is biologically meaningless and the number of spikes used to encode the odour should be reduced. Thus the increase in excitation during active sampling could contribute to the efficiency of odour coding, by selectively facilitating the transfer of information only when

it is biologically relevant. Alternatively, the rapid sniffing in highly attentive mice could primarily be used to speed up odour acquisition, reducing the latency of response onset (Fig. 4.7A), with the FR changes occurring only as a by-product. The changes do appear to increase the detectability and discriminability of odour response across the population however (Fig. 4.4G-H), so it is plausible that the mean response changes do impact on odour representation itself. In either case, it is hard to imagine how the firing rate changes seen here are necessary for odour identity coding, since mice can perform the task even in absence of sniff changes, and because some stability in the identity code must be maintained to facilitate learning.

Overall, I have shown that highly motivated mice will alter their active sampling strategies according to the behavioural task. This sniffing is a strong predictor of the response changes associated with learning animals both within trials and across the population – particularly positive changes in response over the course of learning. While we can make some propositions, mechanistic basis underlying how the changes in sniffing evoke response changes is as yet unclear. The next chapter will investigate the mechanistic relationship between sniffing and response.

CHAPTER 5. **RESULTS**

MECHANISTIC RELATIONSHIP BETWEEN SNIFFING AND RESPONSE CHANGE

5.1. INTRODUCTION

I have thus far shown that changes in the active sampling state of the mouse coincide with overt changes in the representation of odours in the OB. The mechanism linking these changes in active sampling with changes in response are at this point, less clear.

There are two conceivable ways that changes in active sampling could alter responses in the OB. The first is the 'bottom up' effect on sensory input pattern. Each inhalation delivers a 'packet' of sensory information to the OB via OSNs, giving rise to a sniff modulation of the membrane potential. This has often been referred to as a 'theta oscillation' in the literature due to its frequency band similarity with that seen in the hippocampus, but to avoid confusion, I will only term it sniff modulation, since we know this comes as a result of direct rhythmic sensory input following inspiration (Grosmaitre et al., 2007; Margrie and Schaefer, 2003). Thus far sniff modulation has largely been demonstrated in anaesthetised animals (Cang and Isaacson, 2003; Fukunaga et al., 2012; Macrides and Chorover, 1972; Margrie and Schaefer, 2003; Phillips et al., 2012), though a handful of more recent data has shown consistently in the awake passive animal, that activity is locked to sniffing (Fukunaga et al., 2012; Kato et al., 2012). It follows that changes in the frequency of sniffing would alter the pattern of OSN input, resulting in changes in MTC activity. While there has been some investigation of glomerular activation, and MTC firing responses during changes in active sampling (see previous chapter introduction), no investigation to my knowledge has directly investigated how changes in the sniff cycle in awake mice affect subthreshold principal cell activity in the OB.

The second way active sampling could alter OB responses is via a top-down effect: alongside the change in sniff behaviour, it is conceivable that a cortical or neuromodulatory region sends information to the bulb (Shipley and Adamek, 1984) according to directed attention toward odour stimuli, e.g. preparing the OB for the transfer of olfactory information. For example, serotonergic neurons are known to play a role in sniff frequency control in the brainstem and

also gate OB odour responses (Petzold et al., 2009), so have been hypothesised to be involved in sensorimotor coordination of sniffing and olfactory activity (Dugué and Mainen, 2009). Orexigenic neurons of the brainstem also show activity correlated to rapid sniffing (unpublished data), and orexin has known effects on the OB (Apelbaum et al., 2005; Prud'homme et al., 2009).

While there is no evidence about the relative contributions of each in the OB during active sampling, in the barrel cortex during state changes accompanying spontaneous bouts of active whisking, evidence has been found for both bottom-up, whisk-locked contributions (Crochet and Petersen, 2006), as well as 'top-down' effects from cholinergic inputs (Eggermann et al., 2014). There is also an interaction between the two: top-down modulation can boost the whisk-locked contribution according to context, e.g. during social touch (Lenschow and Brecht, 2015). In the cortex, compared to the OB, deciphering the contributions is in some ways trickier, since there are multiple processing stages between peripheral sensory nerves and the cortex. However, in the whisker system, deciphering the bottom up contribution is in other ways easier since the peripheral nerves can be easily cut, or whiskers removed. Additionally, in our study, uninterrupted sniffing and OSN input is a necessity for olfactory behaviour. Thus to investigate the mechanisms, we must utilise different approaches to those previously used in cortex.

There are two broad predictions we can make if the effect of sniffing on activity is based on bottom-up input changes from OSNs. Firstly, we would expect sniff changes to have similar effects on response even in absence of olfactory attention (where there is no olfactory behaviour), and even in absence of wakefulness (where top-down input is presumably absent). Secondly, since sniff-modulation of the membrane potential is inherited from this bottom-up pathway as shown by naris occlusion experiments (Margrie and Schaefer, 2003; Courtiol et al., 2011), we would predict that strongly sniff locked cells would be more sensitive to changes in sniffing compared to weakly sniff-locked cells.

To test these predictions, I utilise whole cell recordings during changes in sniff behaviour in a range of situations: a) during evoked fast sniff behaviour during odour stimulus in passive mice, b) during controlled, simulated fast sniffing in double-tracheotomised mice, and c) during the ITI (in absence of odour) in passive and behaving mice. The latter also provides a way to distinguish mitral and tufted cell phenotype, and allows us to compare response changes across learning in mitral and tufted cells.

5.2. CHAPTER METHODS

5.2.1. EFFECT OF FAST SNIFFING ON BASELINE V_M

For each ITI, the mean V_m was calculated during sniffs of duration of less than 0.2 s given the preceding sniff was also within this duration range ('fast sniffs'). This mean V_m was then normalised according to the mean V_m during sniffs of duration 0.25 and 0.3 s within the same ITI to calculate the 'fast sniff-evoked V_m'. Only cells with at least 20 such 'fast sniffs' within the recording were considered for the analysis. To determine significance, a bootstrapping method was used: the mean V_m for all sniffs within a trial was randomly shuffled, and the shuffled data analysed as before 100 times. The actual fast-sniff evoked V_m was then compared to the 5^{th} and 95^{th} percentiles of the shuffled distribution in order to assign significance.

5.2.2. SURPRISING TACTILE STIMULUS EXPERIMENTS

To evoke fast sniffing behaviour during odour stimuli in passive animals, on a small proportion of trials (20%), a tactile air puff stimulus accompanied the odour stimulus, and was applied to the whisker pads. To compare groups of responses with maximal difference in mean inhalation duration, the five trials with lowest mean inhalation duration were selected and compared to the five trials with highest mean inhalation duration, regardless of whether or not the low inhalation duration was elicited by the whisker stimulus.

5.2.3. DOUBLE TRACHEOTOMY

Two mice were anaesthetised with 'sleep-mix' (0.05 mg/kg Fentanyl, 5 mg/kg Midazolam, 0.5 mg/kg Medetomidine), and both local and general analgesia applied as above for head-fixation. After the head-plate surgery, a double tracheotomy was performed by exposing the trachea and inserting two catheters, one directed to the lungs through which the mouse could freely breathe, and the other directed to the nasal passages through which flow was controlled. To mimic sniffing, a peristaltic pump (Ismatec) was used to generate flow inward through the nares, with a flow controller to buffer out fluctuations and the periodic opening of a 3-way valve used to simulate regular inhalations, either at 3.3 Hz (100 ms opening times), or 6.6 Hz (50 ms opening times).

5.2.4. PUTATIVE MITRAL CELL VERSUS TUFTED CELL IDENTIFICATION FROM THETA TUNING

For each cell both the phase preference and effect of fast-sniffing on baseline V_m was calculated. An initial cutting angle was arbitrarily placed at 4.11 radians, where there visibly appears a clear separation between depolarising and hyperpolarising cells tuned to differing phases (Fig. 5.4G). A second cutting angle was systematically used to separate the population into two groups according to phase preference. For every cutting angle, a p-value was calculated using an unpaired t-test between the values for the fast-sniff evoked V_m from each group. The cutting angle (0.39 radians) giving the most significant difference ($p = 9x10^{-4}$, Ranksum, n = 15 pMCs, 11 pTCs; Fig. 5.4F) was considered the optimal angle to separate putative mitral cells from putative tufted cells. The putative assignment to MC or TC was confirmed morphologically for 8 cells, with MC and TC distinction based largely on soma location relative to the mitral cell layer, as dentritic reconstruction was in many cases incomplete (Fukunaga et al., 2012).

5.3. RESULTS

5.3.1. FAST SNIFFING EVOKES ODOUR RESPONSE CHANGES IN PASSIVELY EXPOSED AWAKE MICE

Since MTC activity in the awake mouse is indeed modulated by the sniff cycle, it is possible that changes in response occurring with rapid sniffing in behaving mice could result from bottom-up changes in the sniff-locked input pattern from OSNs. If response changes due to fast sniffing are mediated by such a bottom-up mechanism, one prediction is that, since sniff modulation amplitudes during learning are comparable (and in some cases even larger) in passive mice relative to learning mice (Chapter 4, Fig. 4.7F), that sniff changes even in a passive mice will evoke changes in activity. I thus wanted to assess changes in odour response where changes in sniffing have been evoked during the stimulus in absence of an olfactory task. Non-olfactory, surprising stimuli have previously been reported to evoke fast sniffing (Wesson et al., 2008a). Here I attempted to evoke fast sniffing using gentle, unexpected tactile stimulation to the whiskers (Fig. 5.1A).

Indeed, when tactile stimulation was paired with odour stimulation, sniff rates were increased (reduced MID: Fig. 5.1B) quantitatively mimicking the MID changes seen during learning (learning ΔMID (fast-slow) = -34±8 ms n = 26; passive ΔMID = -38±12 ms, n = 10; p = 0.29, unpaired t-test; Fig. 5.1C) and even exceeding sniff frequency changes seen in learning mice (learning Δfrequency (fast-slow) = 1.38±0.8 Hz, n = 26; passive Δfrequency = 2.2±0.5 Hz, n=10; p = 0.01, unpaired t-test; Fig 5.1C). When comparing slow sniff and fast sniff trials from such animals, fast sniffing evoked a variety of different changes in V_m response between -0.6 and 2 mV, with some very weak insignificant changes (bottom example, Fig. 5.1D), and some very strong significant changes (top example, Fig. 5.1D). Over the 10 cell-odour pairs, fast sniffing resulted in a significant change in response for only one cell odour pair, and across the sample caused significantly more positive responses during fast sniffing (fast-slow ΔV_m = 0.65±0.82 mV, p = 0.03, paired T-test, n = 10; Fig. 5.1E). This is congruent with the results of the previous chapter

in rapidly sniffing behaving mice, where positive response changes occurred alongside large MID changes (Chapter 4, Fig. 4.4 and 4.6). This suggests that changes in sniff pattern cause changes in response in awake animals, even in absence of olfactory attention.

These changes could be mediated through bottom-up changes in input pattern, or they could be a result of a top-down input associated with the surprising tactile stimulus. To test this I considered the second prediction of the bottom-up mechanism: the variance in response changes associated with fast sniffing should be explained by variance in the sniff locking properties of the cell. For example, a cell with a high sniff modulation amplitude will necessarily have a high degree of sniff locked input from OSNs, and if sniffing changes, we expect the impact on the activity of this cell to be dramatic. Conversely, if a cell shows very little sniff locked input, and a low sniff modulation amplitude, we would expect the impact of sniffing to be relatively low on the cell's activity.

To test whether the variable response changes seen alongside fast sniffing in the passive mice were explained by sniff locking properties, I compared sniff modulation amplitudes of subthreshold membrane potential during the odour stimulus with absolute response changes seen between slow and fast sniff trials. It was noted that responses with large sniff modulation amplitudes showed large and overt changes in response due to fast sniffing, while others with much lower sniff modulation showed relatively small changes (Fig. 5.1D). Indeed, the magnitude of the response changes across all cell-odour pairs were highly correlated with the amplitude of sniff modulation ($R^2 = 0.71$, $p = 0.002$, $n = 10$; Fig. 5.1F). Thus it seems likely that such response changes evoked by sniff changes in passive mice are a result of bottom-up changes in the sniff-locked input pattern.

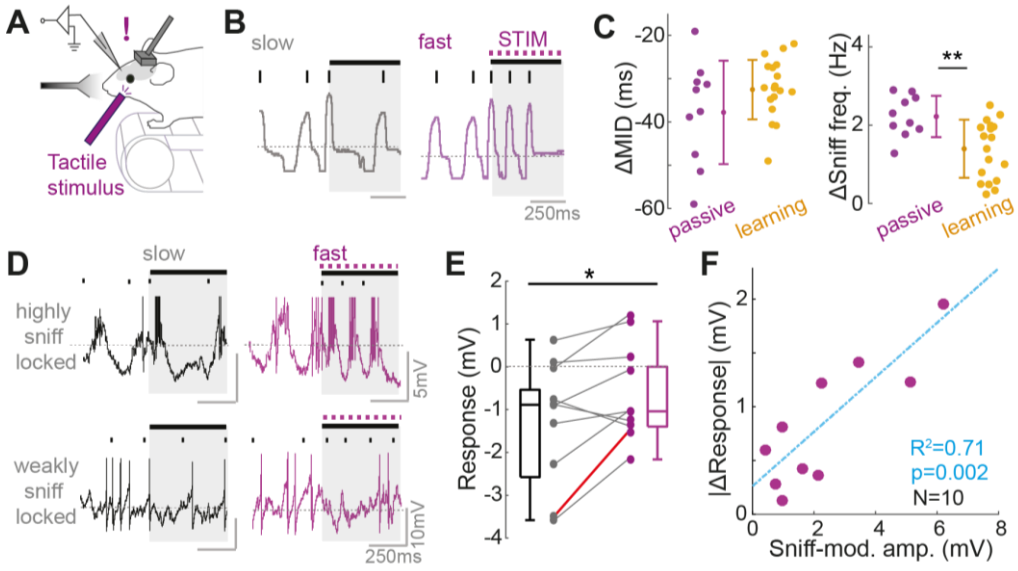

Figure 5.1. Sniff-related response changes in passive mice evoked by surprising tactile stimulation

(A) Experimental set up for tactile stimulation of passive mice: surprising tactile stimulus from gentle air stream to whisker pads is coupled to odour stimulus on a random subset of trials. (**B**) Example traces show nasal flow of one mouse during a control trial (grey, 'slow') and a tactile stimulus trial (purple, 'fast') (**C**) Right: Graph to show changes in MID between 5 trials of 'slow' sniffing and 5 trials of 'fast' sniffing for 10 mice. The same is shown in gold for learning mice (n = 26) which showed the emergence of rapid active sampling across learning. Left: As for right, but for sniff frequency changes. Frequency changes in passive mice significantly exceeded those seen in learning mice. (**D**) As for B, but for V_m response traces. Black ticks show inhalation onsets. Top example shows a cell with a large sniff modulation amplitude during response, while the bottom example shows a cell with a small sniff modulation amplitude during response. (**E**) Mean response changes for 10 cells between 'slow' and 'fast' sniff trials ($p<0.05$, paired T-test). Red line shows the only cell-odour pair to show significant change. (**F**) Scatter of response change between slow and fast sniff trials versus sniff modulation amplitude during the odour.

5.3.2. FAST SNIFFING EVOKES ODOUR RESPONSE CHANGES IN ANAESTHETISED MICE

While the correlation between sniff modulation amplitude and response change makes it likely that changes in response seen in passive animals during evoked sniff changes are due to changes in OSN input pattern, it is still possible that top-down inputs could play a role. To test further whether the response changes seen in passive mice could be due to tactile or neuromodulatory input, I sought to evoke similar sniff changes in anaesthetised mice, where top-down input is presumably silenced. To this end, a double tracheotomy was performed on two anaesthetised mice (Fig. 5.2A), and flow was controlled through the naris to mimic either slow sniffing (valve opening = 3.3 Hz, duration = 110 ms), or fast sniffing (valve opening = 6.6 Hz, duration = 60 ms) during the odour stimulus, independent of tracheal breathing. The resulting changes in nasal flow quantitatively matched or even exceeded those seen during learning for both MID change (learning: ΔMID (fast-slow) = -34±8 ms n=26; anaesthetised: ΔMID = -43±5 ms, n = 9; p = 0.004 unpaired t-test) and sniffing frequency change (learning: Δfrequency (fast-slow) = 1.38±0.8 Hz, n = 26; anaesthetised: Δfrequency = 3.7±0.4 Hz, n = 9; $p = 5x10^{-8}$; Fig. 5.2B).

Alongside the sniff changes, odour response changes could again occur during the first 500ms of the stimulus (Fig. 5.2C). However, unlike for passive mice, these did not show a consistent positive change between slow and fast sniffing (mean ΔV_m (fast-slow) = 0.28±0.66 mV p = 0.8, paired-t-test; Fig. 5.2D). Overall, 2 out of 9 cell-odour pairs showed a significant change, while there were 7 responses that remained fairly stable. Again, the variance in these response changes could be explained by the amplitude of sniff modulation of the responses, with a significant correlation between theta amplitudes and response change magnitude ($R^2 = 0.67$, p = 0.006, n = 9; Fig. 5.2E). This correlation, though slightly shifted downward in the y-axis (potentially due to the difference in absolute MID values), showed a very similar gradient to that seen in passive mice (0.25). Thus it seems that the response changes due to sniff changes in both

passive and anaesthetised mice are a common result of changes in the pattern of sniff locked input.

Previous work looking at how sustained high sniff rates affect odour responses in glomeruli in fact report an attenuation of response magnitude at long timescales, perhaps owing to adaptation mechanisms (Verhagan et al. 2007). While this was not true of the initial 500 ms in my anaesthetised mice, I did note that at longer timescales (500-2000 ms after odour onset), some responses showed dramatic changes that were not present at the start, including diminishing responses and even reversals of polarity (Fig. 5.2F). Such changes resulted in significantly more positive responses at late timescales during fast sniffing. Instead of being a function of theta amplitude ($R^2 = 0.001$, $p = 0.91$, $n = 9$), these changes appeared to depend on the response type, with larger inhibitory responses showing the largest positive changes ($R^2 = 0.49$, $p = 0.03$, $n = 9$; Fig. 5.2G), indicating a different mechanism to changes occurring early in the stimulus, and congruent with the idea that these are a result of response attenuation (Verhagan et al., 2007). Since I focus only on the first 500 ms of the response in my behaving mice, (arguably the only behaviourally relevant part of the stimulus based on reaction times (see Chapter 2, Fig. 2.5), this result is of little use to deciphering the mechanism of response change, but it is interesting to note that the mechanisms on play at longer timescales of rapid sniffing may be different to those at earlier ones.

Thus, early response changes due to evoked sniff changes in anaesthetised mice are similarly the result of bottom-up changes in input pattern.

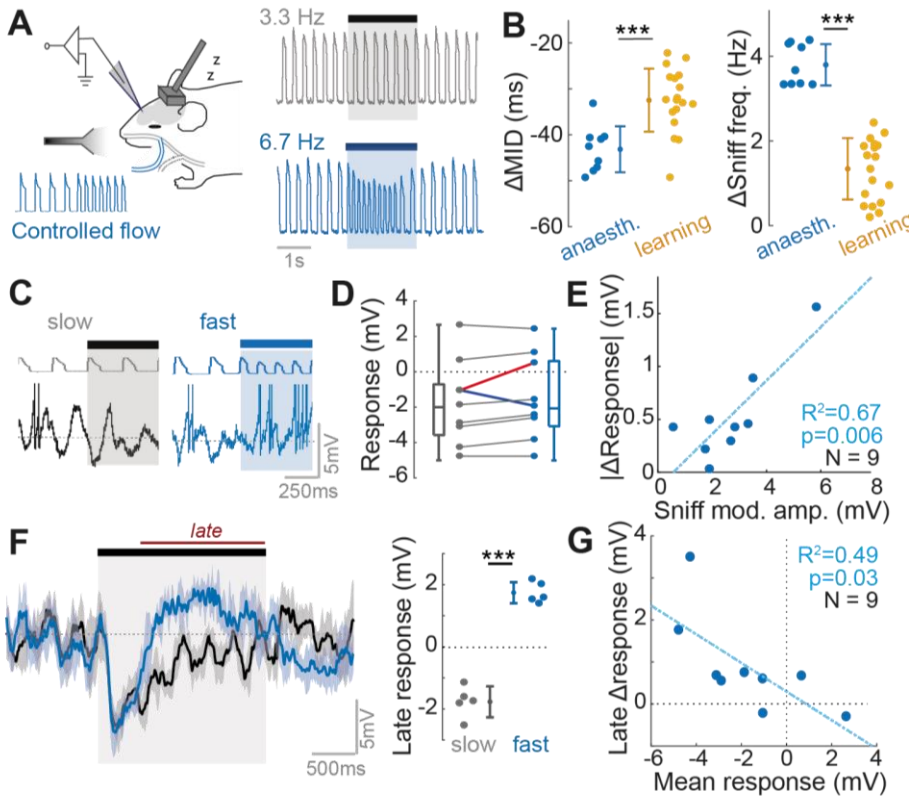

Figure 5.2. Sniff changes in double-tracheotomised anaesthetised mice result in response changes

(**A**) Right: diagram to show experimental set up: anaesthetised mice breathe freely through one tube connecting the trachea to the lungs, while flow is manually controlled through the nasal passage via a separate tracheotomy. Left: example nasal pressure waveforms measured externally from the naris during controlled nasal flow. Top trace shows the pressure during a slow sniff trial (3.3 Hz sniffing), and below shows the same during a fast sniff trial (6.7 Hz sniffing). (**B**) Graphs to show changes in MID and sniff frequency between 5 trials of 'slow' sniffing and 5 trials of 'fast' sniffing for 10 mice. The same is shown in gold for learning mice which showed large MID changes (n = 18). (**C**) As for nasal pressure traces in A, but for V_m response traces for one cell-odour pair with a large sniff modulation amplitude. (**D**) Mean response changes for 9 cells between 'slow' and 'fast' sniff trials. In thick red is the example in D, in thick blue is the only other significant response change. (**E**) Scatter of response change between slow and fast sniff trials versus sniff modulation amplitude during the odour. (**F**) Right: example mean response waveforms during 5 slow (black) and 5 fast (blue) sniff trials for one cell-odour pair showing a prominent change late in the odour. Shaded area shows standard deviation. Red bar indicates region of stimulus considered the 'late' response. Left: mean response late in the odour (0.5-2 s after odour onset) compared for example in G for 5 slow sniff and 5 fast sniff trials. P<0.001, t-test. (**G**) Scatter of late odour response changes as in F for all 9 cell-odour pairs as a function of the mean response in slow sniff trials.

5.3.3. RESPONSE CHANGES DURING BEHAVIOUR EXCEED THAT PREDICTED BY SNIFF LOCKING PROPERTIES

In absence of olfactory behaviour, the response changes due to sniffing in both anaesthetised and passive mice are dependent on sniff locking properties, making them likely to come largely from bottom-up mechanisms. How do the response changes occurring with active sniffing changes during behaviour correspond to those seen during sniff changes in absence of olfactory behaviour? To analyse this, I pooled MTC recordings in both mice learning the task, and mice in the task engagement vs disengagement paradigm, and selected the cell-odour pairs where MID was changed by at least 20ms between early and late (or engaged vs disengaged) trials (e.g. Fig. 5.3A; n = 26 cell-odour pairs). Response changes for behaving mice undergoing large sniff changes showed a generally wider spread than in anaesthetised or passive mice, and showed a much higher incidence of significant response change (behaving: 54%, 14/26 cell-odour pairs, passive: 10%, 1/10 cell-odour pairs, anaesthetised: 22%, 2/9 cell-odour pairs; $p<0.05$, unpaired t-test between 5 fast and 5 slow sniff trials; Fig. 5.3B).

Secondly, since the response changes due to fast sniffing showed a common relationship with sniff-locked input properties in both passive and anaesthetised cell-odour pairs, this provided a tool with which I could test whether the response changes during learning could be predicted by their sniff-locking properties in the same way. I noted that in behaving mice, even cells with low sniff modulation amplitude could undergo large changes in response alongside the emergence of rapid sniffing (e.g. Fig. 5.3A). Correlating response change with sniff modulation amplitude revealed no relationship in the behaving cohort ($R^2 = 0.02$, $p = 0.55$, $n = 26$), and compared to the correlations in passive and anaesthetised cases, the response changes in behaving animals were far larger than that predicted by their sniff-locking properties (Fig. 5.3C). Using the linear regression model calculated between sniff modulation amplitude and response change in passive cell-odour pairs, I calculated the expected change due to sniffing for all cell-

odour pairs in behaving mice based on their sniff modulation amplitudes (ΔV_{ex} = 0.26*T+0.21 mV, where ΔV_{ex} = expected absolute V_m response change in mV, and T = sniff modulation amplitude in mV). Comparing actual changes to expected changes revealed that changes in behaving mice significantly exceeded the expected change (mean difference (actual-expected) = 0.55±1.2 mV, p = 0.03, paired t-test, n = 26; Fig. 5.3D). With this analysis it was also possible to show that response changes for passive mice were also slightly larger than those seen for tracheotomised anaesthetised mice, as response changes in the latter were significantly smaller than those expected based on the linear regression calculated from passive data (mean actual-expected = -0.38±0.26 mV, p = 0.002, paired t-test, n = 9; paired t-test; Fig. 5.3D), which may be due to state-dependent differences, or differences in overall sniff changes.

While this suggests that sniff-evoked response changes in behaving mice exceed those expected based purely on sniff-locked feed-forward input, this does not mean that such response changes are any less linked to the sampling behaviour of the animal. When comparing R^2 values for the correlation between MID and V_m response across trials for each cell odour pair, we found no significant differences in the distributions between anaesthetised, passive and behaving mice (Fig. 5.3E), and the latter if anything show larger R^2 values (behaving: median = 0.16, IQR = 0.03-0.27; passive: median = 0.10, IQR = 0.03-0.21; anaesthetised: median = 0.03, IQR = 0.01-0.20; $p>0.05$, ranksum) and more frequent significant relationships (behaving: 46%; passive: 40%; anaesthetised: 20%; $p<0.05$ linear regression).

Thus, the response changes in behaving animals across learning cannot fully be explained by the bottom-up effect of sniff frequency on input alone, and rather it seems there may be an additional component which boosts the changes during odour-directed active sampling.

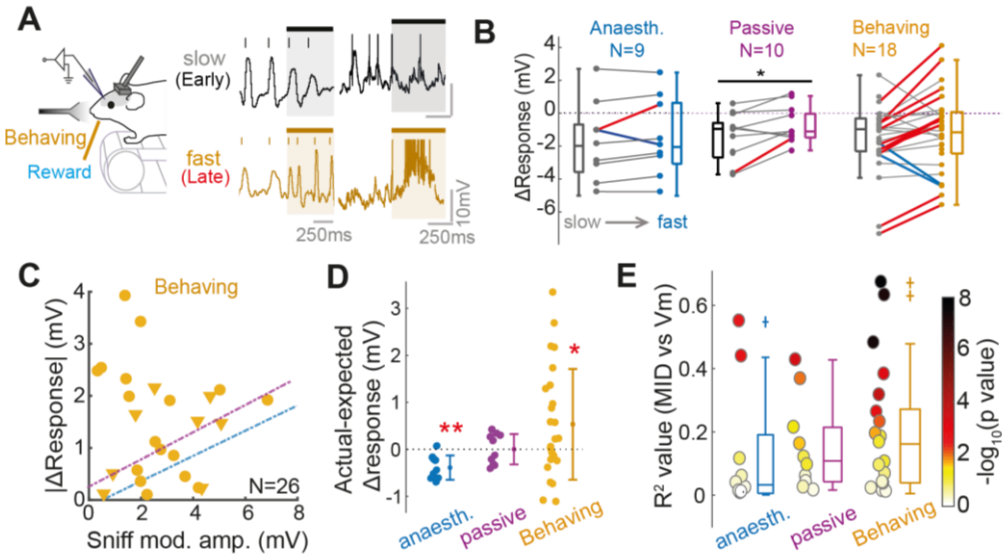

Figure 5.3. Response changes due to fast sniffing in behaving mice exceed those predicted by bottom-up mechanisms

(**A**) Experimental set up: pooling data from all behaving mice (both those undergoing learning, and those taking part in task engagement/disengagement paradigm) where emergence of fast sniffing occurred as in example nasal pressure traces and associated V_m response traces (with very small sniff modulation amplitude) from one example learning cell-odour pair. (**B**) Graph to show changes in V_m response between 5 trials of 'slow' sniffing and 5 trials of 'fast' sniffing across all three paradigms, anaesthetized, passive and behaving. Thick lines indicate significant changes ($p<0.05$, unpaired t-test between slow and fast trials; red=positive; blue=negative), thin grey lines indicate insignificant changes. (**C**) Scatter of absolute response change against sniff modulation amplitude of the odour response for cell-odour pairs recorded during learning (circle, n = 18) and task-engagement/disengagement (triangle, n = 8), where a large change in MID (>20 ms) occurred. Correlations for passive (purple) and anaesthetized (blue) are included for comparison. (**D**) Comparison of errors (actual-expected) when calculating expected response change based on the sniff modulation amplitude of the response (0.26 mVxT_{amp}+0.21 mV, where T_{amp} = sniff modulation amplitude), for anaesthetized (blue), passive (purple), and behaving (gold = learning or task engaged/disengaged). Red asterisks indicate significant differences when analyzing each dataset with a paired t-test between actual and expected response changes. (**E**) Comparion of R^2 values between MID and V_m response calculated across trials for each cell odour pair undergoing large MID change in anaesthetised, passive and behaving mice.

5.3.4. SPONTANEOUS SNIFF BOUTS IN ABSENCE OF ODOUR CAUSE ACTIVITY CHANGES

A previous study in the visual system has shown that modulation of response by saccades happens in a way temporally locked to the period of sampling (50 ms prior to saccade; Han et al., 2009). I wanted to test whether this was also the case in my behaving mice. Since activity even in absence of odour is widely modulated by the sniff cycle (Cang and Isaacson, 2003; Fukunaga et al., 2012; Macrides and Chorover, 1972; Chapter 3, Fig. 3.1H), and response changes are dependent on sniff locking properties during the odour, this made it likely that any sniff change even in absence of odour would cause activity changes. I wanted to test whether in behaving mice, the increased sensitivity of responses to fast sniffing occur only during the odour stimulus, or whether there is a generally increased sensitivity that extends even outside the stimulus sampling period. To examine this, I made use of spontaneous bouts of rapid (>5Hz) sniffing that occur in awake mice during the inter-trial interval – i.e. in absence of odour (Fig. 5.4A).

It was clear that in certain cells, overt changes in activity would occur coinciding with such rapid sniff bouts. Such overt changes could be both excitatory and inhibitory (Fig. 5.4A). Quantifying the mean membrane potential during sniffs of duration <0.2 s (>5 Hz), and comparing this to the membrane potential of adjacent sniffs of slower sniff durations (between 3 and 5 Hz) across 26 MTCs (pooled between passively exposed and behaving cell-odour pairs) revealed almost two thirds significantly changed their mean potential during fast sniffing, with 7 depolarizing and 9 hyperpolarizing ($p<0.05$, bootstrapping – see methods, Fig. 5.4A). Thus, sniff changes evoke response changes even in absence of odour.

To test any differences in sensitivity to sniff change caused by behavioural state, I then split the data into those from behaving mice (n = 16) and those from passive mice (n = 10). To test how these depended on bottom-up sniff locked input, I again compared the magnitude of the response changes to their sniff modulation amplitudes, as I did for those during odour response.

Like response changes during the odour stimulus, passive cell-odour pairs displayed significant correlations between sniff modulation amplitude and the magnitude of V_m change during fast sniffing (R^2 = 0.56, p = 0.01, n = 10), while for behaving mice this was not true (R^2 = 0.07, p = 0.31, n = 16). However, the pooled datasets together resulted in an even more robust correlation (R^2 = 0.46, p = 0.001, n = 26; Fig. 5.4B), indicating that the generally smaller variance in sniff modulation amplitudes in the behaving sample (mean sniff modulation amplitude = 1.4±1.0 mV, n = 16) compared to passive mice (2.4±1.7 mV) was likely the cause of the lack of significant result in the behaving mice. When comparing the expected V_m change (as calculated using the linear model generated from the linear regression, $\Delta V_{ex} = 0.31*T+0.01$, where ΔV_{ex} = expected absolute V_m change in mV, and T = sniff modulation amplitude in mV), I found that the difference between expected and actual V_m change did not significantly differ from zero for either passive (mean actual-expected = 0.17±0.57 mV, p = 0.37, paired t-test, n = 10) or behaving cell-odour pairs (mean actual-expected = -0.11±0.36 mV, p = 0.25, paired t-test, n = 16; Fig. 5.4C). Additionally, the differences did not significantly differ between passive and behaving datasets (p = 0.14, unpaired t-test; p = 0.1, Bartlett test). Altogether this indicates that increased sensitivity to sniff change during behaviour is only true during odour sampling.

Since there was high heterogeneity as to whether a cell would depolarise or hyperpolarise during fast sniffing, I sought to determine whether the sign of response change was also predictable from sniff-locking properties. It is known that the sniff-driven circuits of mitral and tufted cells differs during baseline activity. MCs are thought to be driven by feed-forward inhibition, while TCs are driven by feed-forward excitation (Fig. 5.4D; Fukunaga et al., 2012), and this is thought to give rise to their differential sniff tuning properties: inhalation and exhalation is preferred by each respective cell type. To test this in awake mice, I recovered 9 morphologies of MTCs (e.g. Fig. 5.4E, and categorised them as MCs (n = 5) or TCs (n = 4) based on soma location relative to the mitral cell layer (Fig. 5.4J). Congruent with the previous data in anaesthetised

mice, the two cell types had subthreshold membrane potential which was locked to different phases of the sniff cycle: morphologically-confirmed MCs locked to inhalation, and the post-inhalation pause seen in awake animals, while TCs locked to exhalation (Fig. 5.4F). Given the feedforward circuit architecture proposed from anaesthetised mice (Fukunaga et al., 2012), it follows that, for each cell type, we have different expectations for activity change during fast sniffing: MCs would relatively hyperpolarise when sniff frequency increases, while TCs would depolarise. To test whether these sniff-driven circuit differences could contribute to the sign of fast-sniff induced activity change, I examined the relationship between phase preference and the effect of fast sniffing. Indeed, the sign of the change in activity during fast sniffs was strongly related to the phase coupling of the cell to the sniff cycle (Fig. 5.4G), with inhalation-locked cells hyperpolarising and exhalation-locked cells depolarising. Defining the phase boundaries for best separation of hyperpolarising and depolarising cells (as drawn in Fig. 5.4G) allowed definition of putative MC and TC based on phase, and the phase preferences of morphologically identified MCs and TCs conformed to these boundaries (Fig. 5.4G, red triangles and blue diamonds). Cells within the putative MC boundaries showed significantly more hyperpolarising effects of fast sniffing than those within the putative TC boundaries (putative MC, median ΔV_m = -0.39 mV, IQR = -0.66 to -0.17 mV, n = 16; putative TC median ΔV_m = 0.19, IQR = 0.08-0.66, n = 11; p = $9x10^{-4}$, Ranksum; Fig. 5.4H).

Thus, in absence of olfactory stimulation, the effect of fast sniffing on response is again strongly predicted by the sniff-driven input of the cell.

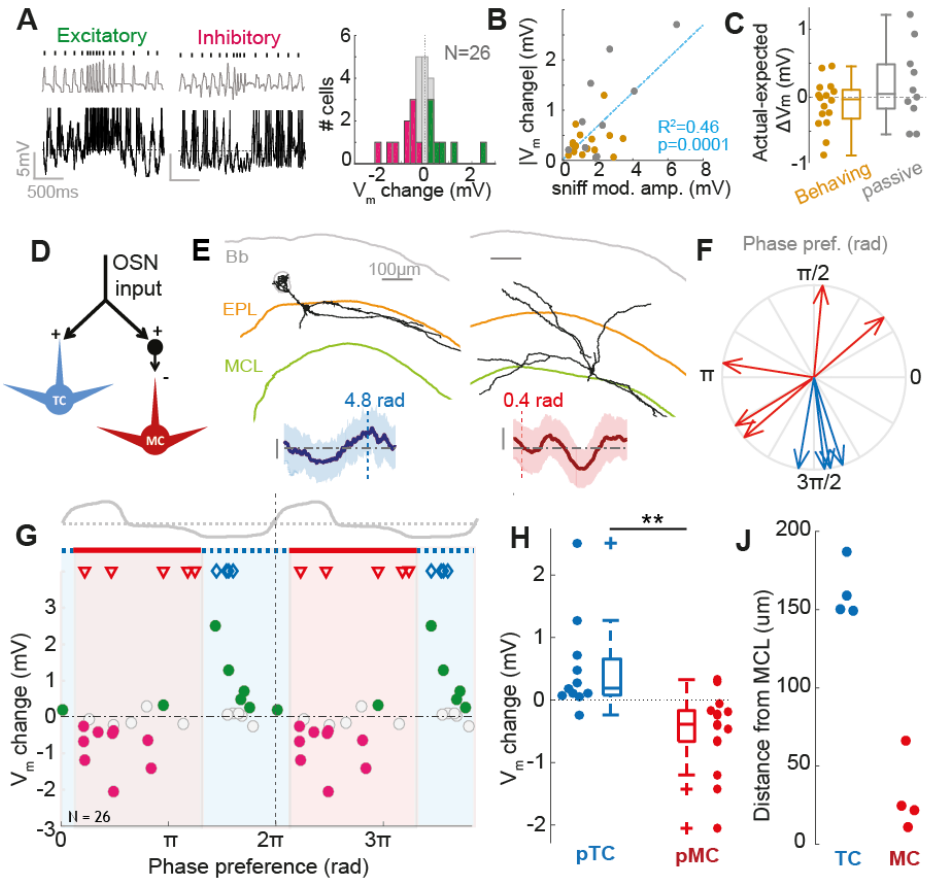

Figure 5.4. Activity changes during spontaneous rapid sniff bouts in absence of odour.

(**A**) Right: awake mice will sometimes make spontaneous rapid sniff bouts in absence of odour during the inter-trial interval. Example traces show such sniff bouts, and coincident V_m traces showing overt activity changes. Left: Histogram to show distribution of V_m changes during spontaneous rapid sniffs (>5 Hz) for 26 MTCs in which there were >20 fast sniffs. (**B**) Correlation between absolute sniff change between slow and fast sniffs, and amplitude of baseline theta modulation. Grey dots show data from passive mice (n = 10), gold dots show data from behaving mice (n = 16). (**C**) Comparison of errors (actual-expected) when calculating expected V_m change based on the sniff modulation amplitude of the baseline membrane potential ($0.31xT_{amp}+0.01$, where T_{amp} = sniff modulation amplitude), for passive (grey), and behaving cell-odour pairs. (**D**) Schematic of potential sniff driven circuit of MCs and TCs. MCs are thought to be driven by feed-forward inhibition and TCs by direct feed-forward excitation (Fukunaga et al., 2012). (**E**) Morphologies of a reconstructed TC (left) and MC (right), with mean membrane potential as a function of phase shown below (shaded area = SD), with their respective phase preferences. Bb=brain border; EPL=external plexiform layer; MCL = mitral cell layer. (**F**) Phase plot to show preferences of 4 reconstructed MCs (red) and 5 reconstructed TCs (blue). *Continued on next page…*

(**G**) V_m change between fast and slow sniffing (fast-slow) as a function of the phase preference of the cell. Red shaded region corresponding to inhalation and subsequent pause shows the phases which best encompass hyperpolarising cells, thought to be MCs, and blue region best encompasses depolarising cells, thought to be TCs. Symbols show phase preferences of morphologically recovered cells: red triangles = MCs; blue diamonds = TCs. Green dots show significant depolarisation, while magenta dots show significant hyperpolarisation. (**H**) Comparison of V_m change due to fast sniffing for putative TCs and MCs defined by the phase boundaries shown in F. (**J**) As for G, but for soma location relative to mitral cell layer (MCL). MC and TC phenotype were designated based on this: any cell with a soma < 70 μm from MCL was designated a MC, and any cell exceeding this distance was designated a TC.

5.3.5. TUFTED CELLS SHOW MORE HIGHLY CORRELATED CHANGES DURING BEHAVIOUR THAN MITRAL CELLS

Since the data suggests involvement of extrabulbar circuits in shaping responses during active sampling, and previous work has suggested that both learning and neuromodulators may have divergent effects on MC responses compared to TC responses (Kapoor et al., 2016; Yamada et al., 2017), I wanted to compare the response changes across learning for the two groups of cells. I thus used the phase boundaries determined in Fig. 5.4G as a way of determining putative MC (pMC) or putative TC (pTC) type for the rest of the data.

The distribution of early responses (prior to learning) for putative MCs and TCs did not significantly differ (pTCs: -1.1±1.9 mV, n = 16; pMCs: -1.8±2 mV n=26; p = 0.26, unpaired t-test; Fig. 5.5A), however pTCs showed significantly more positive responses compared to pMCs in late responses after learning was complete (pTCs: median = 0.3 mV, IQR = -1.3-1.1 mV, n = 16; pMCs: median = -2.1mV, IQR = -3.2-0.5 mV, n = 26; p = 0.01, Ranksum), consistent with previous findings that MCs receive more lateral inhibition than TCs, and show more excitatory responses (Christie et al., 2001; Nagayama et al., 2004). Comparing response changes across learning for putative MCs and TCs, we found that the two groups did not significantly differ in terms of mean or variance of response changes (pTCs: 0.64±1.7 mV; pMCs: -0.14±1.4 mV; p = 0.1, unpaired t-test; p = 0.46, Bartlett test; Fig. 5.5B). Comparing the R^2 values for the correlations between

mean inhalation duration and V_m response across trials also indicated that in general, pMCs and pTCs do not show differing effects of sniffing on responses (pTCs: median R^2 = 0.09, IQR = 0.01-0.29; pMCs: median = 0.06, IQR = 0.03- 0.18; p = 0.88, Ranksum; p = 0.35, Brown-Forsythe test; Fig. 5.5C).

We next compared the response changes for CS+ and CS- stimuli across learning for pMCs and pTCs individually. For tufted cells, response changes for the two stimuli were highly significantly correlated (R^2 = 0.65, p = 0.002, n = 12 cells), whereas this was not the case for MCs (R^2 = 0.21, p = 0.13, n = 13 cells; Fig. 5.5D). The same difference was seen when looking at the R values between MID and V_m response across trials: pTCs showed highly correlated R values between CS+ and CS- stimuli (R^2 = 0.72, p = 0.001, n = 11), while pMCs did not (R^2 = 0.26, p = 0.1, n = 12; Fig. 5.5E). Since response changes were overall less correlated between CS+ and CS- for pMCs, we wanted to compare the change in discriminability of the responses across learning for pMCs compared to pTCs. Using the Euclidean distance between population response vectors for CS+ and CS- stimuli, we found that pTCs did not show a significant change in peak discriminability across learning (mean peak early = 9.4±1.6 mV; late = 10.4±2.6 mV, p = 0.41 unpaired t-test, n = 5), however pMCs did show a significant increase in peak discriminability (mean peak early = 10.1±0.4 mV; late = 13.1±1.9 mV, p = 0.01 unpaired t-test, n = 5; Fig. 5.5F). Both cell types however significantly contributed to increased detectability of the stimulus across learning, though this was more pronounced for pTCs rather than pMCs (pTCs: peak early = 15.9±1.2 mV, peak late = 21.5±1.8 mV, p = 0.001, unpaired t-test; pMCs: peak early = 31.0±2.2 mV, peak late= 33.9±1.1 mV, p = 0.01, unpaired t-test; Fig. 5.5G).

Thus, while response changes across learning were generally quite similar for pMCs and pTCs, pTCs showed highly correlated changes and pMCs showed less correlated changes, consistent with recent findings that neuromodulators have more heterogeneous effects on MCs than TCs (Kapoor et al., 2016).

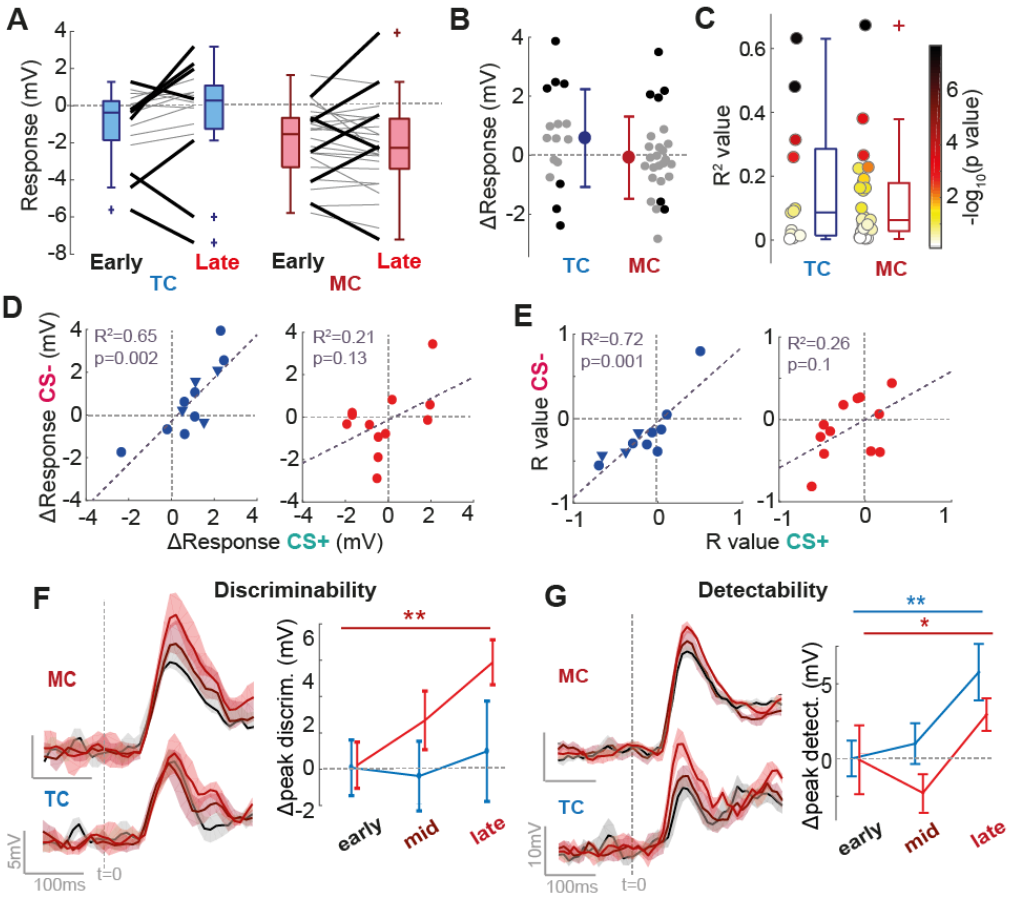

Figure 5.5. Comparison of putative mitral and tufted cell response changes

(**A**) Plot of early and late membrane potential responses (first 500 ms) across learning for pTCs (left; n = 16 cell-odour pairs) and pMCs (right; n = 26 cell-odour pairs) separately. (**B**) Comparison of response changes (late-early) for TCs and MCs cell-odour pairs. Red dots show significant positive changes ($p<0.01$) and blue dots show significant negative changes. (**C**) Comparison of R^2 values between MID and V_m response across trials for TC and MC cell-odour pairs. Colour shows p-value of the correlation ($-\log_{10}$). (**D**) Scatter of response change for CS+ vs response change for CS- for TCs (left) and MCs (right) independently. Triangles show data from task-engaged/disengaged recordings (as in Figure 6), where response change is calculated as engaged-disengaged response, while circles are from learning data (response change = late-early response). (**E**) As for G, but for the R value between MID and V_m response across trials for each cell odour pair. (**F**) Right: euclidean distance for the discriminability between CS+ and CS- during early (black), mid (maroon) and late (red) trials, for TCs (left) and MCs (right) independently. Left: plot of average peak discriminability in the first 150 ms of the stimulus for early, mid and late trials for TCs (blue) and MCs (red) Plot shows mean, and errorbars show SD across 5 trial subsets. (**G**) Right: euclidean distances (as in Figure 5) for the detectability between CS+ and CS- during early (black), mid (maroon) and late (red) trials, for TCs (left) and MCs (right) independently. Left: plot of average peak detectability in the first 150 ms of the stimulus for early, mid and late trials for TCs (blue) and MCs (red) Plot shows mean, and errorbars show SD across 5 trial subsets.

5.4. DISCUSSION

Here I have shown that sniff changes evoke response changes even in non-behaving mice, and that the extent of these response changes are dependent on cell sniff-locking. Meanwhile, sniff-locking properties cannot explain the entirety of response change alongside active sniffing in behaving mice engaged in an olfactory task. While this shows that sniff changes will always have an effect on at least a subset of responses in the OB, it seems likely that there are context-dependent top-down mechanisms for how active sampling alters responses.

The activity of the olfactory system is strongly patterned by the sniff cycle. Alteration in active sampling behaviour has the potential to affect odour responses of MTCs in two broad ways. The first is the 'bottom-up' consequence of sniffing on the pattern of ORN input coming into the OB. ORNs are activated and deliver a 'packet' of olfactory input to the OB on each inhalation, and as a result, MTCs show clear modulation of their activity by the sniff cycle, both during baseline and during odour stimulus (Adrian, 1950; Cang and Isaacson, 2003; Fukunaga et al., 2012; Macrides and Chorover, 1972). A large portion of such evidence comes from anaesthetised mice, but consistently I find that nearly all MTCs in awake mice are significantly modulated by the sniff cycle, with varying tuning phases and amplitudes of modulation. Mechanoreceptors are known to transduce information about pressure changes occurring with each sniff (Grosmaitre et al., 2007). The cell to cell variation in sniff modulation amplitude, particularly at baseline, could conceivably be due to differing levels of this mechanoreceptor input.

There is already some evidence that multiple parameters of sniff behaviour can have an effect on ORN input. As each inhalation delivers a 'packet' of sensory input from ORN terminals, increased frequency of inhalations is predicted to increase the rate of input to MTCs. One prediction of this is that a cell which is highly modulated by the sniff cycle will display a greater effect of input frequency than a cell with weak modulation. We find this prediction holds true in situations lacking olfactory attention – i.e. in passive and anaesthetised mice, and during the ITI

(Fig. 5.1F, 5.2E and 5.4B). Such changes are thus likely to be primarily the effect of 'bottom-up' changes in ORN input frequency accompanying the changes in sniff cycle. A notable imaging study in tracheotomised, anaesthetised mice manually altering inhalation frequency shows that prolonged bouts of high frequency sniffing causes a reduction of glomerular activity, perhaps owing to adaptation mechanisms (Verhagen et al., 2007). In our tracheotomised preparation where sniff bouts were prolonged, we found very similar results at for late timescales of the response (Fig. 5.2F-G). However, this dampening of activity did not apply to the earliest portions of the rapid sniff bout and arguably only this early information would be used in decision. Additionally, in awake animals, rapid sniff bouts were not usually prolonged (except in the case of response to novel odours), instead only incorporating a few sniff cycles (Wesson et al., 2009).

While input frequency can explain a portion of the change in mean activity within the first 500 ms of the stimulus (a timescale in which the number of inhalations can change), the response changes in learning animals occur within the first sniff cycle – an effect which cannot be explained by a change in the number of inhalations. Alongside sniff frequency changes, it is possible that a single 'packet' of ORN input can be altered according to modification of the parameters of a single inhalation: the flow, velocity and/or volume of air coming into the naris, in turn altering odour concentration profiles (Shusterman et al., 2017). Modulation of these may alter odourant sorption in the nasal passage, in turn affecting ORN activation in a way dependent on the odourant chemical properties and the position of the glomerulus along the nasal epithelium (Mozell et al., 1991; Youngentob et al., 1987). Indeed this hypothesis predicts that glomeruli that are not activated at low sniff effort could become activated when the flow velocity increases, and vice versa, which has been supported physiologically (Cenier et al., 2013; Oka et al., 2009). Increased nasal flow rate is also hypothesized, via the simple rules of fluid dynamics, to alter the concentration profile in the naris (higher air velocity = higher peak concentration within the nose; Shusterman et al., 2017), so a cell with very little response at low

sniff frequency may show responses at higher sniff frequencies, as the concentration exceeds the threshold to activate the cell. A notable extensive study of sniff properties on MTC responses revealed that, in anaesthetised, double-tracheotomised rats, peak glomerular responses to odours within a sniff increased with the flow rates of each sniff, though in the awake state, this was not the case (Cenier et al., 2013). This could indicate some mechanism by which the olfactory system will reduce odour sensitivity in the OB during high sniff amplitudes, such that the olfactory system does not show overwhelming response when the animal is displaying high sniff frequency. This could be done by continually balancing of sniff frequency and sniff amplitude in awake mice, which are thought to have opposing effects on the response (Courtiol et al., 2011), but it could also be achieved through top-down modulation. Such a role has been hypothesized for serotonin neurons, which both increase sniff frequency, and dampen odour responses in the OB (Dugué and Mainen, 2009; Petzold et al., 2009). Finally, another mechanism by which changing the parameters of a single sniff could conceivably alter odour response is if the altered sniff results in increased activation of ORN mechanoreceptors, as such stimulation is known to boost weak ORN responses odours in an *ex vivo* preparation (Grosmaitre et al., 2007).

As there are multiple bottom-up mechanisms by which sniff behaviour can alter the sensory input onto a MTC, this could in part explain why response changes in the behaving state do not show the same dependency on sniff modulation strength as in the passive and anaesthetised cases. While the inhalation duration and frequency change is very similar in each scenario, other parameters inaccessible with external flow measurement – such as amplitudes and flow velocities – may differ, and this could explain the additional variation in response changes.

The second way in which active sampling could affect responses in behaving odour-attentive mice is via the 'top-down' effect of directed attentional processes (Wachowiak, 2011). Such processes are thought to modulate sensory processing in precise coordination with active sampling of the stimulus in the task-engaged state, and are thought to be precisely timed to the

bout of active sampling. In V4 neurons, it is known that 50ms prior to a saccade, visual sensitivity starts to become modulated (Han et al., 2009). Similarly here, while the response changes during stimulus sampling are much greater for sniff changes in task-engaged active sampling mice compared to passive mice (Fig. 5.3), this is not true for the effect of sniff changes in absence of odour (Fig. 5.4A-C), so the enhancement of response change in behaving mice is specific to the sampling period. The OB receives an abundance of top-down input from both neuromodulatory centres and cortical regions (Shipley and Adamek, 1984; Niedworok et al. 2010; Steinfeld et al., 2015), which could give rise to such a directed attentional signal. For example, noradrenergic neurons of the locus coeruleus are thought to be involved in attentional processes in multiple sensory systems (Sara, 2009), while cholinergic inputs in particular have been linked to both control of whisking, and state changes during active sampling and attentional processes in the barrel cortex (Eggermann et al., 2014), and visual cortex (Herrero et al., 2008).

Sniff changes have the most profound effect on odour responses during olfactory attention, but even in absence of olfactory attention in passive and anaesthetised mice, sniff changes can evoke strong changes given that the cell is strongly locked to the sniff cycle. Since there will always be a subset of cells strongly locked to sniffing, sniff changes will always evoke large changes in a subset of cells regardless of behavioural state, and even regardless of whether an olfactory stimulus is present. Since mice alter their sniffing frequency for many reasons, including non-olfactory reasons, such as reward expectation and surprising non-olfactory stimuli, sniff changes could provide a parsimonious explanation for the plentitude of different contextual modulations described in olfactory bub output.

Overall, though sniffing evokes response changes regardless of behavioural state, bottom up effects of sniffing prevail in non-odour-attentive mice, while a coordinated top-down and bottom-up mechanism is likely to drive response changes in the odour-attentive mouse. The

next chapter will focus on how stable encoding may be achieved despite the changes in response occurring alongside sniff changes.

CHAPTER 6. **RESULTS**

IMPACT OF SNIFF VARIANCE ON INTENSITY PERCEPTION AND NEURAL CORRELATES OF ODOUR CONCENTRATION

6.1 INTRODUCTION

A fundamental problem for sensory processing is extracting stable features of stimuli in the face of variance in other parameters, for example encoding object size independent of distance in the visual system (Helmholtz, 1867). In the previous chapters, we have seen that sniffing can cause drastic changes in odour responses, both in behaving animals, as well as in passive animals (depending on their feedforward input). A conceptual problem that this poses is one of coding: presumably perceptual features of the odour stimulus, such as identity, must remain stable across different contexts to facilitate learning about the stimulus. How then, does perception and coding remain stable despite such overt changes in cellular response?

Previous studies have already looked at how odour identity may be encoded independent of odour concentration (Cleland et al., 2012; Uchida and Mainen, 2008; Wachowiak et al., 2002; Wilson et al., 2017) and sniff cycle variance (Cury and Uchida, 2010). An olfactory problem that has received less attention, however, is stable encoding of odour intensity (but see Shusterman et al., 2017). Increasing concentration is known to affect neural activity in many ways (Mainland et al., 2014). At the level of glomerular input from OSNs, increasing concentration increases the activity of already responsive glomeruli, as well as incorporate new glomeruli into the activity profile, overall resulting in a broadening of the spatial 'map' of activity (Rubin and Katz, 1999; Spors and Grinvald, 2002). Changes in spike rate also be seen at the level of the olfactory bulb output cells, mitral and tufted cells (MTCs), though this can be a more complex mixture of inhibitory and excitatory effects (Bathellier et al., 2008; Cury and Uchida, 2010; Fukunaga et al., 2012; Meredith, 1986), and is thought to be restrained within a range via inhibitory circuits (Kato et al., 2013; Miyamichi et al., 2013; Roland et al., 2016). The perhaps more ubiquitous correlate of concentration increase however, is temporal response changes, notably with early excitation undergoing a latency reduction in OSNs (Ghatpande and Reisert, 2011; Rospars et al., 2000),

MTCs (Cang and Isaacson, 2003; Fukunaga et al., 2012; Sirotin et al., 2015), as well as in piriform cortex (Bolding and Franks, 2017).

Since we know from the previous results presented in this thesis that sniffing alters both onsets (Chapter 4, Fig. 4.7A-C) and mean activity (Chapter 4, Fig. 4.4 and 4.6), sniff changes may provide a confounding factor when deciphering response changes due to concentration change. What precise problems may sniff variance provide for concentration coding? Firstly, changing flow will alter the number of odour molecules entering the nasal passage, causing a nasal increase in concentration against a stable environmental concentration (Mainland and Sobel, 2006; Shusterman et al., 2017; Teghtsoonian et al., 1978). Secondly, altering the velocity of air in the nasal epithelium will alter the time at which odourised air reaches the olfactory epithelium, which will cause issues for temporal coding of concentration (Shusterman et al., 2017). Despite these potential problems, previous work suggests that humans can perceive concentration independent of the inhalation flow rate (Teghtsoonian et al., 1978), and this has recently been confirmed in rats (Shusterman et al., 2017). Here, again using whole cell patch recordings in awake passively exposed mice, I show that stronger sniffs evoke response changes identical to those caused by increasing concentration. Surprisingly however, variance in sniffing parameters has little effect on the performance of mice trained to make fine concentration discriminations. Finally, I propose that the olfactory system can make an inference about whether a response change was caused by concentration change or sniff change by encoding the parameters of sniffing on fast timescales via mechanoceptive input to mitral and tufted cells, which respond to inhalation change in distinct, cell-type specific ways.

6.2 CHAPTER METHODS

6.2.1. BEHAVIOURAL TASK AND TRAINING

On day 0 (48 hours after surgery), mice with head-plates implanted would begin water restriction. On day 1, mice were habituated to the experimenter and hand-fed 0.5 ml of highly

diluted sweetened condensed milk with a Pasteur pipette. On day 2, mice were habituated to head-fixation: mice were head-fixed above a treadmill and allowed access to free reward upon licking. On day 3, successfully habituated mice underwent operant conditioning with repeated presentations of CS+ concentration of the odour mixture until the mouse learned to lick in the 1 s after odour offset to receive the reward. On day 5, the CS- concentration was also presented alongside the CS+ concentration in a pseudorandom order, until the mice learned to refrain from licking to the CS-. Licking to the CS- would evoke an addition of 6 s to the inter trial interval. 5 mice were trained with high concentration stimuli as the CS+, and 3 mice were trained on the reverse contingency. On day 6-8, mice would be presented with 5 different concentrations (3 additional concentrations spanning the range between the previously two learned concentrations), and contingencies as depicted in Fig. 6.7A. On day 9, five mice went on to a final session: after observing criterion performance on the binary odour concentration task with the mixture as learned previously, the odour would switch to vanillin with the same contingency between concentrations. Mice were carefully monitored to maintain their body-weights within 80% of their pre-restriction weight and were ensured a minimum of 1 ml water per day regardless of performance.

6.2.2. ODOURS USED

Odours applied to animals included two different odour mixtures (for recordings, either mixture A: Methyl salicylate, eugenol, cinnamaldehyde, creosol and 1-nonanol; or mixture B: guaiacol, valeric acid, (+)-carvone, 2-phenyl ethanol and 4-allylanisol). The components of each mixture were of similar vapour pressure and proportions were adjusted according to relative vapour pressure values. For behaviour, either mixture A or pure vanillin odour were applied at various concentrations.

6.2.3. CELL NUMBERS

Altogether 14 cells were recorded in passive mice and presented with two different odour concentrations, as well as puff stimuli to evoke fast sniffing (Fig. 6.2A). Some cells were presented two different odour stimuli (e.g. two different mixtures), such that there were 20 cell-odour pairs in total. Concentrations were presented in a pseudorandom order and puff stimuli occurred on a random subset of trials only for the low concentration. Puff stimuli were applied in concert with the odour stimuli with a gentle clean air stream to the flank. For some analyses, e.g. Fig. 6.4A-D, 6.5A-D and for Fig. 6.8 and 6.10, data was supplemented with cells recorded in previous chapters from the passive mouse presented the same odour mixtures at 1% vapour pressure (n = 6 for Fig. 6.4A-D and 6.5A-D, and n=38 for Fig. 6.8 and 6.10).

6.2.4. SPIKE RATE RESPONSES AND ONSETS

Long timescale (Fig. 6.2): for each cell, mean spike count was calculated in 250 ms time bins for the full 2 s odour stimulus. These were then averaged across trials to generate PSTHs for low concentration and fast sniffing (5 trials of lowest mean inhalation duration), low concentration and slow sniffing (5 trials with highest mean inhalation duration) and high concentration and slow sniffing. Values were quadrupled to estimate FR in Hz.

Short timescale (Fig. 6.4): for each cell, spike counts were calculated in 10 ms time bins for only the first 250 ms from odour onset (aligned to first inhalation onset). These spike counts were then averaged across trials for low concentration and fast inhalation (>70th percentile peak inhalation slope), low concentration and slow inhalation (<30th percentile inhalation slope) and high concentration and slow inhalation (<30th percentile inhalation slope). Onset for excitatory responses was defined at the point the mean spike count exceeded the mean + 2 SDs of the baseline spike rate in the 250 ms prior to odour onset, and remained there for at least 2 consecutive points. For phase-warped responses, each spike was initially assigned to its phase within the sniff cycle, rather than absolute time after odour onset, and the analysis repeated.

6.2.5. CORRELATIONS BETWEEN RESPONSE CHANGES DUE TO SNIFFING AND CONCENTRATION CHANGE

For both long and short timescale mean FR responses, changes in FR response were calculated for sniff change (fast-slow sniffing, low concentration odour) and concentration change (high-low concentration, slow sniffing). For all cell-odour pairs across the sample, a single regression was made between FR changes for sniff change and FR changes for concentration change in the corresponding time bins within the odour stimulus, generating an actual R and p value (Fig. 6.2E and 6.4G). For shuffle controls, low concentration trials were shuffled in respect to the sniff behaviour on each trial, and the same regression analysis was repeated 100 times.

6.2.6. EUCLIDEAN DISTANCE ANALYSIS OF CONCENTRATION DISCRIMINABILTY

In reference to Fig. 6.4K and 6.5G. Euclidean distance was taken across the population between mean spike counts for high concentration and low concentration (evoked by slow inhalation). This generated a measure of discriminability between concentrations when the inhalation was slow for both concentrations. To test how much of the discriminability was due to latency (or phase) shift of excitation, responses for whom had been calculated a latency (or phase) shift between high and low concentrations had the spike counts at low concentration manually shifted forward according to the latency shift occurring when concentration was high. Euclidean distance was then recalculated between spike counts for high concentration and the latency/phase-shifted spike counts at low concentration. Finally, Euclidean distances were taken between spike counts for high concentration (slow inhalation) and low concentration (fast inhalation). Time for discrimination was calculated, if possible, as the point at which the Euclidean distance exceeded the mean + 2 SDs of the baseline Euclidean distance (250 ms prior to odour onset) for at least 2 consecutive 10 ms time bins.

6.2.7. BASELINE ACTIVITY CORRELATIONS WITH INHALATION DURATION

For each cell (n = 48), 800-2000 sniffs were analysed in absence of odour. Sniffs were categorised according to their inhalation duration, 35-45 ms, 45-55 ms, 55-65 ms and so forth. For each individual sniff, different parameters were calculated from the corresponding neural activity. Mean membrane potential was calculated from the subthreshold membrane potential occurring from 0 to 250 ms from inhalation onset. Time of the peak membrane potential was calculated at the time of maximum membrane potential. Spike counts were calculated by summing all action potentials occurring within the same timeframe. To calculate the correlations for each parameter, each was averaged across all sniffs within the category and regression analysis was used to generate an R and p value between the resulting activity parameters and the corresponding inhalation duration (minimum of the category). For each cell, inhalation duration categories were excluded from the correlation if they contained less than 25 sniffs, and cells that had less than 4 valid categories were additionally excluded. For shuffle controls, inhalation duration was shuffled throughout the data and the regression analysis repeated 10 times per cell. Phase preferences were calculated as in previous chapters.

6.2.8. EUCLIDEAN DISTANCE ANALYSIS OF DETECTABILITY OF SNIFF CHANGE

For this analysis only cells with more than 50 sniffs during baseline in each category: 55-65 ms, 75-85 ms and 95-105 ms inhalation duration were included. A random subset of 25 sniffs in each group were selected and spike activity within these samples were used to construct PSTHs. PSTHs were put in sequence, either 4 consecutive 95 ms inhalation duration sniffs (control sequence), or the same sequence but with the final sniff of a different inhalation duration, either 75 ms or 55 ms. Each PSTH was normalised such that the first 30 ms started at zero. Euclidean distance across the population of these sequences were then calculated between the control sequence and sequences ending in 55 ms or 75 ms inhalation duration sniffs. Detection time for

the change in inhalation duration was calculated where the Euclidean distance in the last sniff exceeded the mean + 2 SDs of the baseline Euclidean distance from the first 3 sniffs.

6.2.9. MODULATION OF SNIFF-ACTIVITY RELATIONSHIPS ACROSS PHASE PREFERENCE

In reference to Fig. 6.10. To determine whether the sign of relationships between inhalation duration and the various activity parameters is modulated by the sniff phase preference of the cell, R values for the various correlations were plotted as a function of phase preference. Only correlations with a significant p value (<0.05) and with an R^2>0.6 were included. A sliding window of 2 radians was then used to calculate the mean R value for all cells with phase preference within the window, resulting in a mean R value as a function of phase preference. The modulation strength of mean R value as a function of phase was then calculated: the plot of mean R value was normalised to the minimum value across all phases, and the result plotted as Cartesian coordinates. The length of the mean vector calculated by averaging these Cartesian coordinates was taken as the modulation strength of the R value across phase. To determine the significance of this modulation, R values were shuffled across phase preference 10000 times, and the resulting distribution of shuffled modulation strength was compared to the actual value for the unshuffled data.

6.3 RESULTS

6.3.1 CHANGES IN SNIFFING CAN MIMIC EFFECT OF INCREASED CONCENTRATION ON FIRING RATE RESPONSE

I first wanted to determine whether the effect of sniff changes on MTC odour response could qualitatively mimic concentration changes at the level of FR change. To do this, I used whole cell recordings from identified MTCs in awake passive mice, resulting in recordings from 20 cell-odour pairs. To evoke fast sniffing, mice would again be stimulated using a gentle air puff to the flank during the odour stimulus, which I used to evoke fast sniffing behaviour in the previous chapter (Fig. 6.1A). This evoked a robust increase in sniffing frequency during the odour stimulus

compared to control trials as well as a reduction in mean inhalation duration, including in the very first inhalation (Fig 6.1B). It is useful to note that even in absence of odour, several parameters of sniffing co-vary with inhalation duration (Fig. 6.1C), including the slope of the inhalation (Fig. 6.1D), the current sniff duration (Fig 6.1E), and previous sniff duration (Fig 6.1F), and thus wherever I refer to 'fast sniffing', this will necessarily refer to variance in these multiple parameters.

On each trial, mice were presented randomly with 2 s long odour stimuli calibrated to either 1% (low) or 2.5% (high) (saturated vapour pressure) square pulses using a miniPID (Fig. 6.2A). On a small percentage of low concentration trials, the puff stimulus would additionally be used to evoke fast sniffing. During recordings, it was apparent that some cells showed overt changes in FR with the increase in concentration, and the most salient of these were increases in excitatory FR response (Fig. 6.2B, cell a and cell b). When comparing changes in FR evoked by concentration increase to those taking place as a result of increased sniff frequency, it was apparent that very similar changes took place (Fig. 6.2B). Altogether I recorded from 20 MTC pairs in such a manner, with a range of FR responses to the low concentration odourant (Fig. 6.2C). Comparing heat maps of the changes in FR due to increased concentration and due to increased sniff frequency strikingly revealed a very similar set of changes across the dataset (Fig. 6.2D), which were significantly correlated (Fig. 6.2E; $R = 0.63$, $p = 5x10^{-19}$), compared to shuffle controls (see methods). When taking a broad measure of the change in firing rate across the first second of the stimulus, changes in FR were significantly correlated between those resulting from concentration change and those resulting from sniff frequency change ($R^2 = 0.62$, $p = 5x10^{-5}$, $n = 20$, Fig. 6.2F).

While in the output of MTCs, the effect of sniffing and concentration increase were highly similar, differences were seen in the subthreshold response changes that suggest input in the two cases were not perfectly the same: inhibitory increases for concentration increase were in

general larger than for fast sniffing (Fig. 6.3A-C). I hypothesize that this could be the result of inhibitory networks which act to normalise (within boundaries) olfactory output in the face of changing concentration (Kato et al., 2013; Miyamichi et al., 2013; Roland et al., 2016).

Thus, increases in sniff frequency result in changes in gross FR responses that mimic those resulting from increases in concentration.

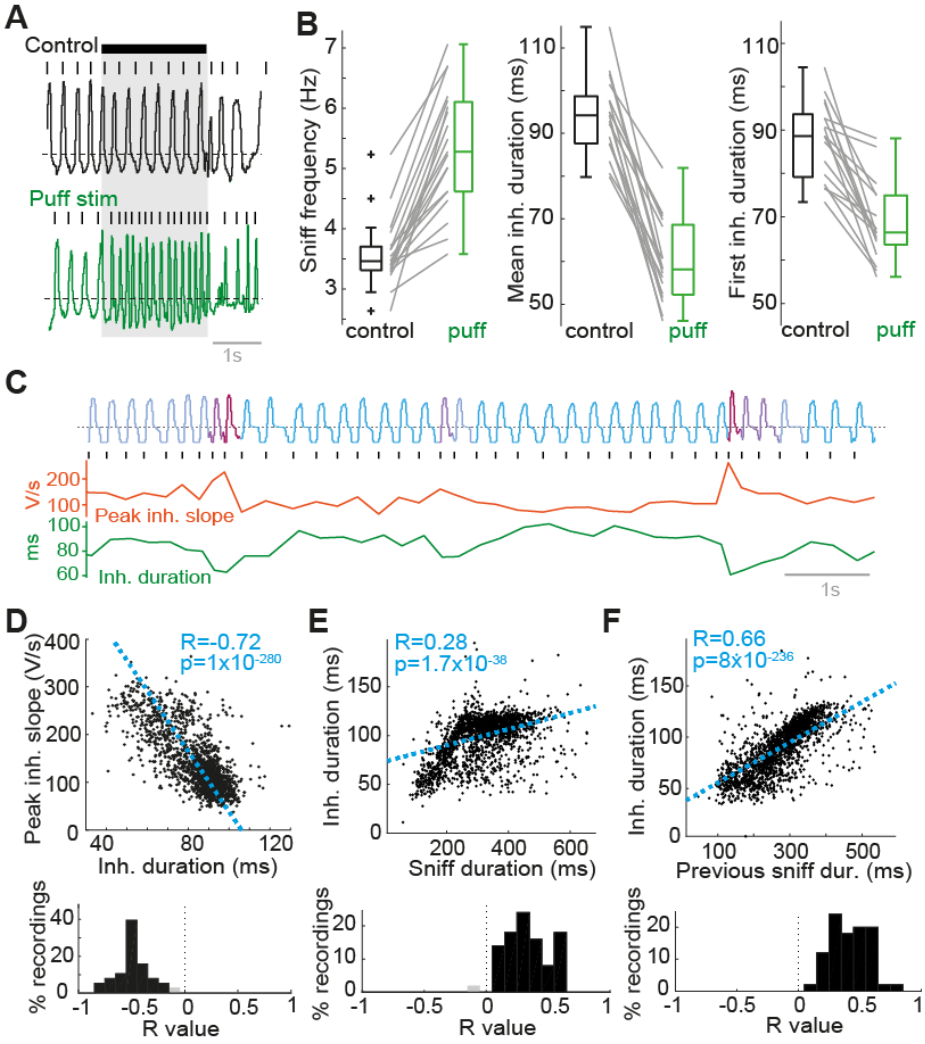

Figure 6.1. Effect of puff on sniffing and covariance between sniffing parameters

(**A**) Example nasal flow traces from one animal during a control trial (no puff stimulus accompanying 2 s odour stimulus) and a trial with a puff stimulus. Shaded area shows odour stimulus. (**B**) Plots to show average change in sniff frequency, mean inhalation duration, and first inhalation duration between five slow (black, control) and five fast (green, puff) trials for all 20 cell-odour pairs. (**C**) Example nasal flow trace during an inter-trial interval (no odour), with sniffs coloured according to their inhalation duration (blue to red = long to short duration). Black ticks show time of inhalation onset, orange plot shows peak inhalation slope for each inhalation aligned to the inhalation onset, and green plot shows inhalation duration for each inhalation. (**D**) Example correlation between inhalation duration and peak inhalation slope for 1988 sniffs in 1 animal (top), and histogram of correlation R values between inhalation duration and peak inhalation slope across 45 animals. Black bars indicate significant correlations. (**E**) As for D, but for correlation between sniff duration and inhalation duration. (**F**) As for D, but for the correlation between the previous sniff duration and the current inhalation duration.

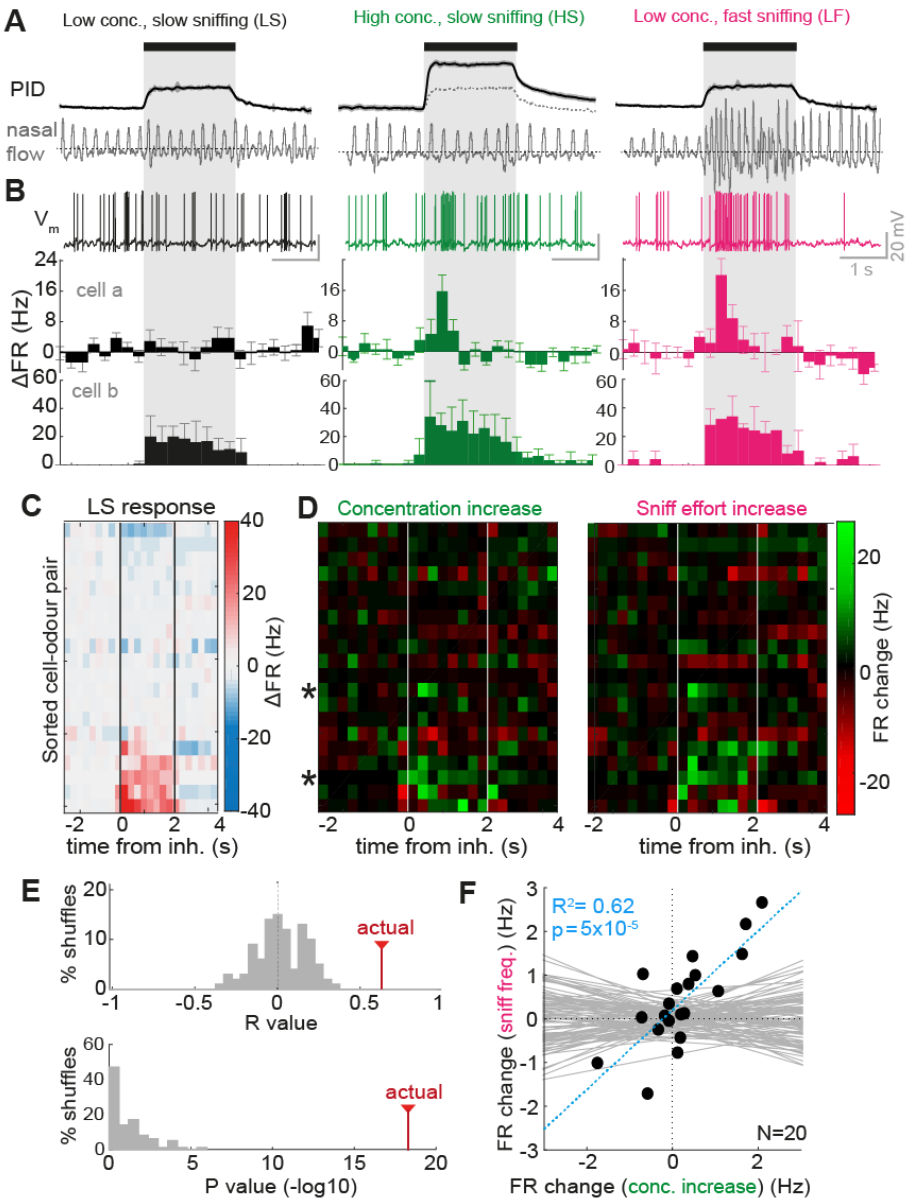

Figure 6.2. Sniff change and concentration change have similar effects on FR responses of MTCs

(**A**) Stimulation paradigm during whole cell recordings. PID traces show response of photoionisation detector (magnitude proportional to odour concentration), while nasal flow traces shows example sniffing recorded using external flow sensor for 3 trials. Black bar and grey box shows where odour is on, aligned to first inhalation onset. (**B**) Example odour responses recorded in each stimulus condition. V_m traces show example responses for cell a, while PSTHs below show averaged FR responses in 250 ms time bins for 5 trials in each case. Bottom-most PSTHs are calculated for a different example, cell b. Error bars show standard deviation. (**C**) Heatmap of average FR respones for all cell odour pairs in the low concentration low sniff effort condition, ordered by mean FR response. (**D**) Heatmap of response changes (difference between PSTHs): Concentration increase = HS-LS, sniff-effort increase = LF-LS. Asterisks indicate cell a and cell b examples. *Continued on next page….*

(**E**) Top: R values for correlation between FR change during odour time bins due to concentration change and sniff effort change. Histogram shows R values for shuffle controls, actual shows R value for real data. Bottom: as for above, but histogram showing p-values for the correlations ($-\log_{10}$) (**F**) Correlation between mean FR response change for concentration change and sniff effort change across first second of odour stimulus. N = 20 cell-odour pairs. Grey lines show correlations calculated for 100 shuffle controls, blue line shows real correlation.

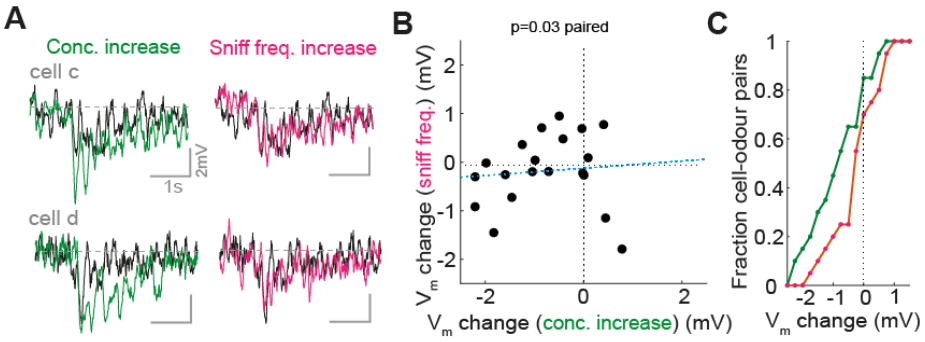

Figure 6.3. Changes in subthreshold response are more inhibitory for concentration increase than for fast sniffing.

(**A**) Example average subthreshold response traces for low concentration, slow sniffing (black), high concentration, slow sniffing (green) and low concentration, fast sniffing (magenta), for two different cells, cell c (top) and cell d (bottom). Each trace is the average of 5 spike-subtracted trials. (**B**) Scatter to show average change in membrane potential response for the first 1000 ms of the odour stimulus for concentration increase (high conc.-low conc.) and sniff frequency change (fast sniffing-slow sniffing). (**C**) Cumulative histograms of membrane potential response change for concentration increase (green) and sniff effort increase (magenta).

6.3.2. FASTER INHALATION MIMICS EFFECT OF CONCENTRATION INCREASE ON LATENCY RESPONSE IN THE TIMESCALE OF A SINGLE SNIFF

It has been reported several times that increased concentration causes changes in response on finer temporal timescales, in particular the advance of excitatory bursts (Cang and Isaacson, 2003; Fukunaga et al., 2012; Sirotin et al., 2015). Are such changes constant in the face of changing sniffs?

To determine this, I analysed 13 excitatory cell-odour pairs recorded in passive mice (data from sets in previous chapters) over the first sniff cycle of response. Comparing the FR response over the first 250ms for 'fast' sniff trials (>70th percentile peak inhalation slopes), and 'slow' sniff trials (<30th percentile), it was apparent that in almost every case, faster inhalation caused an advance of the excitatory burst (Fig. 6.4A-B). Faster inhalation caused a significant latency reduction in mean response onset (mean latency reduction = -16±14 ms, p = 0.002 paired t-test between onsets for slow and fast inhalations; Fig. 6.4C). The extent of the latency advance was significantly positively correlated with the onset time for slow inhalation, such that if the response was of longer latency for a slow sniff, the latency reduction was greater (R^2 = -0.46, p = 0.01, n = 13; Fig. 6.4D), which could indicate a lower limit on the latency of odour response, as noted in chapter 4 (Fig. 4.7B).

Could this effect of sniff speed mimic concentration effects at this timescale? Indeed, when comparing high and low concentration stimuli over the first 250 ms in MTC recordings from passive mice (same dataset as in Fig. 6.2), the only overt changes in response to increased concentration was an advance of excitatory burst stimuli (Fig. 6.4E and F). When correlating changes in spike count as before (Fig. 6.2E) between those occurring for sniff change and those occurring for concentration change, there was a highly significant positive correlation between the two (R = 0.71, p = 4x10^{-72}, n = 525 time bins), that could not be recreated in shuffle controls (Fig. 6.4G). Latency reductions for concentration increase were on a similar timescale to those

seen due to sniff change (mean onset reduction = -18±10 ms, p = 0.04, n = 4 paired t-test between onsets for low and high concentration; Fig. 6.4H). This latency change contributed to the entirety of the discriminability of the two different concentrations on this timescale, with the Euclidean distance between the two dropping to baseline if the excitatory bursts were manually shifted forward for the low concentration (Fig. 6.4K, 'slow sniff' vs 'slow sniff adv.', see chapter methods). Faster inhalations on low concentration trials mimicked the latency shifts caused by concentration increase, rendering the high and low concentration stimuli indistinguishable (Fig. 6.4K, 'slow sniff' vs 'fast sniff).

Thus, even on short timescales, a more rapid inhalation mimics concentration increases at the level of the olfactory bulb output, rendering it difficult to distinguish faster sniffing from increased concentration without knowing what kind of sniff occurred.

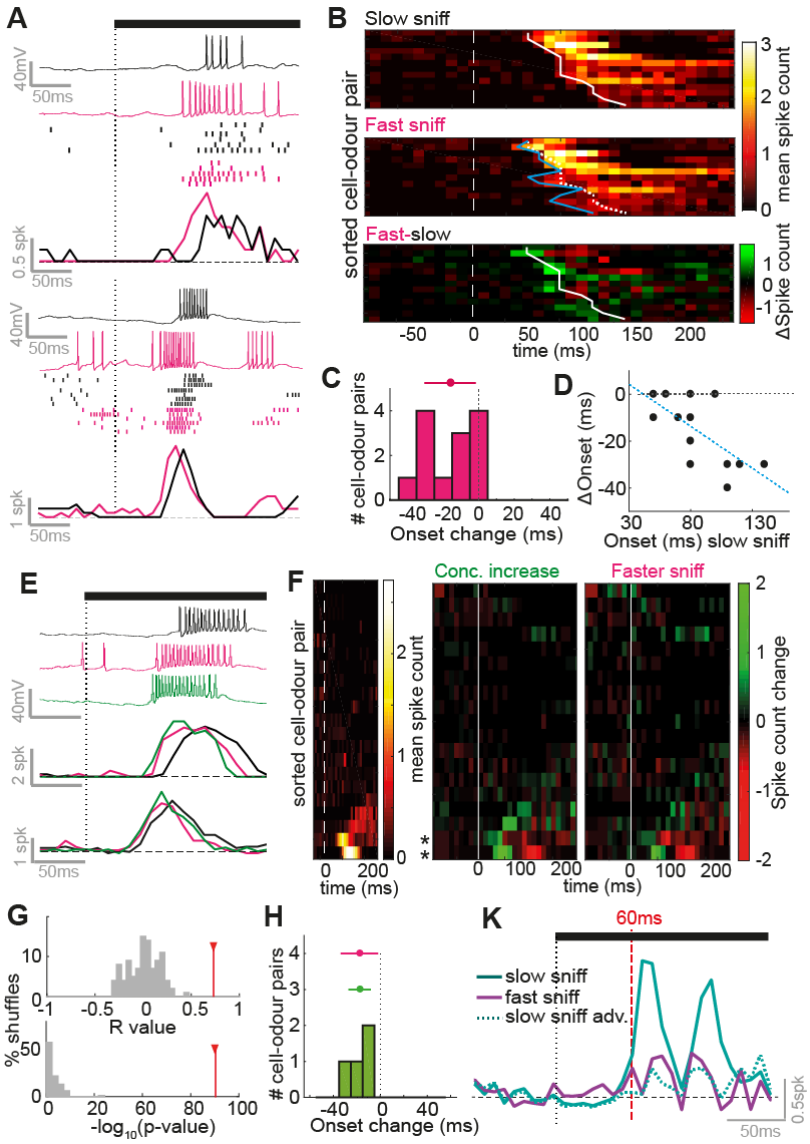

Figure 6.4. Excitatory onset latencies shift in response to inhalation change and concentration change in similar ways.

(**A**) Example traces, spike rasters and mean spike counts for early excitatory responses for both slow inhalation (black) and fast inhalation (pink), for two different cell-odour pairs. (**B**) Heatmaps of mean spike count for 13 cell odour pairs showing early excitation in response to slow inhalation (top) and fast inhalation (middle). Cell odour pairs are sorted from short to long onset latency at slow inhalation. Bottom heatmap shows the difference between the two above (fast-slow). White solid and dotted line indicates onset latency of each cell-odour pair for slow inhalation. Blue line indicates onset latency for fast inhalation. (**C**) Histogram of onset latency changes (fast-slow) for all 13 cell-odour pairs. (**D**) Scatter plot to show relationship between onset latency for slow inhalation, and the onset change between fast and slow inhalation. (**E**) Example traces and mean spike counts for early excitatory responses. Black shows response at low concentration and slow inhalation, pink shows response at low concentration and fast inhalation, and green shows response for high concentration and slow inhalation. *Continued on next page…*

(**F**) Left: Heatmap to show early spike counts of all 20 cell odour pairs recorded for low concentration slow inhalation. Cell-odour pairs are sorted by the mean spike count, from low to high. Middle: Heatmap to show difference in spike counts between high concentration and low concentration (slow inhalation). Left: heatmap to show difference in spike count between fast inhalation and slow inhalation (low concentration). (**G**) Top: R values for correlation between spike count change during odour time bins due to concentration change and sniff effort change. Histogram shows R values for shuffle controls, red bars show R value for real data. Bottom: as for above, but histogram showing p-values for the correlations ($-\log_{10}$). (**H**) Histogram to show response onset changes due to concentration increase. Errorbar in green shows mean and SD of this data, and in pink shows the distribution of changes as in panel C for comparison. (**K**) Euclidean distance over time between population vectors for high and low concentration spike counts where the inhalation was slow ('slow sniff'; solid cyan), for high concentration and time-shifted low concentration ('slow sniff adv.': where excitatory latency changes due to concentration change were undone via time shifting of the data; dotted cyan), and for high concentration and low concentration where low concentration data came from fast inhalation trials ('fast sniff'; solid purple).

6.3.3. PHASE ADVANCE WITHIN SNIFF CYCLE REMAINS STABLE DESPITE CHANGES IN SNIFF RISE TIME

Given that using absolute latency, sniff parameters can render concentrations indiscriminable, it must be the case that the coding of concentration takes sniff parameters into account. One way of doing this would be to code relative to phase of the sniff cycle (Shusterman et al., 2011). I thus repeated the above analysis, with spikes registered to phase of sniff cycle rather than absolute time.

First I looked at the effect of changing sniff flow rate on excitatory bursts across the 13 cell-odour pair population as above. When registered to phase, I noticed that fast sniffing did not appear to evoke any consistent shift in excitatory response onset (Fig. 6.5A). Overall there were variable changes in the detected onset phase between high and low sniff flow rate, with no significant systematic change seen (mean latency change = -0.17±0.37 rad, n = 13, p = 0.12, paired t-test; Fig. 6.5B). The changes in phase-aligned responses due to flow rate change look particularly small and inconsistent when compared directly to those evoked by latency change

(Fig. 6.5C). The difference was particularly obvious when comparing average change in mean spike count aligned to the onset at low flow rate: for latency aligned responses, there is a clear peak prior to onset that corresponds to the advance of the excitatory bursts, while for phase aligned responses this is much smaller (Latency: 0.47±0.3 spk/bin, phase: 0.16±0.18 spk/bin, $p = 0.004$, unpaired t-test, averaged approx. 20 ms prior to onset; Fig 6.5D). Thus the ubiquitous advance of onset latency calculated before is not present when registering to sniff cycle phase.

Using phases, increasing concentration again evoked an advance in excitatory bursts, however, unlike for absolute latency, increasing the flow of the first sniff did not mimic this effect in the early excitatory responses (Fig. 6.5E). Directly comparing the phase changes evoked by increasing concentration with those evoked by fast sniffing revealed that, in 3 of 4 cases, the change evoked by concentration was larger. As for latency, the changes in the excitatory responses again contributed to almost the entirety of the discriminability, as manually shifting the slow sniff responses forward caused a dramatic reduction in discriminability (Fig. 6.5G, 'slow sniff adv.'). The remainder of the discriminability seen was due to changes in the peak excitation, as excluding the four excitatory responses altogether reduced discriminability to baseline (data not shown). However, unlike for latency, increased flow of the first sniff did not cause a reduction in discriminability (Fig. 6.5G, 'fast sniff').

Thus, taking sniff cycle phase into account enables concentration to be discriminated from the olfactory bulb output regardless of changes in sniff effort.

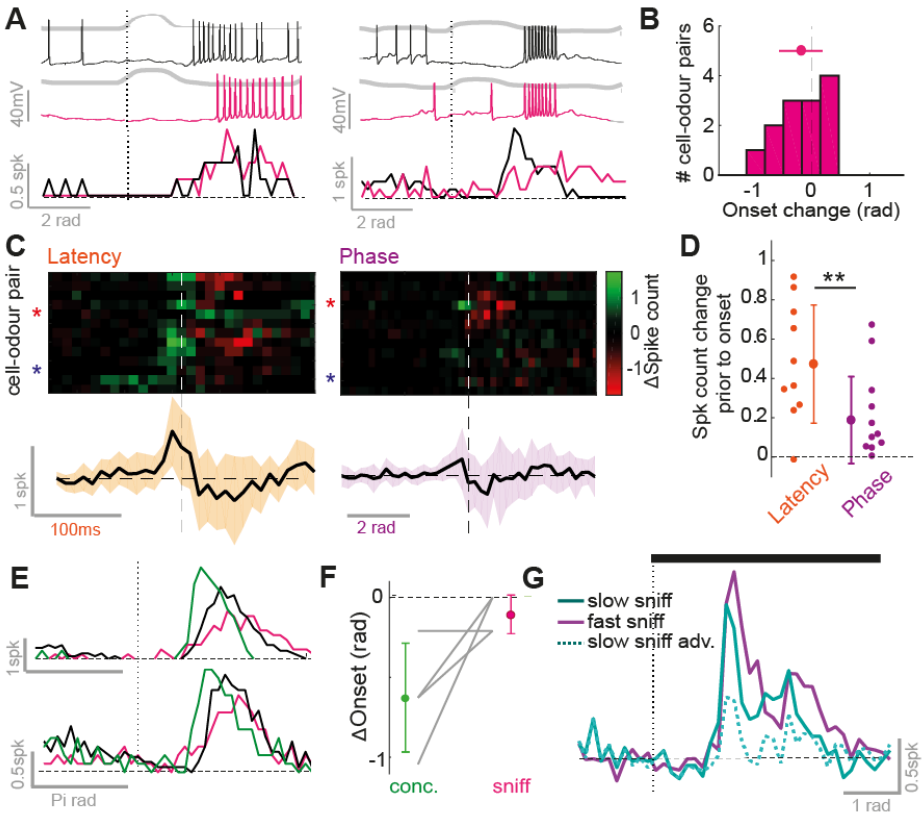

Figure 6.5. Fast sniffing does not replicate effect of concentration change when aligning to sniff phase.

(**A**) Example trace, and corresponding mean spike counts for early excitatory responses for both slow inhalation (black) and fast inhalation (pink), for two different cell-odour pairs, with each time-point warped to the phase of the sniff cycle. Grey trace shows phase-aligned nasal flow. (**B**) Histogram of onset phase changes (fast-slow) for all 13 cell-odour pairs. (**C**) Above: heatmaps of the change in mean spike count between fast and slow sniffs for all 13-cell-odour pairs, aligned to the dashed vertical line using their response onset at slow sniffing. On the right shows the data in absolute time after inhalation onset, while the right heatmap shows the same data warped to sniff phase. Below: plot shows mean change in spike count across the above sample of 13 cell-odour pairs. Shaded area shows standard deviation. (**D**) Mean change in spike count between fast and slow sniffs in the 20 ms time window prior to response onset at slow sniffing for all 13 cell-odour pairs, compared where responses were aligned to absolute time, or sniff phase. (**E**) Example mean spike counts for two early excitatory responses registered to the phase of the sniff cycle. Black shows response at low concentration and slow inhalation, pink shows response at low concentration and fast inhalation, and green shows response for high concentration and slow inhalation. (**F**) For the 4 early excitatory cell-odour pairs in the dataset (as in Fig. 8.5F), a comparison of the change in response onset phase when concentration is changed from low to high (green data), and when the sniff was changed from fast to slow (magenta data). *Continued on next page…*

(**G**) Euclidean distance over time between population vectors for high and low concentration spike counts where the inhalation was slow ('slow sniff'; solid cyan), for high concentration and time-shifted low concentration where excitatory phase changes due to concentration change were undone via time shifting of the data('slow sniff adv.'; dotted cyan), and for high concentration and low concentration where low concentration data came from fast inhalation trials ('fast sniff'; solid purple). Spike counts for population response vectors were registered to sniff phase.

6.3.4. MICE CAN SUCCESSFULLY DISCRIMINATE CONCENTRATIONS ON RAPID TIMESCALES

Rodents have previously demonstrated the ability to discriminate odour concentrations (Abraham et al., 2004; Parthasarathy and Bhalla, 2013; Slotnick and Ptak, 1977; Wojcik and Sirotin, 2014). Given the physiology (Fig. 6.2 and 6.4), and that sniff parameters are constantly varying in awake mice (Wachowiak, 2011; Chapter 6) I next sought to determine whether and how fast mice could distinguish such concentrations of the odour mixture in a simple go/no-go paradigm (Fig. 6.6A). The overall trial timing is the same as was used for the odour identity go/no-go task in previous chapters.

First, mice were trained to simply distinguish high (3%) versus low (1%) concentration stimuli. 3 mice were trained with the low concentration stimulus as the CS+ ('low go'), and 5 mice were trained with high concentration as the CS+ ('high go'). After pre-training (Fig. 6.6B), all mice learned the distinction within a single training session (85±19 trials to 80% correct, n = 8; Fig. 6.6C). Mice were not only able to learn quickly, but also make rapid decisions based on concentration: analysis of the reaction time of mice based on anticipatory lick probability showed that mice could perform the task successfully within as low as 200 ms (median = 300 ms, range = 200 to 1050 ms, calculated as in Chapter 4 methods; Fig. 6.6D). Similarly, using divergence of sniffing behaviour between CS+ and CS- stimuli (calculated as in chapter 4 methods), reaction times could be estimated at 214±60 ms, and as low as 160 ms (Fig. 6.6E) - in every case the first exhalation already showing significant difference. Thus, as for odour identity

(Chapter 2, Fig. 2.5), mice can make decisions about concentration on the timescale of a single inhalation.

Mice were not using flow changes from the olfactometer output to make the discrimination, as our olfactometer design keeps flow at the nose piece constant (Fig. 6.6F). Secondly, trigeminal stimulation was likely not being used since mice subsequently learned to discriminate the same concentrations of vanillin (an odour which is thought not to stimulate trigeminal afferents – Frasnelli et al., 2011), within a significantly shorter timeframe (16±14 trials to criterion, $p = 0.001$, paired t-test, $n = 6$; Fig. 6.6G), suggesting they may have learned the rule for the concentration. Moreover, reaction times for vanillin were not significantly different than for the mixture (Fig. 6.6H, licking RT: $p = 0.46$, paired t-test, $n = 6$; sniffing RT: 237±45 ms, $p = 0.5$, unpaired t-test). Finally, learning in the task was likely the result of acquiring the response to the stimulus rather than learning how to perceive the difference in concentration, since on the very first presentation of the CS- concentration after pre-training on the CS+ concentration, mice typically displayed a rapid sniffing response (Fig. 6.6J) classically associated with novel odour identity (Roland et al., 2016; Verhagen et al., 2007).

Thus, mice can very rapidly make decisions based on relatively modest concentration differences within the timescale of a single sniff, comparing very well to their abilities in odour identity tasks (Rajan et al., 2006; Uchida and Mainen, 2003; Wesson et al., 2008a).

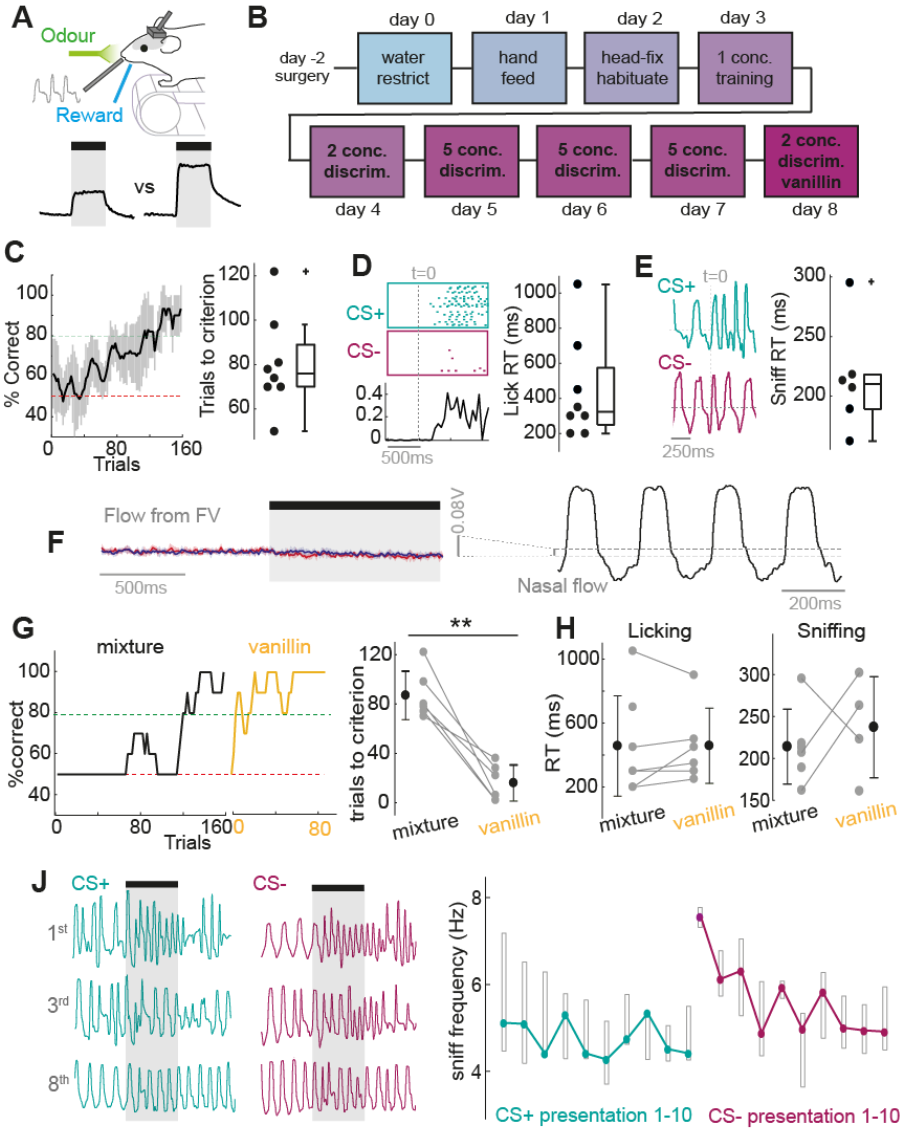

Figure 6.6. Mice rapidly learn to discriminate concentrations on fast timescales.

(**A**) Diagram of go/no-go task paradigm. (**B**) Diagram to show training sequence for mice (described in methods). (**C**) Left: Average learning curve for 8 mice. % correct is calculated as a moving average over 5 CS+ and 5 CS- trials. Errorbars indicate SD. Right: Distribution of learning time to criterion (4 successive learning curve points at or above 80% correct). (**D**) Left: Example to show calculation of reaction time from lick behaviour. Rasters of licking during criterion performance are shown for CS+ and CS-. A difference in mean lick count over time is then calculated (bottom) and lick RT is determined where this difference first exceeds 2 SDs of the baseline difference. Right: distribution of lick RTs calculated in this way. (**E**) Left: example sniff traces for CS+ and CS- during driterion performance. Prior to licking mice show rapid sniff bouts such that RT may be determined earlier using divergence of sniff timing (see Methods Chapter 2). Right: distribution of RTs calculated using sniff time divergence. *Continued on next page…*

(**F**) Mean flow change recorded 1mm from olfactometer output for high concentration stimulus (red) and low concentration stimulus (blue). Average of 10 trials; shaded area shows standard deviation. Y scale bar is compared to that of nasal flow traces recorded in the same manner to demonstrate the negligible nature of flow change from the olfactometer. (**G**) Example learning curves for 1 mouse for 2 concentration discrimination, first for the odour mixture (in black) and subsequently for vanillin (yellow). Right hand plot compares the number of trials to criterion for the initial mixture and vanillin for each mouse. (**H**) Plots to compare the reaction time as estimated from lick behaviour (right) and sniff behaviour (left) for the mixture stimulus and vanillin for all 5 mice who underwent training on both stimuli. (**J**) Left: Example sniff traces for the 1st, 3rd and 8th presentation of the CS+ and CS- concentrations for the initial concentration discrimination session. Note that in this session, the CS+ concentration is first presented 10 times to ensure retention of the lick pattern learned the day before, and then the CS- is interleaved in a pseudorandom order. Right: plot to show median sniff frequency across 8 mice for presentations 1-10 of the CS+ and CS- concentration in the first 2 concentration discrimination session. Boxes show upper and lower quartiles.

6.3.5. VARIANCE IN SNIFFING HAS NO OVERT IMPACT ON PERFORMANCE IN A FINE CONCENTRATION DISCRIMINATION TASK

To determine whether sniff variation impacts on the concentration decisions of mice, after learning the initial discrimination, mice advanced to a task in which 3 new intermediate concentrations between the two previously learned concentrations were presented. The concentration most similar to the learned CS+ was rewarded as a CS+ also, while the other two concentrations, including one exactly halfway between the previously learned concentrations, were treated as CS- (Fig. 6.7A). 2-3 sessions of 200 trials were performed on this task, and mice displayed a graded probability of a go response according to the concentration of the stimulus relative to previously learned CS+ and CS- concentrations (Fig. 6.7B). Mice generally performed at a high level of accuracy (mean percent correct across session = 75±6%, n = 8 mice; Fig. 6.7C).

Three lines of evidence suggests that sniff variance does not grossly affect concentration discrimination. First, I separated trials according to whether the first sniff was fast (<30th

percentile inhalation duration) or slow (>70th percentile) (Fig. 6.7D), which resulted in a comparison of trials between which the difference in the mean first inhalation duration even exceeded that which made responses to high and low concentrations indistinguishable in the physiology (Fig. 6.7E). I recalculated performance curves for each subset, there were no large or significant differences in the performance curves for mice performing on either contingency (Fig. 6.7F; $p>0.01$ paired t-tests). Secondly, on a small selection of trials, the puff stimulus (as used during the physiological recordings) was used to evoke fast sniffs, including the first inhalation (Fig 6.7G). The mean changes in first inhalation duration evoked by this puff was again highly comparable to that used for analysis of fast and slow sniffs in the physiological data above (Fig. 6.7H). While this had a minor but insignificant effect on error rate likely owing to distraction (Percent correct: control trials = 83±8%, probe trials = 77±9%, $p = 0.16$ paired t-test, $n = 7$ mice), there were remarkably no gross differences in the performance curves compared to control trials ($p>0.01$, paired t-tests; Fig 6.7J). Finally, when separating trials for each concentration according to the response of the mouse (either 'go' or 'no go', Fig. 6.7K), the mean difference in first inhalation between go and no-go trials in general was smaller than used in the physiological analysis (Fig. 6.7L), and across different concentrations there were no large or significant differences in the first inhalation duration according to the response ($p>0.01$, paired t-tests; Fig. 6.7M).

Overall, reductions of inhalation duration of 10-20ms rendered 1% and 2.5% concentrations indiscriminable from MTC responses (Fig. 6.3 and 6.4). Here I am comparing similar and even larger reductions in inhalation duration, yet ability to discriminate concentration shows no dramatic differences. Thus, variable sniffing appears to have no overt negative impact on concentration perception.

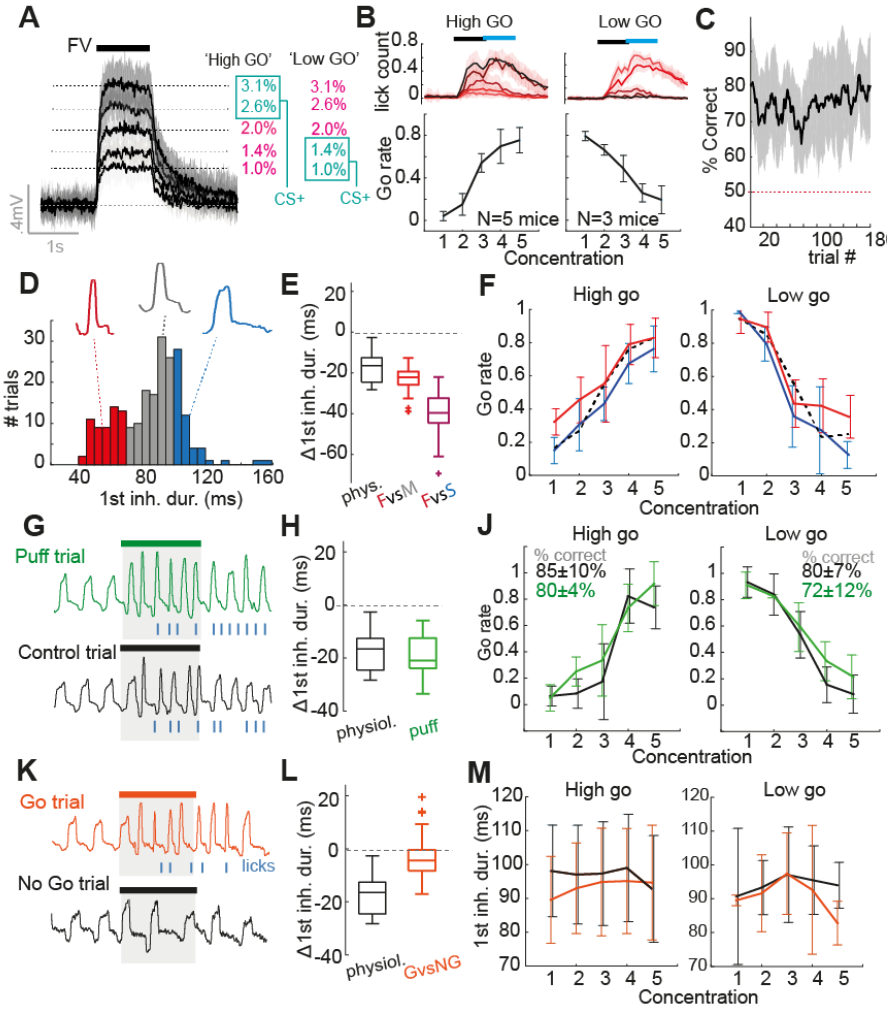

Figure 6.7. Mice are capable of good concentration discrimination in the face of fluctuating inhalations.

(**A**) Diagram to show average PID traces for the 5 different concentrations and contingency schemes. Shaded area shows SD. (**B**) Top: Mean lick counts for the 5 different concentrations (darkest = strongest) for both high go and low go contingencies. Black bar indicates odour stimulus, and blue bar indicates response period. Bottom: average go rate across mice for all 5 concentrations. (**C**) Average % correct across all sessions of the 5 concentration discrimination task (n = 3 sessions x 8 mice). Shaded area shows standard deviation. (**D**) Example histogram of inhalation durations of the first sniff in an odour stimulus across trials. Data for each mouse is partitioned into fast inhalations (30th percentile, red), slow inhalations (>70th percentile, blue), and other (grey). Example nasal flow waveforms for the whole sniff for each subset are shown. (**E**) Comparison of changes in the first inhalation between physiology and behavioural experiment. Black ('physiol') shows distribution of mean change used for analysis of odour responses (Fig. 6.4) for 20 cell odour pairs recorded in passive mice. Red ('FvsM') shows mean difference between red and grey sections of the inhalation distribution as in panel D for all mice and concentrations (n = 8 mice x 5 concentrations); Purple 'FvsS' shows the same as for 'FvsM', but shows mean difference between red and blue sections of the inhalation duration distribution as in panel D. *Continued on next page…*

(**F**) Go rate as a function of concentration when splitting trials according to speed of first inhalation as in D. Dotted line shows mean go rate for sniffs with inhalation between 30th and 70th percentile. (**G**) Example sniff traces for one animal for a puff trial (a trial in which an air puff to the flank was used to evoke fast sniffing) and an adjacent control trial of the same odour. (**H**) Comparison of changes in mean first inhalation duration for physiological analysis (Fig. 6.4, n = 20) and for puff vs control during behaviour (n=8 mice x 5 concentrations). (**J**) Mean go rate as a function of concentration across mice for puff trials (green) vs control trials (black). (**K**) Example sniff traces for one animal for a go trial and a no go trial for a given odour concentration. (**L**) General comparison of mean first inhalation change for physiological analysis (Fig 6.4, n = 20) and between go and no-go trials during behaviour (n = 8 mice x 5 concentrations). (**M**) Mean first inhalation duration for go vs no go trials across all mice in each concentration category.

6.3.6. MITRAL AND TUFTED CELLS ENCODE CHANGES IN THE INHALATION ON RAPID BEHAVIOURAL TIMESCALES

I have so far shown that it is highly difficult to disseminate the effect of a change in inhalation speed or a change in concentration physiologically (Fig. 6.2 and 6.4), yet mice are perfectly capable of fine concentration discrimination in the face of fluctuating inhalations (Fig. 6.7). I thus conjecture that the olfactory system receives information about the kind of inhalation that just occurred in order to infer whether concentration or sniffing evoked the response change. This could either be achieved through efferent copy of the sniffing control signal, or reafference (the sensory result of the sniff motor command). Congruent with the latter idea, OSNs have been demonstrated to respond to pressure changes (Grosmaitre et al., 2007), giving rise to the sniff coupling in the olfactory bulb that has already been discussed multiple times in previous chapters (Cang and Isaacson, 2003; Fukunaga et al., 2012). Already in the previous chapter, I showed that fast sniffing generally affects baseline activity with heterogeneity between cells (Chapter 5, Fig. 5.4). I thus wanted to determine whether the olfactory bulb reports sniff effort changes in a graded way, and if it does so within a behaviourally relevant timescale.

To do this I analysed the cellular activity of 45 MTCs recorded in passive mice across 1000-2000 sniffs occurring in absence of the odour. Sniffs were categorised according to inhalation duration, and peristimulus time histograms (PSTHs) and average membrane potential waveforms were calculated over 250 ms triggered by inhalation onset for each subset (Fig. 6.8A-C). I found that individual mitral and tufted cells would show linear transformations in their activity according to the duration of the inhalation just occurring. For example, some cells showed increased spike count (Fig. 6.8A_1-B_1) and depolarising membrane potential (Fig. 6.8C_1) as inhalations became faster, while others showed decreasing spike count (Fig. 6.8A_2-B_2) and more hyperpolarising membrane potential (Fig. 6.8C_2). 24% of cells showed significant ($p<0.01$) relationships between spike count and inhalation duration compared to only 3% in shuffle controls (Fig 6.8D). R^2 for the actual correlations were also significantly higher than for shuffle controls (actual R^2 median = 0.54, IQR = 0.17-0.82; shuffled median = 0.18, IQR = 0.04-0.45, $p = 2x10^{-4}$, Ranksum, n = 41 vs 369; Fig. 6.8D). Similarly, 22% showed significant correlations with mean membrane potential compared to 2% of shuffle controls ($p<0.05$, linear regression), with R^2 values for the actual data being significantly higher than for shuffled data (actual R^2 median = 0.56, IQR = 0.20-0.73; shuffled median = 0.18, IQR = 0.04-0.41, $p = 9x10^{-7}$, Ranksum, n = 41 vs 369; Fig. 6.8D). Timing of activity was also often linearly correlated with inhalation duration (e.g. Fig. 6.8C_{1-2}), generally with the peak of the membrane potential shifting to earlier times as inhalation duration reduced (significant R values in 32% of cells vs 2% in shuffle controls (actual R^2 median = 0.50, IQR = 0.22-0.86; shuffled median = 0.20, IQR = 0.05-0.43, $p = 2x10^{-6}$; Fig. 6.8D). Altogether 51% of cells showed a significant relationship ($p<0.01$) between inhalation duration and at least one or more of these activity parameters (Fig. 6.8E).

For all cells with enough sniff variation (>50 sniffs in each inhalation duration category), I then calculated sequences of spike histograms for different inhalation durations using random subsets of sniffs within each group (Fig. 6.9B; see methods). I constructed either a sequence with

three consecutive sniffs of 95ms inhalation duration, or a sequence with 2 consecutive sniffs of 95 ms, with the last PSTH instead constructed from 55 ms inhalation duration sniffs (Fig. 6.9B). Using these, it was possible to determine a change in sniff effort (95 to 55 ms inhalation duration) within only 70±12 ms by calculating euclidean distances for population vectors of the two different sequences (Fig. 6.9B). Smaller duration changes could also be detected, e.g. 95 to 75 ms change could be detected within 94±9 ms (Fig. 6.9C).

Thus, mitral and tufted cell baseline activity is informative of the inhalation that just occurred, which could be utilised by the system to distinguish sniff changes versus concentration changes.

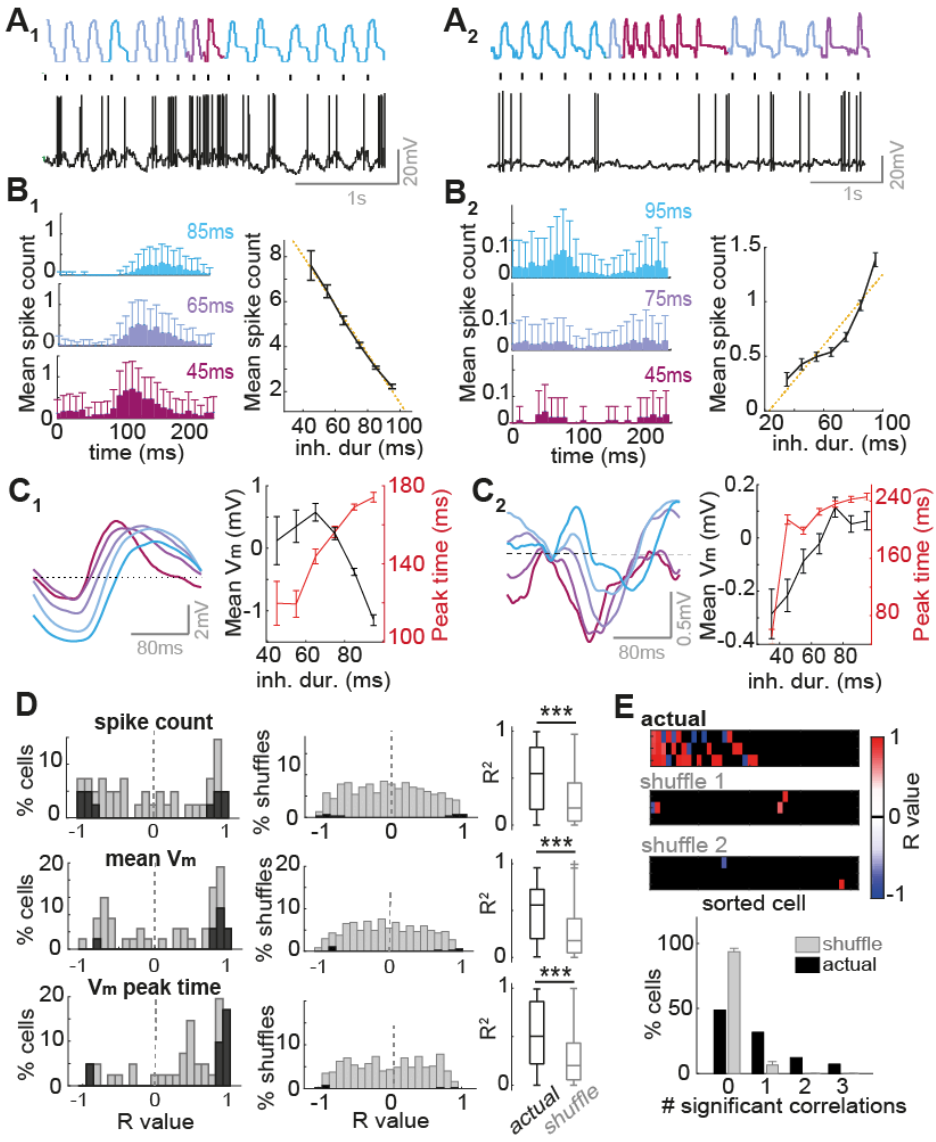

Figure 6.8. Inhalation duration transforms mean baseline MTC activity in a large proportion of cells. (**A**) Example nasal flow traces and V_m traces in absence of odour. Sniffs are colour coded according to inhalation duration (blue = slow, and red = fast). Black ticks indicate inhalation onset. (**B**) Left: Average spike count triggered by inhalations of different durations (denoted on each histogram). Right: mean spike count per sniff as a function of inhalation duration. Errorbars = SE. (**C**) Left: Inhalation triggered mean membrane potential waveforms for sniffs of different inhalation duration. Right: mean V_m and timing of V_m peak for membrane potential waveforms across all sniffs as a function of inhalation duration. Errorbars = SE. (**D**) Left: Histograms of R values for correlations between inhalation duration and different activity variables: (from top to bottom) spike count, mean membrane potential, and the timing of peak membrane potential. Middle: histograms of R values between the different activity parameters and inhalation duration for shuffle controls (n = 10 shuffles x 45 cells). Dark bars show significant correlations. Right: Boxplots show comparison of actual R^2 values for the correlations as compared to shuffle controls. *Continued on next page…*

(**E**) Top: Heatmap of R values for correlations between inhalation duration and 3 different activity parameters (spike count per sniff, mean membrane potential and timing of peak membrane potential, rows 1-3 respectively), for 45 mitral and tufted cells. Cells are sorted left-right by largest number of significant correlations to lowest number. Black squares show where the correlation was insignificant ($p>0.01$, regression analysis). Two lowest heatmaps show the same data but for 2 example shuffle controls, where inhalation durations were shuffled with respect to the physiology, and the data re-analysed. This gives an indication of false positive rates in this analysis. Bottom: histogram to show proportion of cells with 0 to 3 significant correlations between the different activity parameters and inhalation duration. Grey shows proportion for shuffle controls.

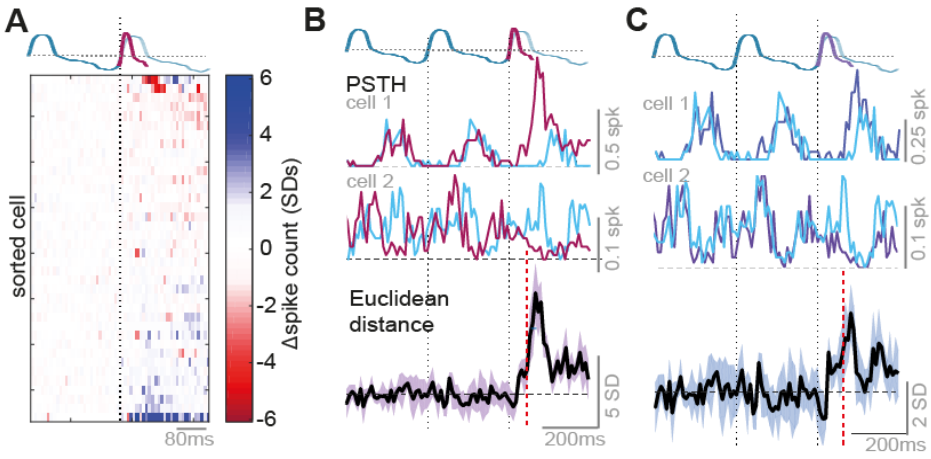

Figure 6.9. Population activity allows detection of an inhalation change on behavioural timescales.

(**A**) Difference between PSTH sequences (fast-slow inhalation) across population of cells, sorted by the mean difference between PSTHs for fast (55 ms) and slow (95 ms) inhalation. (**B**) Top: diagram to show construction of sniff sequences of different inhalation duration: either three of 95 ms inhalation duration, or two of 95 ms with the final sniff of 55 ms duration. Middle: two example PSTH sequences averages from random subsets of sniffs that show the particular inhalation duration. Blue line shows the PSTH sequence for 3 sniffs of 95 ms, and purple shows sequence in which the last inhalation is of 55 ms. Bottom: mean euclidean distance calculated between population vectors constructed from the two sniff sequences as above. Plot shows the average of 5 different subsets of data, and shaded area shows standard deviation. Dashed red line indicates time of significant detection of change. (**C**) As for panel B, but looking at a smaller change between inhalation duration of 95 ms and 75 ms.

6.3.7. PUTATIVE MITRAL AND TUFTED RESPOND TO CHANGING INHALATION PARAMETERS IN DIVERGENT WAYS

Since, with the exclusion of timing, there was significant variety within the polarity with which changing inhalation duration affected cell activity (Fig. 6.8), I wanted to test whether this could be explained by cell type. As mentioned in the previous chapter, we can utilise phase preferences to disseminate putative mitral and tufted cells, and these two cell types appeared to generally hyperpolarise or depolarise respectively during fast sniff bouts (Chapter 5, Fig. 5.4G). Could cell type consistently explain the divergent effects of changing inhalations across the population?

I wanted to see whether activity correlations with inhalation duration (as in Fig. 6.8) conformed to the putative mitral and tufted cell phase boundaries. In some cases, morphologically reconstructed cells showed graded changes in their activity as inhalation duration decreased. For example, the tufted cell in Fig. 6.10A_1-C_1 showed depolarisation as inhalation duration reduced (increased spike count and more depolarised V_m waveform), while the mitral cell in Fig. 6.10A_2-C_2 showed the opposite displayed increasing inhibition as inhalation duration reduced. I thus plotted R values for the correlations between inhalation duration and mean V_m or spike count as a function of phase preference for all cells showing strong correlations ($p<0.05$, $R^2>0.6$). Indeed, for both parameters analysed (mean V_m and spike count), there was a significant organisation according to phase (Fig. 6.10D and E; mean V_m: $p<0.01$; spike count: $p<0.001$; bootstrapping test, see methods). Moreover, comparing R values between the phase boundaries assigned for putative MCs and TCs resulted in significant differences between the two groups in each case (mean V_m: pMC: median = 0.93, IQR = 0.84-0.95 n = 6, ; pTC: median = -0.83, IQR = -0.96 to -0.82, n = 10; p = 0.002, Ranksum; spike count: pMC: median = 0.84, IQR = -0.88-0.96 n = 22, ; pTC: median = -0.92, IQR = -0.94 to -0.89, n = 12; p = 0.008, Ranksum). In some cases, there were regions of phase space where both positive and negative R values would occur

(around the transition from inhalation to exhalation for spike count), indicating potential overlap of the phase preference of the two cell types.

Since pMCs and pTCs displayed divergent effects of sniff change on their activity in absence of odour, I wanted to test whether there were any notable differences in the effect of sniffing on early odour responses – i.e. the reduction in latency of excitatory responses reported earlier (Fig. 6.4A-D). The dataset of 13 excitatory cell-odour pairs analysed contained 5 pMC cell-odour pairs and 8 pTC cell-odour pairs. Exemplary reductions in latency according to fast sniffing could be found for both pMCs and pTCs (Fig. 6.10F). Across this population, onset latency during slow sniffing displayed a strong relationship with the peak firing rate during the response ($R^2 = 0.61$, $p = 0.002$, $n = 13$; Fig. 6.10G), suggesting that the most strongly activated cells respond earlier. Consistent with previous reports from anaesthetised mice (Fukunaga et al., 2012; Griff et al., 2008a; Nagayama et al., 2004), pTCs showed both shorter latency responding on average (pTC onset median = 75 ms, IQR = 55-90 ms; pMC onset median = 110 ms, IQR = 80-113 ms, $p = 0.13$, Ranksum) and higher peak firing rates compared to pMCs (pTC peak spike count=2.1±0.7 spikes; pMC: peak spike count=1.1±0.5 spikes; $p=0.02$, unpaired t-test; Fig 6.10G). Comparing response onsets between fast and slow sniffs, pMCs showed robust significant reductions in latency (-30±7 ms, $p = 7x10^{-4}$, paired t-test; Fig. 6.10H), while pTCs showed a collectively smaller reduction which did not reach significance (-8±10 ms, $p = 0.08$, paired t-test; Fig. 6.10H). Altogether, pMCs displayed greater reductions in onset latency according to sniff changes than TCs ($p = 0.001$, unpaired t-test; Fig. 6.10J), which matches well with previously reported latency changes in anaesthetised mice due to concentration increase (Fukunaga et al., 2012): MCs show significant reductions, while the already short-latency TC responses do not.

Thus, phase locking, which very likely relates to MC and TC phenotype, determines how a cell will respond to changing sniff parameters.

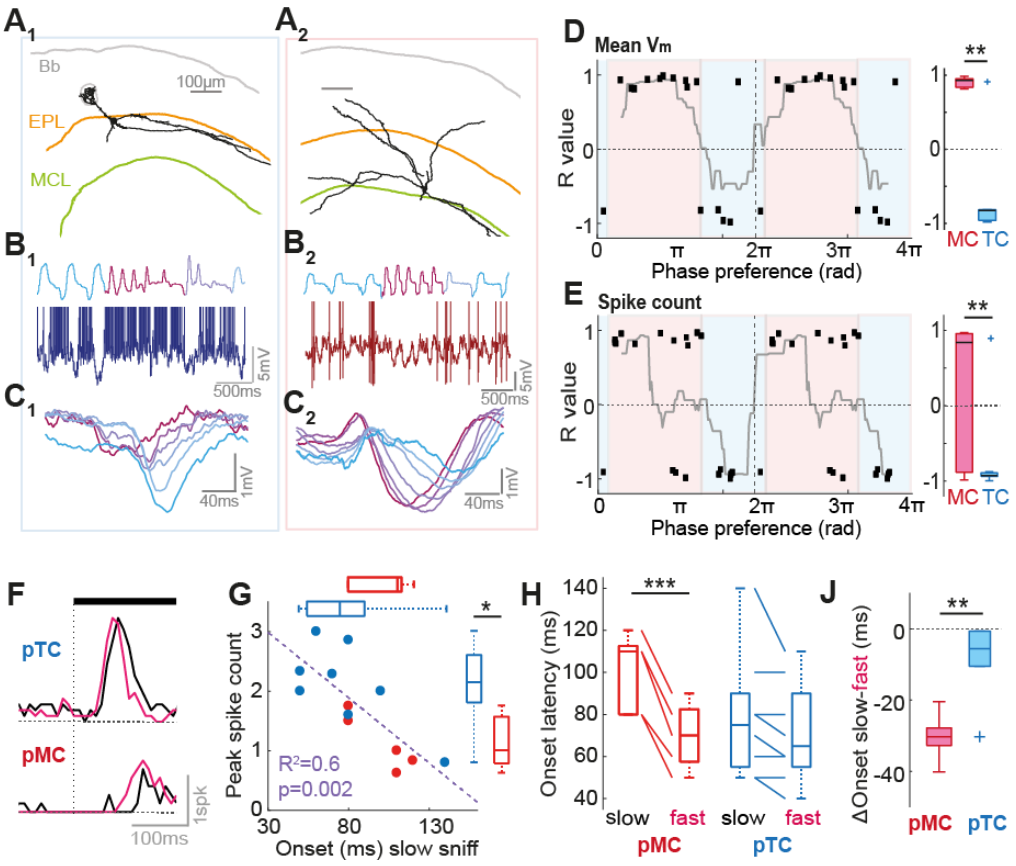

Figure 6.10. Cell type specificity of effect of inhalation.

(**A_1**) Reconstructed morphology of a tufted cell recorded in awake mouse. 'Bb' refers to brain border, 'EPL' refers to external plexiform layer and 'MCL' refers to mitral cell layer, as visualised with DAPI. Blue waveform shows mean V_m as a function of sniff phase, indicating a phase preference of 4.8 radians. (**B_1**) Example nasal flow and V_m trace during a rapid sniff bout (blue to purple represents slow to fast inhalation on flow trace. Spikes have been cropped. (**C_1**) Mean membrane potential waveform for different bands of inhalation duration: blue = long inhalation duration, purple = short. (**A_2**)-(**C_2**) as for A_1-C_1, but for a filled mitral cell recorded in an awake mouse. (**D**) R values for correlations between inhalation duration and mean V_m as a function of phase preference. Only strong correlations have been included ($p<0.05$ and $R^2>0.6$). Grey line shows mean R value for all cells within a 2 radian moving window (centred), to give an idea of the phase modulation strength of the data. Boxplots to the right compare all values within the putative MC (red) and putative TC (blue) phase boundaries. (**E**) As for panel D, but for mean spike count per sniff. (**F**) Examples of mean spike counts for early excitatory responses for both slow inhalation (black) and fast inhalation (pink), for two different cell-odour pairs: top=pTC, bottom=pMC. (**G**) Correlation between response onset latency and peak spike count for early excitatory odour responses evoked by a slow sniff. Blue data comes from pTCs and red data comes from pMCs. Boxplots compare the two parameters for pTCs and pMCs. (**H**) Comparison of response onset latencies for excitatory responses evoked by fast and slow sniffs for pMCs and pTCs. (**J**) Comparison of response onset latency change (slow-fast sniff) for pMCs and pTCs.

6.4. DISCUSSION

For stable perception, the sensory system must find ways of encoding of stimulus features in the face of fluctuating parameters. Here I show that faster sniffs can evoke response changes that appear indistinguishable from those caused by increasing concentration (Fig. 6.2 and 6.4), yet mice are highly capable of perceiving concentration on fast timescales, regardless of sniffing parameters (Fig. 6.6-6.7). I reason that the only way the system can distinguish these two occurrences is via information about the kind of sniff that just occurred. Consistently, I find that olfactory bulb activity provides just this kind of information on rapid behavioural timescales, and that this is likely generated from feed-forward input in a cell type specific way.

Given the timescale of decision making for concentration (Fig. 6.6D and E), it seems likely that the information used by the mouse is the fast timescale temporal shifts in excitation that have been previously described (Cang and Isaacson, 2003; Fukunaga et al., 2012; Sirotin et al., 2015). Congruently, this temporal information contributes to the entirety of concentration discriminability on such a timescale in my dataset (Fig. 6.4K). It has been suggested that high baseline firing rates of MTCs could obscure such a latency code for concentration being used (Mainland et al., 2014), however this was based on the high estimation of baseline FRs from unit recordings. The whole cell recordings I employ here are unbiased in terms of baseline FRs (Kollo et al 2014), and discriminability of MTC responses based on latency shifts is overt (Fig. 6.4K). Congruently it is known that mice can perceive the latency difference in optogenetic glomerular activation in the order of tens of milliseconds (Smear et al., 2013).

Sniff changes have been hypothesized to alter odour concentration profiles within the nasal cavity (Shusterman et al., 2017; Teghtsoonian et al., 1978). Here I show for the first time directly that sniff changes can indeed mimic the effect of concentration change at the level of both firing rates (Fig. 6.2), and temporal shifts (Fig. 6.4). It has been known for some time that the olfactory bulb is highly modulated by the sniff cycle (Cang and Isaacson, 2003; Fukunaga et al., 2012;

Margrie and Schaefer, 2003). Since sniff modulation is more overt in anaesthetised mice and is reduced at higher sniff frequencies (Bathellier et al., 2008; Carey and Wachowiak, 2011; Cazakoff et al., 2014; Kay and Laurent, 1999), it may lead some to call into question the importance of sniff modulation in the awake animal. Here I find that sniff patterning of activity gives rise to linear transformations of baseline activity as inhalation parameters are changed, a feature which is widespread throughout MTCs (Fig. 6.8). I thus reason that a primary function of sniff modulation may be to inform the olfactory system of what kind of inhalation took place, such that a change in concentration and a change in sniffing are distinguishable.

Encoding of 'sniff effort' has been hypothesized previously when psychophysics showed that humans could categorise concentrations well despite large changes in inhalation flow rate (Teghtsoonian et al., 1978). Airway resistance is subject to continual changes, and even differs between the two nostrils (Principato and Ozenberger, 1970; Sobel et al., 1999), which will naturally result in varying sniff pressure for identical respiratory motor commands. Thus reafference using mechanoceptive encoding of sniff pressure, rather than efference copy of the motor commands (which would require internal models to calculate the effect on airway flow) may be the optimal solution to encoding of inhalation parameters. This could be the reason that olfactory receptors respond to pressure changes as well as olfactory stimuli (Connelly et al., 2015; Grosmaitre et al., 2007) and is backed up by the fact that theta modulation all but disappears if the naris is occluded (Margrie and Schaefer, 2003). Consistently, concentration perception in humans can be affected when the nostril flow rate was changed via experimenter-induced changes in airway resistance instead of volitional changes in sniff pressure (Teghtsoonian and Teghtsoonian, 1984) – i.e. only when flow changes and pressure stays constant. I can use averaged activity from subsets of sniffs across my sample to detect that a change in inhalation has occurred within 70 ms (Fig. 6.9B), suggesting that it is possible to read out what kind of inhalation just occurred. However, my sniff recordings were made externally,

and thus I don't have the full range of sniff dynamics present in my data (e.g. amplitudes), while my cells were recorded independently rather than simultaneously. This limits what we can infer about decoding of the inhalation dynamics from population activity. Further large scale recordings from a true population, alongside intranasal measurement of flow will be required to know exactly how much information is present about the sniff in the OB output.

A recent study intuitively suggests that the advance of odour-driven excitation as sniff frequency increases is the result of fluid dynamics in the nasal cavity (Shusterman et al., 2017). They compared several modes of time-warping and time-shifting the spiking responses of cells in how much they could improve concentration discrimination from the population spiking given high variance in sniff dynamics. Congruent with their results, here I find that phase-warping cellular activity relative to the sniff cycle improves the ability to distinguish concentrations from cellular activity (Fig. 6.5). However, Shusterman and colleagues find that an even more reliable concentration read-out could be made in the face of high sniff variance by shifting spike timing according to a parameter equivalent to the time at which the inspired air reaches a given distance within the nasal cavity – a time which changes as a function of the inhalation duration. Indeed, a large fraction of our cells show an advance of their baseline activity peak as the inhalation becomes faster (Fig. 6.8C-D). I could thus hypothesise that non-odour responsive MTCs within a region of the bulb can provide information about the timing of inspired air reaching the epithelium. If the inhalation becomes faster, both responsive and unresponsive cells show a latency reduction in their peak activity, while if concentration has increased, only the much sparser odour responsive population will show this latency shift. Exactly how the two kinds of information are integrated downstream to form sniff invariant encoding of concentration should be the objective of future investigations, though recent evidence from the piriform cortex of awake mice already suggests that cortical interneurons sharpen the latency

shifts evoked by concentration change and encode concentration via the synchronicity of ensemble firing (Bolding and Franks, 2017).

There are certain limitations to my dataset. Firstly, given the relatively small number of cells sampled here, it is possible that I miss an uncommon population of neurons which are capable of reporting concentration invariant of sniff effort. I think this less likely since the complimentary unit recording study finds that the latency shift of excitatory response due to sniff change is widespread throughout MTCs (Shusterman et al., 2017). However, it is also possible that I have missed activity parameters at the population level, such as spike synchrony, which could conceivably be more stable reporters of concentration in the face of fluctuating sniffs. Finally, it is possible that in a mouse performing a concentration guided task, the bulb physiology is altered in such a way as to generate a sniff invariant representation of concentration. Future large scale neural recordings in behaving mice will be required to determine this.

In conclusion, I show that mice are remarkably good at concentration discrimination in the face of fluctuating sniffing, and that while concentration and sniff changes cause identical odour response changes, the early olfactory system already contains all the tools required to report the inhalation change.

CHAPTER 7.

OVERALL CONCLUSIONS AND GENERAL DISCUSSION

OVERALL CONCLUSIONS

1) There is very little difference in the basic spontaneous and passive properties of MTCs between passively exposed and olfactory task-engaged states.

2) There are however detectable differences in certain response features according to behavioural state – including increased response diversity, faster response onsets and reduced sniff locking in behaving mice relative to passive mice.

3) There are diverse changes in odour responses of MTCs across olfactory learning. These changes enhance stimulus detectability and discriminability within the timescale of decision-making.

4) Highly motivated mice show the development of rapid active sampling of odour stimuli as they learn to perform the olfactory task – something which is associated with faster reaction times.

5) Rapid active sampling is highly correlated with the development of positive response changes, which often result in enhanced excitation; modulating active sampling state rapidly by ending and restarting the task regulates excitatory responses in a profound way.

6) State dependent changes in sniffing can also account to a degree for the reduced response onset latencies and reduced sniff locking seen in behaving mice.

7) Evoking sniff changes in mice lacking olfactory attention (namely passive and anaesthetised mice) evokes robust changes in neural responses, but only when sniff locked input amplitude is high. This occurs via a bottom-up mechanism.

8) The response changes due to active sampling in behaving mice exceed what is predicted based on the bottom-up mechanism, pointing to top-down sources of additional response change.

9) Mitral and tufted cells undergo different kinds of change during learning, with mitral cells primarily increasing discriminability, while the more correlated changes in tufted cells only tend to increase detectability of the odour.

10) Mice can perform concentration discrimination in the face of variance in sniff dynamics even though changes in sniffing alone can cause response changes identical to those caused by concentration change

11) The olfactory bulb, in absence of odour, responds to changing inhalation parameters in a cell-type specific way that may allow inference about the kind of sniff that just occurred on a behavioural timescale.

GENERAL DISCUSSION

Contextual information has been widely reported in early sensory systems, and the olfactory bulb is certainly no exception. Some have even gone so far as to say that the OB firing rate in freely moving rodents varies more due to contextual cues than due to olfactory stimuli (Kay and Laurent, 1999). To investigate the mechanisms of such context dependent modulation of OB activity alongside learning, I optimised whole cell recording procedures in behaving mice, alongside a learning paradigm for rapid task learning within whole cell timescales. This allowed me to perform the first experiments tracking subthreshold activity from single identified cells during the entire course of task learning. With these experiments, I sought to better understand the mechanisms of context dependent changes in MTC activity across learning. I show profound diverse changes in single cell responses to olfactory stimuli across learning which act to enhance early stimulus detectability and discriminability. Rapid active sampling strongly predicts these response changes, and indeed modulating active sampling state on rapid timescales dynamically regulates excitation. Exogenously evoking sniff changes in non-behaving mice also alters neural responses, but cannot entirely recreate the kind of changes we see in the behaving active sampling mouse. I find evidence for a bottom-up mechanism, in which sniff changes result in changes in the input pattern and consequently alter firing rates, in addition to top down mechanisms: response changes during active sampling exceed those predicted from bottom up input. The relative contribution of each is dependent on the behavioural context. Here I will elaborate upon the impact of these findings for our understanding of the olfactory bulb, the future of its research, and our understanding of sensory processing in general.

7.1 New perspectives on olfactory bulb function

7.1.1 The bulb as an olfactory thalamus

The olfactory bulb is the only neural bottleneck between the sensory periphery and the olfactory cortex, and as such it is in prime position to regulate the flow of information coming into the olfactory system – i.e. to remove redundant information as far as is optimal, and facilitate the robust encoding of olfactory stimuli that are of current biological importance. Its abundance of interneurons (Shepherd, 2004), as well as top-down connections from higher brain centres (Niedworok et al., 2012; Shipley and Adamek, 1984), makes it well equipped for such a task. This circuit architecture is very similar to that displayed by the thalami of other sensory systems, which are hypothesized to be the gate-keepers of information flow according to context (Kay and Sherman, 2007).

Coincident with changes in active sampling state I find prominent changes in responses to odour that are markedly absent in passive mice, even when undergoing sniff changes. These changes are associated with both increased early detectability and discriminability of the odour representation across the sample, and this is congruent with the more rapid reaction times that are linked to active sampling. Mice which displayed rapid sniffing showed shorter reaction times, while previous studies with an increased trial number show that rapid stimulus sampling in rats is associated with enhanced discrimination performance (Kepecs et al., 2007). Unlike any change occurring alongside a sniff change in absence of olfactory attention, the extent of these changes cannot be predicted by sniff locking properties, and as such are not explainable purely by bottom-up mechanisms. Thus it would appear, when olfactory attention is high, mice display rapid active sampling of the odour stimulus, and this coincides with facilitation of odour responses that likely occurs though a top-down mechanism. Such a phenomenon fits very well into the idea that the olfactory bulb exerts control over the flow of odour information according to its current relevance to the animal.

Despite the prominent changes in mean response, animals are still capable of performing the task in absence of the response changes coincident with rapid sniff behavior. Thus, it is unlikely that the changes have a critical role in coding for odour identity. Indeed, as different MTCs will have their rates of response affected to different degrees by sniff effort, this could have negative implications for an odour-identity code that is based on relative firing rates – i.e. the pattern of activation across MTCs would be unstable over changes in active sampling, as has found to be the case for glomerular maps of activation in response to odour mixtures at different sniff frequencies in tracheotomized, anaesthetized mice (Oka et al., 2009). In light of this, an identity code based on rapid and/or temporal features of spiking seems more likely, and the high speed with which mice can make olfactory decisions is consistent with this (Abraham et al., 2004, 2010; Resulaj and Rinberg, 2015; Uchida and Mainen, 2003).

So what could be the function of these firing rate changes? The active sampling changes may rather alter other more subtle perceptual qualities of the odours, for instance intensity, which is consistent with our finding that peak detectability increases across learning alongside changes in active sampling (Chapter 4, Fig. 4.4D). This is possible despite the fact that sniff variance in passive mice does not affect intensity perception (Chapter 6, Fig. 6.8), since the changes are qualitatively different according to behavioural state (Chapter 5, Fig.5.3). Congruently, some investigations in human psychophysics have shown that increased sniff effort increases odour intensity perception (Laing, 1983; Sobel et al., 2000). It is also possible however, that in absence of olfactory attention, a small proportion of strongly excited MTCs encode the odour identity with changes in firing rate, and that active sampling (and increased olfactory attention) boosts weakly excited cells to incorporate more cells into the ensemble coding for the odour, and increase reliability of encoding – this could function to increase the signal to noise ratio. Finally, imaging of glomeruli in behaving mice shows that the only detectable aspect of ORN input change with rapid sniffing is the onset of activity, which occurs at smaller latency when the

animal is sniffing rapidly (Wesson et al., 2009). I find consistently that responses in behaving mice occur with shorter latency than in passive mice (Chapter 3, Fig. 3.2C), an effect we can attribute to the speed of the first inhalation (Chapter 4, Fig. 4.7C). Thus rapid sniffing in highly motivated mice may also function to speed up stimulus acquisition. If this is the case, it is conceivable that the firing rate changes occur only as an unavoidable, but functionless by-product of the sniff change which has its true function in activating a MTC ensemble at an earlier timescale. However, the fact that fast sniffs are equally capable of reducing response onset in both passive and behaving states (Chapter 4, Fig. 4.7A), while the effect on average V_m responses are much larger when the mouse is engaged in a task, suggests that such a simple explanation is unlikely.

7.1.2 'CONTEXTUAL INFORMATION' IN THE BULB - A MISNOMER?

An increasing amount of reports indicate contextual modulation of OB output, either across learning episodes or other behavioural events. Despite this, mechanistic understanding of such phenomena is limited, though the most highly touted explanations relate to the abundance of top-down information coming into the olfactory bulb. At the same time, active sampling is a universal feature across sensing in all animals, from invertebrates to vertebrates, and across all sensory modalities – e.g. sniffing in olfaction, saccadic eye movement in vision, pinnae orientation in audition and active touch in somatosensation. It follows that active sampling is of fundamental importance to sensation in general. In fact, so important are the active sampling processes to sensory processing, that cessation of the sampling behaviours leads to a complete blocking of sensory perception: when the eye does not move relative to the visual scene, no image is conveyed to the brain (Pritchard, 1961); when odours are applied to the olfactory epithelium in absence of sniffing, no olfactory percept is reported (Bocca et al., 1965). Sensory processing in the behaving animal can therefore *only* be understood in the framework of active sampling, and yet astoundingly many previous (and even very recent) reports on contextual

modulation of the OB not only forget to record sniffing behaviour, but fail to discuss it as a possible mechanism altogether.

Behaving animals display complex variance in sniff behaviour which is modulated according to behavioural context (Wachowiak, 2011). I show that active sampling during an olfactory task causes very overt changes in odour response during behaviour (Chapter 4, Fig. 4.4 and 4.6), but even in absence of olfactory attention, prominent changes during any sniff change occur given that the cell is highly sniff locked (Chapter 5, Fig. 5.1 and 5.2). The latter can even occur in absence of an odour (Chapter 5, Fig. 5.4; Chapter 6, Fig. 6.8). Thus, *all* changes in sniff frequency will profoundly alter MTC activity in a cell-type and context-dependent manner. Sniff changes could thus provide a parsimonious explanation for multiple contextual modulations present in OB activity. Indeed, every instance in which MTC firing in behaving mice is reported to be 'contextually modulated' in previous studies, there is equally evidence that sniffing behaviour is modulated by such a context (Table 7.1). Thus, it is possible that sniffing and active sampling may account for many instances of contextual modulation of activity in the literature. In fact, if this turns out to be the case, we could go as far as to say that a large portion of the study of contextual modulation of olfactory bulb activity may equate to a study of sniff-modulation of the OB in different behavioural scenarios.

While active sampling could plausibly account for a large number of contextual changes, there are certain cases where this is unlikely to explain the modulations seen. For example, in cases where the preparation was in the anaesthetised state it is less likely that sniffing was modulated, such as the study by Kass et al. (2013), which showed potentiation of CS+ specific inputs after fear conditioning. Congruently, in my own data sniffing does not appear to account well for increased inhibitory responding across learning (Chapter 4, Fig. 4.4). Thus, active sampling does not account for all contextual changes, but every study into such phenomena must account for sniffing behaviour to prove this.

Context	MTC modulation	State	Report sniffing?	Modulation of sniffing
Learning of odour task	Chu et al., 2016 Yamada et al., 2016 Doucette & Restrepo, 2008	awake, HF awake, HF awake, FM	no no no (R)	Wesson et al. 2009, Kepecs et al., 2007 own data (Fig. 4.2)
Motivational state	Pager et al., 1974	awake, FM	no	own data (Fig. 4.3D)
Task type	Fuentes et al., 2008 Beshel et al., 2010	awake, FM awake, FM	no no	Wesson et al., 2008a
Reward expectation	Kay and laurent, 1999 Doucette & Restrepo, 2008 Doucette et al., 2011	awake, FM awake, FM awake, FM	no (R) no (R) no	Wesson et al. 2008a Ikemoto & Panksepp,1994 Kepecs et al., 2007
Fear conditioned stimuli	Kass et al., 2013 Freeman & Schneider 1982	anaesthetised awake, FM	yes (separate mice) no	Leer et al. 2011 Blanchard et al., 2001
Non-olfactory event	Kay and Laurent, 1999 Rinberg et al., 2006	awake, FM awake, FM	no (R) no	Own data (Fig. 5.1) Wesson et al., 2008a

Table 7.1. Context dependent modulation of MTC activity and sniffing in the literature.

The first column indicates the type of contextual modulation being considered. The second column indicates studies which have described such a contextual modulation in the output of the olfactory bulb. The third column indicates the behavioural state of the mice used in the study. 'HF' means head-fixed, 'FM' means freely moving. The fourth column indicates whether or not the authors attempted to account for their results according to sniffing behaivour. (R) indicates that the authors did record sniffing to a degree, but did not relate contextual modulation of activity to sniffing behaviour in either analysis or discussion. The one case where sniffing was recorded (Kass et al., 2013), did so in a separate cohort of mice to those used in the physiology. The final column indicates studies which describe modulation of sniffing behaviour by the same context.

Note that this is by no means an exhaustive list.

7.1.3 THE OLFACTORY BULB AS AN ENCODER OF SNIFF DYNAMICS

Activity in the olfactory system has long been known to be modulated by the sniff cycle (Cang and Isaacson, 2003; Fukunaga et al., 2012; Macrides and Chorover, 1972; Margrie and Schaefer, 2003). Most of this evidence came from anaesthetised mice, but here in awake mice I find consistently that the sniff cycle shapes activity in almost every cell, though to varying degrees. It is thought that, in absence of odour, these oscillations are a result of activation of mechanoceptive receptors as a result of the pressure changes coincident with each inhalation (Grosmaitre et al., 2007; Margrie and Schaefer, 2003). I found that, in absence of olfactory attention, a change in the frequency of the sniff pattern can have predictable effects on the mean activity of the cell depending on its sniff locking properties: the amplitude of sniff modulation determines the extent of the activity change, and the phase preference determines the sign of the change (during baseline).

What could be the function of such mean activity changes coincident with changes in sniffing? Of course, it is possible that such changes have no function, and one must be cautious not to assign a biological meaning to any detectable phenomenon. One plausible possibility however, is that for olfaction, it is fundamentally necessary to encode the parameters of sniffing. Since olfactory transduction is dependent on air being delivered to the epithelium through sniffing, you might need to know the sniff parameters in order to decode features of the odour stimulus. For example, the Teghtsoonian model predicts that, increased air velocity during a sniff will alter the number of odour molecules taken in and transduced at the epithelium in a given unit of time, such that an ambiguity arises: the number of odour molecules inhaled is not only affected by true changes in concentration, but also by the parameters of the sniff itself - a more forceful sniff draws in more odour molecules. Thus, you in fact must encode the sniff effort to disambiguate these effects (Teghtsoonian et al., 1978). In Chapter 6, I found highly congruent evidence for such a hypothesis, and this is further backed up by the recent work of Shusterman

and colleagues (2017). Fast sniffing at the very least causes changes that mimic the effect of concentration increases, while sniff variance seems conversely to have no overt impact on concentration perception. Thus the olfactory system must actively account for sniff change, and this could even be a primary function of sniff locking in the olfactory bulb. Congruently, imaging of the olfactory cortex in humans identified different regions, one which primarily responds to the sensory effect of sniffing in absence of odour, and another which responds primarily to olfactory stimuli (Sobel et al., 1998).

The wide variation in sniff modulation amplitudes across the MTC population could have benefits in this respect. This could also be the purpose of having two populations of principal cell, namely MCs and TCs, which respond in different ways to sniffing changes in absence of odour – with hyperpolarization and excitation respectively (Fig. 5.4 and Fig. 6.10). In general, heterogeneity within a population allows that population to carry more information (Padmanabhan and Urban, 2010); in this case, heterogeneity may allow the bulb to encode more information about the sniff that just occurred. This encoding of sniff cycle effort could underlie the function of ORN mechanoreceptors. As physiological changes in the naris, such as blood flow, can alter airway resistances (Bojsen-Moller and Fahrenkrug, 1971; Principato and Ozenberger, 1970), it is not trivial to calculate parameters of nasal flow accurately by only considering the motor output controlling sniffing. This could perhaps account for the fact that theta oscillations in the OB are generated through sensory input, rather that corollary discharge (Margrie and Schaefer, 2003).

Thus, the olfactory bulb may function to encode sniff effort in order to extract features of the odour stimulus which would otherwise be ambiguous.

7.2. Active sampling modulation of olfactory responses – potential mechanisms

A large amount of work in the olfactory field has been done on the 'bottom-up' effect of sniff change on activity – i.e. the effect of changes in OSN input - and the large majority of this work

has been done in the anaesthetised tracheotomised mouse (Wachowiak, 2011). While it has been demonstrated previously that olfactory task-engaged mice display rapid active sniffing during the odour stimulus (Kepecs et al., 2007; Wesson et al., 2009), only a handful of physiological work has been done in awake mice (Cury and Uchida, 2010; Shusterman et al., 2011; Verhagen et al., 2007; Wesson et al., 2009), and in particular very little of this been done in the framework of active sampling during olfactory behaviour. Here I have demonstrated the impact of active sampling during behaviour on the olfactory responses of individual mitral and tufted cells. In other sensory modalities, the active sampling process is thought to engage 'top down' mechanisms that act to modulate sensory processing in precise coordination with stimulus sampling and behavioural state. For the first time in the olfactory system, I have shown the effect of active sampling on odour response greatly exceeds what we would expect from simple changes in sniff locked input, and that this enhanced effect of sniffing on response is specific to the odour sampling period. Thus, changes during active sampling likely involves top-down modulation during the active sampling process. However, beyond this, our mechanistic understanding of the process is still quite lacking, and there remains a lot of detail to uncover in the future.

7.2.1 LOCAL CIRCUIT MECHANISM

The first question is how exactly the changes during active sampling are effected in the olfactory bulb circuit. For the majority of affected cell-odour pairs, increasingly positive responses appeared alongside the increasingly rapid active sampling, however, in rare cases, the opposite effect was also noted (data not shown). In the task engage/disengage paradigm (Chapter 4, Fig. 4.6), the change due to active sampling could be predicted according to the response of the cell during task engagement. Thus it would seem that the active sampling process affects the response of the cell to the olfactory input specifically, which could be achieved in a number of ways (Fig. 7.2). It could be done for example by directly increasing the excitability of the mitral

and tufted cell – and it is known that activation of certain neuromodulatory pathways in absence of odour *in vivo* does indeed have a general excitatory effect on MTCs (Bendahmane et al., 2016; Brunert et al., 2016; Rothermel et al., 2014). Secondly, the top-down input may act to disinhibit OSN input. A population of periglomerular cells, that are also known to be dopaminergic, provide inhibitory input onto the OSN presynaptic terminal (Ennis et al., 2001; Wachowiak et al., 2005). If a neuromodulator is capable of inhibiting such a population during active sampling, this could explain the increased response diversity, as more direct olfactory driven input is provided. Some lines of evidence argue against this however: imaging OSN terminals during active sniffing reveal no increase in the amplitude of response (Wesson et al., 2009). A similar effect could be achieved intrinsic to bulbar circuitry by downregulating inhibitory networks that appear to normalise overall MTC odour-evoked activity in the olfactory bulb, such as short axon cell networks (Burton et al., 2017) or parvalbumin cells (Kato et al., 2013; Miyamichi et al., 2013). Since in some cases, inhibitory responses during natural sniffing could become excitatory responses during active sampling (e.g. Chapter 4, Fig. 4.4D and 4.7A-B), the latter mechanism could be supported. Congruent with such mechanisms, we know that neuromodulatory centres, especially serotonergic projections from the raphe nuclei, as well as cholinergic neurons from the horizontal limb of the diagonal band of Broca, send abundant projections to the mitral cell layer as well as glomerular layer interneurons (Shipley and Adamek, 1984). I deem granule cells less likely to be involved, since silencing them seems to have no impact on average activity during odour (Fukunaga et al., 2014).

Some of these hypotheses could be tested using 2-photon imaging of periglomerular interneurons, in particular the dopaminergic population, as well as mitral and tufted cells, during shifts in active sampling state alongside task engagement and disengagement. This on its own will provide further evidence of top down modulation: if the phenomenon is purely feed-forward, we expect periglomerular cell odour responses to be modulated in the same direction

as mitral and tufted cell responses, since the effect on their OSN input will be the same (given that both directly sample from the OSN input). Alternatively, if we note a general reduction in PG cell responsiveness, top-down mediated disinhibition seems more likely. Imaging DAT positive (dopaminergic) cells, or co-labelling them with a reporter, could allow us to refine any modulation to this sub-population or otherwise.

7.2.2 TOP DOWN CONTROL

Secondly, the top-down pathways engaged during active sampling need to be identified. The bulb receives abundant top down input from several regions, providing many candidates for the source of modulation, and thus a difficult task when deciphering which one (or combination) of these inputs is involved. In the sensory cortices of other modalities, it is known that regions which regulate the relevant active sampling process both project to and modulate sensory activity. For example, several areas that are involved in the generation of saccades, including to frontal eye fields, appear to contribute to the modulation of responses by selective visual attention on an area - something which is inherently linked to the spatial focusing on the area mediated by saccades (Noudoost et al., 2010, 2014). Similarly, the vibrissae motor cortex which controls whisking behaviour (Ebbesen et al., 2017), also projects directly to the barrel cortex, where it can amplify responses to whisker touch (Khateb et al., 2017).

The control of active sniffing is perhaps less well understood than the control of saccadic eye movement or whisking. The pre-bötzinger complex, alongside a number of other respiratory nuclei in the brainstem, are known to perform a critical component of the central pattern generator that underlies breathing (Smith et al., 2009). Activating the pre-bötzinger complex optognetically results in rapid sniffing behaviour (Alsahafi et al., 2015; Sherman et al., 2015). However, other areas are known to have similar properties in this respect: activation of a number of cortical areas, which project to the brainstem breathing centres, causes exploratory-like sniff behaviour in anaesthetised animals, for example the infralimbic cortex (Alexandrov et

al., 2007). This is also seen during self-stimulation of reward-associated areas (Ikemoto and Panksepp, 1994), and orexin neurons of the hypothalamus (Kuwaki, 2008; Young et al., 2005). Thus, fast sniffing could be controlled by multiple centres in a likely highly interconnected network of brain regions. With regard to modulation of the olfactory bulb by active sniffing, there are already some candidate pathways by which areas controlling sniffing could act to modulate the bulb physiology. Firstly, serotonergic neurons which have effects on gating olfactory responses and modulating MTCs odour responses (Brunert et al., 2016; Kapoor et al., 2016; Petzold et al., 2009), also project to the brainstem areas in control of respiratory rhythm generation (Bonham, 1995), leading some to hypothesize that serotonin may play a role in the coordination of sniffing and olfactory response (Dugué and Mainen, 2009). Secondly, it has recently been noted that the pre-bötzinger complex, directly projects to the locus coeruleus (Yackle et al., 2017), which in turn sends abundant projections to the olfactory bulb. Orexin neurons in the hypothalamus are also known to project to the olfactory bulb (unpublished data from Denis Burdakov lab), and orexin has effects on olfactory bulb physiology (Apelbaum et al., 2005). Whether cortical areas that appear to modulate sniffing behaviour, such as the infralimbic cortex, in turn have an effect on OB physiology, remains to be tested.

Finally, cholinergic afferents appear to have a central role in the modulation of sensory cortices during active sampling behaviours. In the barrel cortex, cholinergic axons are active during spontaneous whisking, and have dramatic effects on circuit physiology (Eggermann et al., 2014), while in the visual cortex acetylcholine modulates visual responses via a muscarinic pathway, and contributes to modulation via selective attention (Goard and Dan, 2009; Herrero et al., 2008). Activation of cholinergic projections to the OB *in vivo* have dramatic effects on the glomerular input, boosting weak activation and slightly dampening the most highly activated glomeruli, as well as adding excitatory bias to mitral and tufted cell responses (Bendahmane et

al., 2016; Rothermel et al., 2014). Thus, cholinergic afferents would be a highly plausible mediator of changes in the OB during active sampling.

Due to the current lack of understanding of the control of active sniffing, alongside the huge numbers of potential mechanisms indicated by the literature, there is a long road ahead for understanding how active sampling modulates the olfactory bulb. Imaging the axons of different kinds of top-down afferents in the bulb in the behaving actively sampling animal would provide great help in deciphering which pathways are involved in the coordination of active sampling and sensory modulation. This alongside manipulation of identified candidates would contribute greatly to our mechanistic understanding of this effect.

7.2.3 POPULATION LEVEL EFFECTS

Finally, it will be of great use to record from populations of neurons simultaneously during active sampling state and otherwise. This would allow us to confirm more robustly the beneficial effects of active sampling for the odour representation across the population, and would also allow us to see changes in dynamics on a population level, such as changes in cell synchrony. Such changes have been noted across learning olfactory tasks using unit recordings in the olfactory bulb (Doucette et al., 2011). Furthermore, imaging from large populations of mitral and tufted cells has shown both increased discriminability and robustness of odour representation across learning (Chu et al., 2016; Yamada et al., 2017), congruent with our results. However, since neither measured sniffing, it is impossible to know whether these were driven by active sampling.

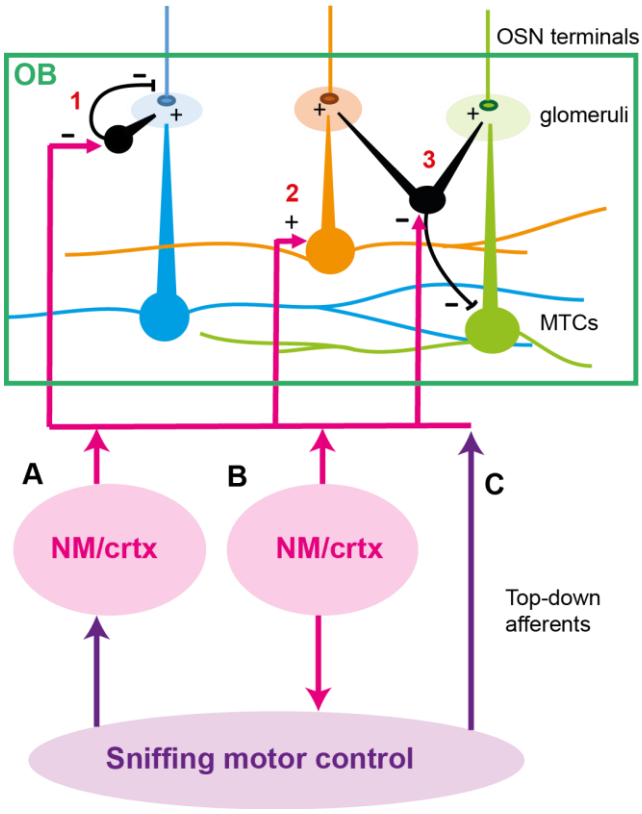

Figure 7.2. Potential mechanisms for top-down control of olfactory bulb responses during active sampling.

This shows a simple schematic for three potential non-mutually exclusive local circuit mechanisms for how olfactory bulb responses are facilitated during active sampling. (1) Top-down inputs inhibit periglomerular interneurons that provide inhibitory feedback terminals onto OSN inputs (disinhibition of input). (2) Top down inputs increase excitability of mitral and tufted cells directly. (3) Top-down inputs inhibit interneurons which provide widespread, normalising inhibition onto mitral and tufted cells (disinhibition of lateral inhibition). There are additionally several potential central mechanisms for how the motor effect of fast sniffing and the sensory effect on the olfactory bulb are coordinated. (A) The motor control centre for sniffing projects to neuromodulatory or cortical centres that feed into the olfactory bulb (an example would be the pre-bötzinger→locus coeruleus→olfactory bulb pathway). (B) Neuromodulatory or control centres act to modulate both the sniffing motor control centre alongside the sensory responses in the olfactory bulb (an example would be serotonergic neurons of the raphe, which project both to the bulb and respiratory brainstem circuits). (C) Direct projections from the sniffing motor centre to the olfactory bulb (I can find no evidence for this in the literature).

7.3 THE IMPACT ON FUTURE RESEARCH

7.3.1 RESEARCH IN THE OLFACTORY SYSTEM

Why has sniffing behaviour been altogether overlooked as a mechanism in so many previous papers? This could first and foremost owe to the difficulties associated with measuring sniffing in a freely moving animal. However, there are even recent instances in head-fixed mice (where sniff recording is well established), in which sniff behaviour was not only unrecorded, but not even given a mention (e.g. Chu et al., 2016). With the results of this project I hope to a) drive more people working with olfaction during behaviour to measure and account for the sniff cycle, or at least acknowledge sniffing as a plausible mechanism; b) convince the field and those around it that a mechanism based on active sampling could be a prevalent mechanism underlying contextual modulation; and c) show that this is in fact a highly interesting phenomenon, with complex mechanistic underpinnings including top-down components, rather than a basic effect on the frequency of OSN input.

What I hope not to do is to stagnate research into 'contextual modulation' of the olfactory bulb by providing this evidence. Now that most mechanistic studies are increasingly performed in the head-fixed animal due to unprecedented advantages in stimulus control and mechanical stability, accounting for sniff behaviour is straightforward, particularly with newer techniques, such as infrared imaging of the mouse nares (Esquivelzeta Rabell et al., 2017). New advances in techniques to control changes in sniffing behaviour in the awake animal more directly, e.g. via control of the pre-bötzinger complex which coordinates sniffing, or the vagal nerve which controls sniff frequency (Alsahafi et al., 2015; Sherman et al., 2015), may greatly facilitate mechanistic study of the OB during behaviour.

Furthermore, the sheer abundance of different kinds of top-down input to the olfactory bulb and the huge number of interneurons, presumably must do something complex. The olfactory

go/no-go task we present here is a simple task for the animal to perform, as indicated by rapid learning times. It is well possible that more complex tasks that more greatly challenge the OB circuitry will incorporate more extensive top-down mechanisms and/or differing sniff strategies, and perhaps evoke long term potentiation within the circuitry, as is known to be possible via top-down cortical connections (Gao and Strowbridge, 2009). It is known for example that LFP gamma activity differs according to task difficulty (Beshel et al., 2007), and recent imaging data shows that the nature of changes in MTC responses across long learning timescales is different according to task difficulty (Chu et al., 2016). Further experimentation will be required to tease out the relative role of task-specific sniff strategies and top-down influence during more complex tasks.

Furthermore, these findings bring up new questions about sniffing strategies, and the function and impact of sniff strategies on olfactory function. One such question I addressed here in Chapter 6. The variation in firing rate responses to odours across trials according to active sampling state will allow us to ask further such interesting questions about the nature of coding of odour identity within the olfactory bulb. Since the firing rate is unstable, yet perceptual stability must on some level be maintained to facilitate learning, this points towards coding for odour identity based on only small numbers of spikes, such as the activation of the earliest and strongest responding glomeruli (Cury and Uchida, 2010; Kepple et al., 2016; Wilson et al., 2017), which would be congruent with the very fast olfactory discrimination times of mice. A powerful tool to determine the features of the odour response that remain stable across variable trials would be the task engagement/disengagement paradigm used in Chapter 4 (Fig. 4.5 and 4.6). One would need to monitor the activity of large numbers of neurons across task switches, and ask what features of spiking activity could be used to predict the odour stimulus regardless of the current task engagement state. Are the earliest detectable excitation bursts stable across such changes? Initial evidence recording from presumptive MTC units in behaving rats has

shown that indeed, the early, transient sub-sniff pattern of spiking in response to an odour was stable across sniff frequencies, and conveyed more information about odour identity than the average activity across the sniff (Cury and Uchida, 2010).

Overall, I would hope the current findings inspire more careful recording and/or control of sampling behaviour when studying context dependent neural activity, and inspire research into a rich new set of questions that arise as a result of such findings.

7.3.2 BROADER IMPACT ON SENSORY NEUROSCIENCE

It has been hypothesized that changes in sampling behaviour during tasks helps to optimise sensory representation according to behavioural context. This comes as a result of theoretical modelling and psychophysical measurements (Ahissar and Assa, 2016; Yang et al., 2016), but direct physiological evidence that this is the case has, to my knowledge, not yet been demonstrated. Here I present the first such demonstration that this is indeed the case – mice display active sniffing according to behavioural need, with profound impact on the representation of odours at one of the earliest stages in the olfactory pathway.

Complex orchestration of active sampling is similarly present in other sensory systems. For example, rodents are known to adjust whisking strategies to the behavioural task at hand (Grant et al., 2009; Mitchinson et al., 2011), and whisking activity strongly influences neural activity in both somatosensory thalamus and cortex through both bottom-up and top-down pathways (Crochet and Petersen, 2006; Ferezou et al., 2006; Lenschow and Brecht, 2015). This overt change in physiology according to active sampling has now been demonstrated many times, and shows context dependent changes itself, but the function for somatosensory processing is still a matter of speculation. Control of eye movement can be complex, with variation across tasks and individuals, in particular in natural settings (Hayhoe and Ballard, 2014; Rayner et al., 2007). Saccadic movements have an impact on visual responses at various locations along the visual pathway. For example, in the primary visual cortex, neurons undergo a biphasic modulation of

activity during saccades (McFarland et al., 2015), while visual responses in V4 undergo heterogeneous changes in sensitivity 50ms prior to the onset of a saccade (Han et al., 2009). The data presented in this dissertation extends such findings to the olfactory bulb. However, the findings here go further in that the functional benefits of such activity changes are clearer: early odour representation is enhanced both in detectability and discriminability on the behavioural timescale, and this occurs in highly motivated mice with shorter average reaction times. Whether active modification of the sampling behaviours of other sensory modalities according to task performance similarly improves early stimulus representation remains to be seen.

In conclusion, contextual modulation of sensory-evoked activity early in the sensory pathway is not necessarily due to plasticity in centrifugal inputs or in the immediate sensory circuit itself. It might rather be the indirect consequence of ongoing, context-dependent adjustments in the "closed-loop" neural pathway that dynamically coordinates active sampling behaviour (Ahissar and Assa, 2016), in order to yield optimized sensory acquisition and processing according to ongoing context-dependent behavioural demands.

References

Abraham, N.M., Spors, H., Carleton, A., Margrie, T.W., Kuner, T., and Schaefer, A.T. (2004). Maintaining accuracy at the expense of speed: stimulus similarity defines odor discrimination time in mice. Neuron *44*, 865–876.

Abraham, N.M., Egger, V., Shimshek, D.R., Renden, R., Fukunaga, I., Sprengel, R., Seeburg, P.H., Klugmann, M., Margrie, T.W., Schaefer, A.T., et al. (2010). Synaptic inhibition in the olfactory bulb accelerates odor discrimination in mice. Neuron *65*, 399–411.

Adrian, E.D. (1950). The electrical activity of the mammalian olfactory bulb. Electroencephalogr. Clin. Neurophysiol. *2*, 377–388.

Ahissar, E., and Assa, E. (2016). Perception as a closed-loop convergence process. ELife *5*, e12830.

Alexandrov, V.G., Ivanova, T.G., and Alexandrova, N.P. (2007). Prefrontal control of respiration. J. Physiol. Pharmacol. Off. J. Pol. Physiol. Soc. *58 Suppl 5*, 17–23.

Alsahafi, Z., Dickson, C.T., and Pagliardini, S. (2015). Optogenetic excitation of preBötzinger complex neurons potently drives inspiratory activity in vivo. J. Physiol. *593*, 3673–3692.

Apelbaum, A.F., Perrut, A., and Chaput, M. (2005). Orexin A effects on the olfactory bulb spontaneous activity and odor responsiveness in freely breathing rats. Regul. Pept. *129*, 49–61.

Aungst, J.L., Heyward, P.M., Puche, A.C., Karnup, S.V., Hayar, A., Szabo, G., and Shipley, M.T. (2003). Centre–surround inhibition among olfactory bulb glomeruli. Nature *426*, 623–629.

Balu, R., Pressler, R.T., and Strowbridge, B.W. (2007). Multiple modes of synaptic excitation of olfactory bulb granule cells. J. Neurosci. Off. J. Soc. Neurosci. *27*, 5621–5632.

Bathellier, B., Buhl, D.L., Accolla, R., and Carleton, A. (2008). Dynamic ensemble odor coding in the mammalian olfactory bulb: sensory information at different timescales. Neuron *57*, 586–598.

Bendahmane, M., Ogg, M.C., Ennis, M., and Fletcher, M.L. (2016). Increased olfactory bulb acetylcholine bi-directionally modulates glomerular odor sensitivity. Sci. Rep. *6*, 25808.

Berditchevskaia, A., Cazé, R.D., and Schultz, S.R. (2016). Performance in a GO/NOGO perceptual task reflects a balance between impulsive and instrumental components of behaviour. Sci. Rep. *6*, 27389.

Beshel, J., Kopell, N., and Kay, L.M. (2007). Olfactory Bulb Gamma Oscillations Are Enhanced with Task Demands. J. Neurosci. *27*, 8358–8365.

Bhalla, U.S., and Bower, J.M. (1997). Multiday recordings from olfactory bulb neurons in awake freely moving rats: spatially and temporally organized variability in odorant response properties. J. Comput. Neurosci. *4*, 221–256.

Blauvelt, D.G., Sato, T.F., Wienisch, M., Knöpfel, T., and Murthy, V.N. (2013). Erratum: Distinct spatiotemporal activity in principal neurons of the mouse olfactory bulb in anesthetized and awake states. Front. Neural Circuits *7*, 114.

Bocca, E., Antonelli, A.R., and Mosciaro, O. (1965). Mechanical Co-Factors in Olfactory Stimulation. Acta Otolaryngol. (Stockh.) *59*, 243–247.

Bojsen-Moller, F., and Fahrenkrug, J. (1971). Nasal swell-bodies and cyclic changes in the air passage of the rat and rabbit nose. J. Anat. *110*, 25–37.

Bolding, K.A., and Franks, K.M. (2017). Complementary codes for odor identity and intensity in olfactory cortex. ELife *6*, e22630.

Bonham, A.C. (1995). Neurotransmitters in the CNS control of breathing. Respir. Physiol. *101*, 219–230.

Bouret, S., and Sara, S.J. (2004). Reward expectation, orientation of attention and locus coeruleus-medial frontal cortex interplay during learning. Eur. J. Neurosci. *20*, 791–802.

Boyd, A.M., Sturgill, J.F., Poo, C., and Isaacson, J.S. (2012). Cortical feedback control of olfactory bulb circuits. Neuron *76*, 1161–1174.

Bramble, D.M., and Carrier, D.R. (1983). Running and breathing in mammals. Science *219*, 251–256.

Brunert, D., Tsuno, Y., Rothermel, M., Shipley, M.T., and Wachowiak, M. (2016). Cell-Type-Specific Modulation of Sensory Responses in Olfactory Bulb Circuits by Serotonergic Projections from the Raphe Nuclei. J. Neurosci. Off. J. Soc. Neurosci. *36*, 6820–6835.

Buck, L., and Axel, R. (1991). A novel multigene family may encode odorant receptors: a molecular basis for odor recognition. Cell *65*, 175–187.

Burton, S.D., LaRocca, G., Liu, A., Cheetham, C.E.J., and Urban, N.N. (2017). Olfactory Bulb Deep Short-Axon Cells Mediate Widespread Inhibition of Tufted Cell Apical Dendrites. J. Neurosci. *37*, 1117–1138.

Bywalez, W.G., Patirniche, D., Rupprecht, V., Stemmler, M., Herz, A.V.M., Pálfi, D., Rózsa, B., and Egger, V. (2015). Local Postsynaptic Voltage-Gated Sodium Channel Activation in Dendritic Spines of Olfactory Bulb Granule Cells. Neuron *85*, 590–601.

Cang, J., and Isaacson, J.S. (2003). In vivo whole-cell recording of odor-evoked synaptic transmission in the rat olfactory bulb. J. Neurosci. Off. J. Soc. Neurosci. *23*, 4108–4116.

Carey, R.M., and Wachowiak, M. (2011). Effect of sniffing on the temporal structure of mitral/tufted cell output from the olfactory bulb. J. Neurosci. Off. J. Soc. Neurosci. *31*, 10615–10626.

Cazakoff, B.N., Lau, B.Y.B., Crump, K.L., Demmer, H.S., and Shea, S.D. (2014). Broadly tuned and respiration-independent inhibition in the olfactory bulb of awake mice. Nat. Neurosci. *17*, 569–576.

Cenier, T., McGann, J.P., Tsuno, Y., Verhagen, J.V., and Wachowiak, M. (2013). Testing the Sorption Hypothesis in Olfaction: A Limited Role for Sniff Strength in Shaping Primary Odor Representations During Behavior. J. Neurosci. *33*, 79–92.

Chery, R., Gurden, H., and Martin, C. (2014). Anesthetic regimes modulate the temporal dynamics of local field potential in the mouse olfactory bulb. J. Neurophysiol. *111*, 908–917.

Christie, J.M., and Westbrook, G.L. (2006). Lateral Excitation within the Olfactory Bulb. J. Neurosci. *26*, 2269–2277.

Christie, J.M., Schoppa, N.E., and Westbrook, G.L. (2001). Tufted cell dendrodendritic inhibition in the olfactory bulb is dependent on NMDA receptor activity. J. Neurophysiol. *85*, 169–173.

Chu, M.W., Li, W.L., and Komiyama, T. (2016). Balancing the Robustness and Efficiency of Odor Representations during Learning. Neuron *92*, 174–186.

Chubykin, A.A., Roach, E.B., Bear, M.F., and Shuler, M.G.H. (2013). A cholinergic mechanism for reward timing within primary visual cortex. Neuron *77*, 723–735.

Clarke, S. (1971). Sniffing and fixed-ratio behavior for sucrose and brain stimulation reward in the rat. Physiol. Behav. *7*, 695–699.

Cleland, T.A., Chen, S.-Y.T., Hozer, K.W., Ukatu, H.N., Wong, K.J., and Zheng, F. (2012). Sequential mechanisms underlying concentration invariance in biological olfaction. Front. Neuroengineering *4*.

Connelly, T., Yu, Y., Grosmaitre, X., Wang, J., Santarelli, L.C., Savigner, A., Qiao, X., Wang, Z., Storm, D.R., and Ma, M. (2015). G protein-coupled odorant receptors underlie mechanosensitivity in mammalian olfactory sensory neurons. Proc. Natl. Acad. Sci. *112*, 590–595.

Courtiol, E., Amat, C., Thévenet, M., Messaoudi, B., Garcia, S., and Buonviso, N. (2011). Reshaping of Bulbar Odor Response by Nasal Flow Rate in the Rat. PLOS ONE *6*, e16445.

Crochet, S., and Petersen, C.C.H. (2006). Correlating whisker behavior with membrane potential in barrel cortex of awake mice. Nat. Neurosci. *9*, 608–610.

Cury, K.M., and Uchida, N. (2010). Robust Odor Coding via Inhalation-Coupled Transient Activity in the Mammalian Olfactory Bulb. Neuron *68*, 570–585.

Davison, I.G., and Katz, L.C. (2007). Sparse and selective odor coding by mitral/tufted neurons in the main olfactory bulb. J. Neurosci. Off. J. Soc. Neurosci. *27*, 2091–2101.

Dhawale, A.K., Hagiwara, A., Bhalla, U.S., Murthy, V.N., and Albeanu, D.F. (2010). Non-redundant odor coding by sister mitral cells revealed by light addressable glomeruli in the mouse. Nat. Neurosci. *13*, 1404–1412.

Di Prisco, G.V., and Freeman, W.J. (1985). Odor-related bulbar EEG spatial pattern analysis during appetitive conditioning in rabbits. Behav. Neurosci. *99*, 964–978.

Doucette, W., and Restrepo, D. (2008). Profound context-dependent plasticity of mitral cell responses in olfactory bulb. PLoS Biol. *6*, e258.

Doucette, W., Gire, D.H., Whitesell, J., Carmean, V., Lucero, M.T., and Restrepo, D. (2011). Associative cortex features in the first olfactory brain relay station. Neuron *69*, 1176–1187.

Dowling, J.E. (1996). Retinal Processing of Vision. In Comprehensive Human Physiology, (Springer, Berlin, Heidelberg), pp. 773–788.

D'Souza, R.D., and Vijayaraghavan, S. (2014). Paying attention to smell: cholinergic signaling in the olfactory bulb. Front. Synaptic Neurosci. *6*, 21.

Dugué, G.P., and Mainen, Z.F. (2009). How serotonin gates olfactory information flow. Nat. Neurosci. *12*, 673–675.

Ebbesen, C.L., Doron, G., Lenschow, C., and Brecht, M. (2017). Vibrissa motor cortex activity suppresses contralateral whisking behavior. Nat. Neurosci. *20*, 82–89.

Eckmeier, D., and Shea, S.D. (2014). Noradrenergic plasticity of olfactory sensory neuron inputs to the main olfactory bulb. J. Neurosci. Off. J. Soc. Neurosci. *34*, 15234–15243.

Economo, M.N., Hansen, K.R., and Wachowiak, M. (2016). Control of Mitral/Tufted Cell Output by Selective Inhibition among Olfactory Bulb Glomeruli. Neuron *91*, 397–411.

Eggermann, E., Kremer, Y., Crochet, S., and Petersen, C.C.H. (2014). Cholinergic Signals in Mouse Barrel Cortex during Active Whisker Sensing. Cell Rep. *9*, 1654–1660.

Engel, A.K., Fries, P., and Singer, W. (2001). Dynamic predictions: Oscillations and synchrony in top–down processing. Nat. Rev. Neurosci. *2*, 704–716.

Ennis, M., Linster, C., Aroniadou-Anderjaska, V., Ciombor, K., and Shipley, M.T. (1998). Glutamate and synaptic plasticity at mammalian primary olfactory synapses. Ann. N. Y. Acad. Sci. *855*, 457–466.

Ennis, M., Zhou, F.M., Ciombor, K.J., Aroniadou-Anderjaska, V., Hayar, A., Borrelli, E., Zimmer, L.A., Margolis, F., and Shipley, M.T. (2001). Dopamine D2 receptor-mediated presynaptic inhibition of olfactory nerve terminals. J. Neurophysiol. *86*, 2986–2997.

Esquivelzeta Rabell, J., Mutlu, K., Noutel, J., Martin Del Olmo, P., and Haesler, S. (2017). Spontaneous Rapid Odor Source Localization Behavior Requires Interhemispheric Communication. Curr. Biol. CB *27*, 1542–1548.e4.

Ferezou, I., Bolea, S., and Petersen, C.C.H. (2006). Visualizing the cortical representation of whisker touch: voltage-sensitive dye imaging in freely moving mice. Neuron *50*, 617–629.

Fiser, A., Mahringer, D., Oyibo, H.K., Petersen, A.V., Leinweber, M., and Keller, G.B. (2016). Experience-dependent spatial expectations in mouse visual cortex. Nat. Neurosci. *19*, 1658–1664.

Franks, K.M., and Isaacson, J.S. (2006). Strong single-fiber sensory inputs to olfactory cortex: implications for olfactory coding. Neuron *49*, 357–363.

Frasnelli, J., Hummel, T., Berg, J., Huang, G., and Doty, R.L. (2011). Intranasal Localizability of Odorants: Influence of Stimulus Volume. Chem. Senses *36*, 405–410.

Freeman, W.J., and Schneider, W. (1982). Changes in spatial patterns of rabbit olfactory EEG with conditioning to odors. Psychophysiology *19*, 44–56.

Fuentes, R.A., Aguilar, M.I., Aylwin, M.L., and Maldonado, P.E. (2008). Neuronal activity of mitral-tufted cells in awake rats during passive and active odorant stimulation. J. Neurophysiol. *100*, 422–430.

Fukunaga, I., Berning, M., Kollo, M., Schmaltz, A., and Schaefer, A.T. (2012). Two distinct channels of olfactory bulb output. Neuron *75*, 320–329.

Fukunaga, I., Herb, J.T., Kollo, M., Boyden, E.S., and Schaefer, A.T. (2014). Independent control of gamma and theta activity by distinct interneuron networks in the olfactory bulb. Nat. Neurosci. *17*, 1208–1216.

Gao, Y., and Strowbridge, B.W. (2009). Long-term plasticity of excitatory inputs to granule cells in the rat olfactory bulb. Nat. Neurosci. *12*, 731–733.

Ghatpande, A.S., and Reisert, J. (2011). Olfactory receptor neuron responses coding for rapid odour sampling. J. Physiol. *589*, 2261–2273.

Ghosh, S., Larson, S.D., Hefzi, H., Marnoy, Z., Cutforth, T., Dokka, K., and Baldwin, K.K. (2011). Sensory maps in the olfactory cortex defined by long-range viral tracing of single neurons. Nature *472*, 217–220.

Giessel, A.J., and Datta, S.R. (2014). Olfactory maps, circuits and computations. Curr. Opin. Neurobiol. *24*, 120–132.

Goard, M., and Dan, Y. (2009). Basal forebrain activation enhances cortical coding of natural scenes. Nat. Neurosci. *12*, 1444–1449.

Grabska-Barwińska, A., Barthelmé, S., Beck, J., Mainen, Z.F., Pouget, A., and Latham, P.E. (2017). A probabilistic approach to demixing odors. Nat. Neurosci. *20*, 98–106.

Grant, R.A., Mitchinson, B., Fox, C.W., and Prescott, T.J. (2009). Active touch sensing in the rat: anticipatory and regulatory control of whisker movements during surface exploration. J. Neurophysiol. *101*, 862–874.

Gray, C.M., Freeman, W.J., and Skinner, J.E. (1986). Chemical dependencies of learning in the rabbit olfactory bulb: acquisition of the transient spatial pattern change depends on norepinephrine. Behav. Neurosci. *100*, 585.

Griff, E.R., Mafhouz, M., and Chaput, M.A. (2008a). Comparison of identified mitral and tufted cells in freely breathing rats: II. Odor-evoked responses. Chem. Senses *33*, 793–802.

Griff, E.R., Mafhouz, M., Perrut, A., and Chaput, M.A. (2008). Comparison of Identified Mitral and Tufted Cells in Freely Breathing Rats: I. Conduction Velocity and Spontaneous Activity. Chem. Senses *33*, 779–792.

Grosmaitre, X., Santarelli, L.C., Tan, J., Luo, M., and Ma, M. (2007). Dual functions of mammalian olfactory sensory neurons as odor detectors and mechanical sensors. Nat. Neurosci. *10*, 348–354.

Gschwend, O., Abraham, N.M., Lagier, S., Begnaud, F., Rodriguez, I., and Carleton, A. (2015). Neuronal pattern separation in the olfactory bulb improves odor discrimination learning. Nat. Neurosci. *18*, 1474–1482.

Guerin, D., Peace, S.T., Didier, A., Linster, C., and Cleland, T.A. (2008). Noradrenergic neuromodulation in the olfactory bulb modulates odor habituation and spontaneous discrimination. Behav. Neurosci. *122*, 816–826.

Guo, Z.V., Hires, S.A., Li, N., O'Connor, D.H., Komiyama, T., Ophir, E., Huber, D., Bonardi, C., Morandell, K., Gutnisky, D., et al. (2014). Procedures for Behavioral Experiments in Head-Fixed Mice. PLOS ONE *9*, e88678.

Haberly, L.B., and Price, J.L. (1978). Association and commissural fiber systems of the olfactory cortex of the rat. I. Systems originating in the piriform cortex and adjacent areas. J. Comp. Neurol. *178*, 711–740.

Han, X., Xian, S.X., and Moore, T. (2009). Dynamic sensitivity of area V4 neurons during saccade preparation. Proc. Natl. Acad. Sci. *106*, 13046–13051.

Hayar, A., Karnup, S., Ennis, M., and Shipley, M.T. (2004). External Tufted Cells: A Major Excitatory Element That Coordinates Glomerular Activity. J. Neurosci. *24*, 6676–6685.

Hayhoe, M., and Ballard, D. (2014). Modeling task control of eye movements. Curr. Biol. CB *24*, R622-628.

Helmholtz, H. von (1867). Handbuch der physiologischen Optik (Leipzig : Leopold Voss).

Herrero, J.L., Roberts, M.J., Delicato, L.S., Gieselmann, M.A., Dayan, P., and Thiele, A. (2008). Acetylcholine contributes through muscarinic receptors to attentional modulation in V1. Nature *454*, 1110–1114.

Homma, R., Cohen, L.B., Kosmidis, E.K., and Youngentob, S.L. (2009). Perceptual stability during dramatic changes in olfactory bulb activation maps and dramatic declines in activation amplitudes. Eur. J. Neurosci. *29*, 1027–1034.

Hubel, D.H., and Wiesel, T.N. (1959). Receptive fields of single neurones in the cat's striate cortex. J. Physiol. *148*, 574–591.

Hubel, D.H., and Wiesel, T.N. (1962). Receptive fields, binocular interaction and functional architecture in the cat's visual cortex. J. Physiol. *160*, 106–154.2.

Igarashi, K.M., Ieki, N., An, M., Yamaguchi, Y., Nagayama, S., Kobayakawa, K., Kobayakawa, R., Tanifuji, M., Sakano, H., Chen, W.R., et al. (2012). Parallel mitral and tufted cell pathways route distinct odor information to different targets in the olfactory cortex. J. Neurosci. Off. J. Soc. Neurosci. *32*, 7970–7985.

Ikemoto, S., and Panksepp, J. (1994). The relationship between self-stimulation and sniffing in rats: does a common brain system mediate these behaviors? Behav. Brain Res. *61*, 143–162.

Ito, M., and Gilbert, C.D. (1999). Attention modulates contextual influences in the primary visual cortex of alert monkeys. Neuron *22*, 593–604.

Jacobs, B.L., and Fornal, C.A. (1993). 5-HT and motor control: a hypothesis. Trends Neurosci. *16*, 346–352.

Jahr, C.E., and Nicoll, R.A. (1982). Noradrenergic modulation of dendrodendritic inhibition in the olfactory bulb. Nature *297*, 227–229.

Kapoor, V., Provost, A.C., Agarwal, P., and Murthy, V.N. (2016). Activation of raphe nuclei triggers rapid and distinct effects on parallel olfactory bulb output channels. Nat. Neurosci. *19*, 271–282.

Kass, M.D., Rosenthal, M.C., Pottackal, J., and McGann, J.P. (2013). Fear learning enhances neural responses to threat-predictive sensory stimuli. Science *342*, 1389–1392.

Kato, H.K., Chu, M.W., Isaacson, J.S., and Komiyama, T. (2012). Dynamic sensory representations in the olfactory bulb: modulation by wakefulness and experience. Neuron *76*, 962–975.

Kato, H.K., Gillet, S.N., Peters, A.J., Isaacson, J.S., and Komiyama, T. (2013). Parvalbumin-expressing interneurons linearly control olfactory bulb output. Neuron *80*, 1218–1231.

Kay, L.M., and Beshel, J. (2010). A beta oscillation network in the rat olfactory system during a 2-alternative choice odor discrimination task. J. Neurophysiol. *104*, 829–839.

Kay, L.M., and Laurent, G. (1999). Odor- and context-dependent modulation of mitral cell activity in behaving rats. Nat. Neurosci. *2*, 1003–1009.

Kay, L.M., and Sherman, S.M. (2007). An argument for an olfactory thalamus. Trends Neurosci. *30*, 47–53.

Kepecs, A., Uchida, N., and Mainen, Z.F. (2007a). Rapid and precise control of sniffing during olfactory discrimination in rats. J. Neurophysiol. *98*, 205–213.

Kepecs, A., Uchida, N., and Mainen, Z.F. (2007b). Rapid and precise control of sniffing during olfactory discrimination in rats. J. Neurophysiol. *98*, 205–213.

Kepple, D., Giaffar, H., Rinberg, D., and Koulakov, A. (2016). Deconstructing Odorant Identity via Primacy in Dual Networks. ArXiv160902202 Q-Bio.

Khateb, M., Schiller, J., and Schiller, Y. (2017). Feedforward motor information enhances somatosensory responses and sharpens angular tuning of rat S1 barrel cortex neurons. ELife *6*.

Kikuta, S., Fletcher, M.L., Homma, R., Yamasoba, T., and Nagayama, S. (2013). Odorant response properties of individual neurons in an olfactory glomerular module. Neuron *77*, 1122–1135.

Kleene, S.J. (2008). The electrochemical basis of odor transduction in vertebrate olfactory cilia. Chem. Senses *33*, 839–859.

Kollo, M., Schmaltz, A., Abdelhamid, M., Fukunaga, I., and Schaefer, A.T. (2014). “Silent” mitral cells dominate odor responses in the olfactory bulb of awake mice. Nat. Neurosci. *17*, 1313–1315.

Kuwaki, T. (2008). Orexinergic modulation of breathing across vigilance states. Respir. Physiol. Neurobiol. *164*, 204–212.

Laing, D.G. (1983). Natural sniffing gives optimum odour perception for humans. Perception *12*, 99–117.

Lenschow, C., and Brecht, M. (2015). Barrel cortex membrane potential dynamics in social touch. Neuron *85*, 718–725.

Lepousez, G., and Lledo, P.-M. (2013). Odor discrimination requires proper olfactory fast oscillations in awake mice. Neuron *80*, 1010–1024.

Livneh, Y., Adam, Y., and Mizrahi, A. (2014). Odor processing by adult-born neurons. Neuron *81*, 1097–1110.

Louis, M., Huber, T., Benton, R., Sakmar, T.P., and Vosshall, L.B. (2008). Bilateral olfactory sensory input enhances chemotaxis behavior. Nat. Neurosci. *11*, 187–199.

Lowe, G., and Gold, G.H. (1993). Nonlinear amplification by calcium-dependent chloride channels in olfactory receptor cells. Nature *366*, 283–286.

Macrides, F., and Chorover, S.L. (1972). Olfactory bulb units: activity correlated with inhalation cycles and odor quality. Science *175*, 84–87.

Macrides, F., Eichenbaum, H.B., and Forbes, W.B. (1982). Temporal relationship between sniffing and the limbic theta rhythm during odor discrimination reversal learning. J. Neurosci. Off. J. Soc. Neurosci. *2*, 1705–1717.

Magklara, A., and Lomvardas, S. (2013). Stochastic gene expression in mammals: lessons from Olfaction. Trends Cell Biol. *23*, 449–456.

Mahler, S.V., Moorman, D.E., Smith, R.J., James, M.H., and Aston-Jones, G. (2014). Motivational activation: a unifying hypothesis of orexin/hypocretin function. Nat. Neurosci. *17*, 1298–1303.

Mainland, J., and Sobel, N. (2006). The Sniff Is Part of the Olfactory Percept. Chem. Senses *31*, 181–196.

Mainland, J.D., Lundström, J.N., Reisert, J., and Lowe, G. (2014). From Molecule to Mind: an Integrative Perspective on Odor Intensity. Trends Neurosci. *37*, 443–454.

Malnic, B., Hirono, J., Sato, T., and Buck, L.B. (1999). Combinatorial Receptor Codes for Odors. Cell *96*, 713–723.

Mandairon, N., Kermen, F., Charpentier, C., Sacquet, J., Linster, C., and Didier, A. (2014). Context-driven activation of odor representations in the absence of olfactory stimuli in the olfactory bulb and piriform cortex. Front. Behav. Neurosci. *8*, 138.

Margrie, T.W., and Schaefer, A.T. (2003). Theta oscillation coupled spike latencies yield computational vigour in a mammalian sensory system. J. Physiol. *546*, 363–374.

Margrie, T.W., Meyer, A.H., Caputi, A., Monyer, H., Hasan, M.T., Schaefer, A.T., Denk, W., and Brecht, M. (2003). Targeted whole-cell recordings in the mammalian brain in vivo. Neuron *39*, 911–918.

Markopoulos, F., Rokni, D., Gire, D.H., and Murthy, V.N. (2012). Functional properties of cortical feedback projections to the olfactory bulb. Neuron *76*, 1175–1188.

Martin, C., Gervais, R., Messaoudi, B., and Ravel, N. (2006). Learning-induced oscillatory activities correlated to odour recognition: a network activity. Eur. J. Neurosci. *23*, 1801–1810.

Matsutani, S., and Yamamoto, N. (2008). Centrifugal innervation of the mammalian olfactory bulb. Anat. Sci. Int. *83*, 218–227.

McFarland, J.M., Bondy, A.G., Saunders, R.C., Cumming, B.G., and Butts, D.A. (2015). Saccadic modulation of stimulus processing in primary visual cortex. Nat. Commun. *6*, 8110.

McGinley, M.J., David, S.V., and McCormick, D.A. (2015). Cortical Membrane Potential Signature of Optimal States for Sensory Signal Detection. Neuron *87*, 179–192.

McLean, J.H., Shipley, M.T., Nickell, W.T., Aston-Jones, G., and Reyher, C.K. (1989). Chemoanatomical organization of the noradrenergic input from locus coeruleus to the olfactory bulb of the adult rat. J. Comp. Neurol. *285*, 339–349.

Meredith, M. (1986). Patterned response to odor in mammalian olfactory bulb: the influence of intensity. J. Neurophysiol. *56*, 572–597.

Mitchinson, B., Grant, R.A., Arkley, K., Rankov, V., Perkon, I., and Prescott, T.J. (2011). Active vibrissal sensing in rodents and marsupials. Philos. Trans. R. Soc. Lond. B. Biol. Sci. *366*, 3037–3048.

Miyamichi, K., Amat, F., Moussavi, F., Wang, C., Wickersham, I., Wall, N.R., Taniguchi, H., Tasic, B., Huang, Z.J., He, Z., et al. (2011). Cortical representations of olfactory input by trans-synaptic tracing. Nature *472*, 191–196.

Miyamichi, K., Shlomai-Fuchs, Y., Shu, M., Weissbourd, B.C., Luo, L., and Mizrahi, A. (2013). Dissecting local circuits: parvalbumin interneurons underlie broad feedback control of olfactory bulb output. Neuron *80*, 1232–1245.

Mizrahi, A. (2007). Dendritic development and plasticity of adult-born neurons in the mouse olfactory bulb. Nat. Neurosci. *10*, 444–452.

Mombaerts, P., Wang, F., Dulac, C., Chao, S.K., Nemes, A., Mendelsohn, M., Edmondson, J., and Axel, R. (1996). Visualizing an Olfactory Sensory Map. Cell *87*, 675–686.

Moreno, M.M., Linster, C., Escanilla, O., Sacquet, J., Didier, A., and Mandairon, N. (2009). Olfactory perceptual learning requires adult neurogenesis. Proc. Natl. Acad. Sci. U. S. A. *106*, 17980–17985.

Mori, K., Kishi, K., and Ojima, H. (1983). Distribution of dendrites of mitral, displaced mitral, tufted, and granule cells in the rabbit olfactory bulb. J. Comp. Neurol. *219*, 339–355.

Mouret, A., Lepousez, G., Gras, J., Gabellec, M.-M., and Lledo, P.-M. (2009). Turnover of newborn olfactory bulb neurons optimizes olfaction. J. Neurosci. Off. J. Soc. Neurosci. *29*, 12302–12314.

Mozell, M.M., Kent, P.F., and Murphy, S.J. (1991). The effect of flow rate upon the magnitude of the olfactory response differs for different odorants. Chem. Senses *16*, 631–649.

Nagayama, S., Takahashi, Y.K., Yoshihara, Y., and Mori, K. (2004). Mitral and tufted cells differ in the decoding manner of odor maps in the rat olfactory bulb. J. Neurophysiol. *91*, 2532–2540.

Nagayama, S., Enerva, A., Fletcher, M.L., Masurkar, A.V., Igarashi, K.M., Mori, K., and Chen, W.R. (2010). Differential axonal projection of mitral and tufted cells in the mouse main olfactory system. Front. Neural Circuits *4*.

Nakamura, T., and Gold, G.H. (1987). A cyclic nucleotide-gated conductance in olfactory receptor cilia. Nature *325*, 442–444.

Niedworok, C.J., Schwarz, I., Ledderose, J., Giese, G., Conzelmann, K.-K., and Schwarz, M.K. (2012). Charting Monosynaptic Connectivity Maps by Two-Color Light-Sheet Fluorescence Microscopy. Cell Rep. *2*, 1375–1386.

Niell, C.M., and Stryker, M.P. (2010a). Modulation of Visual Responses by Behavioral State in Mouse Visual Cortex. Neuron *65*, 472–479.

Niell, C.M., and Stryker, M.P. (2010b). Modulation of visual responses by behavioral state in mouse visual cortex. Neuron *65*, 472–479.

Nigrosh, B.J., Slotnick, B.M., and Nevin, J.A. (1975). Olfactory discrimination, reversal learning, and stimulus control in rats. J. Comp. Physiol. Psychol. *89*, 285–294.

Noudoost, B., Chang, M.H., Steinmetz, N.A., and Moore, T. (2010). Top-down control of visual attention. Curr. Opin. Neurobiol. *20*, 183–190.

Noudoost, B., Clark, K.L., and Moore, T. (2014). A distinct contribution of the frontal eye field to the visual representation of saccadic targets. J. Neurosci. Off. J. Soc. Neurosci. *34*, 3687–3698.

Nunes, D., and Kuner, T. (2015). Disinhibition of olfactory bulb granule cells accelerates odour discrimination in mice. Nat. Commun. *6*, 8950.

Nusser, Z., Kay, L.M., Laurent, G., Homanics, G.E., and Mody, I. (2001). Disruption of GABAA Receptors on GABAergic Interneurons Leads to Increased Oscillatory Power in the Olfactory Bulb Network. J. Neurophysiol. *86*, 2823–2833.

Ojima, H., Mori, K., and Kishi, K. (1984). The trajectory of mitral cell axons in the rabbit olfactory cortex revealed by intracellular HRP injection. J. Comp. Neurol. *230*, 77–87.

Oka, Y., Takai, Y., and Touhara, K. (2009). Nasal Airflow Rate Affects the Sensitivity and Pattern of Glomerular Odorant Responses in the Mouse Olfactory Bulb. J. Neurosci. *29*, 12070–12078.

O'Kusky, J., and Colonnier, M. (1982). A laminar analysis of the number of neurons, glia, and synapses in the adult cortex (area 17) of adult macaque monkeys. J. Comp. Neurol. *210*, 278–290.

Orona, E., Rainer, E.C., and Scott, J.W. (1984). Dendritic and axonal organization of mitral and tufted cells in the rat olfactory bulb. J. Comp. Neurol. *226*, 346–356.

Otazu, G.H., Chae, H., Davis, M.B., and Albeanu, D.F. (2015). Cortical Feedback Decorrelates Olfactory Bulb Output in Awake Mice. Neuron *86*, 1461–1477.

Packer, O., Hendrickson, A.E., and Curcio, C.A. (1989). Photoreceptor topography of the retina in the adult pigtail macaque (Macaca nemestrina). J. Comp. Neurol. *288*, 165–183.

Padmanabhan, K., and Urban, N.N. (2010). Intrinsic biophysical diversity decorrelates neuronal firing while increasing information content. Nat. Neurosci. *13*, 1276–1282.

Pager, J. (1974). A selective modulation of the olfactory bulb electrical activity in relation to the learning of palatability in hungry and satiated rats. Physiol. Behav. *12*, 189–195.

Parthasarathy, K., and Bhalla, U.S. (2013). Laterality and symmetry in rat olfactory behavior and in physiology of olfactory input. J. Neurosci. Off. J. Soc. Neurosci. *33*, 5750–5760.

Petzold, G.C., Hagiwara, A., and Murthy, V.N. (2009). Serotonergic modulation of odor input to the mammalian olfactory bulb. Nat. Neurosci. *12*, 784–791.

Phillips, M.E., Sachdev, R.N.S., Willhite, D.C., and Shepherd, G.M. (2012). Respiration drives network activity and modulates synaptic and circuit processing of lateral inhibition in the olfactory bulb. J. Neurosci. Off. J. Soc. Neurosci. *32*, 85–98.

Pissonnier, D., Thiery, J.C., Fabre-Nys, C., Poindron, P., and Keverne, E.B. (1985). The importance of olfactory bulb noradrenalin for maternal recognition in sheep. Physiol. Behav. *35*, 361–363.

Potts, A.M., Hodges, D., Shelman, C.B., Fritz, K.J., Levy, N.S., and Mangnall, Y. (1972). Morphology of the primate optic nerve. I. Method and total fiber count. Invest. Ophthalmol. *11*, 980–988.

Pressler, R.T., and Strowbridge, B.W. (2006). Blanes cells mediate persistent feedforward inhibition onto granule cells in the olfactory bulb. Neuron *49*, 889–904.

Principato, J.J., and Ozenberger, J.M. (1970). Cyclical changes in nasal resistance. Arch. Otolaryngol. Chic. Ill 1960 *91*, 71–77.

Pritchard, R.M. (1961). Stabilized images on the retina. Sci. Am. *204*, 72–78.

Proetz, A. (1938). Applied physiology of the nose and the accessory nasal sinuses. Am. J. Surg. *42*, 190–193.

Prud'homme, M.J., Lacroix, M.C., Badonnel, K., Gougis, S., Baly, C., Salesse, R., and Caillol, M. (2009). Nutritional status modulates behavioural and olfactory bulb Fos responses to isoamyl acetate or food odour in rats: roles of orexins and leptin. Neuroscience *162*, 1287–1298.

Rajan, R., Clement, J.P., and Bhalla, U.S. (2006). Rats smell in stereo. Science *311*, 666–670.

Ravel, N., Chabaud, P., Martin, C., Gaveau, V., Hugues, E., Tallon-Baudry, C., Bertrand, O., and Gervais, R. (2003). Olfactory learning modifies the expression of odour-induced oscillatory responses in the gamma (60-90 Hz) and beta (15-40 Hz) bands in the rat olfactory bulb. Eur. J. Neurosci. *17*, 350–358.

Rayner, K., Li, X., Williams, C.C., Cave, K.R., and Well, A.D. (2007). Eye movements during information processing tasks: Individual differences and cultural effects. Vision Res. *47*, 2714–2726.

Resulaj, A., and Rinberg, D. (2015). Novel Behavioral Paradigm Reveals Lower Temporal Limits on Mouse Olfactory Decisions. J. Neurosci. *35*, 11667–11673.

Rinberg, D. (2006). Sparse Odor Coding in Awake Behaving Mice. J. Neurosci. *26*, 8857–8865.

Rinberg, D., Koulakov, A., and Gelperin, A. (2006). Sparse odor coding in awake behaving mice. J. Neurosci. Off. J. Soc. Neurosci. *26*, 8857–8865.

Roland, B., Jordan, R., Sosulski, D.L., Diodato, A., Fukunaga, I., Wickersham, I., Franks, K.M., Schaefer, A.T., and Fleischmann, A. (2016). Massive normalization of olfactory bulb output in mice with a “monoclonal nose.” ELife *5*, e16335.

Rospars, J.P., Lánský, P., Duchamp-Viret, P., and Duchamp, A. (2000). Spiking frequency versus odorant concentration in olfactory receptor neurons. Biosystems *58*, 133–141.

Rothermel, M., Carey, R.M., Puche, A., Shipley, M.T., and Wachowiak, M. (2014). Cholinergic Inputs from Basal Forebrain Add an Excitatory Bias to Odor Coding in the Olfactory Bulb. J. Neurosci. *34*, 4654–4664.

Rubin, B.D., and Katz, L.C. (1999). Optical imaging of odorant representations in the mammalian olfactory bulb. Neuron *23*, 499–511.

Rubin, B.D., and Katz, L.C. (2001). Spatial coding of enantiomers in the rat olfactory bulb. Nat. Neurosci. *4*, 355–356.

Saha, D., Li, C., Peterson, S., Padovano, W., Katta, N., and Raman, B. (2015). Behavioural correlates of combinatorial versus temporal features of odour codes. Nat. Commun. *6*, 6953.

Sara, S.J. (2009). The locus coeruleus and noradrenergic modulation of cognition. Nat. Rev. Neurosci. *10*, 211–223.

Schneider, S.P., and Scott, J.W. (1983). Orthodromic response properties of rat olfactory bulb mitral and tufted cells correlate with their projection patterns. J. Neurophysiol. *50*, 358–378.

Schoenbaum, G., and Eichenbaum, H. (1995). Information coding in the rodent prefrontal cortex. I. Single-neuron activity in orbitofrontal cortex compared with that in pyriform cortex. J. Neurophysiol. *74*, 733–750.

Schoppa, N.E. (2006). Synchronization of olfactory bulb mitral cells by precisely timed inhibitory inputs. Neuron *49*, 271–283.

Shepherd, G.M. (2004). The Synaptic Organization of the Brain (Oxford University Press, USA).

Sherman, D., Worrell, J.W., Cui, Y., and Feldman, J.L. (2015). Optogenetic perturbation of preBötzinger complex inhibitory neurons modulates respiratory pattern. Nat. Neurosci. *18*, 408–414.

Shipley, M.T., and Adamek, G.D. (1984). The connections of the mouse olfactory bulb: A study using orthograde and retrograde transport of wheat germ agglutinin conjugated to horseradish peroxidase. Brain Res. Bull. *12*, 669–688.

Shoham, S., O'Connor, D.H., and Segev, R. (2006). How silent is the brain: is there a "dark matter" problem in neuroscience? J. Comp. Physiol. A Neuroethol. Sens. Neural. Behav. Physiol. *192*, 777–784.

Short, S.M., Morse, T.M., McTavish, T.S., Shepherd, G.M., and Verhagen, J.V. (2016). Respiration Gates Sensory Input Responses in the Mitral Cell Layer of the Olfactory Bulb. PloS One *11*, e0168356.

Shuler, M.G., and Bear, M.F. (2006). Reward Timing in the Primary Visual Cortex. Science *311*, 1606–1609.

Shusterman, R., Smear, M.C., Koulakov, A.A., and Rinberg, D. (2011). Precise olfactory responses tile the sniff cycle. Nat. Neurosci. *14*, 1039–1044.

Shusterman, R., Sirotin, Y.B., Smear, M.C., Ahmadian, Y., and Rinberg, D. (2017). Sniff invariant odor coding. BioRxiv 174417.

Sirotin, Y.B., Shusterman, R., and Rinberg, D. (2015). Neural Coding of Perceived Odor Intensity,,. ENeuro *2*.

Slotnick, B.M., and Ptak, J.E. (1977). Olfactory intensity-difference thresholds in rats and humans. Physiol. Behav. *19*, 795–802.

Smear, M., Resulaj, A., Zhang, J., Bozza, T., and Rinberg, D. (2013). Multiple perceptible signals from a single olfactory glomerulus. Nat. Neurosci. *16*, 1687–1691.

Smith, J.C., Abdala, A.P.L., Rybak, I.A., and Paton, J.F.R. (2009). Structural and functional architecture of respiratory networks in the mammalian brainstem. Philos. Trans. R. Soc. B Biol. Sci. *364*, 2577–2587.

Sobel, N., Prabhakaran, V., Desmond, J.E., Glover, G.H., Goode, R.L., Sullivan, E.V., and Gabrieli, J.D. (1998). Sniffing and smelling: separate subsystems in the human olfactory cortex. Nature *392*, 282–286.

Sobel, N., Khan, R.M., Saltman, A., Sullivan, E.V., and Gabrieli, J.D. (1999). The world smells different to each nostril. Nature *402*, 35.

Sobel, N., Khan, R.M., Hartley, C.A., Sullivan, E.V., and Gabrieli, J.D. (2000). Sniffing longer rather than stronger to maintain olfactory detection threshold. Chem. Senses *25*, 1–8.

Sosulski, D.L., Lissitsyna Bloom, M., Cutforth, T., Axel, R., and Datta, S.R. (2011). Distinct representations of olfactory information in different cortical centres. Nature *472*, 213–216.

Spehr, M., and Munger, S.D. (2009). Olfactory receptors: G protein-coupled receptors and beyond. J. Neurochem. *109*, 1570–1583.

Spors, H., and Grinvald, A. (2002). Spatio-temporal dynamics of odor representations in the mammalian olfactory bulb. Neuron *34*, 301–315.

Spors, H., Wachowiak, M., Cohen, L.B., and Friedrich, R.W. (2006). Temporal Dynamics and Latency Patterns of Receptor Neuron Input to the Olfactory Bulb. J. Neurosci. *26*, 1247–1259.

Steinfeld, R., Herb, J.T., Sprengel, R., Schaefer, A.T., and Fukunaga, I. (2014). Divergent innervation of the olfactory bulb by distinct raphe nuclei. J. Comp. Neurol.

Takahashi, Y.K., Kurosaki, M., Hirono, S., and Mori, K. (2004). Topographic representation of odorant molecular features in the rat olfactory bulb. J. Neurophysiol. *92*, 2413–2427.

Tan, J., Savigner, A., Ma, M., and Luo, M. (2010). Odor information processing by the olfactory bulb analyzed in gene-targeted mice. Neuron *65*, 912–926.

Teghtsoonian, R., and Teghtsoonian, M. (1984). Testing a perceptual constancy model for odor strength: the effects of sniff pressure and resistance to sniffing. Perception *13*, 743–752.

Teghtsoonian, R., Teghtsoonian, M., Berglund, B., and Berglund, U. (1978). Invariance of odor strength with sniff vigor: an olfactory analogue to size constancy. J. Exp. Psychol. Hum. Percept. Perform. *4*, 144–152.

Trombley, P.Q., and Shepherd, G.M. (1992). Noradrenergic inhibition of synaptic transmission between mitral and granule cells in mammalian olfactory bulb cultures. J. Neurosci. Off. J. Soc. Neurosci. *12*, 3985–3991.

Uchida, N., and Mainen, Z.F. (2003). Speed and accuracy of olfactory discrimination in the rat. Nat. Neurosci. *6*, 1224–1229.

Uchida, N., and Mainen, Z.F. (2008). Odor Concentration Invariance by Chemical Ratio Coding. Front. Syst. Neurosci. *1*.

Uchida, N., Takahashi, Y.K., Tanifuji, M., and Mori, K. (2000). Odor maps in the mammalian olfactory bulb: domain organization and odorant structural features. Nat. Neurosci. *3*, 1035–1043.

Urbain, N., Salin, P.A., Libourel, P.-A., Comte, J.-C., Gentet, L.J., and Petersen, C.C.H. (2015). Whisking-Related Changes in Neuronal Firing and Membrane Potential Dynamics in the Somatosensory Thalamus of Awake Mice. Cell Rep. *13*, 647–656.

Vassar, R., Chao, S.K., Sitcheran, R., Nuñez, J.M., Vosshall, L.B., and Axel, R. (1994). Topographic organization of sensory projections to the olfactory bulb. Cell *79*, 981–991.

Verhagen, J.V., Wesson, D.W., Netoff, T.I., White, J.A., and Wachowiak, M. (2007). Sniffing controls an adaptive filter of sensory input to the olfactory bulb. Nat. Neurosci. *10*, 631–639.

Vinck, M., Batista-Brito, R., Knoblich, U., and Cardin, J.A. (2015). Arousal and locomotion make distinct contributions to cortical activity patterns and visual encoding. Neuron *86*, 740–754.

Wachowiak, M. (2011a). All in a sniff: olfaction as a model for active sensing. Neuron *71*, 962–973.

Wachowiak, M. (2011b). All in a sniff: olfaction as a model for active sensing. Neuron *71*, 962–973.

Wachowiak, M., Cohen, L.B., and Zochowski, M.R. (2002). Distributed and concentration-invariant spatial representations of odorants by receptor neuron input to the turtle olfactory bulb. J. Neurophysiol. *87*, 1035–1045.

Wachowiak, M., McGann, J.P., Heyward, P.M., Shao, Z., Puche, A.C., and Shipley, M.T. (2005). Inhibition [corrected] of olfactory receptor neuron input to olfactory bulb glomeruli mediated by suppression of presynaptic calcium influx. J. Neurophysiol. *94*, 2700–2712.

Welker, W.I. (1964). Analysis of Sniffing of the Albino Rat 1). Behaviour *22*, 223–244.

Wesson, D.W., Donahou, T.N., Johnson, M.O., and Wachowiak, M. (2008). Sniffing behavior of mice during performance in odor-guided tasks. Chem. Senses *33*, 581–596.

Wesson, D.W., Carey, R.M., Verhagen, J.V., and Wachowiak, M. (2008). Rapid encoding and perception of novel odors in the rat. PLoS Biol. *6*, e82.

Wesson, D.W., Verhagen, J.V., and Wachowiak, M. (2009). Why sniff fast? The relationship between sniff frequency, odor discrimination, and receptor neuron activation in the rat. J. Neurophysiol. *101*, 1089–1102.

Wilson, C.D., Serrano, G.O., Koulakov, A.A., and Rinberg, D. (2017). Concentration invariant odor coding. BioRxiv 125039.

Wojcik, P.T., and Sirotin, Y.B. (2014). Single scale for odor intensity in rat olfaction. Curr. Biol. CB *24*, 568–573.

Yackle, K., Schwarz, L.A., Kam, K., Sorokin, J.M., Huguenard, J.R., Feldman, J.L., Luo, L., and Krasnow, M.A. (2017). Breathing control center neurons that promote arousal in mice. Science *355*, 1411–1415.

Yamada, Y., Bhaukaurally, K., Madarász, T.J., Pouget, A., Rodriguez, I., and Carleton, A. (2017). Context- and Output Layer-Dependent Long-Term Ensemble Plasticity in a Sensory Circuit. Neuron.

Yang, S.C.-H., Wolpert, D.M., and Lengyel, M. (2016). Theoretical perspectives on active sensing. Curr. Opin. Behav. Sci. *11*, 100–108.

Young, J.K., Wu, M., Manaye, K.F., Kc, P., Allard, J.S., Mack, S.O., and Haxhiu, M.A. (2005). Orexin stimulates breathing via medullary and spinal pathways. J. Appl. Physiol. Bethesda Md 1985 *98*, 1387–1395.

Youngentob, S.L., Mozell, M.M., Sheehe, P.R., and Hornung, D.E. (1987). A quantitative analysis of sniffing strategies in rats performing odor detection tasks. Physiol. Behav. *41*, 59–69.

Zhang, X., and Firestein, S. (2002). The olfactory receptor gene superfamily of the mouse. Nat. Neurosci. *5*, 124–133.

Zinyuk, L.E., Datiche, F., and Cattarelli, M. (2001). Cell activity in the anterior piriform cortex during an olfactory learning in the rat. Behav. Brain Res. *124*, 29–32.

Zuo, Y., Perkon, I., and Diamond, M.E. (2011). Whisking and whisker kinematics during a texture classification task. Philos. Trans. R. Soc. B Biol. Sci. *366*, 3058–3069.